Investigations into the potential effectiveness of new and existing corneal cross-linking therapies

Nada H. Aldahlawi

Thesis submitted to Cardiff University in fulfilment of the requirements for the degree of

DOCTOR OF PHILOSOPHY

School of Optometry and Vision Sciences

Structural Biophysics Research Group

Cardiff University

Wales, United Kingdom

March 2018

Abstract

The studies comprising this thesis were conducted to examine the potential of a range of cross-linking therapies; in particular, to investigate the effect of a novel cross-linking therapy (involving a bacteriochlorophyll derivative and near-infra red illumination (WST-D/NIR)) on the structure of the cornea, and to develop a trans-epithelial riboflavin/Ultraviolet-A (UVA) corneal cross-linking protocol that was equally effective to that of the standard protocol (SCXL), without the need for epithelium removal. A number of laboratory techniques were used to investigate changes in the structure of the cornea and its biochemical and biomechanical properties following cross-linking. X-ray scattering and electron microscopy data provided evidence that treatment with WST-D/NIR resulted in no change in corneal collagen organisation and confirmed its potential as an alternative to riboflavin/UVA cross-linking for stiffening diseased or surgically weakened corneas. Enzyme digestion studies and strip extensometry were performed to compare the effectiveness of newly developed riboflavin/UVA protocols to that of the SCXL protocol in terms of their ability to increase the enzymatic resistance and stiffness of the cornea. The studies indicated that the intensity and distribution of cross-links formed within the cornea vary with different protocols, and that the outcome of trans-epithelial riboflavin/UVA cross-linking may be significantly enhanced through the use of higher concentrations of riboflavin, a longer duration of iontophoresis and the use of pulsed and higher energy dose UVA.

As the precise amount of CXL required to prevent disease progression is still unidentified, and an effective depth of cross-linking less than that achieved with SCXL may prove sufficient, the modified trans-epithelial protocols identified in this thesis may be an effective means of halting keratoconus progression. Further clinical studies, especially randomized prospective trials, are, however, required to confirm the encouraging results of these modified procedures.

Dedication

I proudly dedicate my dissertation to my lovely husband and gorgeous girls, Amaya and Alana, for they give up their time to support me and believe in me. Their encouraging words mean the world to me. I also dedicate this work and give special thanks to my beloved parents, for their endless love, support and valuable prayers. Thank you both for encouraging me in all of my pursuits and inspiring me to reach for the stars and chase my dreams. Thanks also to my sisters and brothers, who have never left my side and have always been there for me and supported me over the years. Last but by no means least, I cannot go without recognising my high school biology teacher, Miss. Nawal Mammon. I would have never embarked on a PhD without her contagious enthusiasm for Science and unfailing faith in me.

Acknowledgement

Prima facea, all praises to God for the strength, wellbeing and His blessings in completing this thesis. I wish also to express my sincere gratitude to my three supervisors, each one has played a vital role in my PhD.

My earnest thanks to Prof. Keith Meek not only for his continuous support of my PhD studies and his insightful comments and encouragement, but also for the challenging questions which gave me the incentive to widen my research from various perspectives. I could not have imagined having a better advisor for my PhD studies. He is a source of knowledge and wisdom. I have been extremely lucky to have a supervisor who cared so much and always responded immediately to my emails, regardless of his health.

I would also like to extend a special heart-felt thanks to my supervisor, Dr. Sally Hayes, for the continuous support, valuable advice, positive appreciation and all the days and nights we worked together. Indeed, this work would not have been possible without her guidance and involvement, her encouragement on a daily basis from the start of the project to date. Under her guidance I successfully overcame many difficulties and learnt a lot. She even taught me how to maintain a good life balance between work and family. Her own enthusiasm for perfection, passion and conviction, has always inspired me to do more. For all these, I sincerely thank her from the bottom of my heart and will be truly indebted to her throughout my life.

I am greatly indebted to my research guide Prof. David O'Brart, a talented physician, for his motivation, zeal, constructive criticism and immense knowledge. His advice and experience has been tremendously helpful throughout the research tenure. His unflinching courage pushed my boundaries for more effective work. I also truly appreciate the opportunity of completing clinical training in one of the remarkable hospitals in London.

Besides my advisors, I would like to extend my gratitude to my collaborators Dr. Arie Marcovich, Dr. Jurriaan Brekelmans and Dr Alexa Goz for the support received through the collaborative work undertaken with the Weizmann Institute of Science, Rehovot.

My sincere thanks also go to Dr. Rob Young, Dr. Phil Lewis, Dr. James Bell, Dr. Ahmad Abass, Mr. Martin Spong, Dr. Carlo Knupp, Dr. Siân Morgan, Miss. Eleanor Feneck and Dr. Tom White for their help with laboratory and research facilities, without their precious support it would not be possible to conduct this research. I am so proud to be part of the Structural Biophysics group. I want to thank every single one of them for providing such a welcoming and helpful environment to work within and making my experience in Cardiff a magical one.

It is my fortune to gratefully acknowledge the support of my fellow lab mates, Dr. Alina Akhbanbetova, Dr. Stacy Littlechild and Naomi O'Brart for their help and the sleepless nights we have worked together, as well as all the fun we had in the last four years.

To the CXL Experts, thank you for the rich research and the amazing meetings. Special thanks to Prof. Eberhard Spoerl for his kind advice in the transepithelial

method and sweet words. His kindness means the world to me.

I am also grateful for the financial support received through the Saudi government. I am indebted to King Saud University for the scholarship and the research fund to undertake my PhD. I owe thanks to Veni Vidi for the early gratuitous provision of riboflavin and loan of the Phoenix CXL System. I am equally thankful to Dr. Dario Rusciano and Dr. Giulio Luciani for their kind offer of hosting me in their Italian lab and generous help for sending me rabbit eyes.

Many thanks go to my Cardiff family Shymaa and Manna, Hawazen and Loay, Afnan and Homam, Nada and Emad, Mai and Anas, Saba and Amer, Farah Alesaei, Shahad Alahdali, and Nada Almazroa, who have provided both friendship and support, and with whom I have shared laughter, frustration and companionship. You have been more than family to me. Thank you for all of your help with the girls when I needed it the most. A special thank you to Dr. Liyana, our friendship will not be forgotten, your distance support was incredibly effective. The best of luck to you in all of your endeavours!

I would like to extend my sincerest thanks and appreciation to my parents for all of the love, support, encouragement and prayers they have sent my way along this journey. Your unconditional love and support has meant the world to me and I would never be able to pay back the love, affection and sacrifice you provided to shape my life. I hope that I have made you proud. To my siblings, the rivalry between us has pushed me to succeed. I am so proud of all of your accomplishments and share in all of the joy in your lives. In particular, I am grateful to my sister Dr. Rana, and her family (Hatem, Lamar, Malik and Lareen), for their selfless love, care and dedicated efforts to settle my family in the first years of my PhD.

My heart felt regard goes to my dear husband, Ahmad for his continued and unfailing love, support and understanding during my pursuit of a PhD degree that made the completion of my thesis possible. He was always around at times I thought that it is impossible to continue, he helped me to keep things in perspective. I greatly value his contribution and deeply appreciate his belief in me. I appreciate my daughters, who have given me much happiness and keep me hopping. Each one is deeply loved in a unique way. Amaya, has grown up watching me study and juggle between family and work, encouraging me to finish my book. Alana, the little one, who always tries to do everything to make me smile, each has contributed immeasurably to family enjoyment in a special way. Words would never say how grateful I am to the three of you. I consider myself the luckiest person in the world to have such a lovely and caring family, standing beside me with their love and unconditional support.

Finally, this thesis is the culmination of my PhD journey, which was just like a treasure hunting exercise accompanied with encouragement, hardship, trust and frustration. We have been around the world to find our treasure (Middle East, Australia, USA and UK). When I reached the top, experiencing the feeling of fulfilment, I realised that although only my name appears on the cover of this dissertation, a great many people, including my family members, well-wishers, my friends, colleagues and various institutions have contributed to accomplish this huge task. Success always depends on teamwork and the best strategy. I cannot thank you enough for helping me to turn my dream into a reality. THANK YOU ALL.

Contents

List of Figures

List of Tables

List of abbreviations

ACXL	Accelerated cross-linking
ACXL (A18)	Accelerated 18 mW/cm^2 cross-linking
ACXL (A9) or ACXL 5.4 J/cm^2	Accelerated 9 mW/cm^2 cross-linking
BAC	Benzalkoniumchloride
Bchl-Ds	Bacteriochlorophyll Derivative photosensitiser
BDMA	Benzyl dimethylamine
BSCVA	Best spectacle corrected visual acuity
c-HCXL	Continuous, high intensity and high energy UVA cross-linking
CXL	Corneal cross-linking
D	Dextran only
DDSA	Dodecenyl succinic anhydride hardener
Dis-CXL	Disrupted epithelium cross-linking
Dis-ribo	Disrupted epithelium non-irradiated control
DW	Distilled water
EDTA	Ethylenediaminetetraacetic
ex vivo	Out of the living organism
FT	Fibril transform
HCl	Hydrochloric acid
HCXL	Accelerated, and high energy UVA cross-linking
HCXL 5.4 J/cm^2	Epithelium-off, standard riboflavin concentration, and high UVA intensity CXL 5.4
HCXL 7.2 J/cm^2	Epithelium-off, standard riboflavin concentration, and high UVA energy dose CXL 7.2
HPMC	Hydroxypropyl methycellulose
ICNIRP	International Commission on NonIonizing Radiation Protection
IF	Interference function
IFS	Interfibrillar spacing
IM	Intramuscular
in vivo	In a living organism
Ion-CXL 5.4 J/cm^2	Epithelium intact, basic iontophoresis protocol
Ion-CXL 6.75 J/cm^2	Epithelium intact, basic iontophoresis protocol with high UVA energy dose 6.75
Medio-CXL 5.4 J/cm^2	Epithelium intact high riboflavin concentration cross-linking
Medio-ribo	Epithelium intact non-irradiated control
MEM	Minimum Essential Medium Eagle buffer

MMPs	Matrix metalloproteases
NaOH	Sodium hydroxide
NIR	Near infrared
p-ACXL	Pulsed light accelerated cross-linking
PBS	Phosphate buffered saline
PFA	Paraformaldehyde
p-HCXL	Pulsed, high intensity and high energy UVA cross-linking
p-HCXL 7.2 J/cm^2	Epithelium-off, standard riboflavin concentration, and pulsed high UVA energy dose CXL 7.2
p-HCXL 7.56 J/cm^2	Epithelium-off, standard riboflavin concentration, and pulsed high UVA energy dose CXL 7.56
p-TC-ion-HCXL	Pulsed, high intensity and high energy UVA cross-linking with iontophoretic riboflavin delivery
p-TC-ion-HCXL 7.56 J/cm^2	Epithelium intact, high riboflavin concentration, prolonged iontophoresis and pulsed high UVA energy dose CXL 7.56
R	Riboflavin only
RGP	Rigid gas-permeable
SAXS	Small-angle x-ray scattering
SCXL or S3	Standard riboflavin/UVA cross-linking, epithelium-off, 3mW/cm^2 for 30 minutes 5.4 J/cm^2, also called standard Dresden CXL procedure
SLRPs	Small leucine-rich proteoglycan
SOD1	Superoxide dismutase 1 gene
TC-ion–CXL 5.4 J/cm^2	Epithelium intact, high riboflavin concentration and prolonged iontophoresis cross-linking
TC-ion-CXL 6.75 J/cm^2	Epithelium intact, high riboflavin concentration, prolonged iontophoresis and high UVA energy dose CXL 6.75
TC-ion-ribo	Epithelium intact, high riboflavin concentration and prolonged iontophoresis non-irradiated control
TEM	Transmission Electron Microscope
U	Untreated
UA	Uranyl acetate
UCE	Reichert-Jung Ultracut E ultramicrotome
UVA	Ultraviolet A
VSX1	Visual system homeobox 1 gene
WST11	Bacteriochlorophyll Derivative photosensitiser
WST-D/NIR	Epithelium-off, Bacteriochlorophyll Derivative with dextran and Near Infrared Light

CHAPTER 1

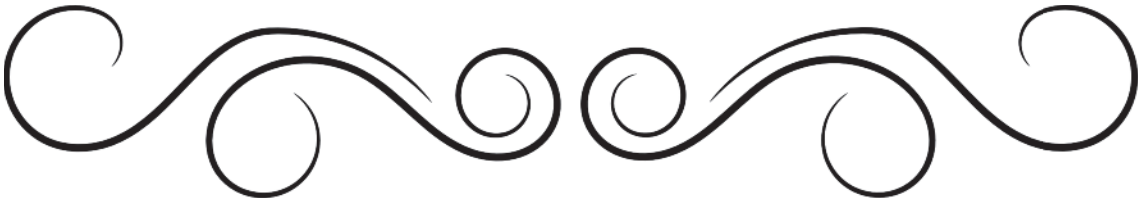

INTRODUCTION

1.1 Introduction

Each part of the eye plays a crucial role to deliver clear vision. Our window to the world is provided by the cornea on the front surface of the eye. The cornea's clarity and refractive power are vital to maximize the visual potential of the eye, and any disorder that affects the transparency or shape of the cornea will affect its performance. Therefore, the integrity and functionality of the cornea is essential for vision. This chapter overviews the anatomy and cell biology of the human cornea, providing an insight into the substructure and biological features of the cornea.

1.2 Cornea: Cellular and molecular biology

The cornea is the distinctive transparent connective tissue of the outer ocular surface of the eye that plays a vital role in the vision pathway. Along with the covering tear film, it acts as the primary infectious barrier as well as a barrier to fluid loss from the surface of the eye (Evans et al. 2013; Kaufman et al. 1998; Zhang et al. 2017). Corneal transparency may alter due to any change in the anatomical and physiological structure (DelMonte et al. 2011; Huang et al. 2001). The corneal extracellular matrix provides the mechanical strength of the cornea, and is also crucial to the maintenance of corneal tissue hydration and hence transparency (Kaufman et al. 1998; Meek et al. 2015). The cornea provides a significant optical refractive element, which constitutes about two-thirds of the total refractive power of the eye (Asgari et al. 2013; Ortiz et al. 2012), with the residual optical power provided by the lens (Savini et al. 2013b). As the major refractive surface of the eye, the anterior surface of the cornea provides 40 to 44 dioptres of the total refractive power of the eye (Krachmer et al. 2011). Both the corneal anterior radius of curvature ($\approx$ 7.8 mm) and the refractive index (1.376) (Savini et al. 2013a) generate this refractive power. The cornea evolved as an avascular structure that dissolves oxygen supplies mostly from the atmosphere through the superficial corneal surface and relies on the aqueous humor for other nutritional requirements (Seal et al. 2007). The connective tissue serves not only

as a structural support but also as the conduit of fluid and nutrients, it also houses support cells that provide for maintenance of the matrix and overlying epithelium (Smolin et al. 2005).

1.2.1 Gross Anatomy

The eye has three primary layers: a fibrous tunic which covers the whole outer surface of the eye and a choroid and neural retina layer, which comprise the middle and innermost layers of all but the anterior-most portion of the eye. The cornea is positioned at the front of the eye and constitutes one-sixth of the outer fibrous tunic, the posterior opaque fibrous tissue of the eyeball called sclera, forms the remaining five-sixths of the outer tunic (Ashalatha et al. 2012) (Figure 1.1).

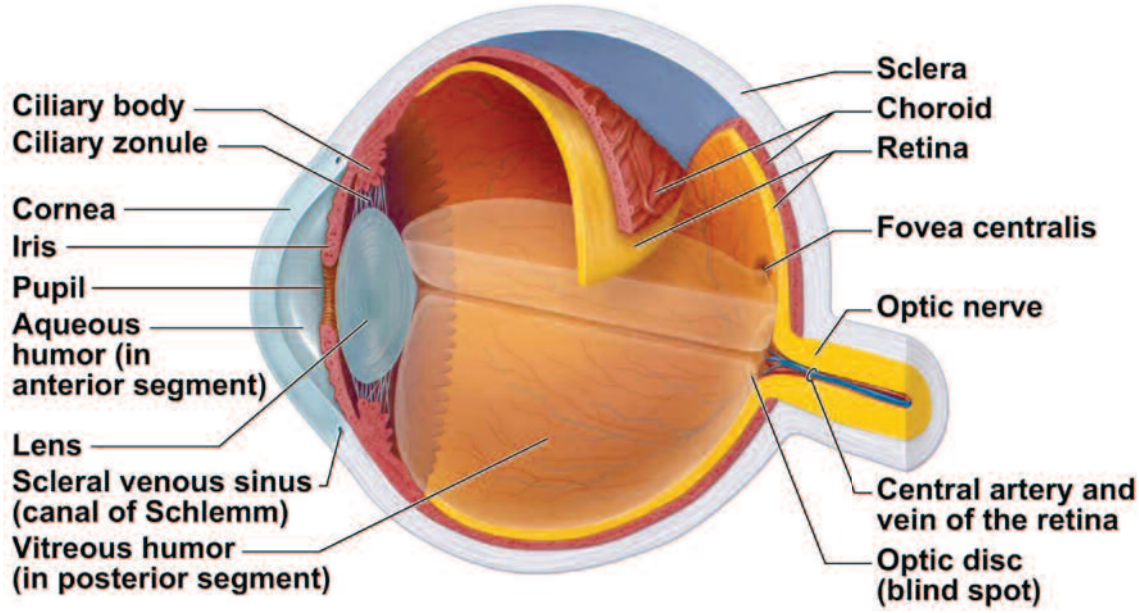

Figure 1.1: The anatomy of the eye. The eye has three primary layers: an outer fibrous tunic, a middle choroid, and an inner neural retina layer. Reproduced from *https://nurseslabs.com/special-senses-anatomy-physiology/* [accessed 31 December 2017]

The normal cornea has an asymmetrical anterior and posterior viewing surface, it has an elliptic shape on the anterior surface and a circular shape at the posterior, because of scleralization superiorly and inferiorly (He et al. 2010). The anterior surface dimensions of the adult human cornea are 11-12 mm horizontally by 9-11 mm vertically. The

average diameter of the posterior surface is 11.76 mm (Lens et al. 2008). The cornea is approximately 550 μm thick at the centre (Feizi et al. 2014), and progressively increases in thickness toward the periphery, where it is roughly 650 μm thick (DelMonte et al. 2011; Land 2014). The corneal curvature is not uniform, being steeper centrally and flatter at the periphery, more so nasally than temporally (Albert et al. 2008). The central one-third of the cornea is called the optical zone, where the surface is almost spherical. The average radius of curvature is between 7.5 and 8.0 mm (Sideroudi et al. 2013).

1.2.2 Corneal histology

The human cornea is divided into five specialized layers: epithelium, Bowman's layer, stroma, Descemet's membrane and the endothelium. The structure of the cornea and its component layers are shown in (Figure 1.2).

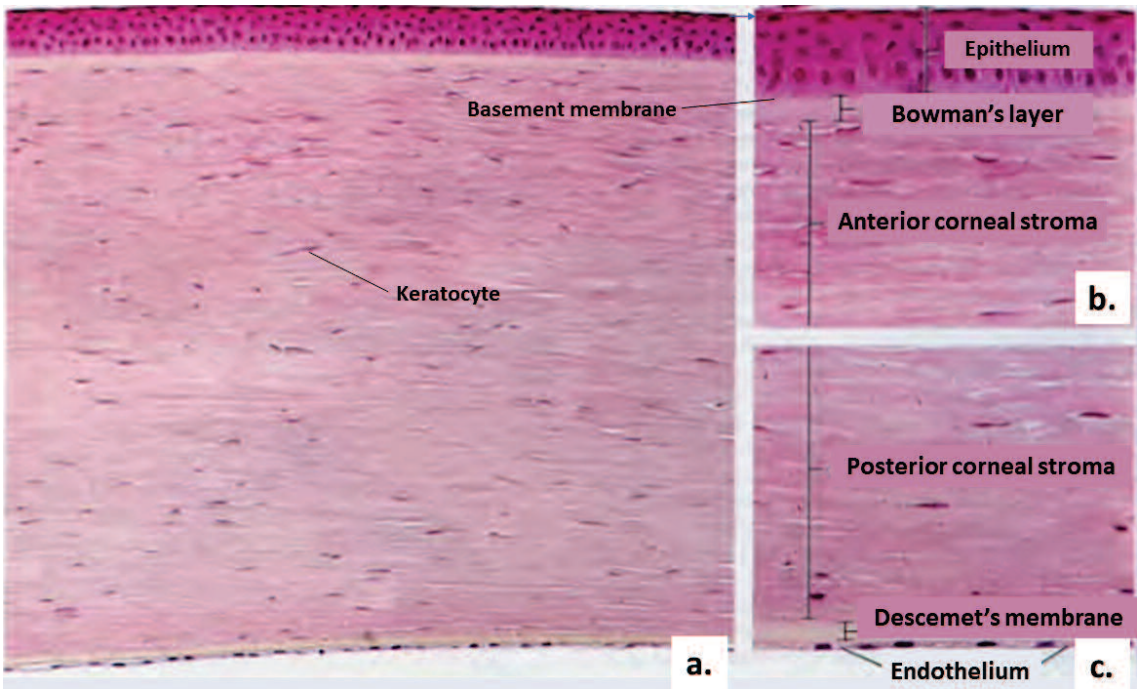

Figure 1.2: (a) The structure of the cornea and its principle layers. (b) Shows epithelium, Bowman membrane and anterior stroma. (c) Illustrations the posterior corneal stroma, Descemet's membrane and endothelium. Reproduced from (Ross et al. 2006).

Epithelium

The corneal epithelium is the superficial layer of cells that is bathed by the tear film; it thus has a smooth, wet optical refractive surface (Lens et al. 2008; Torricelli et al. 2013b). The epithelium has an extraordinary density of sensory nerve endings per unit area, making the cornea one of the most innervated tissues in the body. This high level or innervation results in a high pain sensitivity (Hirata et al. 2017; Lens et al. 2008) and a rapid response to environmental harm (Holland et al. 2013). The epithelium also facilitates the stabilizing of fluid balance within the cornea and protects against pathogen entry (Smolin et al. 1994). Perhaps in keeping with this requirement, the epithelium has a short life span; it is self-renewed and takes five to seven days to complete turnover under normal conditions (McLaughlin et al. 2008). However, in response to injury, the cells are stimulated to undergo a much more rapid regeneration and healing may occur within a day (Lens et al. 2008).

Human epithelium is a non-keratinized stratified squamous epithelium, with a thickness of 50 μm which represents 10% of total corneal thickness. It has five to seven layers of cells, consisting of three to four superficial squamous cell layers, one to three layers of middle or wing cell and monolayer of deep or columnar basal cells. The junctions of these layers are slightly different and characteristic of each layer. The outer squamous layers have tight junctions, with gap junctions in the middle and deep layers (Figure 1.3a). Desmosomes and hemidesmosomes are present basal cell membrane along all of these cell borders (Holland et al. 2013; Smolin et al. 2005) (Figure 1.3a).

The superficial squamous layers are flat, polygonal cells and are about 40 to 60 μm in diameter. The membranes of these cells have surface microvilli which form microplicae. Electron microscopy studies have shown that this superficial squamous layer has two cell types: dark and light cells depending on the amount and pattern of microplicae. The dark cells are larger, and the microvilli are denser (Doughty 2016). These dark cells are older, hyper-mature and are ready to desquamate. On the other hand, the younger cells with lower density of microvilli are the light cells (Smolin et al. 2005). The microplicae

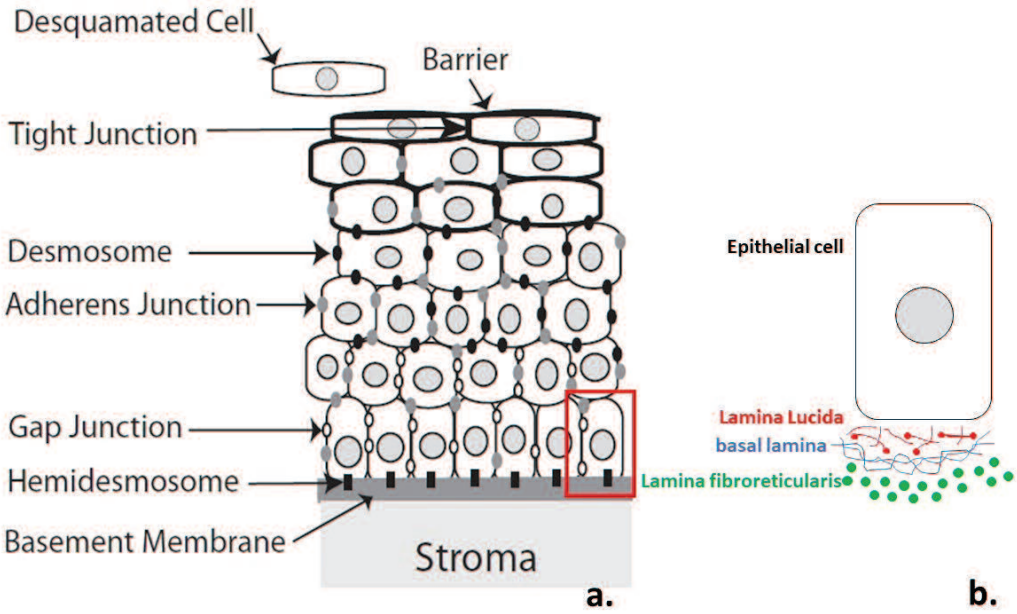

Figure 1.3: (a) Corneal epithelium has tight junctions in the outer squamous layers, with gap junctions in the middle and deep layers. Desmosomes are present along all of these cell borders. Reproduced from (Swamynathan et al. 2011) with permission from the copyright holder, the Association for Research in Vision and Ophthalmology (License No: 4286520001719). (b) The three layers of basement membrane are only visible under electron microscopic examination. These layers are the lamina lucida, lamina densa also known as basal lamina and lamina reticularis. adapted from: $http://www.histology.leeds.ac.uk/tissue_types/connective/con_basal_lam.php$ [accessed 29 November 2017].

increase surface area by folding, which increases oxygen and nutrition taken from the tear film (Holland et al. 2013) and increases adherence of the mucin layer of the tear film to gylcocalyx leading to tear film stability. This filamentous gylcocalyx found on the top of the microplicae is formed of glycolipid and glycoprotein (Holland et al. 2013; Smolin et al. 2005).

Middle or wing cell layers are also called suprabasal epithelial cells, and are transitional cells between basal and superficial that occasionally undergo cell division. These cells migrate superficially to terminally differentiate into superficial squamous epithelial cells (Holland et al. 2013).

The deep or basal cell layer consists of single columnar cells attached to the epithelial basement membrane (Holland et al. 2013), which is adjacent to Bowman's layer. The basement membrane is observable under light microscopy but its three layers are only

visible by electron microscopy (Torricelli et al. 2013a). These layers are the lamina lucida (electron-lucent), lamina densa also known as basal lamina (electron-dense), and lamina fibroreticularis (electron-lucent) (Torricelli et al. 2013a) (Figure 1.3b). In the human cornea, new epithelial basal cells migrate from limbal stem cells into the corneal epithelium (Chang et al. 2008). The basal cells also have mitotic activity. As the proliferation begins, the movement of daughter cells starts in this layer, continues anteriorly as the cells change shape to form wing cells; as they move further forward to corneal surface, the cells turn into corneal superficial cells. The oldest epithelial cells disintegrate and dead cells are continually being shed into the tear film in a process known as desquamation (Li et al. 2017; Smolin et al. 2005).

Bowman's layer

Bowman's layer is a 15 μm thick, acellular layer of connective tissue that lies under the epithelium. Initially, it was named 'Bowman's membrane' but on the basis that lamellae insert into it from the anterior stroma and no clear interface exists between the two regions, it is now more commonly referred to as 'Bowman's layer' or the 'anterior limiting lamina' (Mathew et al. 2008). The layer comprises a random array of collagen fibrils and laminar fibres (Reinhard et al. 2010) consisting of collagen types I, III, V, VII, XII and XVI (Torricelli et al. 2013b), which are smaller in diameter than stromal collagen fibrils (Komai et al. 1991). Although its role is still undefined, it is thought that it protects the stroma against micro-organisms, supports the epithelium and anchors stromal collagen lamellae to help maintain corneal shape (Lens et al. 2008). It has also been suggested that the layer may act as a corneal ligament to maintain corneal structure, however, the low number of complications following removal of the layer post-excimer laser photorefractive keratecotomy does not support this theory (Wilson et al. 2000).

Stroma

The stroma is the core layer of the cornea and offers the majority of the structural framework of the tissue. It is roughly 500 μm thick (DelMonte et al. 2011) and comprises about 90% of the corneal tissue (Meek et al. 2001). The stroma contains about 78% water and type I and type V collagen fibrils embedded in a proteoglycan-rich matrix. The anatomic and biochemical properties of the stroma play an essential role in many characteristics of the cornea, including its physical strength, stability of shape, and transparency. The collagen within the stroma is contained within 200 - 250 transparent lamellae.

The lamellae in the centre of the human cornea lie in all directions within the plane of the tissue but exhibit a predominant alignment along the superior–inferior and medial–lateral meridians (Boote et al. 2004). The lamellae are narrower and more interlaced in the anterior one-third of the stroma than those in the posterior two-thirds of the stroma (Boote et al. 2006; Li et al. 2014). This tighter lamellar organization increases the strength of the anterior stroma and helps to sustain the corneal curvature (Bron 2001). In addition to water, collagen and proteoglycans, the stroma also contains other components such as glycoproteins, soluble proteins, lipid droplets, salts, keratocytes, lymphocytes, macrophages and polymorphounclear leukocytes; however the latter three cell types only occur in cases of inflammation (Krachmer et al. 2011).

The corneal stroma consists of a flexible collagen network, organized as fibrils within lamellae and associated with proteoglycans. Proteoglycans are produced by stromal keratocytes. Proteoglycans are macromolecules consisting of a protein core covalently bound to glycosaminoglycan side chains (Figure 1.4) (Akhtar et al. 2008a; Cheng et al. 2015). Out of the three glycosaminoglycan types in the stroma, keratan sulphate is the most abundant constituting with about 65% of the total glycosaminoglycan content in cornea. The remaining glycosaminoglycans are dermatan sulphate (or chondroitin sulphate) and a minor amount of heparan sulphate, of which the latter is synthesized mainly by epithelial cells (Michelacci 2003). The core proteins of the proteoglycans are members of the family of small leucine-rich proteoglycans (SLRPs), which comprise a common central domain

containing about 10 leucine-rich repeats (Kao et al. 2003). Initially in the embryonic stroma, they collect as low-sulphate glycoproteins, afterward in typical adult cornea, glycosaminoglycans bind to form proteoglycans (Krachmer et al. 2011).

The SLRPs in the extracellular matrix of corneal stroma are: keratocan, lumican, mimecan (also called osteoglycin) and decorin, each characterised by a different protein core. The first three are keratan sulphate-containing proteoglycans, and the last is a dermatan sulphate-containing proteoglycan. Proteoglycans are involved in regulating collagen fibril diameter, in the control of interfibrillar spacing and in the lamellar adhesion properties of corneal collagens, which make proteoglycans play important role in regulating both hydration and corneal structure properties, and consequently corneal transparency (DelMonte et al. 2011; Lewis et al. 2010; Michelacci 2003; Ruberti et al. 2011).

Figure 1.4: (a) Proteoglycans are macromolecules consist of a protein core with covalent bond to glycosaminoglycan side chains. (b) Proteoglycans from matrix around collagen fibrils.

The main cellular components of the corneal stroma are keratocytes, which are quiescent fibroblasts that are scattered between the lamellae. Keratocytes are flat stromal cells that have a spindle-shape with long extensions (Figure 1.2). Corneal connective tissue turnover is very slow (years) and keratocytes are normally quiescent, but become activated if the cornea is injured (West-Mays et al. 2006). Keratocytes are flat in order to minimise the path of light through them, and are also thought to produce crystallins which serve to minimise light scatter and help preserve corneal transparency (Gardner et al. 2015; Jester et al. 1999). Keratocytes turn over occurs every two to three years (Krachmer et al. 2011). Keratocytes are highest in density in the anterior stroma, lowest in the central cornea and have an intermediate density in the posterior stroma (Berlau et al. 2002). Keratocytes

are involved in synthesizing collagen molecules and glycosaminoglycans and producing matrix metalloproteases (MMPs) to stabilize stroma (DelMonte et al. 2011).

Collagen is the main protein component in connective tissues and constitutes about 70% of the total dry weight of the cornea (Meek et al. 2001).The structural strength of stromal connective tissues is provided by collagen, which exists as fibrils held together by intermolecular covalent bonds (Meek et al. 2001). The fibrils are parallel to one another within lamellae and are packed with a high degree of lateral order. This highly ordered, lattice-like arrangement of collagen fibrils is essential for corneal clarity (Boote et al. 2013; Jester et al. 2001).

At least twenty-nine different types of collagen have been identified in human body (Schegg et al. 2009), roughly fourteen of these collagens are found in the eye. Collagens have been classified into several groups: Fibril-forming collagens (e.g. types I, II, III, V, XI collagen), fibril-associated collagens with interrupted triple helices, known as FACIT collagens (e.g. types IX, XII, XIV, XVI, XIX collagen) and nonfibrillar collagens (e.g. types XIII, XVII and XXV) (Koch et al. 2001; Sandberg-Lall et al. 2000; Snellman et al. 2000). These collagens contain triplet helix structures (Figure 1.5). The triple helices are made of three polypeptide, so-called alpha-chains, which are wrapped around a common axis into a right-handed superhelix, therefore, the final domains is a “rope-like rod” (Michelacci 2003). The α - chains comprise the repetitious amino acid sequence glycine – X – Y, where X and Y are frequently proline or hydroxyproline (Motooka et al. 2012).

The collagen in the corneal stroma is mostly type I (75%), type V (10–20%) and type VI (17%), with minor quantity of type III which undergo a rapid increase during wound healing and inflammation (Birk et al. 1990, 1988, 1986; Krachmer et al. 2005; Nakamura 2003). Corneal collagen fibrils have a uniform 25 - 30 nm diameter (Smolin et al. 1994); homogeneity of both the mean diameter and mean distance between fibrils is responsible for cancellation of scattered light rays, permitting light to pass through the cornea (Remington 2011). The occurrence of corneal fibrosis or edema results in

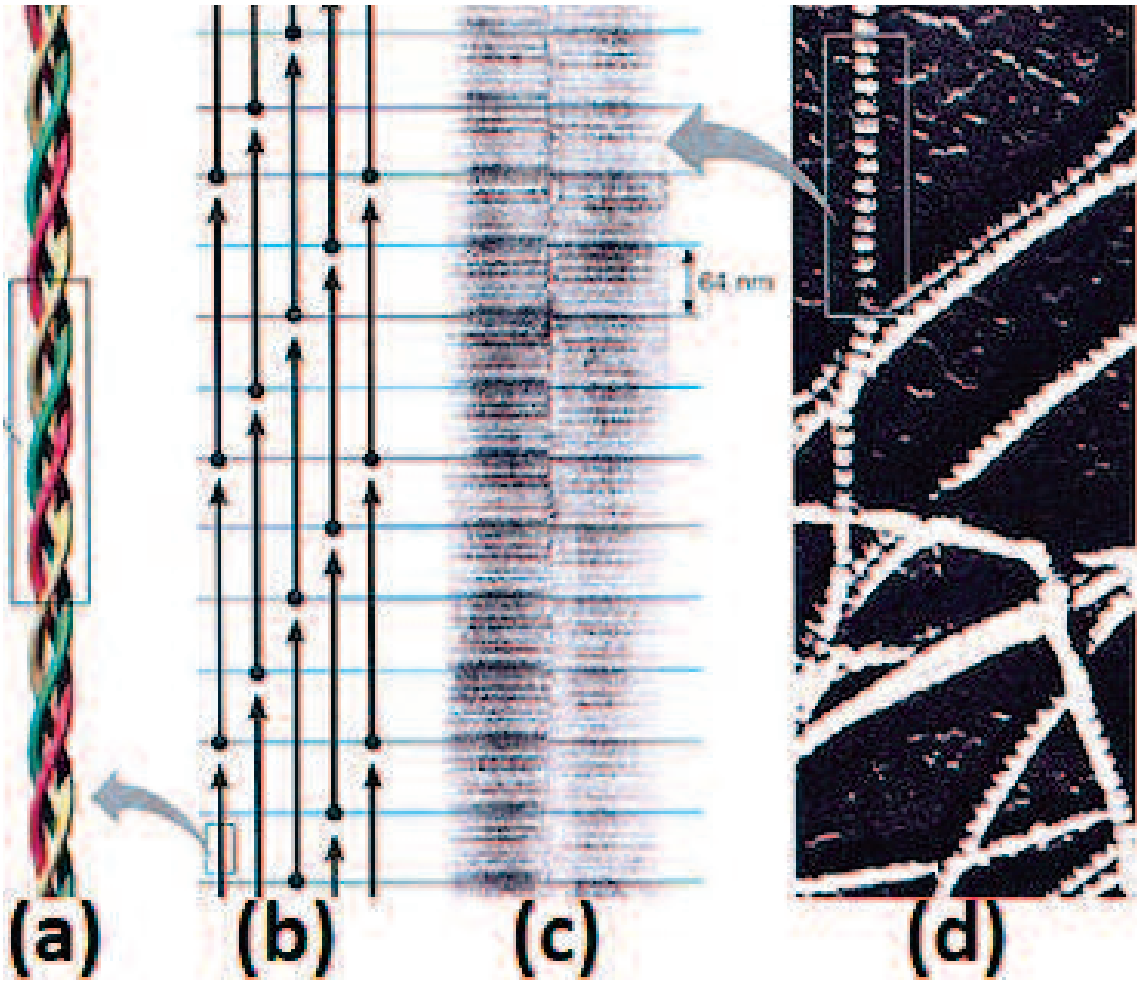

Figure 1.5: Collagen structure. (a) Collagen twisted together into triplet helix. (b) The staggered positioning of adjacent collagen molecules results in alternating gap and overlap regions along the fibril (D-period). (c) The gap and overlap regions create visible striations in positive stained collagen. (d) An electron micrograph of collagen fibrils. Reproduced from https://chempolymerproject.wikispaces.com/Collagen-D-apml [accessed 9 November 2017]. Copyright © 2000 Benjamin/cummings, an imprint of addison wesley longman. Inc.

heterogeneity of this diameter or of the distance between collagen fibrils, which then scatters the incident rays randomly and causes corneal opacity (Krachmer et al. 2011).

When collagen fibrils are stained with heavy metals, dark and light bands are visible. These bands are further divided by cross banding which displays an extraordinarily constant length or "D-period". One dark with light band shows a D-period of ≈67 nm in moist rat-tail tendon (Orgel et al. 2000) and ≈65 nm in physiologically hydrated cornea. The length of the D-period varies in different collagenous tissues and under different condition (Meek et al. 1983) (Figure 1.6). This periodic banding pattern of stained collagen fibrils

detected in the electron microscope can be correlated with the charge distribution realised from the amino acid sequence (Meek et al. 1979). Hodge and Petruska (1963) were the first to find the ordered arrangement of individual collagen molecules along fibrils. The arrangement of individual collagen molecules was organised on the same orientation and packed together side-by-side based on a staggered arrangement of individual collagen monomers (Chapman et al. 1990). Adjacent collagen molecules are offset by approximately a quarter length of a collagen molecule, this is called "axial stagger" arrangement (Goodson 2013). Five different possibility of axial offset positions occurred across the fibril as demonstrated in Figure 1.6a. This produces a regular, distinctive banding pattern as seen on staining intensity. Negative staining depends on molecular density, the dark band where the heavy metal stain has infiltrated regions of low packing density of collagen in the "gap" regions and light where the stain is excluded by higher packing density in the "overlap" regions (Meek et al. 1979). Similar banding with the same regularity and periodicity can also be observed with "positive staining" (Meek et al. 1979) (Figure 1.6), however, the principle of staining is more complex. With negative staining, regions of high stain uptake exist where there is lower molecular density, i.e. it is based on physical accessibility to the stain, whereas positive staining has an electrostatic basis (Tzaphlidou et al. 1982). Under the electron microscope, uranyl acetate (UA) can be used for positive staining to visualise the regions along the fibril containing comparatively high concentrations of acidic amino acids (aspartate and glutamate) due to binding of the positively charged uranyl ion (Tzaphlidou et al. 1982). Because the uranyl ion is small, it tends to be able to move further into the fibril. Therefore, staining by uranyl ions alone tends to result in better definition of the banding pattern (Meek et al. 1983).

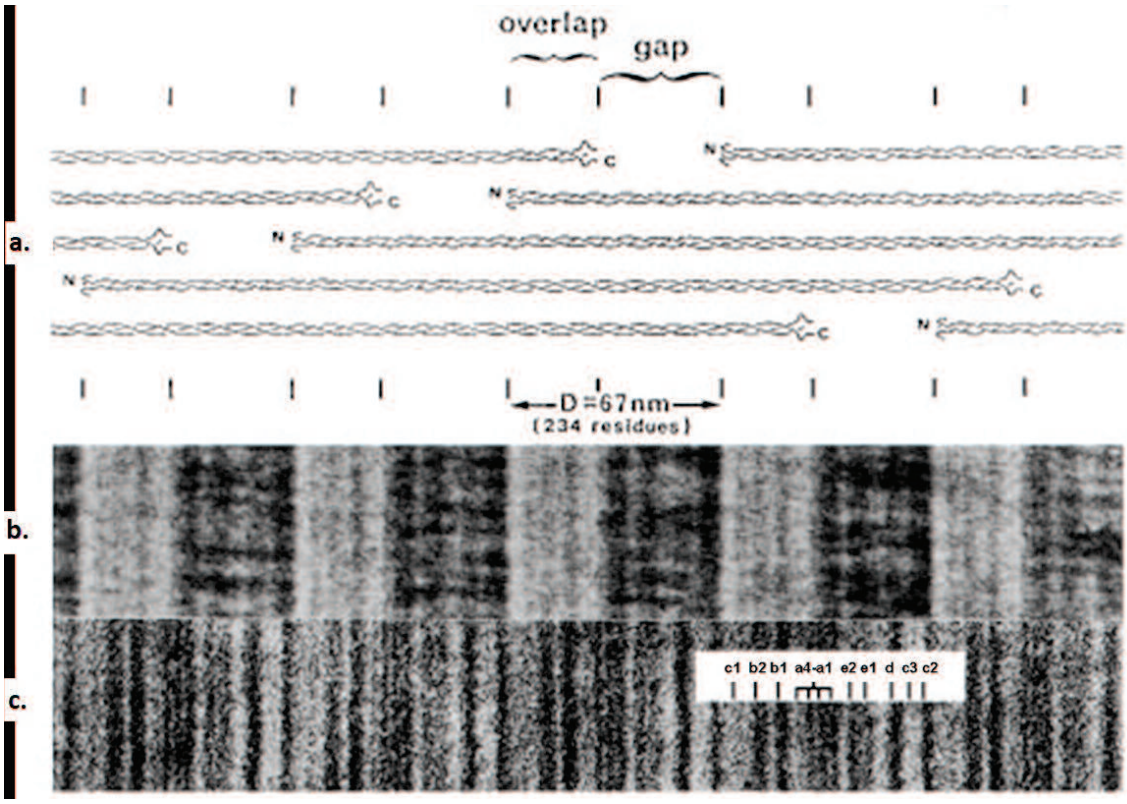

Figure 1.6: (a) A diagrammatic illustration of the axial structure of D-periodic collagen fibrils. The gap (dark) and overlap (light) areas cover a distance (D-period) of roughly 67nm in calfskin collagen. (b) Transmission electron micrograph of a negatively and (c) positively stained calf skin collagen fibril. Negative staining depends on molecular density, with the dark bands marking regions where the heavy metal stain has infiltrated areas of less densely packed collagen, and the "gap" regions occurring where the stain has been excluded by a higher packing density in the "overlap" regions. Similar banding with the same regularity and periodicity can also be observed with "positive staining". There are 12 common positively-stained bands, which is shown in the white box (from left to right) c1, b2, b1, a4, a3, a2, a1, e2, e1, d, c3, c2. Taken from (Chapman et al. 1990) and reproduced with permission from the copyright holder, Elsevier (License No: 4241941117833).

Pre-Descemet's layer (Dua's layer)

Recently, Dua and his colleagues proposed the present of a sixth layer within the cornea in a region immediately above Descemet's membrane, which measures about 6 - 15 μm thick, and contains around 5 - 8 firmly packed mainly type I collagen lamella (Dua et al. 2013, 2014). According to Dua, this layer has few or no keratocytes, a different collagen architecture to the rest of the stroma, and has a substantial impact in relation to corneal surgery such as lamellar keratoplasty using air-injection techniques (Dua et al. 2013, 2014). While there is a general agreement that this layer is biomechanically distinct from the rest

of the cornea (Dua et al. 2016, 2015; Zaki et al. 2015), many other investigations show scepticism that it is a distinct layer, and it is believed that it is just a specialised region of the posterior stroma; this region is now commonly refer to as pre–Descemet's region (Jester et al. 2013; Lewis et al. 2016).

Descemet's membrane

Descemet's membrane is a homogenous layer between the stroma and endothelium. It forms the basement membrane of the corneal endothelium and is composed of two laminated structures, an anterior banded layer and a posterior non-banded layer (Reinhard et al. 2010). The thickness of the anterior banded layer does not change, is roughly 3 - 4 μm at birth while the posterior non-banded layer grows from 3 μm at birth to 20 - 30 μm postnatal life (DelMonte et al. 2011; Reinhard et al. 2010; Smolin et al. 2005). Descemet's membrane contains types IV and VIII collagen, laminin entactin, perlecan and fibronectin. Descemet's membrane structure is a hexagonal array of collagen bundles organized parallel to the surface of the membrane with intervals of 110 μm (Reinhard et al. 2010). Descemet's membrane helps to preserve corneal integral structure and maintains fluids within stroma and aqueous humour which conserves the intraocular pressure (Zavala et al. 2013).

Endothelium

The endothelial layer of the cornea is a neural crest-derived monolayer of honeycomb-like mosaic cells between 455,000 and 338,000 cells over an area of about 130 mm^2 that serves as a major pump to corneal deturgescence which thereby maintains corneal transparency. At birth there are approximately 400,000 cells with a uniform thickness of about 10 μm, with cell density ranging from 3,500 to 4,000 cells per mm^2 (DelMonte et al. 2011; McMonnies 2014; Smolin et al. 2005). In normal corneas, there is an annual reduction of central endothelial cell density at an average rate of 0.6% (Bourne et al. 1997). Between endothelial cells there are gap and tight junctions (Bazzoni et al. 2004; Dejana et al. 1995).

Over time, the endothelial cells flatten and extensively adhere to each other.

During adulthood endothelial cells rarely undergo mitosis, therefore the cell density decreases with age; fortunately, corneas may maintain their clarity with less than 1,000 cells per mm^2 (John 2010). Loss of endothelial cells is compensated by a flattening and enlargement of the remaining cells to maintain a continuous monolayer (Reinhard et al. 2010). The change in the size and shape of the endothelial cells as a result of this flattening and enlargement, reduces the ability of the endothelium to regulate corneal hydration. This emphasises the role of the endothelial layer as an ATP-dependent pump to transport fluid and ions from the stroma to the aqueous humor and explains the mitocodria richness in endothelial cells (Reinhard et al. 2010).

1.3 Corneal Diseases: Keratoconus

In 1854, Nottingham first described keratoconus in detail. Keratoconus derives from the Greek words Kerato (cornea) and Konos (cone). Keratoconus is a bilateral corneal disease often asymmetrical which causes corneal stroma thinning leading to deformation of the normal corneal architecture which in turn results in corneal protrusion (Wang et al. 2010) (Figure 1.7). Keratoconus has been traditionally classified as a non-inflammatory condition, hence there are usually no obvious sign of inflammation such as heat, redness, swelling, and pain associated with the condition (McMonnies 2015). Recent research has discovered several inflammatory processes that have been found in the tears of keratoconus patients along with some inflammation relevant differences in the keratoconus cornea (Galvis et al. 2015; Popescu et al. 2014). The location of keratoconus occurs in the central two-thirds of the cornea, typically the cone apex is concentrated just beneath the visual axis (Krachmer et al. 2011). Irregular astigmatism and high myopia occurs due to corneal protrusion, affecting vision clarity (Wojcik et al. 2013).

The onset of keratoconus is typically early adolescence, because of the progressive changes of normal cornea curvature with age. At birth, the normal cornea tends to

be spherical, but the cornea develops with-the-rule astigmatism during childhood and adolescence, then in middle-aged adults the cornea becomes more spherical, and with aging, the elderly cornea progresses to against-the-rule astigmatism (Wang et al. 2010). Keratoconus initiates in youth and progress for three or four decades in adulthood before cessation.

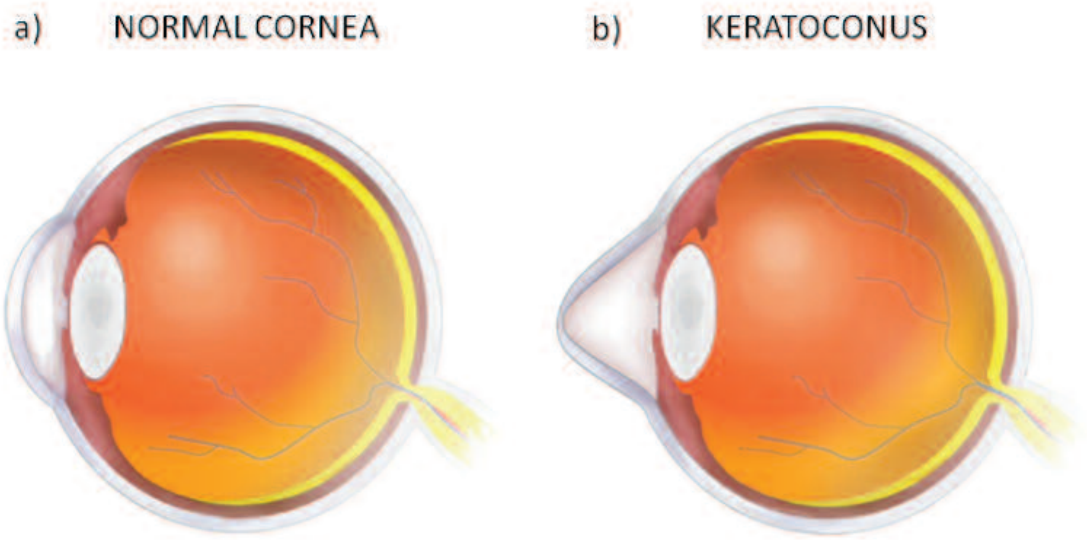

Figure 1.7: Schematic representation of a normal cornea (a) and a keratoconic cornea (b). Image reproduced from (Wojcik et al. 2013).

There are three types of cone morphology: round, oval and keratoglobus shaped cone (Davidson et al. 2014; Perry et al. 1980). The round or "nipple-shaped" cone is the most common cone, this cone usually lies in the infero-nasal quadrant closer to cornea centre and has a diameter of about $\leq$ 5 mm. The oval or sagging cone is usually larger, has a diameter $>$ 5 mm, and locates in the infero-tempral area, paracentral towards the corneal peripheral (Ertan et al. 2009). The keratoglobus cone is generalized corneal thinning, and 75% of the cornea is cone (Davidson et al. 2014).

Disease progression is the main method that ophthalmologists and optometrists use to describe the severity of keratoconus. Table 1.1 describes the classification of keratoconus based on disease severity.

Table 1.1: Clinical classification of keratoconus in stages by (Krumeich et al. 2009).

Stage	**Characteristics**
Stage 1	• Eccentric steepening Induced myopia and/or astigmatism of ≤ 5.0 D • K-reading ≤ 48.00 D • Vogt's lines, typical topography
Stage 2	• Induced myopia and/or astigmatism > 5.0 to ≤ 8.00 D • K-reading ≤ 53.00 D • Pachymetry ≥ 400μm
Stage 3	• Induced myopia and/or astigmatism > 8.0 to ≤ 10.00 D • K-reading > 53.00 D • Pachymetry 200 to 400 μm
Stage 4	• Refraction not measurable • K-reading > 55.00 D • Pachymetry ≤ 200μm • Central scars
Stage is determined if one of the characteristics applies. Corneal thickness is the thinnest measured spot of the cornea.	

1.3.1 Histopathology

The classic histopathological findings in keratoconus are corneal stromal thinning, Bowman's layer rupture and iron deposits in the basal layer of the epithelium (Rahman et al. 2006). Depending on the severity of the disease, keratoconus has consequences in all corneal layers.

Some have reported thinning of the central epithelium of the keratoconic cornea in the presence of breaks in Bowman's membrane (Barbara et al. 2011; Zhou et al. 2014), while others showed central epithelium thickening in keratoconus (Sherwin et al. 2004; Wang et al. 2008). This variation may indicate the variable presentation of keratoconus.

Early degeneration of basal epithelial cells can be seen in the earliest appearances of keratoconus (Wang et al. 2010). Moderate keratoconus usually does not demonstrate changes in either the superficial or wing cells. However, in severe case, keratoconus flattens the superficial epithelial cells and extraordinarily large wing cells with irregular spaced nuclei are observed (Efron et al. 2008). In advanced cases of keratoconus, the basal cell layer diminishes and may even disappear, and noticeable iron deposits are seen within and between epithelial cells (Ucakhan et al. 2006).

Bowman's layer often shows breaks filled by epithelial down-growth or collagen eruptions of the stroma, periodic acid Schiff positive nodules and Z-shaped interruptions caused by the separation of stromal collagen bundles and scar reticulation (Sherwin et al. 2004).

The stromal thinning observed in keratoconus corneas may be related to changes in enzyme levels that cause increases in proteolytic enzymes, decreased concentration of protease inhibitors, which weakens and thins the cornea (Mackiewicz et al. 2006; Sawaguchi et al. 1990, 1994). From confocal microscopy, keratoconus eyes show haziness, hyperreflectivity in stroma, and reduction in keratocytes density (Ku et al. 2008). Keratoconus eyes appear to have an increase in keratocyte apoptosis and change in keratocyte morphology especially in the anterior stroma (Alio 2016; Kim et al. 1999). Transmission electron microscope studies showed that the number of stromal collagen lamellae in the keratoconus cornea is reduced compared to normal eyes, but there was no change in collagen lamellae thickness (Takahashi et al. 1990). Examination of the collagen distribution by x-ray studies found that the orientation of collagen fibrils within the lamellae is altered in the keratoconus cornea, which may affect the strength of cornea and provided evidence of lamella redistribution (Meek et al. 2005; Takahashi et al. 1990). However, there was no distinct difference in the intrafibrillar spacing between collagen, thus, stromal thinning is not a result of closer packing of fibrils in keratoconus (Fullwood et al. 1992). Moreover, x-ray diffraction studies have revealed that alteration in distribution of proteoglycan molecules in the cornea of the keratoconus eye may be associated with some loss of strength of the stroma in keratoconus (Akhtar et al. 2008b; Fullwood et al. 1992).

In severe keratoconus cases, Descemet's membrane breaks and aqueous humour penetrates into the stroma, causing corneal edema, this state known as acute hydrops (Wang et al. 2010). Acute hydrops is found in approximately only 3% of keratoconus corneas (Al Suhaibani et al. 2007). Generally, the endothelium in keratoconic eyes remains intact, rarely, endothelium cell elongation may occur (Weed et al. 2007a).

1.3.2 Signs and Symptoms

The earliest signs and symptoms of keratoconus are typically blurred vision and frequent changes in vision (Lim et al. 2002). This varies from moderate astigmatism to severe vision distortion (Rabinowitz 1998). Although keratoconus is considered a bilateral condition, it is usually asymmetric (Burns et al. 2004). One eye can diagnose with a critical sign of the disease while the other eye detected with a subclinical keratoconus. The reason for this asymmetry is not well understood. In some patients there is a complaint of glare, ghost image, tearing, itching, burning, redness, foreign-body sensation, photophobia, frequent rubbing of the eye and rarely monocular diplopia (Rapuano 2012; Weed et al. 2007b). Frequently, unexplained reduction of visual acuity, change of refractive error or inadequate contact lens fitting leads to topography testing, which exposes the diagnosis. Also a split or scissors motion on retinoscopy indicates keratoconus or high amounts of irregular astigmatism (Rosenfield et al. 2009). On ophthalmoscopy, keratoconus may be marked by the presence of a circular dark red-brown shadow encircled by the usual red fundus reflex, called the oil drop sign or the Charleauc "oil droplet" sign (Abraham et al. 2013). Distorted mires also manifests keratoconus on keratometry (Saxena 2011).

Several keratoconus signs can be detected by slit-lamp biomicroscopy. Some of these signs are: stromal thinning, endothelium reflex, central or eccentric cone, apical stromal scarring, Fleischer's ring, Vogt's striae, Munson's sign, Rizzuti's sign, Axenfeld sign and acute hydrops (Saxena 2011).

Stromal thinning expands gradually from the base of the cone to apex (Sturbaum et al. 1993). The cause of endothelium reflex is increase of corneal concavity (Abraham

et al. 2013). In moderate keratoconus, anterior stromal scars may occur autonomously or secondary to hard contact lens used (Wang et al. 2010). The Fleischer's ring is the most frequently noted slit-lamp sign of keratoconus and is observed using a cobalt blue filter as a line or circle (Weed et al. 2007b). It occurs as a result of epithelial deposition of iron oxide haemosiderin (a yellow-brown to olive-green pigment) in an incomplete annulus surrounding the base of the cone as a result of corneal stretching in the advanced stage of keratoconus and because of an irregular tear film of the cornea in this area (Wagner et al. 2007) (Figure 1.8). Fleischer's ring may be seen prior to evidence of corneal thinning and conical shape change. The second common sign is Vogt's striae, which are fine vertical lines in the Descemet's layer and posterior stroma that temporarily disappear when a gentle limbal pressure is applied (Sundaram et al. 2009) (Figure 1.9).

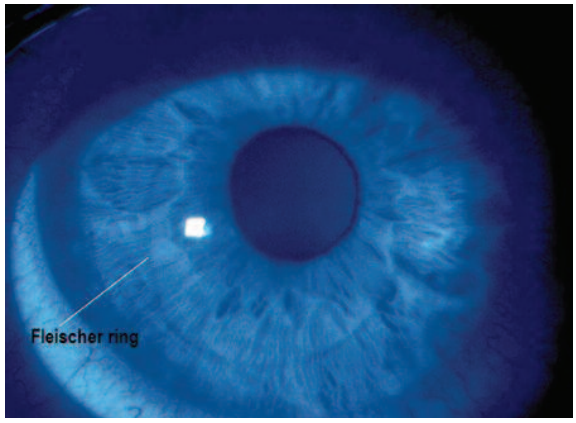

Figure 1.8: Fleischer's ring. Reproduced from *http : //lessons4medicos.blogspot.co.uk/2009/04/corneal − pigmentation − decoded.html* [accessed 9 November 2017].

In advanced disease, the Munson's sign and Rizzuti's sign are not uncommon in keratoconus patients. Munson's sign is detected when the downgaze of a keratonic eye shows a V-shaped pattern on the lower eyelid as it passes over the protrusion corneal cone (Grosvenor 2007) (see Figure 1.10). Rizzuti's sign also called Benedict sign is a triangular conical reflection of focused beam on nasal limbus, formed when lateral illumination is shone from temporal side of the cornea (Ambrósio Jr et al. 2006) (see Figure 1.11). Furthermore, Axenfeld sign is loss of sensitivity on the cone apex (Abraham et al. 2013).

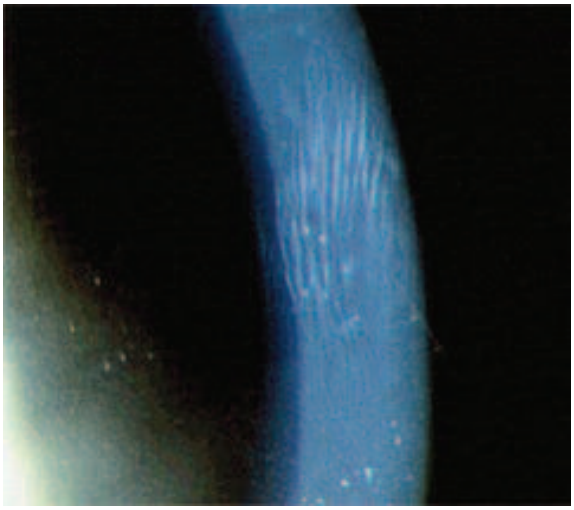

Figure 1.9: Vogt's striae. Reproduced from *http* : *//www.gpli.info/sym* – 2004 – 03/ [accessed 9 November 2017].

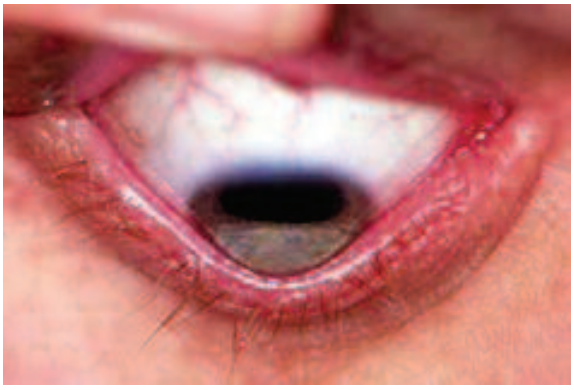

Figure 1.10: Munson's sign. Reproduced from *http* : *//www.pinterest.com /waterlooeyecent/keratoconus/* [accessed 9 November 2017].

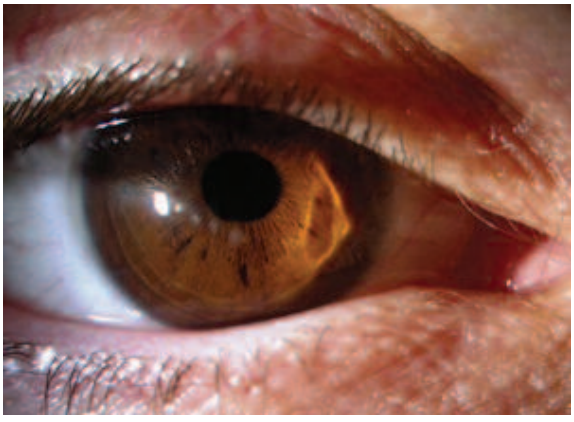

Figure 1.11: Rizzuti's sign. Reproduced from *http* : *//www.cltoday.com /issues/CLToday*_020914.*htm* [accessed 9 November 2017].

Severe keratoconus may present with accompanying corneal hydrops (Figure 1.12). The onset of corneal hydrops is associated with acute pain, sudden blurred vision and photophobia. The oedema usually resolves within 2 to 3 months as the endothelial cells stretch and enlarge to block the breaks in the endothelium (Maharana et al. 2013).

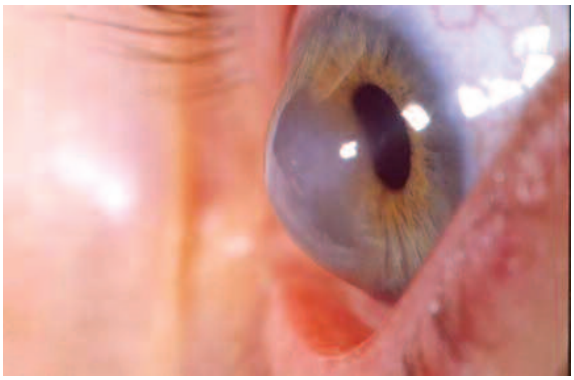

Figure 1.12: Corneal acute hydrops. Reproduced from *http : //www.keratoconus – group.org.uk/expert_contributions/kp/hydrops_and_kc.html* [accessed 9 November 2017].

1.3.3 Epidemiology

The estimation of keratoconus prevalence fluctuates extensively depending on the geographic location, and variation in diagnostic criteria. The prevalence estimation falls between 0.4 to 230 per 100,000 cases (Bykhovskaya et al. 2016; Gokhale 2013; Gordon-Shaag et al. 2015; Krachmer et al. 2011). Keratoconus is known to affect all races (Wagner et al. 2007; Weed et al. 2008) but a UK-conducted study showed that the prevalence in Asians was roughly seven times higher than Caucasians and this was attributed to the higher incidence of consanguineous relations, particularly first-cousin marriages, in the assessed area (Georgiou et al. 2004). In addition, ecological influences may attribute to the wide variation in prevalence. Geographical locations with hot climates and sunshine like Middle East and India (Assiri et al. 2005; Jonas et al. 2009), have higher prevalence than countries with cold weather, such as, Finland, Russia and Denmark (Gorskova et al. 1998; Ihalainen 1986; Nielsen et al. 2007).

The relationship between gender and the incidence of keratoconus is still debated. Some studies have reported no difference in keratoconus prevalence between males and

females (Li et al. 2004) whilst other studies have found either a higher incidence in females (Jonas et al. 2009; Krachmer et al. 1984) or males (Pearson et al. 2000; Wagner et al. 2007).

Keratoconus is commonly considered a bilateral disease. However, advances in computer-assisted topography and pachymetry that have enhanced the ability to detect subtle disease have led to a rise number of patients with only early changes in one eye and no evidence of topographical change in the second eye (Lema et al. 2009).

Although numerous ocular and systemic diseases have been documented in conjunction with keratoconus, few are accepted to be associated. Factors that have been identified as being associated with a higher incidence of keratoconus are eye rubbing, atopy, Down's syndrome, and mitral heart prolapse (Balasubramanian et al. 2013; Barbara et al. 2011; Grünauer-Kloevekorn et al. 2006). However, most often keratoconus incidence is found to be sporadic and not in combination with other diseases.

1.3.4 Aetiology and pathogenesis

Although the accurate aetiology and pathogenesis of keratoconus is still enigma, it has been associated with genetic, mechanical, biochemical and environmental factors.

Genetic

Genetic factors are believed to play a role in the development of keratoconus with between 6% and 23% of keratoconus patients having a family history of keratoconus (Karimian et al. 2008; Owens et al. 2003). Autosomal recessive and autosomal dominant patterns of inheritance seems likely to occur in most keratoconus cases, which suggest a link of genetic factors in keratoconus (Kenney et al. 2003; Mita et al. 2014; Rabinowitz et al. 1992). Studies carried out with corneal topography techniques have revealed that 50% of keratoconus patients have one or more relatives with the condition (Gonzalez et al. 1992). Although various genetic studies have been conducted in an attempt to identity

genetic regions (Loci) for keratoconus (Burdon et al. 2013), it is still not clear exactly which candidate genes are associated with keratoconus. Several studies have indicated a link between keratoconus and the visual system homeobox 1 (VSX1) gene, which plays a significant role in ocular development, in particular cornea development (Bisceglia et al. 2005; Heon et al. 2002; Saee-Rad et al. 2011; Tanwar et al. 2010). In contrast, other studies have shown that there is no correlation between VSX1 and keratoconus, representing the involvement of other genetic factors (Davidson et al. 2014; Stabuc-Silih et al. 2010). Similarly, some studies reported that the superoxide dismutase 1 gene (SOD1) is connected to keratoconus (Liskova et al. 2010), which is an antioxidant defender gene, while other publications did not support this relationship (Stabuc-Silih et al. 2010; Wojcik et al. 2013).

Mechanical

Eye rubbing, contact lens wear, oxidative damage and stromal thinning have also been linked to keratoconus development and progression (Wojcik et al. 2013). The incidence of eye rubbing in keratoconus patients ranges from 66% to 73%, and maybe linked with other diseases such as atopic disease, Down's syndrome, and Leber's tapetoretinal degeneration (Balasubramanian et al. 2013; Krachmer et al. 2011). An increase in tear protease activity and inflammatory mediators in tears after eye rubbing may be involved in keratoconus progression (Balasubramanian et al. 2013). In addition, contact lens wear could prompt the progression of the disease in the form of corneal microtrauma. Macsai et al., recognized that keratoconus patients undergoing long-term contact lens wear tend to have central cones with a flatter corneal curvature than patients with no history of contact lens wear (Macsai et al. 1990). A reduction in number of stromal lamellae in keratoconus causes decrease in corneal rigidly compared to normal eyes (Meek et al. 2005; Sherwin et al. 2004). Some studies showed that stromal thinning in keratoconus is contributed to collagen degradation by proteolytic enzymes (Sherwin et al. 2002) or reduced of proteinase inhibitors levels (Ghosh et al. 2013; Mackiewicz et al. 2006), others proposed that there is no loss of collagen, alteration in collagens distributed of within the cornea by slip between

the lamellae (Polack 1976). Oxidative damage has also been associated with keratoconus progression. Keratoconic corneas have decreased levels of two enzymes that play a vital role in reactive oxygen processes aldehyde dehydrogenase Class 3 (Gondhowiardjo et al. 1993) and superoxide dismutase enzymes (Behndig et al. 2001). The increase of oxidative stress causes cytotoxic deposition resulted from accumulate reactive oxygen species, that could cause damage to the corneal tissues and potentially produce keratoconus (Kenney et al. 2003).

Biochemistry

During the last few decades, our understanding of the biochemistry of keratoconus aetiology has dramatically increased. It is important to note that the results of this research are more related to advance keratoconus. It has been shown that keratoconus is associated with destructive enzyme activity within the cornea (Mita et al. 2014). The increased level of proteases and other catabolic enzymes (Fukuchi et al. 1994), or decreased levels of proteinase inhibitors could results in a degradation of extracellular matrix of the stroma (Wojcik et al. 2014; Zhou et al. 1998). Therefore, corneal thinning occurs due to the loss of corneal structural components (Romero-Jimenez et al. 2010). Several biochemical theories for keratoconus development have been found differences keratoconic corneas in collagen types XIII (Määttä et al. 2006a), XV and XVIII (Määttä et al. 2006b) when compared to non-keratoconus corneas, and that might cause the differences in wound healing process that are observed between normal and keratoconic corneas (Cheung et al. 2013; Croxatto et al. 2010). Moreover, the keratocytes in keratoconus eyes have four times greater numbers of interleukin-1 receptors in contrast to normal eyes (Bureau et al. 1993). Interleukin-1 has also been suggested to induce apoptosis or controlled cell death of the stroma keratocytes. Apoptosis has been found in stromal keratocytes of keratoconus corneas, but not in normal corneas (Kim et al. 1999). Corneal epithelium might release interleukin-1 in response to microtrauma occur in the association of keratoconus with eye rubbing, contact lens wear and atopy (Wilson et al. 1996).

Environment

Environmental factors have also been suggested to contribute to keratoconus pathology, such as overexposure to ultraviolet rays from the sun (Assiri et al. 2005), extreme eye rubbing (Balasubramanian et al. 2013; Shneor et al. 2013), poor contact lenses fitting (Macsai et al. 1990), atopy and chronic eye irritation (Sugar et al. 2012). Ultraviolet light has been observed to be associated with keratoconus. Researchers have suggested in corneas with keratoconus there are some defects in their ability to process accumulated reactive oxygen species (Wojcik et al. 2013). In addition, many studies demonstrated regions with a higher load of airborne allergens have a higher prevalence of keratoconus. Several studies showed that asthma and hay fever are evident in 23% to 30% of keratoconus subjects, respectively (Weed et al. 2008). However, this association may be because patients with allergic symptoms rub their eyes more frequently, which may lead to corneal ectasia (Sugar et al. 2012).

1.3.5 Management and Treatment

Treatment opportunities for keratoconus focus on correcting the distorted vision caused by the thinning and protrusion of the cornea.

Spectacles and contact lenses

Initially, many keratoconic patients develop myopia and simple astigmatism which can be corrected with spectacles or soft contact lenses before signs of the disease become evident. These patients attract the attention of the optometrist as the myopia and astigmatism progress, showing steeper than average keratometry or topography readings. As keratoconus progresses to an intermediate stage, the spectacles and soft contact lenses no longer provide functional vision. Toric soft contact lenses may help with correcting the astigmatism to some extent. When the irregularity of the astigmatism increases, rigid gas-permeable (RGP), hard contact lenses may provide a clear vision by creating a new

anterior refractive surface. However, the contact lens must be fitted with an awareness of patient tolerance, and should be tailored to the individual visual requirements.

Many keratoconus patients can be effectively fitted with hard contact lenses using either the three-point touch technique which allows a light apical corneal touch (Szczotka et al. 2001) or with apical clearance fitting technique (McMahon et al. 2006). Other selections of contact lens include standard biocurved hard lenses, custom-back toric lenses, piggyback systems hybrid lenses design of combined hard lens with a soft skits scleral lenses, and mini-scleral lenses (Lim et al. 2002). Contact lens wear does not halt the progression of corneal ectasia and in some cases it is actually associated with the development of keratoconus (Krachmer et al. 2011). An alternative option for managing keratoconus is intrastromal corneal ring implants.

Intrastromal Corneal Ring implants

Intrastromal corneal ring segments are crescent-shaped/semi-circular, made of polymethylmethacrylate and implanted into a deep corneal stromal tunnel created by a femtosecond laser. The technique reduces corneal curvature by flatting the central cornea, reducing astigmatism and centring the cone, ensuring improved visual acuity and better contact lens fitting (Alio et al. 2014). The safety and effectiveness of intrastromal corneal ring implants are reinforced by many clinical studies (Özertürk et al. 2012; Pron et al. 2011; Vega-Estrada et al. 2016).

Keratoplasty

In the last decade, corneal cross-linking (CXL) treatment reduced the need to corneal transplant performed for keratoconus. Although most patients with keratoconus do not progress to necessitating a transplantation, keratoconus remains one of the leading causes of cornea transplant in the developed world (Davidson et al. 2014; Gharaibeh et al. 2012; Rabinowitz 1998). In advanced keratoconus with severe ectasia and central corneal scarring, fitting a contact lens fails to provide clear vision. As a result, about 10 -

20% of keratoconus patients require invasive surgical intervention such as keratoplasty (Rabinowitz 1998). Although penetrating keratoplasty for keratoconus is still vulnerable to endothelial allograft rejection, it is still the first choice for the severe disease (Sarezky et al. 2017). There are a few different types of corneal transplant which differ in the thickness of grafting: full-thickness penetrating keratoplasty, partial-thickness lamellar keratoplasty, epikeratophakia and Bowman's layer transplantation (Dijk et al. 2014). The overall risk of graft rejection was approximately 6.8% (Dijk et al. 2014). The risk of corneal transplant failure coupled with the limited number of donor corneas available for transplantation, has encouraged the development treatments aimed at halting the progression of keratoconus and reducing the number of keratoconus patients undergoing corneal transplant surgery.

Corneal collagen cross-linking with riboflavin and Ultraviolet irradiation

In 1998, Spoerl and his colleagues introduced a new approach for keratoconus treatment. Their experimental evidence has shown that the non-toxic photosensitizer riboflavin and ultraviolet-A (UVA) induce additional covalent bonds in the cornea by photosensitized oxidation, which leads to strengthening of the corneal stroma (Spoerl et al. 1998). The concept was based on a scientific suggestion that the natural cross-linking effect of glucose increases corneal stiffness in diabetic eyes (Andreassen et al. 1988; Williamson et al. 1986). Applying cross-linking to progressive keratoconus or postoperative refractive surgery ectasia, where the collagen structure is disposed to enzymatic degradation and fibrillar slippage, has been shown to adjust the biomechanical properties of the cornea (Abad et al. 2008; Kohlhaas et al. 2006; Sandner et al. 2004; Wollensak et al. 2003a,b). The biomechanical effect in human eyes has been reported to significantly increase corneal rigidity by 328.9% (Wollensak 2006; Wollensak et al. 2003b). Moreover, enzymatic degradation resistance is increased in porcine eyes, after cross-linking (Spoerl et al. 2004), which may also contribute to biomechanical stability (Krachmer et al. 2011). Usually the cross-linking effect is localized in the anterior 300 μm of the stroma (Kohlhaas et al. 2006). The average collagen fibril diameter in the treated cornea is significantly increased by 12.2% in the anterior stroma while it is increased by only 4.6% in the posterior stroma

(Wollensak et al. 2004b), further indicating that the effect is mostly in the anterior stroma.

Cross-linking the cornea using riboflavin and ultraviolet-A light has been greatly improved in recent years through developments and modification to make it suitable for clinical use. In 2003, the Dresden group carried out the first prospectively designed clinical study in 23 eyes with moderate or advanced progressive keratoconus (Wollensak et al. 2003a). It has been proven that the riboflavin/UVA cross-linking procedure prevent further keratoconus progression, improves the corneal shape and in some cases flattens the cone (Kohlhaas et al. 2005). Also, improvement in best spectacle corrected visual acuity (BSCVA) was reported together with the stability of endothelial cell density (Wittig-Silva et al. 2014). Over the past decades, the standard cross-linking (SCXL) procedure, which involves soaking the corneal stroma with riboflavin and then photoactivating it using 370 nm UVA with an irradiance of 3 mW/cm^2 for 30 minutes, has been widely utilized to halt the progress of keratoconus and other ectasia disease. Following the implantation of cross-linking in the Netherlands, a 25% reduction in the number of corneal transplants required for keratoconus has been documented (Godefrooij et al. 2016). The application of cross-linking is not limited to corneal ectasias it has also been used to successfully treat infectious diseases; specifically, infectious keratitis (Tabibian et al. 2015). In 2000, Schnitzler et al, announced the efficacy of SCXL in the stabilization of corneal melting ulcers. Multiple studies have shown the efficacy of using SCXL as a first line treatment for advanced ulcerative infectious keratitis and early-stage bacterial keratitis as it has the ability to render certain bacteria and viruses inactive (Garg et al. 2017; Makdoumi et al. 2016; Richoz et al. 2014).

Mechanism of cross-linking

There are four key components in the process of CXL: photosensitizer (riboflavin), UVA illumination, oxygen and tissue (Kamaev et al. 2012). Exposing cornea soaked with riboflavin to UVA light in an oxygenated environment forms singlet oxygen species which lead to creation of extra CXL bonds (McCall et al. 2010; Zhang et al. 2011).

Kamaev et al. (2012) investigated the photochemical kinetics of SCXL and observed

oxygen consumption with the cornea during the CXL process. They documented that a photochemical type II reaction was found in cornea tissue during the first 10 - 15 sec of the UVA exposure, which is favoured at high oxygen concentration and generates reactive oxygen species; then complete oxygen depletion takes place and photochemical type I reaction occurred, which is favoured at low oxygen concentration and forms singlet molecular oxygen; after 10 minutes, corneal oxygen concentration increased slowly and the photochemical type II reaction recurred (Kamaev et al. 2012) (Figure 1.13).

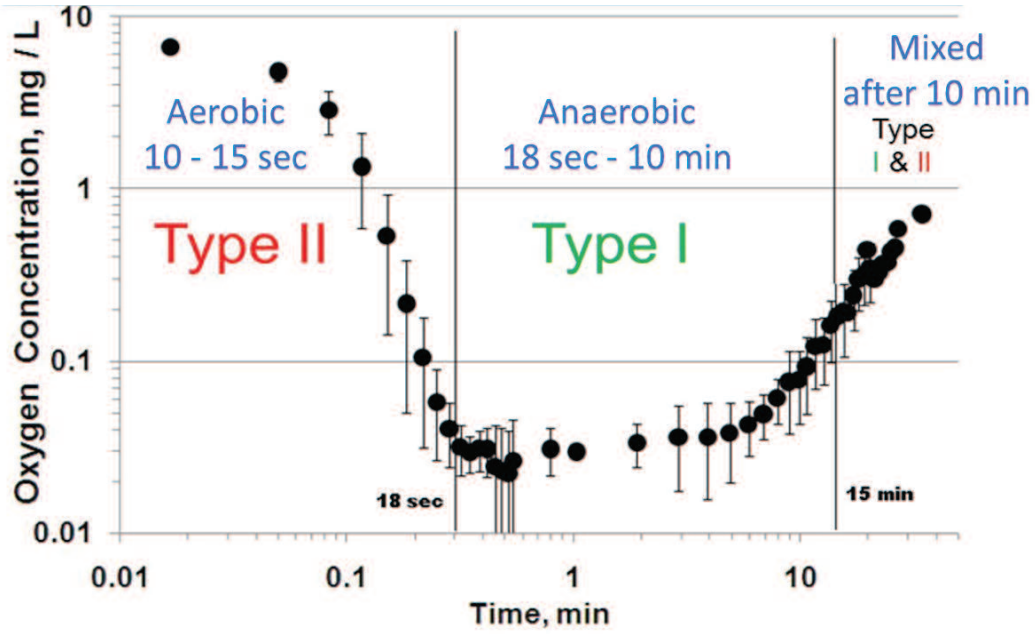

Figure 1.13: The photochemical kinetics mechanism on CXL. photochemical type II reaction was found in cornea tissue during the first 10 - 15 sec of the UVA exposure, which is favoured at high oxygen concentration and generated reactive oxygen species; then complete oxygen depletion occurred and photochemical type I reaction occurred, which is favoured at low oxygen concentration and react with oxygen to form singlet molecular oxygen; after 10 min corneal oxygen concentration has increased gradually and photochemical type II reaction may begin to play a role once again. Image adapted from (Kamaev et al. 2012) with permission from the copyright holder, the Association for Research in Vision and Ophthalmology (License No: 4270240029745).

A study by Zhang et al (2011) into the nature and location of the cross-links formed within the extracellular matrix during riboflavin/UVA cross-linking revealed that the cross-links could occur not just between collagen molecules but also between collagens and proteoglycan core proteins of lumican, mimecan and keratocan and between the proteoglycan core proteins themselves. Although cross-linking may occur within and between proteoglycan core proteins, the covalently attached sulphated glycosaminoglycans (keratan

sulphate and chondroitin sulphate) are not involved in the cross-linking process. Zhang et al. (2011) have shed light on the interaction between collagen and proteoglycan core proteins, showing that the collagen interactions are very different in keratocan and lumican core proteins than in mimecan and decorin.

Moreover, studies using x-ray scattering techniques, enzymatic digestion and stromal swelling behaviour revealed that it is highly unlikely that direct interfibrillar (collagen fibril – collagen fibril) cross-linking occurs and that collagen cross-linking is likely to occur at fibril surfaces only, within and between collagen molecules and within the proteoglycan coating that surrounds the fibrils (Hayes et al. 2013) (Figure 1.14). The probable cross-linking of proteoglycan and collagen molecules shown in Figure 1.14 would explain the increased stiffness of corneas after cross-linking treatment and the increased resistance of stromal tissue to enzymatic digestion.

Morphologically, keratocyte alteration was observed after CXL. Initially, the treatment kills these cells, but the stroma is then repopulated. It has been demonstrated that there is a significant increase in the keratocyte proliferation and moderate apoptotic cells primarily in the anterior part of the cross-linked stroma (Mencucci et al. 2010). Furthermore, it has been well-documented that the collagen fibre diameter increased after cross-linking therapy (Mencucci et al. 2010; Rao 2013). These morphological modifications lead to an increase in biomechanical stability.

Safety

UV irradiation would be expected to damage the endothelial layer and the crystalline lens. However, riboflavin protects the endothelial cell and the crystalline lens by absorbing a high percentage of the irradiation intensity within the stromal layer. Without the riboflavin, the cornea will absorb nearly 30% of the UVA light, and 50% would be transferred to the crystalline lens (Wollensak et al. 2004a). However, with a stromal saturation of 0.1% riboflavin, the UVA light irradiation of 3 mW/cm^2 is significantly decreased by 95% to a non-cytotoxic irradiation of 0.15 mW/cm^2 at the endothelium level, which leaves the crystalline lens intact (Spoerl et al. 2007; Wollensak et al. 2004b). Based on a calcu-

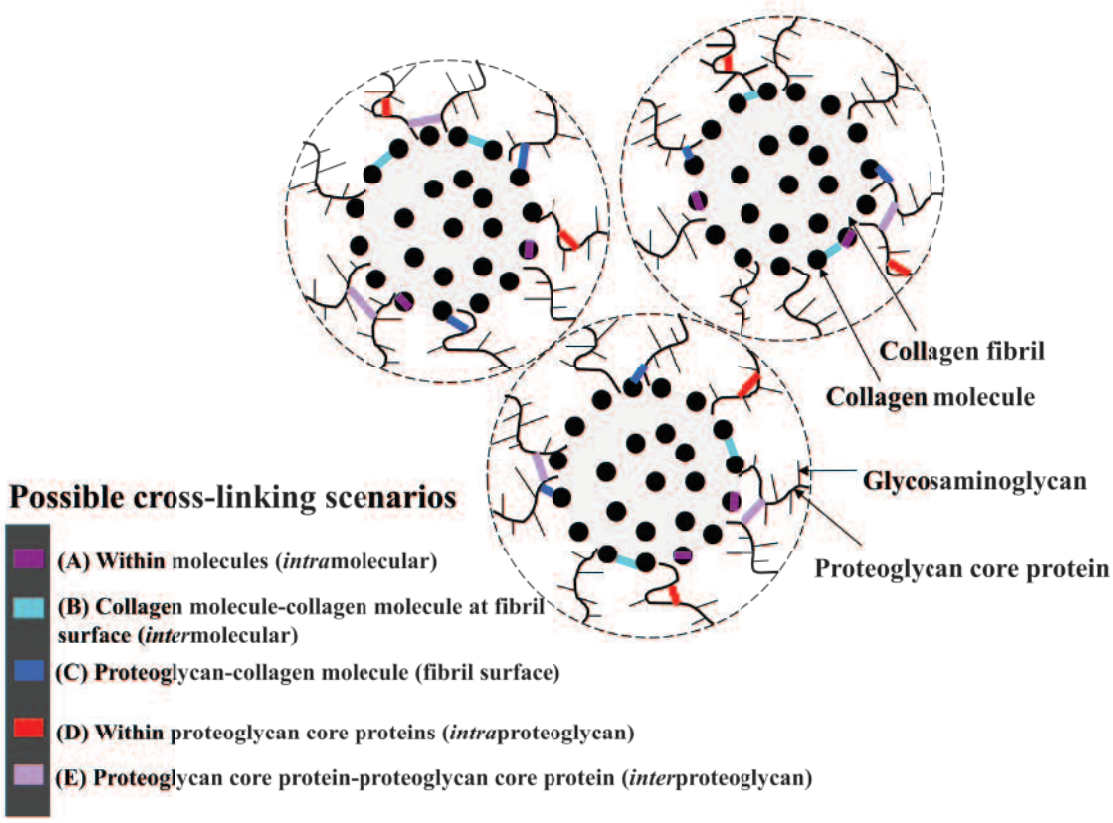

Figure 1.14: A schematic diagram showing the likely locations of riboflavin/UVA induced cross-links. Three collagen fibrils are shown, each with an outer coating (the limit of which is indicated with a dashed line) composed primarily of fibril-attached proteoglycans. The colour key and corresponding coloured lines indicate the possible location(s) of riboflavin/UVA induced cross-links. Image adapted from (Hayes et al. 2013).

lation of endothelial toxicity Spoerl and his colleagues recommended a minimum corneal thickness of 400 μm to ensure safety if the endothelium during CXL (Hafezi et al. 2007; Spoerl et al. 2007; Wollensak et al. 2003c). Therefore, pachymetry should be performed preoperatively to confirm that the corneal thickness is appropriate for the cross-linking procedure.

Although several studies showed a significant small increase in intra-ocular pressure (about 1.45 mmHg) post-CXL treatment, this finding is not considered a safety concern because the IOP seems to be overestimated because of the increased corneal rigidity following treatment (Kymionis et al. 2010; Romppainen et al. 2007).

Inclusion criteria for CXL

CXL requires a minimum corneal thickness of 400 μm after removal of the epithelium,

and an endothelial cell count of more than 3000 cell/mm^2 to minimise the risk of endothelial dysfunction (Wollensak et al. 2003a). However, in thin keratoconus corneas a hypotonic riboflavin solution may be used to increase the pre-operative stromal thickness and permit CXL to be performed (Hafezi et al. 2009).

Other pre-existing conditions would affect the CXL outcomes, such as central corneal haze (Raiskup et al. 2009), infectious eye disease (Pollhammer et al. 2009), Herpes simplex keratitis (Eberwein et al. 2008), severe dry eye (Vinciguerra et al. 2010), and keratometry readings more than 58 D (Koller et al. 2009).

Patients with incisional refractive surgery like radial keratotomy or astigmatic keratotomy are not recommended for treatment because of the possibility of rupture of the incisions (Elbaz et al. 2014; Fuentes-Páez et al. 2012; Mazzotta et al. 2011; Yamamoto et al. 1999). Concomitant autoimmune diseases, collagen vascular disease, pregnant or nursing mothers and patients younger than 4 or over 35 years old are also excluded from the CXL procedure (Hamada et al. 2017; Vinciguerra et al. 2010).

Clinical side effects

To date, multiple clinical trials and observational studies of CXL have been performed which show no remarkable clinical side effects or complications (Caporossi et al. 2010; Raiskup-Wolf et al. 2008; Wittig-Silva et al. 2014; Zotta et al. 2017). After surgery a mild corneal edema is expected with a mild cotton-like hazy appearance within the corneal stroma. This usually settles after four to six weeks without treatment and problems (Rao 2013).

There are consequences by not following the ideal patient selection; focal corneal edema in a small area has been documented in one case only caused by a reduction in endothelial cell count and focal endothelial haziness. This case was found to be below the minimal recommended thickness. Fortunately, this eye returned to normal after one week as a result of compensation of the migration of the surrounding endothelial cells, and there was no further sign of endothelial damage (Wollensak 2010).

Following CXL, most cases develop temporary stromal haze in the first few months depending on the depth of treatment into the stroma as well as the amount of keratocyte apoptosis (Mazzotta et al. 2008). A study evaluating the natural course after CXL demonstrated that haze peaked at 1 month, plateaued between 1 month and 3 months and gradually cleared between 3 and 12 months (Greenstein et al. 2010). Usually this corneal haze does not need treatment but in some cases application of low dose topical steroid eye drops is required (Dhawan et al. 2011). It is possible that the haze formation after CXL is a result of back-scattered and reflected light (Connon et al. 2003), corresponding to the "demarcation line" which Seiler and Hafezi (2006) have proposed to define the depth of cross-linked areas. At the first month, the haze was more distinct in the central anterior stroma (Rehnman et al. 2011). This seems to be associated with immediate loss of keratocytes in the corneal stroma (Dhaliwal et al. 2009; Wollensak et al. 2004b). This is supported by a confocal microscopy study that reported immediate keratocyte apoptosis post-CXL. Activated keratocytes repopulated at 2 months and almost complete repopulation was observed at 6 months (Mazzotta et al. 2007). It is likely that these activated keratocytes are associated with the development of corneal haze post-CXL (Dhawan et al. 2011; Greenstein et al. 2010). Moreover, stromal swelling pressure changes, proteoglycan-collagen interactions and glycosaminoglycan hydration may also contribute to CXL-associated corneal haze (Dohlman et al. 1962; Michelacci 2003; Wollensak et al. 2007).

The most common clinical disadvantages of the cross-linking involving epithelial removal is light sensitivity, risk of infection, discomfort and pain in the first few days until the epithelial layer is completely regenerated. Several case studies have documented that keratitis may occur post-CXL a result of the presence of an epithelial defect (Kymionis et al. 2007; Perez-Santonja et al. 2009; Pollhammer et al. 2009; Sharma et al. 2010). This might present during the postoperative period rather than during the operation because CXL can kill pathogens such as bacteria and fungi on the surface of the cornea (Tabibian et al. 2014). A delay in re-epithelisation was also reported in a few cases, which required corticosteroid medication during the period of epithelisation and bandage soft contact lens wear. The corneal epithelium should recovery be completed within 24 hours and the eye

should be perfectly healthy afterward (Wang et al. 2010).

Also, it has been noted that subepithelial stromal nerve fibres disappear post-operation. Although re-innervation is evident a month later, complete restoration of corneal sensitivity of the anterior subepithelial stroma was seen six months after the procedure (Rao 2013).

Modified protocols

Several methods have been proposed to eliminate some of the limitations of the SCXL protocol, which requires the painful removal of the corneal epithelium, a prolonged treatment time of one hour and is deemed unsuitable for the treatment of very thin corneas. Some of the treatment modifications currently in use are described below:

- ***Trans-epithelial procedures***

  Epithelial debridement in the SCXL procedure may cause postoperative discomfort, potential delay in epithelial healing, infection, and stromal haze. As a result, researchers are investigating modifications to overcome the need for epithelial removal and find a way of getting riboflavin across the intact epithelium and into the corneal stroma to enable the cross-linking process to take place. Some of them used partial epithelial disruption (Samaras et al. 2009), enhanced riboflavin solutions (Kissner et al. 2010; Raiskup et al. 2012), iontophoresis, and intrastromal pockets delivery (Kanellopoulos 2009).

  i) Partial epithelial disruption

  Hayes et al. showed that superficial epithelial trauma and tetracaine administration alone were not adequate to allow the penetration of riboflavin into the corneal stroma (Hayes et al. 2008). Insufficient stromal absorption of riboflavin may impede the efficacy of the cross-linking process. In addition, a later study using spectrophotometry to indirectly measure stromal riboflavin absorption found that loosening the epithelial tight junctions with an application of 20% alcohol solution for 40 seconds or by puncturing the epithelium in a grid pattern also resulted in inadequate pene-

tration of riboflavin into the corneal stroma. Both studies concluded that a complete removal of the epithelium appears to be necessary to permit adequate riboflavin absorption (Hayes et al. 2008; Samaras et al. 2009).

ii) Enhanced riboflavin solutions

On the other hand, a recent publication using the same grid pattern to partially disrupt corneal epithelium with an enhanced riboflavin solution, Ricrolin TE (riboflavin 0.1%, 15% dextran T500) (Sooft Italia S.p.A.), containing two chemical agents, trometamol (Tris-hydroxymethyl-aminometane) and sodium ethylenediaminetetraacetic acid (EDTA), to facilitate passage of riboflavin into the corneal stroma through an intact epithelium, demonstrated significant advantages in terms of reduced pain, faster visual recovery, avoidance of the need for therapeutic contact lens, and a reduction in infection-related complications and the risk of loss of corneal transparency due to abnormal scarring processes (Alhamad et al. 2012). Another research group claimed it is essential to prepare the trans-epithelial riboflavin dextran-free as dextran is a large molecule that hinders the penetration of riboflavin through the intact epithelium. They also showed that adding benzalkoniumchloride (BAC) facilitates trans-epithelial riboflavin stromal absorption (Kissner et al. 2010; Raiskup et al. 2012). Moreover, hydroxypropyl methycellulose (HPMC) is usually used as a riboflavin vehicle (Ramselaar et al. 1988). However, further laboratory and clinical studies are required to evaluate the efficacy of this technique and to compare it with the standard protocol with complete epithelial debridement both with unenhanced and enhanced riboflavin.

iii) Intrastromal pockets delivery

Recently, a novel intrastromal delivery of riboflavin was introduced (Kanellopoulos 2009; Krueger et al. 2008). The aim of this technique was to reduce the complications associated with epithelial debridement by applying the riboflavin through a semi-intact epithelium using femtosecond laser cut of 7 mm diameter at a corneal depth of 100 μm (Kanellopoulos 2009). The riboflavin is injected directly into

the corneal stroma. This facilitates the diffusion of riboflavin and re-epithelization recovery (Kanellopoulos 2009; Krueger et al. 2008). The first clinical case of the intrastromal pockets delivery yielded promising results (Krueger et al. 2008). A laboratory study has shown that the flat cornea and decline of the keratometry readings was achieved within the 6 month follow-up of 10 rabbit eyes, however, the cornea was uneven in all cases (Dong et al. 2011). Other experimental investigation on riboflavin delivery via intrastromal channels measured the biomechanical strength of the cornea post-treatment and revealed that the corneal rigidity in the channel technique is similar to the standard epi-off protocol (Seiler et al. 2014). Further laboratory and clinical investigations are essential to support this mode of CXL.

iv) Iontophoresis

Another method to be considered is iontophoretic delivery of riboflavin, which is a non-invasive delivery system designed to transfer charged molecules throughout the tissues to enhance the penetration. The system uses a low intensity electrical current which flows across the intact epithelium and into the corneal stroma between a negatively charged delivery electrode (located on the cornea) and a counter electrode positioned on the patient's forehead used to drive the riboflavin (Figure 1.15). Experimental studies with riboflavin delivery by iontophoresis imbibition followed by UVA irradiation determined that less tissue damage occurred and the stroma remodelled safely (Cantemir et al. 2017; Cassagne et al. 2016; Lombardo et al. 2014; Mastropasqua et al. 2014; Vinciguerra et al. 2014a). Clinical studies with this technique have demonstrated equivocal results with some suggesting similar efficacy to SCXL (epi-off-CXL) (Bikbova et al. 2014; Buzzonetti et al. 2015; Vinciguerra et al. 2014b), and others showing less pronounced effects (Bouheraoua et al. 2014; Franch et al. 2015; Manetti et al. 2017).

Currently, there is no transepithelial cross-linking therapy that has been shown to consistently achieve the same clinical effectiveness as SCXL and further investigations are needed to develop an equally effective method to SCXL that does not

required epithelial removal and is more comfortable for the patients.

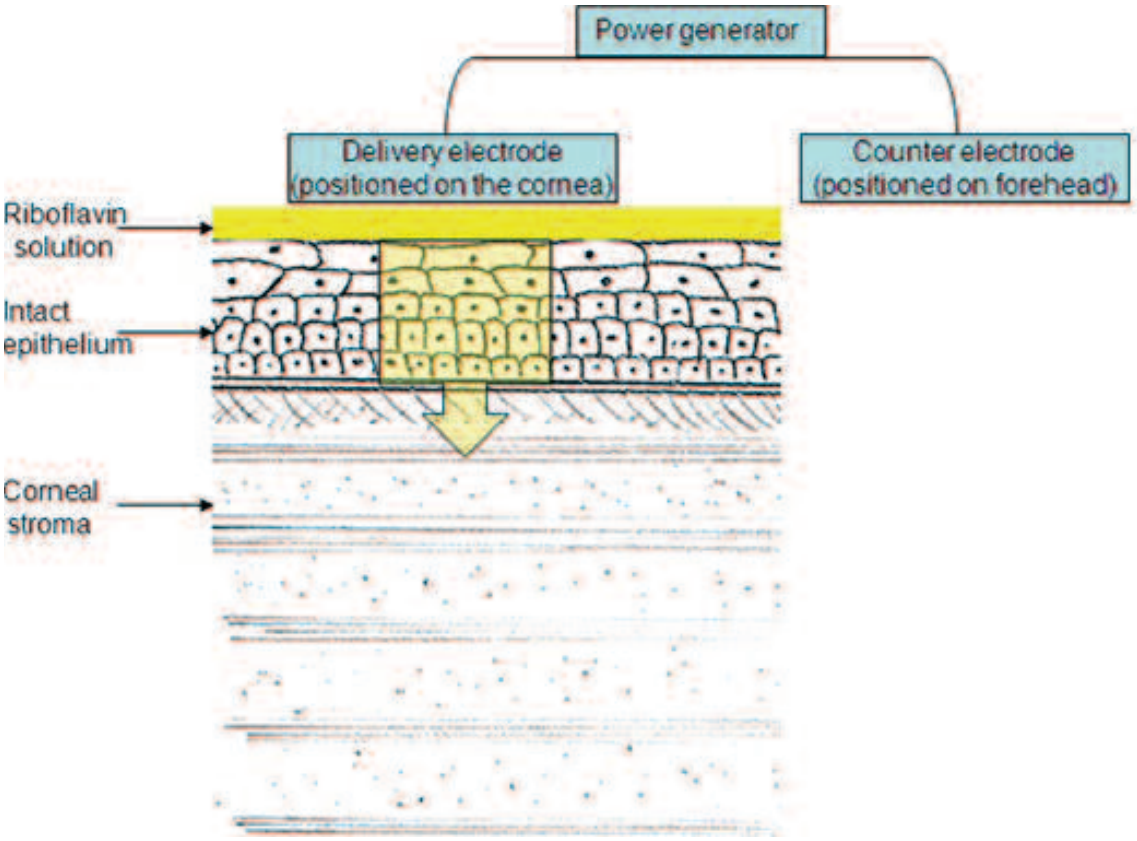

Figure 1.15: Delivery riboflavin into the corneal stroma by iontophoretic using low electrical current. Image reproduced from (Meek et al. 2013).

- ***Accelerated cross-linking***

  With the aim of reducing the procedure time and thereby improving patient comfort and surgeon throughput, researchers theorised that based on the Bunsen-Roscoe law of reciprocity (Bunsen et al. 1862), increasing the intensity and decreasing the time of irradiation such that the total UV dose remained the same (at 5.4 J/cm^2) would achieve the same therapeutic effect as SCXL (Krueger et al. 2014; Schumacher et al. 2011). Consequently, second-generation CXL procedures have been developed to increase the intensity for a shorter time using same level of radiant exposure to accelerate the treatment. This new approach method is called accelerated cross-linking (ACXL). An in vitro study has shown the biomechanical properties of ACXL by increasing the illuminance intensity to 10 mW/cm^2 and reducing the exposure time to 9 minutes produces an equivalent increase in corneal

stiffness to that gained using the SCXL (Schumacher et al. 2011). Wernli et al. observed that the biomechanical stiffness of ex vivo porcine corneas treated with irradiances between 3 mW/cm^2 and 90 mW/cm^2 and illumination times ranging from 30 minutes to 1 minute, respectively. They found up to 45 mW/cm^2 increased in intensity was equivalent to SCXL, however, no statistically significant increase in corneal strength could be obtained at higher levels of irradiance from 50 to 90 mW/cm^2, which demonstrated the failure of the Bunsen-Roscoe reciprocity law at very high intensities (Wernli et al. 2013).

Several studies evaluated the safety of ACXL, and showed no significant change in endothelial cell density using confocal microscopy (Akcay et al. 2017; Kymionis et al. 2014; Touboul et al. 2012); the results contrast with other reports which showed a significant reduction in endothelial cell density using corneal specular microscopy (Cinar et al. 2014; Cingu et al. 2014). These differences might be due to the different microscopies used because the specular microscopy increased scattering and limited imaging of the corneal endothelium in the presence of the usual post-CXL corneal edema results in a reduction of the number of cells discernible; conversely, the use of confocal microscopy permits corneal endothelium examination in the presence of edema and haze (Kymionis et al. 2014).

- ***Treatment of thin corneas using Hypo-osmolar riboflavin solution***

  The standard protocol of CXL requires a corneal thickness of more than 400 μm to be treated (Kymionis et al. 2012; Spoerl et al. 2007; Wollensak et al. 2003c). Unfortunately, many patients with progressive keratoconus have a thinner cornea. A promising method suggested by Hafezi et al. uses hypo-osmolar riboflavin solution that does not contain dextran which thus induces stromal swelling and consequently increases stromal thickness (Hafezi et al. 2009). The technique safely allows treatment of thinner corneas, but the exact biomechanical effect may be lower because the edematous state keeps the collagen fibers apart and may reduce the cross-linking effect (Greenstein et al. 2011; Hafezi 2011).

Hafezi et al. applied the modified protocol to 20 keratoconus patients and found that clinically the amount of swelling showed distinct inter-individual variation (3 minutes to 20 minutes; 36 to 105 μm) (Hafezi et al. 2009). Another study including thirty-two eyes of 29 patients revealed that the mean corneal thickness increase was 114.8 μm and showed a stability of the corneas one year after the cross-linking procedure (Raiskup et al. 2011). Both studies successfully halted the progression of keratoconus in all patients. However, CXL failure using a hypo-osmolar riboflavin solution has been reported in an extremely thin cornea, which suggests that a minimum preoperative stromal thickness of 330 μm is required for a successful CXL (Hafezi 2011).

- ***Accelerated collagen cross-linking with pulsed light (p-ACXL)***

  Oxygen has a crucial role for the photochemical reaction in CXL, and is thought to be a limiting factor in the cross-linking process. Researchers found that it is theoretically likely that increasing UVA intensity in case of ACXL will not permit sufficient time for oxygen to diffuse and not effectively contribute in the photochemical type I and II reactions, which reduce the performance of ACXL (Richoz et al. 2013). Hence, pulsed light accelerated CXL (p-ACXL) of a cycle of (1 second on/ 1 second off) was introduced.

  The modifications are based primarily on current understanding of the photochemical kinetics of UVA exposure and the theoretical principles of the Bunsen–Roscoe's law of reciprocity (Bunsen et al. 1862), which states that a certain biological effect is directly proportional to the total energy dose regardless of the administered regime. Nonetheless, as has been elucidated with other photochemical reactions (Potapenko et al. 1991), this law may only be applicable within a certain dose range and has to be individually defined for each reaction. Recent analysis of the photochemical kinetics observed that the UVA illumination produced a rapid depletion of oxygen in a riboflavin saturated cornea and turning-off the UV light gives rise to replenishment of the oxygen to its original level within 3 to 4 minutes (Figure 1.16) (Kamaev et al.

2012). This study also showed that the oxygen concentration dropped dramatically to zero after approximately 5 second of ACXL compared to 10-15 on SCXL (Figure 1.17). In theory, pulsing the UVA illumination during CXL treatment may start over the photochemical reactions producing an additional oxygen concentration that allows more singlet oxygen release and the formation of "molecular bridges" between and within collagen fibres (Spoerl et al. 1998).

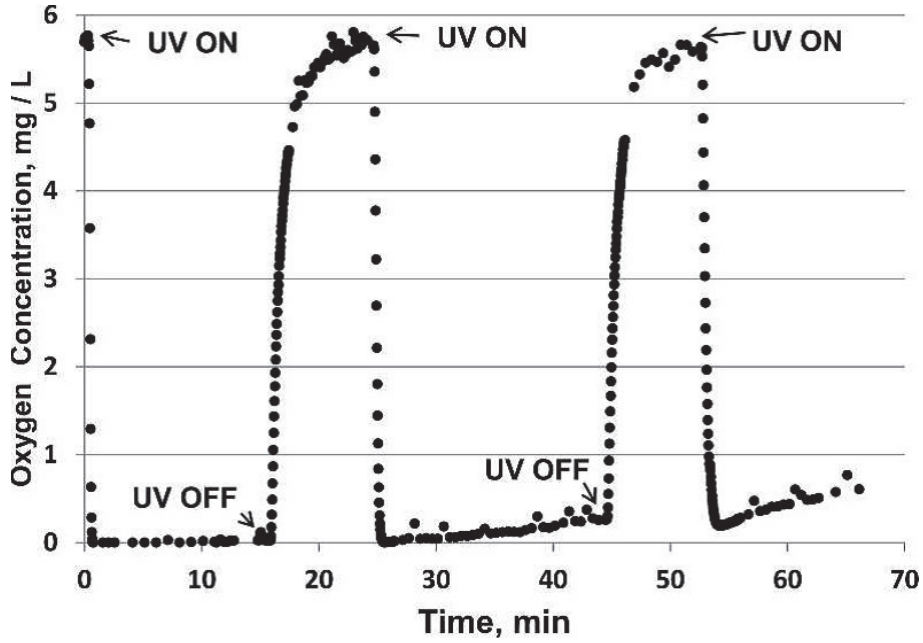

Figure 1.16: Turning-off the UV light gives rise to replenishment of the oxygen to its original level within 3 to 4 minutes. Image reproduced from (Kamaev et al. 2012) with permission from the copyright holder, the Association for Research in Vision and Ophthalmology (License No: 4286520062380).

Several clinical investigations emphasised that the p-ACXL treatment yields a deeper demarcation line than the SCXL protocols (Mazzotta et al. 2014; Moramarco et al. 2015; Peyman et al. 2016). The demarcation line is defined as a biomicroscopically detectable line seen in the slit-lamp, which marks the transition zone between the depth at which keratocytes disappear in the cross-linked anterior corneal stroma region and the untreated posterior corneal stroma region. Although many CXL experts use it as an indication of CXL depth, it is as yet uncertain whether the line represents a region of wound healing or whether it truly represents the effective depth of cross-linking (Seiler et al. 2006). This cell apoptosis causes oxidative stress damaged and produces a toxic nitric oxide molecule (Yuksel et al. 2016). A

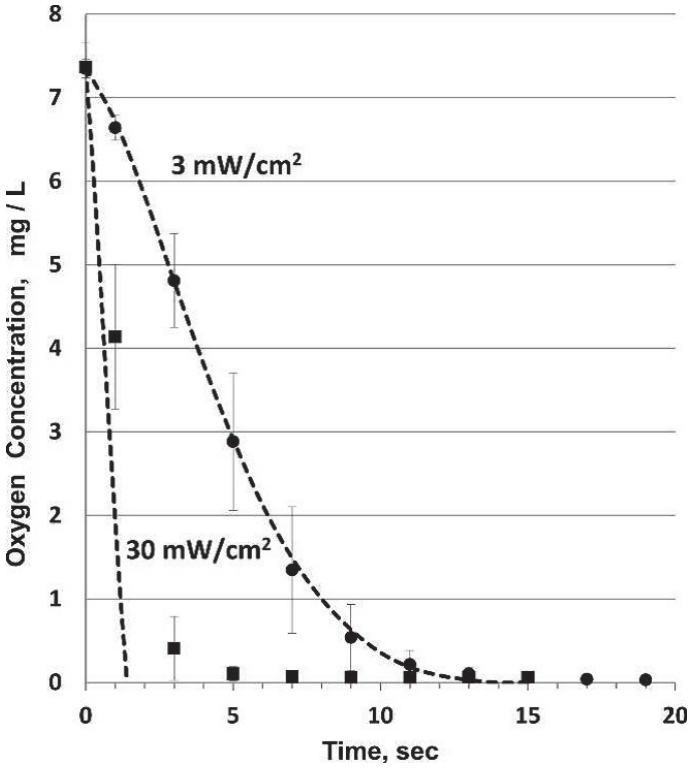

Figure 1.17: The oxygen concentration dropped dramatically to zero after approximately 5 second of ACXL compared to 10-15 on SCXL. Image reproduced from (Kamaev et al. 2012) with permission from the copyright holder, the Association for Research in Vision and Ophthalmology (License No: 4270240029745).

biochemical study advocated that the cornea treated with p-ACXL showed a less nitric oxide levels in aqueous humor than SCXL, which means p-ACXL with 30 mW/cm^2 for 3 minutes (1 sec on / 1 sec off) seems to be a safer treatment (Yuksel et al. 2016). However, pulsed UVA light with 30 mW/cm^2 for 8 min revealed an inferior biomechanical effect than SCXL (Kling et al. 2017). Further investigation is essential to evaluate the strength and stability of the corneas for halting the progression of keratoconus after the p-ACXL method.

1.4 Aims and objectives

The three main objectives of this project are to:

- Assess the effectiveness of existing epithelium-intact and trans-epithelial riboflavin/UVA cross-linking protocols, in terms of their ability to increase the strength and enzymatic resistance of the cornea, and examine the impact of changes in UVA intensity, UVA dosage, UVA delivery mode (pulsed vs continuous) and riboflavin solution.
- Develop improved methods of transepithelial cross-linking that are equally effective to that of SCXL.
- Characterise changes in corneal ultrastructure following photodynamic cross-linking therapy in order to gain a better understanding of the mechanism by which such therapies stiffen the cornea.

  Graphical abstract was included on Appendix I for more illustration.

CHAPTER 2

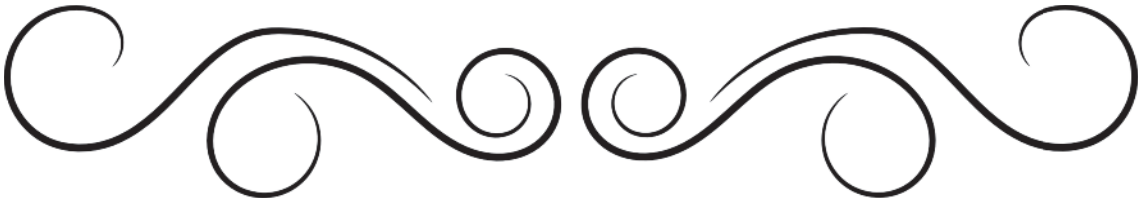

EXPERIMENTAL TECHNIQUES AND GENERAL METHODOLOGY

2.1 Overview

This chapter describes materials and methods that are common to many of the following chapters. Any subtle changes to these general methods are described in the individual chapters.

2.2 Corneal pachymetry

The corneal thickness of both *in vivo* and *ex vivo* eyes was measured using either a Pachette2™ Ultrasonic Pachymeter (DGH Technology, Exton, USA) or a Tomey ultrasound pachymeter (Tomey Corporation, Nuremberg, Germany). The pachymeter probe was placed perpendicular to the centre of the cornea and the mean thickness (based on 8 - 25 consecutive readings) was recorded.

2.3 Enzymatic digestion resistance and dry weight measurements

Three enzymes are typically part of the enzyme panel used to evaluate the efficacy of a cross-linking procedure, these are collagenase, pepsin and trypsin (Charulatha et al. 1997). Spoerl et al. examined the resistance of corneal disks to all three enzymes and found that SCXL significantly increased the resistance of the cornea to digestion by pepsin and collagenase (Spoerl et al. 2004). Most recent studies have used collagenase enzyme to investigate the biochemical resistance of the cornea following different CXL protocols (Fadlallah et al. 2016; Kanellopoulos et al. 2016; Zhu et al. 2017). However, as it is thought that CXL might cause the formation of cross-links not only at the collagen fibril surface but also in the protein network surrounding the collagen (Hayes et al. 2013), pepsin was selected in preference to collagenase for the studies presented in this thesis. As pepsin is a non-specific enzyme it can provide a better assessment of the effectiveness of

different cross-linking procedures in terms of their ability to increase the overall enzymatic resistance of the tissue.

Previous enzyme digest studies have shown that changes in corneal thickness are not a reliable indicator of the rate of enzymatic digestion due to the considerable stromal swelling that occurs in the vertical direction within 24 hours of immersion in pepsin digest solution (Spoerl et al. 2004). As the diameter of the anterior surface of each corneal disk is unaffected by changes in stromal hydration (Spoerl et al. 2004), this parameter was used to monitor the rate of enzymatic digestion. Measurements of anterior surface diameter were made using an electronic digital caliper (Clarke International, model CM145 4500360, Epping, Essex, England) at 24 hourly intervals until complete digestion had occurred. Since the diameter was found to vary slightly between different meridians of an individual specimen, the average of the major axis and minor axis diameter of each corneal disk was recorded at each time point and statistically evaluated. The definition of 'complete digestion' was the point at which the specimen could no longer be distinguished from the surrounding pepsin solution even under microscopical examination (light microscope, Nikon SMZ1000 type 104, Japan). Calculations based on the sample size used (usually 6 per treatment group) and the standard deviation of the diameter measurements confirmed that the sensitivity of the technique was such that differences between groups (in terms of the time taken for complete digestion) of less than 1 day could not be detected by this method.

In order to further assess the effect of each treatment on enzymatic resistance, five corneal disks from each group were removed from the pepsin digest solution midway through the digestion process (after approximately 12 days of digestion). These samples were then placed in a 60°C oven until a constant dry weight was reached. Measurement of the average corneal dry weight for each treatment group, which represents the mass of undigested tissue, allows more subtle differences between treatment groups to be identified.

2.4 Cross-linking using illumination system

2.4.1 The standard Riboflavin/UVA cross-linking protocol

The corneal epithelium was completely removed from enucleated porcine eyes. Riboflavin (vitamin B2) (0.1% solution 10 mg riboflavin-5-phosphate in 10 ml dextran-T-500 20% solution) was applied to the corneal surface 30 minutes before irradiation and at 5 minute interval during a 30 minute exposure to UVA light (Wollensak et al. 2003). The 30 minutes exposure to 370 nm UVA light with an irradiance of 3 mW/cm^2 resulted in a total energy dose of 5.4 J/cm^2. The cross-linking device (CCL-365 Vario cross-linking system, Peschke Trade GmbH) was positioned at a working distance of 5 cm above the cornea to allow the UVA beam to be focussed on the central 9 mm of the cornea (Figure 2.1).

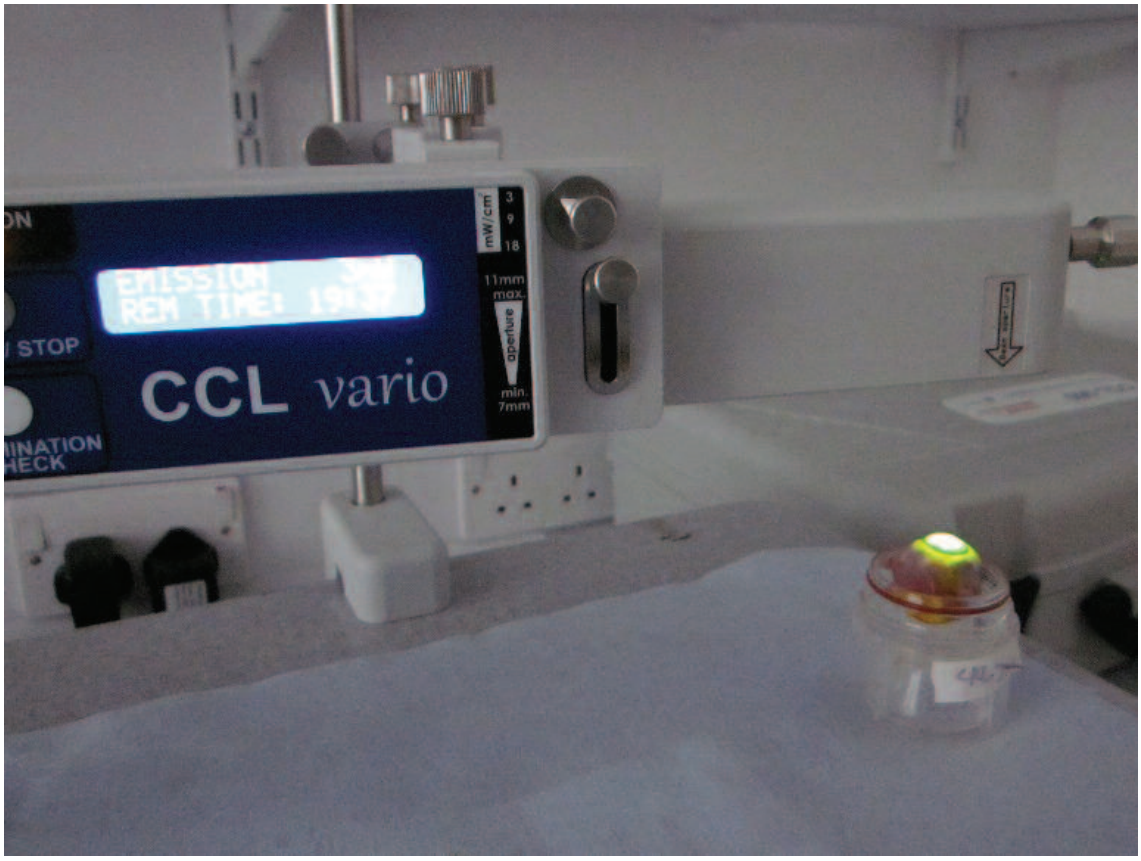

Figure 2.1: Ex-vivo porcine eye was exposed to UVA irradiation using (CCL-365 Vario™ cross-linking system Peschkmed, Huenenberg, Switzerland).

2.4.2 Modifications to the standard cross-linking protocol

In this thesis several modified cross-linking protocols were used, and these are summarised in Table 2.1. Prior to cross-linking, riboflavin was applied to the de-epithelialised cornea in either a drop-wise manner or via a 9 mm diameter corneal annular suction ring (Kestrel Ophthalmics Ltd., Broadstone, Dorset, UK) (Figure 2.2). In the majority of cases, UVA light was provided by a CCL-365 Vario™ cross-linking system (Peschkmed, Huenenberg, Switzerland) (Figure 2.1). However, in studies involving high-intensity, pulsed UVA light (Chapter 5), a Phoenix CXL System was used (Peschke trade GmbH, Huenenberg, Switzerland). Further details relating to specific cross-linking techniques are provided in the methods section of each chapter.

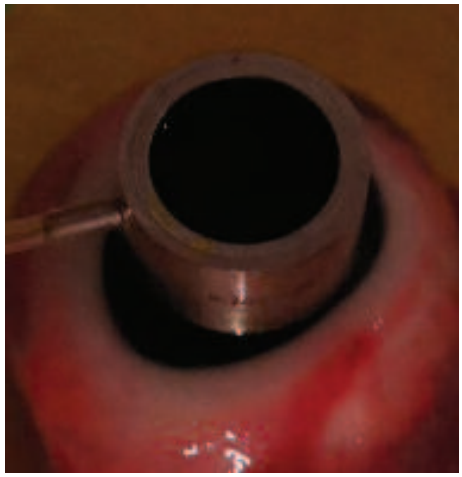

Figure 2.2: The application of riboflavin through a corneal annular suction rings.

Table 2.1: A summary of the cross-linking techniques performed and their controls.

Treatment	Abbreviation	Epithelium	Photosensitising solution	Light intensity (mW/cm^2)	Duration of light exposure (min)	Total Energy Dose (J/cm^2)	Tested on chapter
Untreated	U	off	-	-	-	-	3, 5 and 7 (except on chapter 7 the epi. was intact)
dextran only	D	off	dextran 20%	-	-	-	3
Riboflavin only	R	off	Mediocross D: 0.1% Riboflavin, 20% dextran	-	-	-	3, 4, 5, and 6
standard CXL	SCXL or S3	off	Mediocross D	3	30 min	5.4	3, 5, 6 and 7
accelerated CXL 9 mW	ACXL (A9) or Epi-off-cxl 5.4 J/cm^2	off	Mediocross D	9	10 min	5.4	3 and 4
accelerated CXL 18 mW	ACXL (A18)	off	Mediocross D	18	5 min	5.4	3
Disrupted epithelium non-irradiated control	Dis-ribo	Disrupted	Vitamin B2 Streuli: 0.1% riboflavin, saline	-	-	-	4
Disrupted epithelium CXL	Dis-CXL 5.4 J/cm^2	Disrupted	Vitamin B2 Streuli	9	10 min	5.4	4
Epithelium intact non-irradiated control	Medio-ribo	On	Mediocross TE: 0.25% riboflavin, 1.2% HPMC, 0.01% BACS , Pi-water	-	-	-	4
Epithelium intact high riboflavin concentration CXL	Medio-CXL 5.4 J/cm^2	On	Mediocross TE	9	10 min	5.4	4
Epithelium intact, high riboflavin concentration and prolonged iontophoresis non-irradiated control	TC-ion-ribo	On	Mediocross TE	-	-	-	4
Epithelium intact, high riboflavin concentration and prolonged iontophoresis CXL	TC-ion-CXL 5.4 J/cm^2	On	Mediocross TE	9	10 min	5.4	4

Table 2.1: (Continued).

Treatment	Abbreviation	Epithelium	Photosensitising solution	Light intensity (mW/cm^2)	Duration of light exposure (min)	Total Energy Dose (J/cm^2)	Tested on chapter
Epithelium intact, high riboflavin concentration, prolonged iontophoresis and high UVA energy dose CXL 6.75	TC-ion-CXL 6.75 J/cm^2	On	Mediocross TE	9	12 min 30 sec	6.75	4
Epithelium intact, basic iontophoresis protocol	Ion-CXL 5.4 J/cm^2	On	Mediocross M: 0.1% riboflavin, 1.0% HPMC	9	10 min	5.4	4
Epithelium intact, basic iontophoresis protocol with high UVA energy dose 6.75	Ion-CXL 6.75 J/cm^2	On	Mediocross M	9	12 min 30 sec	6.75	4
Epithelium-off, standard riboflavin concentration, and high UVA intensity CXL 5.4	HCXL 5.4 J/cm^2	off	Mediocross D	30	3 min	5.4	5
Epithelium-off, standard riboflavin concentration, and high UVA energy dose CXL 7.2	HCXL 7.2 J/cm^2	off	Mediocross D	30	4 min	7.2	5
Epithelium-off, standard riboflavin concentration, and pulsed high UVA energy dose CXL 7.2	p-HCXL 7.2 J/cm^2	off	Mediocross D	30	8 min (10 sec-on/10 sec-off)	7.2	5
Epithelium-off, standard riboflavin concentration, and pulsed high UVA energy dose CXL 7.56	p-HCXL 7.56 J/cm^2	off	Mediocross D	9	14 min (stop 15 sec every 1 min)	7.56	6
Epithelium intact, high riboflavin concentration, prolonged iontophoresis and pulsed high UVA energy dose CXL 7.56	p-TC-ion-HCXL 7.56 J/cm^2	On	Mediocross TE	9	14 min (stop 15 sec every 1 min)	7.56	6
Epithelium-off, Bacteriochlorophyll Derivative WST-D and Near Infrared Light	WST-D/NIR	off	WST-D, 20% dextran	10 (NIR)	30 min	18 (NIR)	7

2.5 Calculation of corneal hydration

Measurement of corneal hydration was required as part of the extensometry and SAXS studies. As collagen interfibrillar spacing (IFS) is known to be highly sensitive to the hydration of the tissue, it is necessary to know the water content of the tissue at the time of x-ray data collection (Meek et al. 1991). To calculate an average wet weight of the tissue during data collection, the sample was weighed before and after data collection. Then, to calculate the dry weight, the sample was placed in an oven at 60°C for at least three days until a constant dry weight was obtained. Corneal hydration (H) was calculated using the following equation (Equation 2.1):

$$H = \frac{(Wet\ weight - Dry\ weight)}{Dry\ \ weight} \quad \text{Equation (2.1)}$$

where:

H	=	Corneal hydration
Wet weight	=	Original corneal weight
Dry weight	=	Corneal weight post-dehydration in 60°C oven after removal of all water content

2.6 Extensometry

2.6.1 Corneal strip preparation

Using a custom-made cutter, comprising two parallel razor blades, 5 mm-wide strips of tissue were cut from the endothelial side along the vertical meridian (superior-inferior) (Figure 2.3). The length of the corneal strip was 12 mm plus 2 mm of sclera on both ends. The corneal strips were used for biomechanical testing studies immediately after being cut.

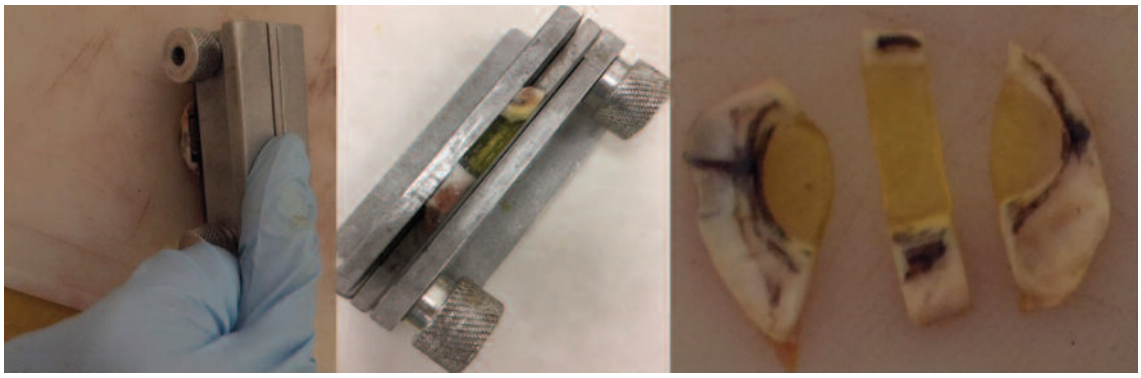

Figure 2.3: Cutting corneal strips for biomechanical testing. A double-blade adjustable strip cutting tool was used to cut 5 mm wide corneal strips from the centre of each cornea.

2.6.2 Extensometer set-up

All stress–strain measurements were performed on a commercial extensometer (Lloyd Instruments Ltd., UK) with a 20 N or 10 N load cell in Chapter 3 and 6, respectively. The steps involved in setting up and carrying out a test are illustrated in (Figure 2.4). Each tensile specimen was clamped to the extensometer arms using serrated grips. Prior to clamping, a guide was used to ensure the extensometer arms were separated by precisely 6 mm, and this distance is referred to as the gauge length. Throughout the test the sample is surrounded by a Perspex tube containing a ball of cotton wool soaked in water, in order to maintain hydration (for details see the preliminary study of the optimal hydration Appendix H) (Figure 2.4).

2.6.3 Biomechanical data analysis

Stress–strain measurements

Using a force of 1 N, three precondition cycles were performed to align the collagen fibrils within the tissue. Hoeltzel et al. found that three precondition cycles were adequate to produce constant results (Hoeltzel et al. 1992). Prior to testing, values for the speed, gauge length, cross-sectional area and break point were entered into the system. The Nexygen 4.1 software package (Lloyd Instruments Ltd., UK) recorded values for load and extension, and calculated the stress and percentage strain for each corneal strip tested. After the test

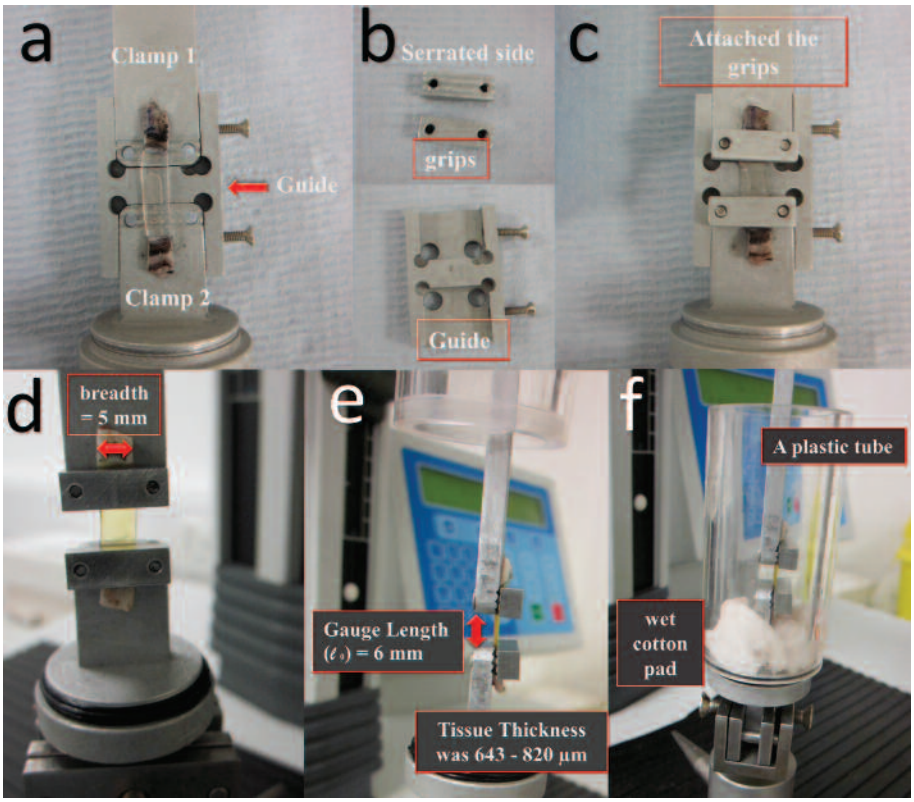

Figure 2.4: Extensometer set-up. (a) The strip was positioned in the middle of the guide. (b and c) Then, the grips were attached firmly; the grips were serrated to reduce the possibility of strip slippage at the grip. (d - f) The guide was removed, and the holder was placed in a plastic tube that contained a wet cotton pad underneath the specimen to maintain hydration.

the data was exported from Nexygen 4.1, transferred to Excel and analysed in MATLAB.

In MATLAB, the cross-sectional area was calculated by inserting the corneal thickness measurement and the breadth for each sample by the equation 2.2:

$$A = \text{Thickness (m)} \times \text{Breadth (m)} \qquad \text{Equation (2.2)}$$

where:

A = Area (m^2)

Thickness = Corneal thickness measured by pachymetry (μm) $\times 10^6$

Breadth = Width of corneal strip (mm) $\times 10^3$

The raw data were loading from the extracted Excel file for each strip, the stress and strain values for each sample had been calculated as equation 2.3, 2.4:

$$\sigma = F\ (N) / A\ (m^2) \qquad \text{Equation (2.3)}$$

where:

σ = Stress (N/m^2 or Pa)

F = Force (N)

A = Area (m^2)

$$\varepsilon = \frac{\Delta l}{l_\circ} = \frac{l - l_\circ}{l_\circ} \qquad \text{Equation (2.4)}$$

where:

ε = Strain (mm/mm), Strain (%) = (mm/mm) × 100

Δl = Change in length (mm) (Extension)

$l_\circ$ = Original length (mm) (Gauge length)

According to Schumacher et al. the stress–strain relationship of connective tissue can be divided into the three regions: (1) an area of nonlinear elasticity, (2) a region of linear elastic behaviour, and (3) a region where irreversible plastic deformation occurs (Schumacher et al. 2011) (Figure 2.5). The region of low-strain nonlinear elasticity (from 2% to 8% strain) was the area of particular interest for examining the effects of various cross-linking protocols on the biomechanical properties of the tissue as they most closely resemble the level of strain experienced *in vivo*. The stress–strain curve was fitted to an exponential function in this region (Elsheikh et al. 2008) as equation 2.5:

$$\sigma = A(e^{B\varepsilon} - 1) \qquad \text{Equation (2.5)}$$

where:

σ = Stress

A,B = Constants

e = Exponential

ε = Strain

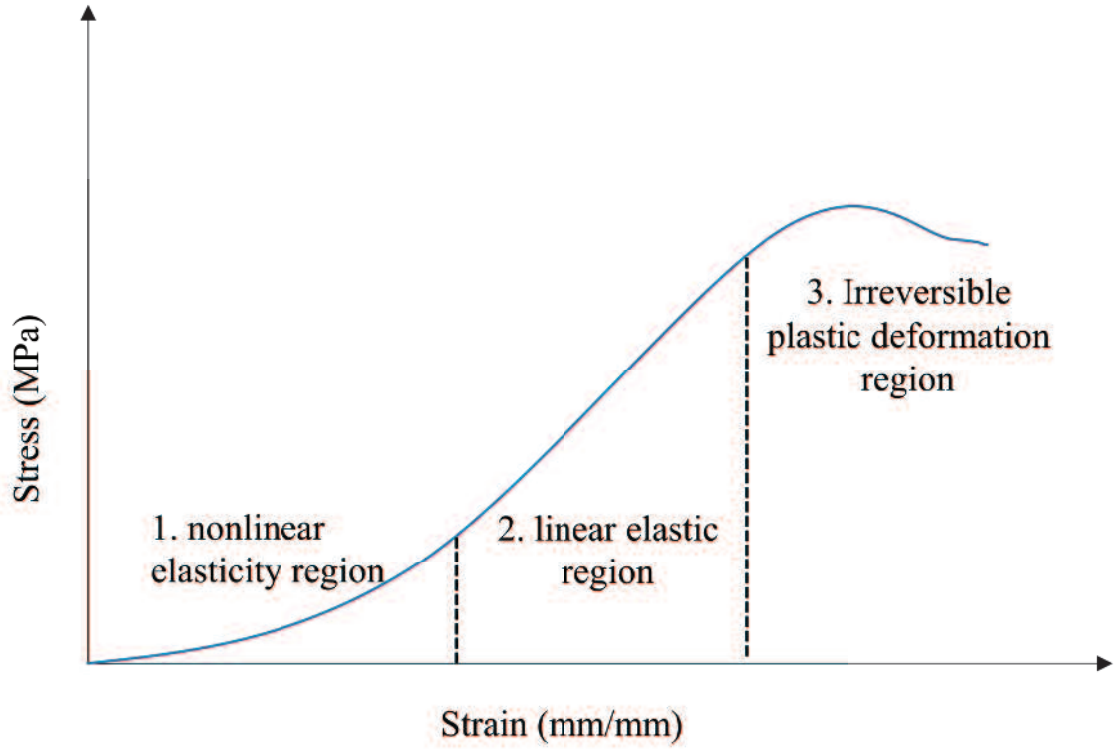

Figure 2.5: Three different elasticity regions on the stress-stain curve.

In order to produce an average stress-strain curve for each treatment group, the mean of A and B values was calculated to plot an individual curve within a particular group. By entering corresponding known values of strain, the equations were utilized to find unknown values of stress i.e. 0.02, 0.04 and onwards up to 0.1. The calculated estimations of stress were then used to find the mean value of stress for a given strain within the treatment group, and plotted against the corresponding strain values to deliver an average stress-strain curve (see Appendix F and G). Examples of raw and fitted curves for single

samples are plotted in Figure 2.6. This strategy was repeated for all treatment groups and correlation diagrams were plotted (see Appendix F and G). In this study, the region of interest was at lower strains, near physiological levels. Consequently, the data was isolated in the region of 0 to 0.10 (0 % - 10 %) strain (see Figure 3.8, and Figure 6.5 in Chapter 3 and 6).

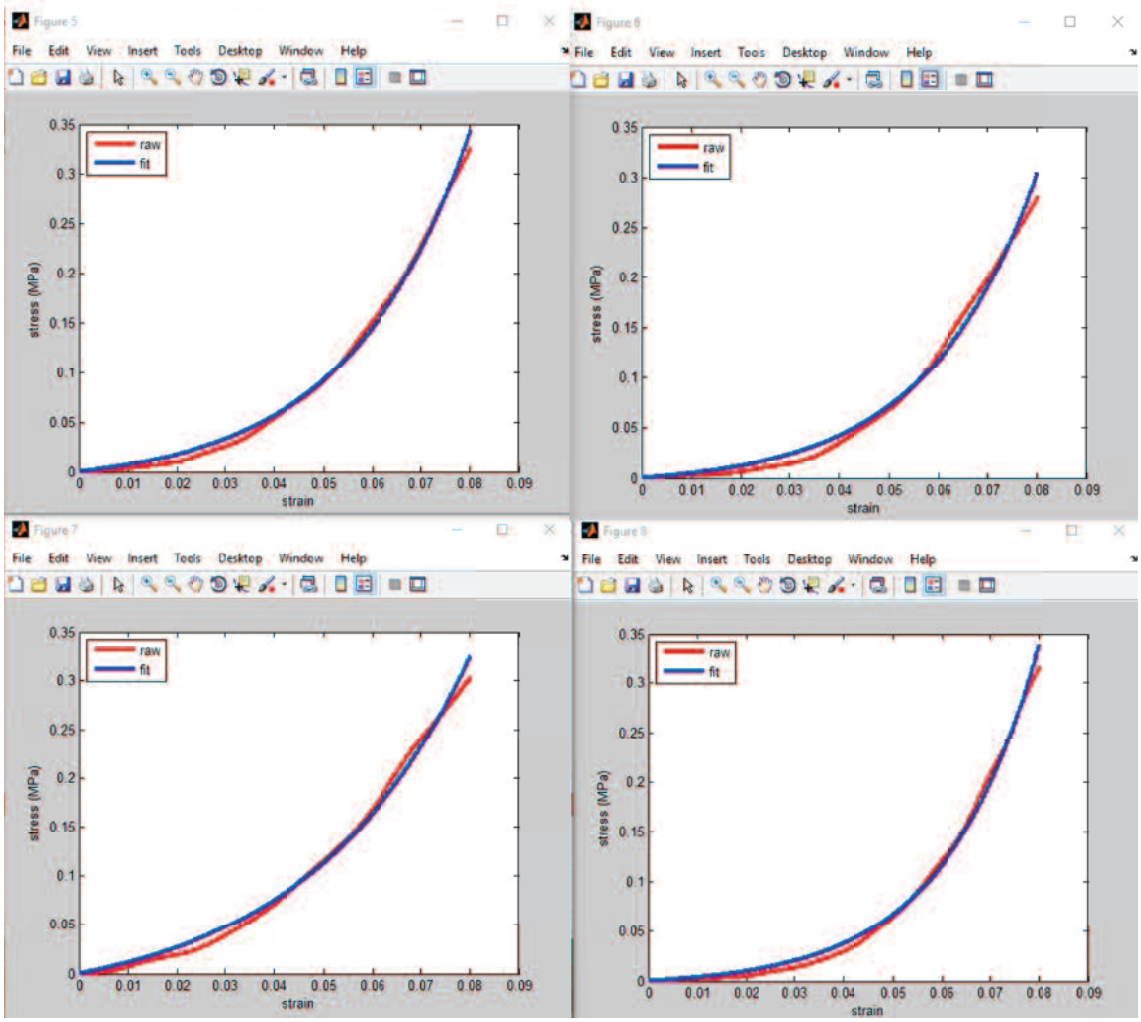

Figure 2.6: Examples of raw and fitted curves for four corneal tissue strips.

Young's modulus

Young's modulus reflects the characteristics of a linearly elastic material experiencing tension. Accordingly, it is a helpful property to look at when attempting to survey the stiffness of a sample. If the material is non-linear, Young's modulus is more accurately referred to as the tangent modulus and is characterized as the slope of tangent in the

stress-strain curve at any point. The modulus at a particular strain can be calculated by finding the slope at that specific point on the curve.

Tangent modulus was calculated for 2%, 4%, 6% and 8% strain as a gradient of the stress–strain curve as equation 2.6:

$$E = \frac{\Delta\sigma}{\Delta\varepsilon} \quad \text{Equation (2.6)}$$

where:

E	=	Tangent modulus
$\Delta\sigma$	=	Difference between two stress points, e.g. $(\sigma_2 - \sigma_1)$
$\Delta\varepsilon$	=	Difference between two stress points, e.g. $(\varepsilon_2 - \varepsilon_1)$

2.7 X-ray diffraction techniques

X-ray scattering techniques can be utilised to measure structural quantitative parameters such as collagen fibril diameter and inter-fibrillar spacing (Meek et al. 2009, 2001). Contrary to electron microscopy, which requires extensive tissue processing preparation that results in shrinkage of the tissue, x-ray scattering data can be obtained from full-thickness of corneal tissue close to its natural hydration state.

All x-ray scattering data presented in this thesis were collected at the UK synchrotron radiation source (Diamond Light Source, Didcot, UK). At the synchrotron, electrons are accelerated to near the speed of light inside a circular storage ring which results in the emission of radiation at all wavelengths, including intense x-rays. The light, in our case the x-rays, generated from this process is directed into laboratories, which are commonly referred to as ‘beam-lines’. Samples placed in the line of the x-ray beam cause the x-rays to be scattered at various angles. Small-angle x-ray scattering beam-lines (such as I22 at the Diamond Light Source) are set up in such a way that x-rays scattered at small-angles (less than 2 degrees) are recorded as an x-ray scatter pattern on a detector positioned several metres behind the specimen. In addition to the scattered x-rays, a proportion of the incident x-rays are absorbed by the specimen itself and others pass directly through

the sample and are absorbed by a lead backstop.

If the sample under investigation has a structure with perfect or near- perfect order, such as a crystal, the scattered x-rays will interfere to produce diffraction maxima known as x-ray reflections. The directions of constructive interference are obtained from Bragg's law which states that, when parallel x-rays are incident on parallel lattice planes in a crystal, each atom acts as a scattering centre and produces a secondary wave. In particular, the angles of both incident and reflected rays (θ) will be equal from any point of these crystal lattice planes (Figure 2.7). Constructive interference between the reflected waves occurs when the optical path difference between waves reflected from successive planes, which can be determined geometrically, equals an integral number of wavelengths. This condition is described by the Bragg equation (Equation 2.7):

$$n\,\lambda = 2d\,\sin\theta \qquad \text{Equation (2.7)}$$

where:

n = an integer numbers of the order of diffraction

d = Distance between the crystal lattice planes

λ = Wavelength of an x-ray beam incident to the crystal planes

θ = Bragg angle

Less organised structures, such as the cornea, produce more diffuse and fewer interference maxima than the true diffraction maxima obtained from crystals but Bragg's law still applies. However, wholly disorganized structure will produce diffuse scattering, which is so-called background scatter (Meek et al. 2001).

When corneal tissue is placed in an x-ray beam, x-rays are scattered parallel to the fibril axis of the constituent collagen to produce a meridional pattern, and at right angles to the fibril axis to form an equatorial pattern (Figure 2.8). The cornea comprises several hundred lamellae and collagen fibrils run in all directions, so when x-rays are passed through different orientations of lamellae, both the meridional and equatorial patterns will result as a series of concentric circles (Meek et al. 2001).

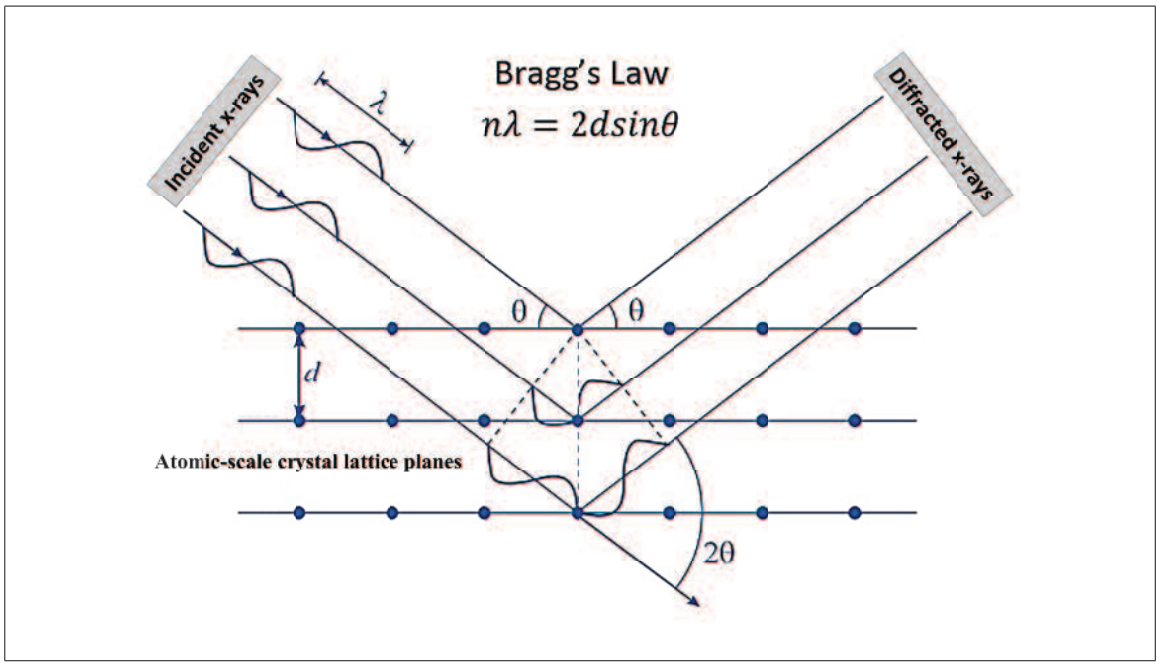

Figure 2.7: Bragg's law states that when a beam of x-rays is incident on a pair of parallel lattice planes in a crystal, each atom acts as a scattering centre and produces a secondary wave. For a given angle of incidence (θ), constructive interference will occur if the path length between adjacent reflected waves (2dsinθ) equals an integral number of wavelengths (nλ).

2.7.1 Small-angle x-ray scattering

Experimental set-up

Cornea can generate a series of small-angle of meridional x-ray patterns, arising from the axial D-periodicity of collagen (65 nm in cornea – (Marchini et al. 1986)) and additional small-angle equatorial x-ray patterns, as a result of the uniform fibril diameters and the regular spacing of collagen fibrils. These additional equatorial peaks give the cornea a distinctive feature compared with most other connective tissues (Boote et al. 2003; Meek et al. 2009). SAXS data collection as elaborated here was applied in Chapter 7. The cornea was gently thawed, and tissue samples were trephined from the centre of each cornea to obtain a 6 mm full-tissue-thickness biopsy. Samples were immediately wrapped in a single layer of Clingfilm^{TM} to minimise tissue dehydration during exposure to the x-ray beam. Samples were then positioned in a polymethyl methacrylate (Perspex; theplastic-shop.co.uk, Coventry, UK) sample cell with transparent Mylar windows (DuPont-Teijin,

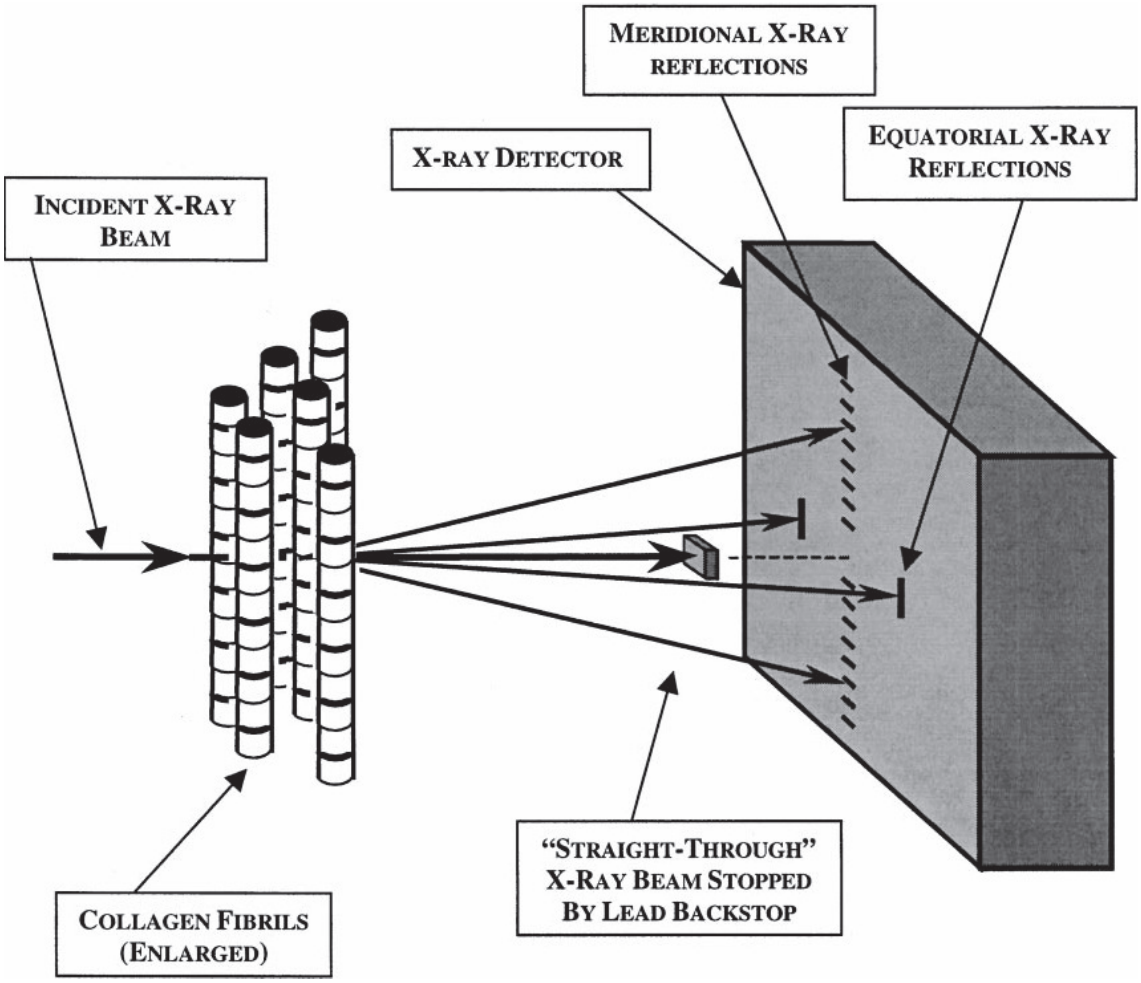

Figure 2.8: A schematic diagram representing fibres placed vertically in an x-ray beam. X-rays that are scattered parallel to fibril axis will produce a meridional pattern resulting from the regular periodicity of the collagen molecular packing along the fibril axis. Meanwhile, at right angles to the fibril axis the x-ray scatter forms an equatorial pattern resulting from the uniform diameter and quasi-regular spacing of the collagen fibrils. Image reproduced from (Meek et al. 2001) with permission from the copyright holder, Elsevier. (License No: 4274230442872).

Middlesbrough, UK) (Figure 2.9). This was mounted on a Perspex cell holder in path of the x-ray beam such that the beam was perpendicular to the plane of the cornea and therefore passed through the whole cornea. The x-ray wavelength was λ = 0.8 nm and the beam cross-section measured $180 \times 300\ \mu m$. The specimen-to-detector distance was set to 5.8 m to collect the SAXS signal. A lead backstop was placed between cornea and detector at the end of camera tube to block the straight-through beam.

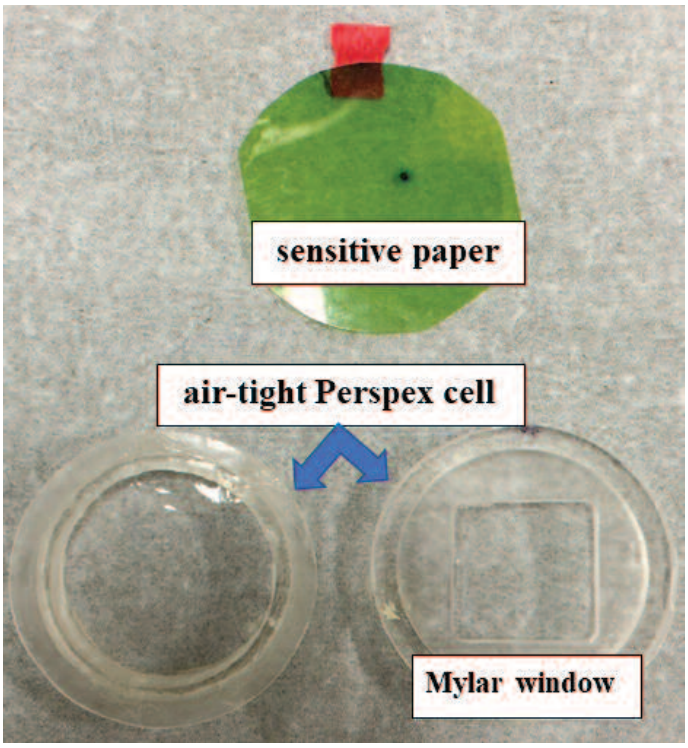

Figure 2.9: Samples were mounted in an air-tight Perspex cell with transparent Mylar windows. During the set-up procedure, green x-ray sensitive paper was used to locate the point within the cell through which the x-ray beam passed. By placing the sensitive paper over the sample holder, it was then possible to correctly position each sample in the cell.

Determining the x-ray beam location and sample position

Before data collection, localizing the precise position of x-ray beam with respect to the specimen was achieved by exposing a piece of x-ray sensitive paper, which was mounted over the front of the specimen cell, to the x-ray beam for 10 seconds. A black dot on the green x-ray sensitive paper identified the point through which the x-ray beam had passed. By temporarily placing the exposed sensitive paper over the sample holder it was then possible to correctly position each sample within the cell (Figure 2.9). The cornea was meticulously situated over the x-ray mark on the green paper to guarantee that the x-ray beam passed through the centre of the corneal disk (epithelium facing the x-ray beam) at the desired location according to the necessities of the investigation; the green paper was then removed. The sample holder was mounted on a motorised stage that could be moved in micron steps in a horizontal and vertical direction.

Initial sample alignment was determined by calibration of a microscope viewer with

the x-ray beam position and the computerised stage. To ensure an acceptable signal-to-noise ratio, an appropriate x-ray exposure time was required to ensure the devices were properly aligned and that the signal was strong enough for following analysis. Furthermore, the initial intensity of the x-ray beam affects the exposure time used, a higher intensity beam enabling a shorter exposure while sustaining an adequate signal-to-noise ratio. An exposure time of 0.5 sec was set up to be the most suitable for the samples. SAXS beamline calibration was carried out using the 58.380 Å peak associated with the first order reflection of powdered silver behanate. The positions of the peak from the centre of the x-ray scatter pattern differs depending on the specimen-detector distance, thus this calibration is essential for every set of experiments conducted on the SAXS beamline. Following data collection in Didcot, UK, the x-ray patterns were electronically analysed in Cardiff University.

SAXS data analysis

The x-ray data were recorded in a BSL file format, which saves the single images as a series of frames within one large file. For processing, the BSL files were converted to TIFF format using Fit2D data analysis program (ESRF, Grenoble, France). SAXS data (in TIFF format) were analysed using MATLAB (MathsWork, UK) with integrated SAXS4COLL software. The SAXS4COLL software was produced by the Structural Biophysics Group at Cardiff University to allow rapid automated analysis of data from different SAXS beamlines (Abass et al. 2017).

A brief description of the SAXS data analysis is given below, for more detail the reader is referred to the guidelines in Abass et al. (2017). The centre of the SAXS pattern was determined using a diffraction pattern acquired from a calibrant of powdered silver behanate, by selecting seven points manually around the circumference of one of the diffraction rings (Figure 2.11a). The x and y coordinates of the centre of the pattern were recorded. The corneal patterns were then calibrated using the 5.838 nm peak associated with the first order reflection of powdered silver behanate. This calibrated pixel value was

Figure 2.10: The small-angle x-ray scattering experimental set-up used to image rabbit corneas at the Diamond synchrotron. Top: specimen cell mounted in the cell holder. Bottom right: Side view showing path of the x-rays as they pass through the specimen. Bottom left: View of the camera tube from the specimen (front) to the detector.

input into the calibration input box alongside the 5.838 nm first order, which was stored and used to automatically calculate the sample collagen peak positions (Abass et al. 2017).

The interference function (IF) and the fibril transform (FT) peaks arise from the spacing and diameter of collagen fibrils, respectively. To determine these two peaks, the background scatter from non-collagenous components of the cornea needed to be removed from the total intensity of the SAXS pattern from the cornea, which consists of IF, FT and the background (Meek et al. 2001). The software allows removal of the background

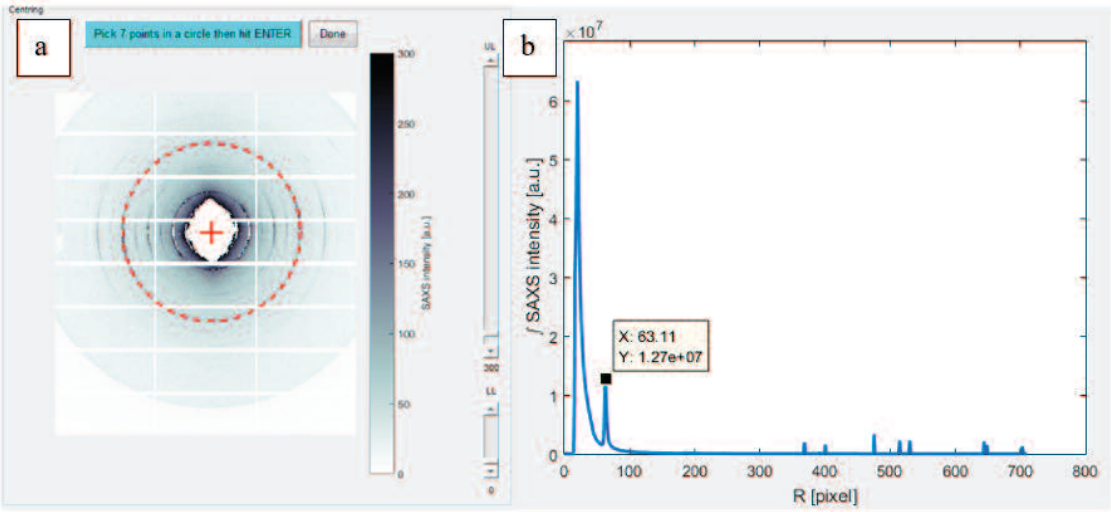

Figure 2.11: Pre-processing the data on SAXS4COLL involved centring and calibrating the image. (a) The image was centred using the diffraction pattern acquired from powdered silver behanate, by selecting seven points manually on the circumference of one of the diffraction rings. (b) The patterns were then calibrated against the position of the first-order reflection (in pixels) of a known calibrant such as silver behanate or as shown here, hydrated rat tail tendon. Image reproduced from (Abass et al. 2017).

scatter by plotting the data logarithmically and interactively fitting a straight line below the data as precisely as possible by selecting three points Figure 2.12.

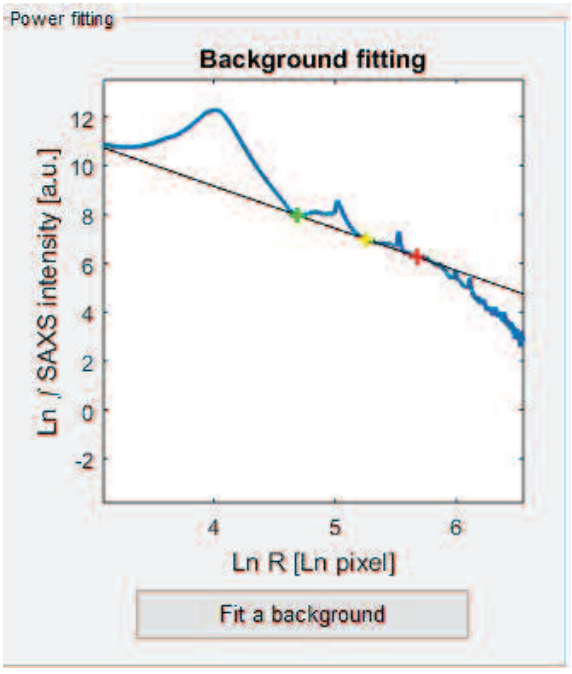

Figure 2.12: Removing background scatter by interactively fitting a straight line below the data as precisely as possible by selecting three points.

After background removal, the interference function (IF) could be identified as shown

in Figure 2.13a. The position of the IF peak was located by clicking close to the peak (Figure 2.13a), then, the software detects and records the closest peak maximum automatically. The SAXS4COLL automatically converts the position of this peak into the interfibrillar Bragg spacing using Bragg's law, and calibrates the Bragg spacing (d) against the position of the first order reflection (pixels) of the silver behenate. The Bragg spacing is determined after first calculating the value of θ, by applying the known parameters of silver behenate to equation 2.7: peak position = 5.838 nm, n = 1, λ = 0.8 nm.

The fibril transform (FT) is a Bessel function that contains a wide, low peak near the third order of collagen. To calculate the average collagen fibril diameter, the screen displays sliding bars that generate Bessel functions from cylinders (representing collagen fibrils) - sliding the bars changes the diameter and scattering intensity of the cylinders. By sliding the bars it was thus possible to stop at a diameter that aligned the position and the intensity of the peak in the calculated Bessel function with the visible peak in the x-ray pattern (Figure 2.13b). As before, the program then calibrated this peak position and converted it to a fibril diameter in nanometres.

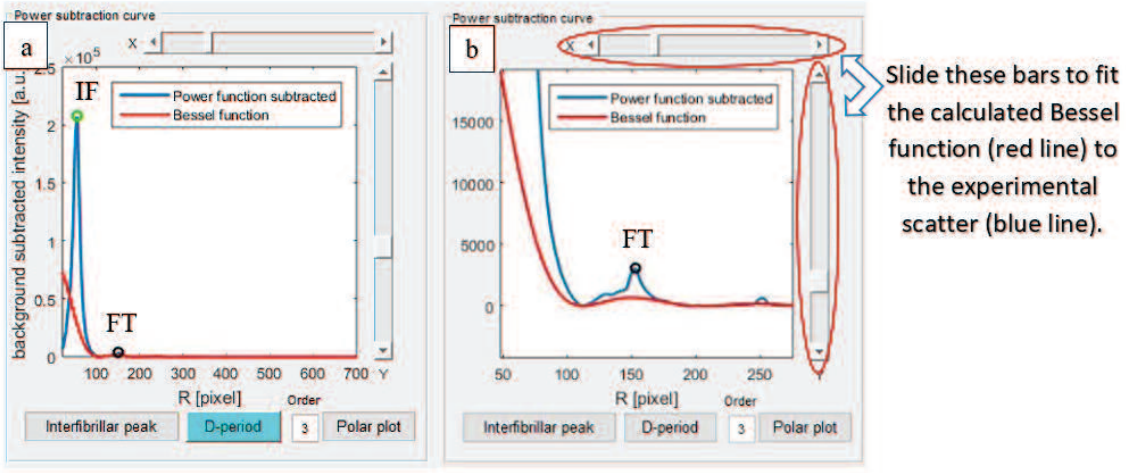

Figure 2.13: Detecting the collagen peaks. (a) The interfibrillar peak IF (green circle) was located by clicking as close to the peak as possible. (b) The fibril transform (FT) contains a wide, low peak near the third order of collagen (circled). To calculate the average collagen fibril diameter, it was necessary to manually slide the bars to fit the calculated Bessel function (red line) to the experimental scatter (blue line).

2.8 General preparation for TEM analysis

Prior to transmission electron microscope (TEM) analysis, the cross-linking treatments were carried out in our collaborator's laboratory at the Weizmann Institute of Science in Rehovot as had been agreed. The Methods section of Chapter 7 explains in detail how the treatment was performed. After treatment, corneas were dissected out from the eye globes with a 2 - 3 mm scleral rim attached to preserve specimen structure and were placed into a fixative solution containing 2.5% glutaraldehyde and 2% paraformaldehyde (PFA) in 0.1M Sorensen phosphate buffer (pH 7.2 - 7.4) for two hours to maintain the tissue (Step 1, Figure 2.14). They were then stored in 0.2M Sodium cacodylate buffer (pH 7.4) and transported to Cardiff University, where electron microscopy processing was performed. The preparation of all fixative was handled according to COSHH.

2.8.1 Fixation and staining

Corneas were washed and placed in 0.1M Sorensen phosphate buffer (pH 7.2 - 7.4) overnight at 4 °C. The following day, the corneal tissue was cut into segments (Step 2, Figure 2.14). Corneal tissue was then post-fixed in 1% osmium tetroxide in 0.1M Sorensen phosphate buffer for one hour and rinsed three times for five minutes with distilled water (DW). Samples were then en-block stained in 0.5% aqueous uranyl acetate (UA) for a further one hour in the dark under foil as UA is light sensitive (Step 3-4, Figure 2.14).

2.8.2 Dehydration and resin embedding

Corneal specimens were then dehydrated through an ethanol series at the following concentrations: 70%, 90%, 100% (2×) each for 15 min (Step 5, Figure 2.14). This dehydration step is necessary to allow for the infiltration of tissue with epoxy resin that is non-water-soluble; this is essential for adequately sectioning the block, otherwise, polymerized blocks have a rubber-like texture (Dykstra 2012).

Table 2.2: Resin mixture used to embed corneal tissue.

Resin Component	Volume (ml)
Araldite monomer CY212	14
DDSA hardener	16
BDMA accelerator	0.6

Following dehydration, specimens were placed into propylene oxide (2×) for 15 min (Step 6, Figure 2.14), to remove any remaining ethanol. Specimens were then placed in a mixture of equivalent proportions of araldite resin and propylene oxide for one hour. This provides an intermediary step between highly volatile propylene oxide and the viscous resin (Step 7, Figure 2.14). Finally, the corneal tissue was embedded in araldite resin into six steps (Step 8, Figure 2.14), which comprised the following components: Araldite monomer CY212, dodecenyl succinic anhydride (DDSA) hardener, and benzyl dimethylamine (BDMA) accelerator in proportions according to the procedure established in our laboratory (Table 2.2). Adding DDSA hardener and BDMA accelerator to the Araldite monomer avoid an overly brittle block and speed the polymerization process, respectively (Hayat 2000). The resin infiltration process was carried out over two days with three changes of fresh resin per day at three hourly intervals - the tops were left off the specimen vials which were placed in a rotator in a fume hood at room temperature. Specimens were then placed into embedding moulds and orientated so that the central cornea produced full thickness transverse cross sections of the tissue. Polymerisation of the resin blocks was carried out at 60°C in an oven for 24 hours (Step 9, Figure 2.14). The polymerised resin blocks were then ready for ultrathin section collection on a Reichert-Jung Ultracut E (UCE) ultramicrotome (Optische Werke AG, Wien, Austria).

2.8.3 Sectioning and positive staining

Resin-embedded sample blocks were fixed into a UCE ultramicrotome specimen chuck. The resin block was then carefully trimmed with a razor blade to reveal the tissue. A small trapezoid shape block face was carefully created by removing excess resin around

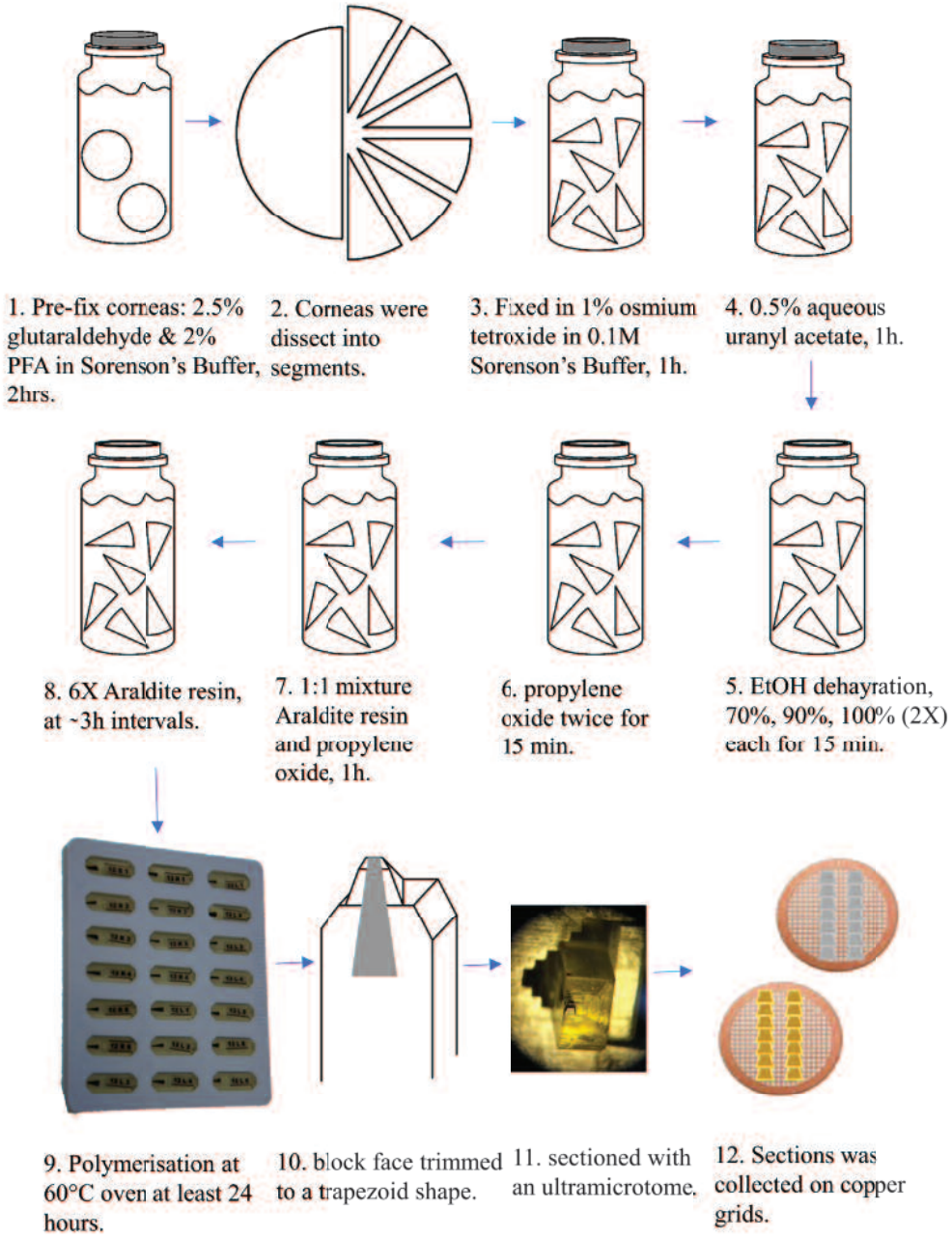

Figure 2.14: Specimen processing steps for transmission electron microscopy. The vial tops on step 5-8 were removed.

the tissue using a razor blade (Step 10, Figure 2.14). The block face was then polished using the UCE by rocking the blockface back and forth over a glass knife-edge until it was sufficiently smooth and reflective (Step 11, Figure 2.14)

Semi-thin sections (approximately 0.25 μm in thickness) were then taken using the UCE ultramicrotome to identify the exact area for TEM ultrastructural analysis using a glass knife made on a Leica EM KMR2 (Leica, Austria). The sections were collected by wire loop from a small water reservoir which was attached to the glass knife. Semi-thin sections were then transferred onto a droplet of water on a microscope slide. After evaporating the water droplet from the slide on a hot plate, the section was stained with a filtered solution of 1% toluidine blue on the hot plate for 1 minute, then washed with DW to remove any excess stain. The sections were then observed under light microscopy to identify the exact region of interest which was the full thickness of the central cornea showing all the corneal layers.

The surface of the block was trimmed further to a smaller trapezoid containing the exact region of interest. A diamond knife was then used to cut ultrathin ≈90 nm thick sections on the UCE for TEM analysis. The ultramicrotome was set to an automatic cutting speed of 1 mm/min and a 90 nm section thickness was selected ribbons of sections with silver and gold interference colours indicating they were ≈ 70 - 90 nm thick were collected on the surface of the diamond knife water reservoir (Step 12, Figure 2.14). The ribbon sections were then stretched using chloroform (Figure 2.15). This stretching is necessary to decompress the sections after cutting on the ultramicrotome. Ultrathin sections (3 - 4) were separated from the ribbons using an eyelash. These were then collected on either 3 mm 300 hex copper grids or on Pioloform support film 3 mm copper 2×1 mm slot grids.

Contrast enhancement with uranyl acetate and Reynolds lead citrate was carried out for prior to transmission electron microscope imaging. These positive staining solutions were all centrifuged at 14,500 × for 5 min and filtered with a 0.2 μm syringe filter, in order to remove any particulates which could contaminate the sections prior to use. At room temperature, the grids were placed sample side down onto the surface of 25 μm

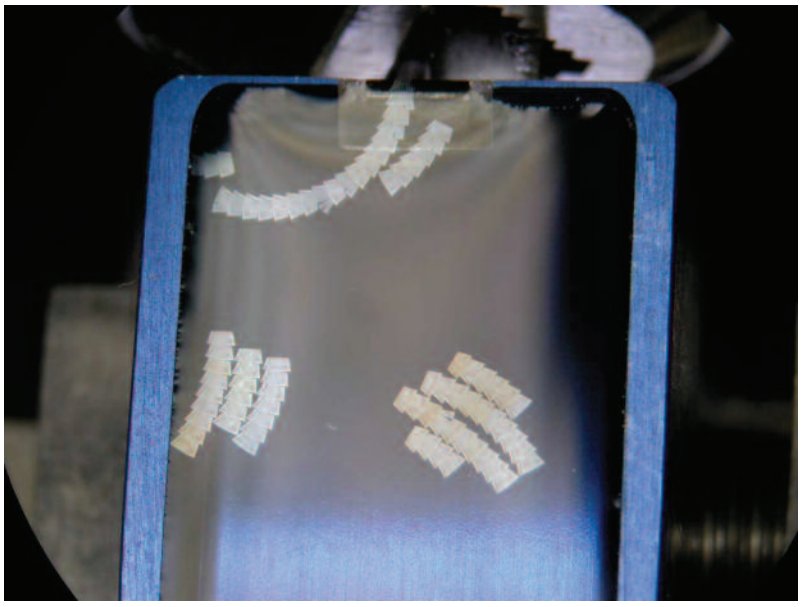

Figure 2.15: A diamond knife was used to obtain ultrathin sections on a UCE ultramicrotome, showing mostly silver and few golden ribbon of sections floating on the water surface.

drops of the stain, placed on parafilm or support film over filter paper. First, samples were stained for 20 minutes with 2% aqueous uranyl acetate, a brown opaque cover was placed over the samples to prevent any light from reacting with the light sensitive UA stain. Next, the samples were stained with Reynolds lead citrate for 7 minutes. NaOH pellets were positioned around the drops to reduce carbon dioxide reacting with the lead citrate which can form electron dense precipitate contamination on the sections. Between the two staining steps, the grids were washed by dipping the grid 20 times each in four cups containing filtered DW. The grids were then dried overnight on filter paper and were then ready for TEM analysis.

2.8.4 TEM Imaging

Grids were placed into a Transmission Electron Microscope (TEM) specimen holder which was then inserted into the TEM via the specimen port of the TEM (Figure 2.16). Electron microscopy was carried out on a Jeol 1010 transmission electron microscope (Jeol UK, Herts, UK), operating at 80 keV. Images were taken in Gatan imaging software (Gatan, Inc., Abingdon, UK) in gatan (.dm3) format, then converted to TIFF (.tif) format

to facilitate using these images in this thesis, Image J/Fiji program, publications, and presentations.

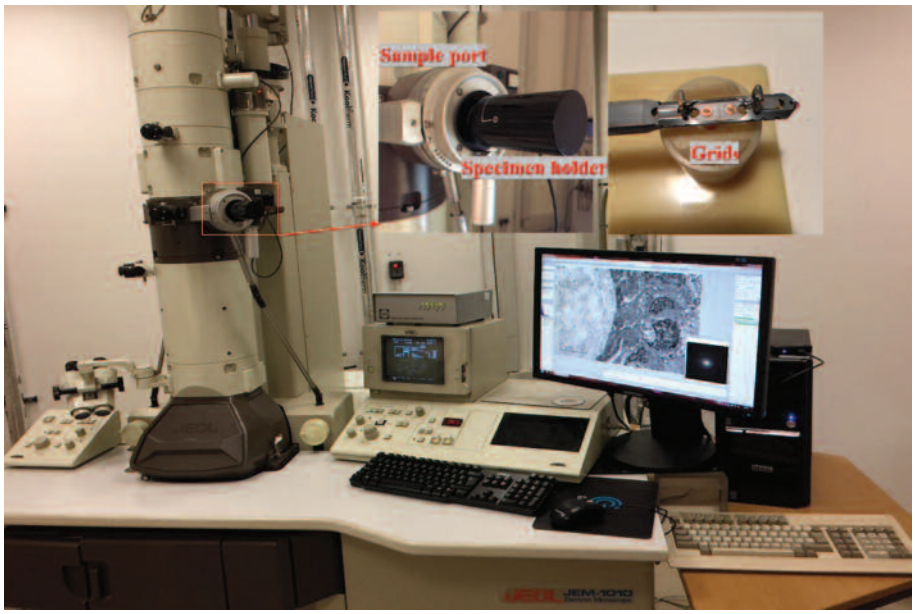

Figure 2.16: JEOL 1010 Transmission electron microscope. Grids were placed on specimen holder then into specimen port on Transmission Electron Microscope (TEM).

2.8.5 Image analysis

Sections 60 – 70 nm thick were collected as mentioned in section 8.3 to provide the minimum interference between lamella layers for better resolution of the image. The TEM images of a positively stained rabbit corneal collagen fibril obtained were digitised and displayed in 2D Viewer on a PC. Micrographs from cross-linking treatments and untreated corneas were processed with Image J/Fiji software ((Abramoff et al. 2004); https://imagej.nih.gov/ij/ accessed 22 November 2017) for analysing the fibril diameter and stain intensity in the anterior and posterior stroma (see Chapter 7). Image J could be provided with Fiji script editor with many bundled plugins, which was used in the standard scientific image analysis. The Image J/Fiji software could display, edit, analyse, process, save and print 8-bit, 16-bit and 32-bit binary images in grey or colour images. In this study the standard 8 bit grey images were used. The Image J/Fiji software were used to perform basic image processing for fibril diameter analysis and to create linear profile plots of the distribution of stain intensity along the axis of positively stained collagen fibrils from high

magnification micrographs (×20,000 - ×30,000).

Fibril diameter analysis

Image J/Fiji software was used to analyse the parts of the micrographs where the collagen fibrils were cut in cross-section, to determine the fibril diameter. First, the scale bar of the dataset was calibrated to 100 nm : 303 pixel. Next, the circular Fibril perimeters were marked manually with a computer mouse and measured with the help of the Image J/Fiji program. Only clearly defined borders of high contrast were marked and used in the analysis; profiles with low contrast and blurry borders were not circled. Only fibrils cut in cross-section were included in the analysis, with those cut at oblique angles being omitted from the study. As a matter of interest, the oblique sections could have been used because the shortest diameter in an ellipsoidal section is equal to the diameter of the corresponding circular section profile (Wollensak et al. 2004), but this was not necessary here as there were sufficient circular cross-sectioned fibrils in the micrographs analysed. This measurement was based on subjective eye detection to distinguish between the cross-section (circle fibrils) from the oblique angle (oval fibril) and a manual detection of the fibrils circumference (Figure 2.17). The diameter was then calculated on an Excel sheet directly from the circled area.

Stain intensity analysis

Using the Image J/Fiji program, the stain intensity was plotted from a longitudinal-section of collagen fibrils. After the image was calibrated, fibrils were selected on the basis of positive staining band clarity and least background contamination. A highlighted line (rectangle) was drawn over several D-periods along each selected fibril (Figure 2.18a). The stain intensity was integrated across the fibril and plotted as a function of the position along the fibril axis using the “plot profile” function. An example of the stain distribution from a single D-period is shown in Figure 2.18b. The stain intensity data were acquired for the entire usable length of the fibril.

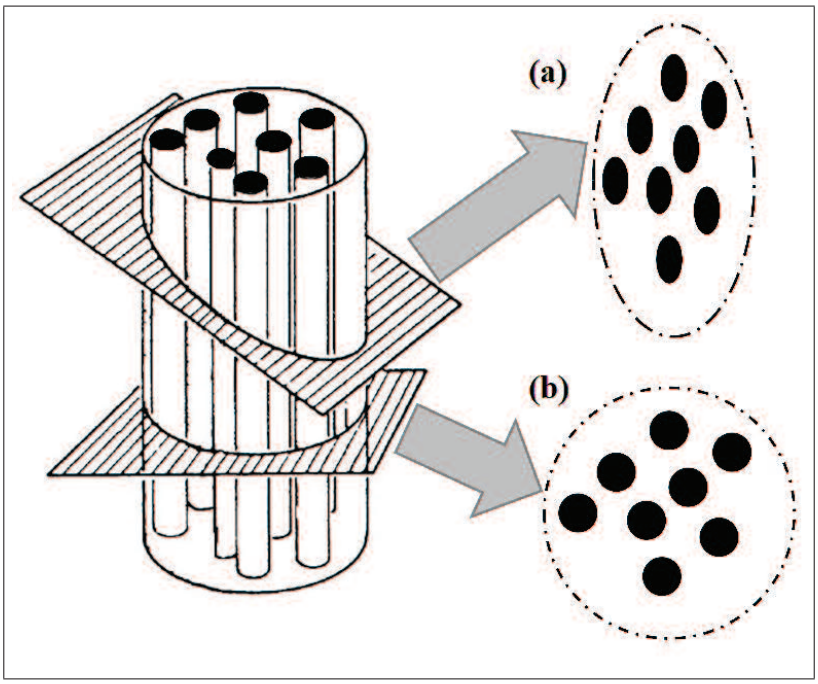

Figure 2.17: Cross-section through the fibrils. (a) Oblique angle sections were omitted from this study. (b) Perpendicular section to the fibrils with a circular shape in cross-section were included in the analysis. Adapted with permission from the copyright holder, Wolters Kluwer Health, Inc. (Wollensak et al. 2004). (License No: 4223690894294), Date: Nov 07, 2017.

The data were transferred to Excel spreadsheets and subdivided to a length of precisely one D-period with the same start and end positions, so that all D-period plots would include the same number of points taking into account the direction and polarities of the fibril. This dataset was defined as one exact D-period. The position along the axis within each D-period of the fibril was identified by the positive staining band (e.g. c1-b2-b1-a4-a3-a2-a1-e2-e1-d-c3-c2) (Chapman et al. 1990). In order to reduce noise, three D-period intensity profiles were averaged from each treatment group. Any background intensity gradient along the D-period was removed by applying a linear ramp to ensure that the intensity value of the first data point in the averaged profile was identical to the intensity value of the last data point. For comparison of the treatment groups, the averaged profiles needed to be correctly aligned. This was done by moving one plot stepwise past the one to which it was being compared until the best visual alignment of the staining bands was achieved.

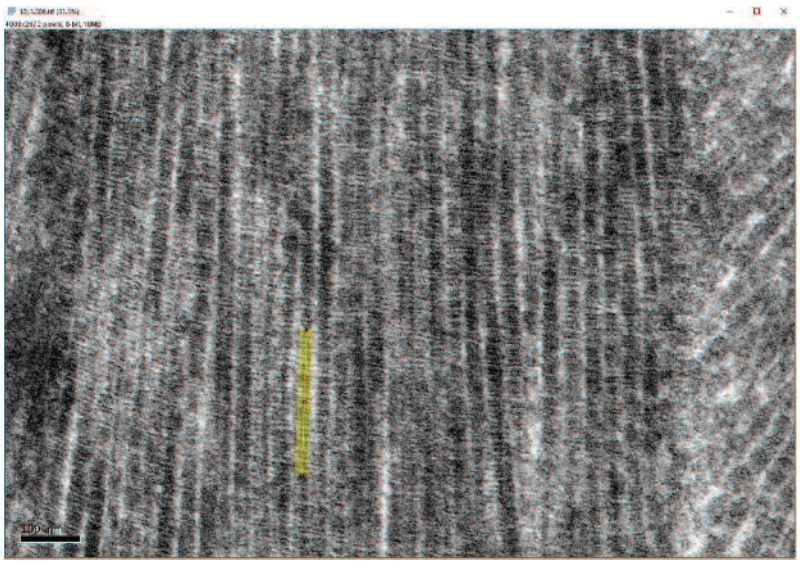

(a)

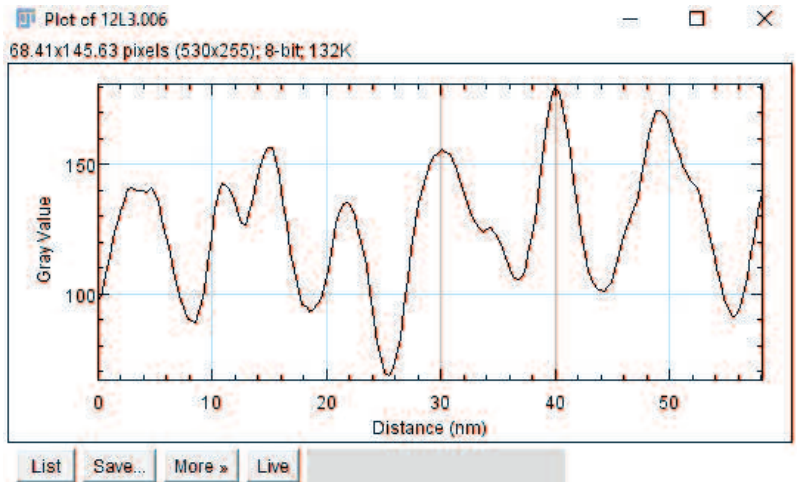

(b)

Figure 2.18: (a) Transmission electron micrograph of a positively stained rabbit corneal collagen fibril analysed using the Image analysis J/Fiji program. Fibrils were carefully chosen for use on the basis of positive staining band clarity. To extract an average band intensity distribution for each D-period, a rectangle (yellow) was drawn over several D-periods along the length of a fibril. The integrated axial stain intensity for the chosen region was then extracted using the "Plot Profile" function. (b) An example of the axial stain intensity distribution along approximately one D-period of the fibril obtained from the Image analysis J/Fiji program.

CHAPTER 3

STANDARD VERSUS ACCELERATED RIBOFLAVIN/ ULTRAVIOLET CORNEAL CROSS-LINKING: ENZYMATIC DIGESTION RESISTANCE AND BIOMECHANICAL STRENGTH.

Parts of this chapter were published as a laboratory science article in J Cataract Refract Surg 2015; 41:1989–1996. Published by Elsevier Inc. on behalf of ASCRS and ESCRS.

3.1 Introduction

The standard Dresden CXL procedure (SCXL) takes a minimum of one hour to achieve the desired clinical effect (Spoerl et al. 1998), as it requires removal of the corneal epithelium, a 20 - 30 minutes instillation of riboflavin eye drops (to achieve a homogeneous stromal uptake of riboflavin (Gore et al. 2014)) and a 30 minutes exposure to 365 nm UVA irradiation at 3 mW/cm^2. Recently, in an attempt to shorten patient treatment time, accelerated CXL protocols (ACXL) have been introduced. The concept of ACXL is based on the Bunsen-Roscoe law of reciprocity (Bunsen et al. 1862) and assumes that increasing UVA fluence while simultaneously reducing the exposure time (to ensure that the total energy dose remains unchanged), will produce the same cross-linking effect as that of the SCXL protocol (Schumacher et al. 2012; Wernli et al. 2013). Numerous clinical studies demonstrate the safety and efficacy of the ACXL procedure in the short term, with no reported adverse effects and a significant reduction in both topographic keratometry and corrected distance acuity at up to 46 months follow-up (Cinar et al. 2014; Hashemi et al. 2015; Kanellopoulos 2012; Kymionis et al. 2017; Ng et al. 2016; Waszczykowska et al. 2015). However, it is unclear if the same amount of tissue is cross-linked with the ACXL and SCXL procedures, and the long-term effects of different cross-linking protocols, in terms of keratoconus stability, remains uncertain.

3.2 Research aim

This study was undertaken to compare the efficacy of two ACXL protocols (9 mW/cm^2 for 10 minutes and 18 mW/cm^2 for 5 minutes) with that of the SCXL procedure (3 mW/cm^2 for 30 minutes), in terms of their ability to enhance the enzymatic resistance and biomechanical properties of the cornea.

3.3 Materials and methods

3.3.1 Treatment groups

The treatment and control groups described in the methods for this chapter are detailed below and summarized in Table 3.1.

1. **Untreated controls** — complete removal of the corneal epithelium using a single edged razor blade, followed by a detailed visual inspection of the tissue to confirm that no damage had occurred to the underlying stroma. These corneas received no further treatment.

2. **Dextran-only controls** — epithelial removal (as described above) followed by application of 20% dextran T500 eye drops comprising 1g of Dextran T500 (Pharmacosmos, Holbaek, Denmark) dissolved in 5 ml of PBS. The solution was applied to the cornea every 5 minutes for 30 minutes with no UVA exposure.

3. **Riboflavin-only controls** — epithelial removal followed by application of commercial riboflavin eye drops comprising 0.1% solution riboflavin-5-phosphate in 20% dextran T-500 solution (Mediocross D, Peschk Meditrade, Huenenberg, Switzerland). The riboflavin eye drops were applied every 5 minutes for 30 minutes with no UVA exposure.

4. **"Standard" 3 mW/cm^2 CXL protocol (SCXL 3 mW)** — epithelial removal followed by application of commercial riboflavin eye drops (Mediocross D). Riboflavin eye drops were applied every 5 minutes for 30 minutes before exposure of the central 9 mm region of the cornea to UVA light with a fluence of 3 mW/cm^2 for 30 minutes (CCL-365 Vario™ cross-linking system Peschkmed, Huenenberg, Switzerland). Riboflavin eye drops were re-applied at 5 minute intervals throughout the period of irradiation.

5. **Accelerated 9 mW/cm^2 CXL protocol (ACXL 9 mW)** — epithelial removal followed by application of commercial riboflavin eye drops (Mediocross D) every 5 minutes for 30 minutes, followed by a 10 minutes exposure of the central 9 mm region to UVA light

with a fluence of 9 mW/cm^2. Riboflavin eye drops were re-applied at 5 minute intervals throughout the period of irradiation.

6. **Accelerated 18 mW/cm^2 CXL protocol (ACXL 18 mW)** — epithelial removal followed by application of commercial riboflavin eye drops (Mediocross D) every 5 minutes for 30 minutes, followed by a 5 minutes exposure of the central 9 mm region to UVA light with a fluence of 18 mW/cm^2.

Table 3.1: A summary of the treatment groups and their controls

Type	Protocol	Epithelium	Eye Drops	Fluency (mW/cm^2)	UVA time (min)	UV-A Dose (J/cm^2)
Control	Untreated	Epi-off	N/A	N/A		
	Dextran only		dextran 20% for 30 min			
	Riboflavin only		Ribo. 0.1% /dextran 20% for 30 min			
Treated	SCXL 3 mW			3	30	5.4
	ACXL 9 mW			9	10	
	ACXL 18 mW			18	5	

3.3.2 Tissue preparation: human donor tissue

Twelve human donor corneas with intact scleral rim were used in this study. The tissue was obtained from NHSBT UK eye banks in accordance with the tenets of the Declaration of Helsinki. The corneas were no longer suitable for corneal graft due to a low endothelial cell count and to minimise the wastage of them, they were provided for experimental research. Therefore, a small sample size was involved in this experiment. The corneas were donated by eleven different donors (six men, five women) of average age 73 ± 6 (65 – 81) years and stored in culture medium (Eagle's MEM buffered with HEPES and containing 26 mM

sodium bicarbonate, 2% fetal bovine serum, 2 mM L-glutamine, penicillin, streptomycin, and amphotericin B) at 34°C for approximately 1 - 5 months (2.76 ± 2.1) prior to use. The corneo-scleral disks were assigned according to age and equally divided into four treatment groups with no pair allocated in the same group (detailed in Section 3.3.1): Untreated, SCXL 3 mW, ACXL 9 mW and ACXL 18 mW. The ages of the corneas in each treatment group were as follows: Untreated (66, 78, and 80 years old), SCXL 3 mW (66, 71, and 73 years old), ACXL 9 mW (67, 74, and 81 years old) and ACXL 18 mW (65, 73, and 80 years old). To ensure corneal curvature was maintained during the respective treatments, each cornea was centred and mounted by its scleral rim in an artificial anterior chamber (Baron, Katena Products, Inc, Denville, New Jersey, USA) and inflated from behind with MEM buffer (Figure 3.1). When applicable, measurements of central corneal thickness were performed pre-and post-epithelium removal, and pre- and post-treatment, using a Pachette2™ Ultrasonic Pachymeter (DGH Technology, Exton, USA). Immediately after treatment each sample was wrapped tightly in catering film and stored at 5°C until all treatments were accomplished.

Figure 3.1: The cornea was centred in an artificial anterior chamber and mounted by its scleral rim. MEM buffer was injected behind the cornea to preserve its curvature during treatment.

3.3.3 Tissue preparation: porcine abattoir tissue

One hundred and eighteen fresh whole porcine eye globes were obtained from a local European Community licensed abattoir within 6 - 8 hours post-mortem. All corneas were visually inspected and found to be free of damage, visual autolytic changes, haze, or scratches. The forty eyes destined for biomechanical testing were randomly and equally divided into five treatment groups (detailed in section 3.3.1): Untreated, Riboflavin-only, SCXL 3 mW, ACXL 9 mW and ACXL 18 mW. The seventy-eight porcine eyes required for enzyme digestion studies were randomly and equally divided into six treatment groups: Untreated, Dextran only, Riboflavin only, SCXL 3 mW, ACXL 9 mW and ACXL 18 mW. When applicable, central corneal thickness measurements were performed pre- and post-epithelium removal, and pre- and post-treatment, using a Pachette2™ Ultrasonic Pachymeter (DGH Technology, Exton, USA). Once the treatments were achieved, the corneas were dissected from each globe with a 2 - 5 mm scleral rim, wrapped tightly in catering film and refrigerated at 5°C.

3.3.4 Enzyme digestion studies: porcine and human corneas

On completion of the treatments, a disposable skin biopsy punch (Kai Europe GmbH, ref BP-80F, Solingen, Germany) was used to trephine an 8 mm corneal disk from the centre of each of the seventy-eight porcine and twelve human corneas prepared for enzyme digestion studies. The corneal disks were weighed, then placed in individual plastic tubes, each containing 5 ml of pepsin solution made up from 1 g of 600–1200 U/mg pepsin from porcine gastric mucosa (Sigma-Aldrich, Dorset, UK) in 10 ml 0.1M HCl at pH 1.2. The human corneal disks had five changes of fresh pepsin approximately every 40 days during the digestion period as enzyme activity decays over time. The corneal disks (in pepsin digest solution were then incubated in a water bath (VwB6, Leuven, Germany) at a temperature of 23°C. Following a preliminary study investigating the effect of temperature on the total digestion time of cross-linked and non-cross-linked porcine corneal disks, 23°C was identified as the optimum temperature for detecting differences of one day or more

between treatment groups (Appendix D).

As detailed in Chapter 2, section 2.3, the diameter of the anterior surface of eight of the thirteen porcine corneal disks from each group, and all twelve human corneal disks, were measured daily using digital calipers. These measurements continued until the tissue could no longer be distinguished from the surrounding pepsin solution (even under microscopic examination), at which point the tissue was considered to have undergone 'total digestion'. In order to further assess the effect of each treatment on enzymatic resistance, the remaining five porcine corneal disks from each group were removed from the pepsin solution after 12 days of digestion and placed in a 60°C oven until a constant dry weight was obtained. The average corneal dry weight (which represents the mass of undigested tissue) was calculated for each group (as described in Chapter 2).

3.3.5 Biomechanical testing studies: porcine corneas only

Within 10 minutes of treatment, a double-blade cutter was used to cut a strip of tissue (measuring 5 mm in width) along the vertical meridian of each of the forty porcine corneas prepared for biomechanical testing. After cutting, the corneal strip was secured within the clamps of an enclosed sample holder and attached to the extensometer. A cotton pad soaked in distilled water was placed within the sample enclosure directly beneath the corneal strip to maintain the hydration of the tissue during testing. Preliminary studies examining the effect of different sample environments on corneal hydration identified this as the method of choice for maintaining hydration, since it resulted in a negligible 0.4% reduction in tissue water content over a typical 35 minutes biomechanical testing period (Appendix F). Further details relating the method of strip cutting and tensile testing are provided in Chapter 2.

Stress–strain measurements

Stress–strain measurements were obtained using a Lloyd extensometer (Lloyd Instruments Ltd., UK) with a 20 Newton force cell. Initial values required to perform a stress–strain test, were inserted as shown in (Table 3.2). Prior to testing each tissue strip, three preconditioning cycles were performed using a force of 1 N. This was followed by a tensile test at a velocity of 1 mm/min. During the measurement, the load, strain, extension and stress were automatically recorded. Then in MATLAB, the stress–strain curve was fitted to an exponential function (A and B) in low strain nonlinear elasticity region from 2% to 8% (for more information see chapter 2). The sample numbers used for each aspect of the biomechanical testing and enzyme digestion studies are shown in Table 3.3.

Table 3.2: The values required by Nexygen 4.1 to perform a stress–strain test. The bold row indicates parameter values that were different for each corneal strip.

Parameter	**Logged value**
Speed	1 mm/min
Specimen dimensions: Gauge length Breadth Thickness	 6 mm 5 mm 0.496 – 0.743 ± 0.071 mm
Maximum force	9.5 N

3.3.6 Statistical evaluation

All data are reported as mean ± standard deviation (SD). Statistical comparisons between means were carried out using one-way ANOVA followed by Bonferroni multiple comparisons between groups also using paired samples t-test. All statistical analyses were performed with the Statistical Package for the Social Sciences (IBM SPSS Statistics 20, New York, USA). The statistical significance of difference was taken as $p \leq 0.05$.

Table 3.3: Treatment groups and sample numbers

Sample number (n)				
Technique	**Biomechanical testing**	**Enzyme digestion studies**		
		Daily measurements of disk diameter		**Day 12 dry weight measurements**
Protocol/species	Porcine	Human	Porcine	Porcine
Untreated	8	3	8	5
Dextran only	0	0	8	5
Riboflavin only	8	0	8	5
SCXL 3 mW	8	3	8	5
ACXL 9 mW	8	3	8	5
ACXL 18 mW	8	3	8	5

3.4 Results

3.4.1 Effect of CXL on corneal thickness

Measurements of central corneal thickness, recorded during the preparation of human and porcine corneas for enzyme digestion studies, are shown in Table 3.4. As a result of long term storage in culture medium, the pre-treatment thickness of the human corneas far exceeded physiological levels and was also greater than that of the porcine corneas ($p < 0.0001$). For each species, no statistically significant differences in corneal thickness were observed between the groups either pre- or post-epithelial removal. However, in the porcine corneas there was a significant reduction in corneal thickness following administration of dextran-containing solutions in both the dextran-only group and the riboflavin-only group ($p < 0.0001$). Application of the riboflavin solution (containing dextran) to the de-epithelialised cornea resulted in a significantly greater reduction in corneal thickness than application of the dextran-only ($p < 0.001$). In both porcine and human corneas, a significant reduction in corneal thickness was also observed following CXL treatments (p

< 0.0001). However, as the post-treatment thickness of the SCXL and ACXL irradiated porcine corneas did not differ from that of the non-irradiated riboflavin treated porcine corneas (p = 1.00), the corneal thinning observed after CXL may be attributed to the application of riboflavin rather than to UVA exposure (Table 3.4). These findings were supported by measurements recorded during the preparation of porcine corneas for biomechanical testing, which showed a significant decrease in tissue thickness after riboflavin application but no further change in corneal thickness as a result of UVA irradiation (p = 1.00) (Figure 3.2).

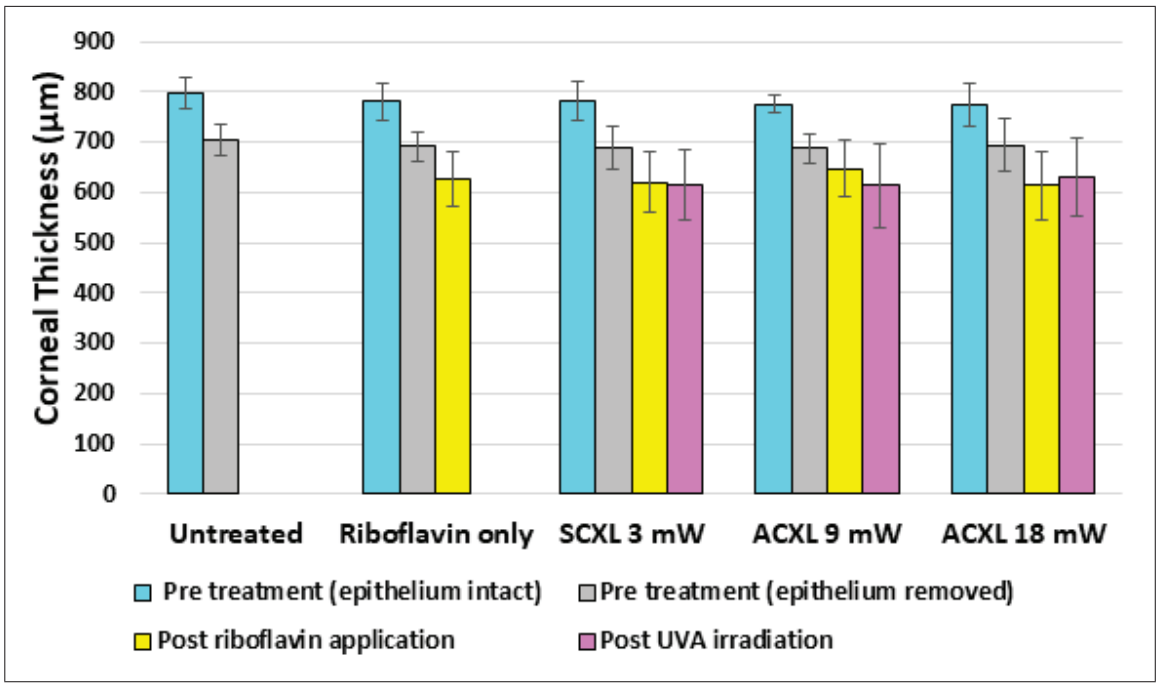

Figure 3.2: Corneal thickness measurements recorded during the preparation of porcine corneas for biomechanical testing. Error bars show standard deviation. Cross-linking treatments: Standard cross-linking (SCXL 3 mW); accelerated cross-linking (ACXL 9 mW and ACXL 18 mW).

Table 3.4: Pre- and post-treatment central Corneal Thickness measurements of human and porcine corneas prepared for enzyme digestion studies.

Type	Central corneal thickness			
	Pre epithelial removal (µm)	Post epithelial removal (µm)	Post treatment (µm)	Change* %
Human corneas				
1) Untreated	1003 ± 32	951 ± 35	N/A	N/A
4) SCXL 3 mW	965 ± 48	919 ± 50	784 ± 84	-17.3
5) ACXL 9 mW	1001 ± 32	952 ± 32	847 ± 33	-12.4
6) ACXL 18 mW	1019 ± 7	976 ± 10	768 ± 55	-27
Porcine corneas				
1) Untreated	816 ± 48	724 ± 47	N/A	N/A
2) Dextran only	827 ± 38	714 ± 36	593 ± 38	-17
3) Riboflavin only	787 ± 45	688 ± 44	520 ± 41	-24.5
4) SCXL 3 mW	802 ± 46	702 ± 46	508 ± 37	-27.7
5) ACXL 9 mW	819 ± 32	714 ± 35	517 ± 28	-27.6
6) ACXL 18 mW	811 ± 33	712 ± 35	501 ± 32	-29.6

*Percentage change from corneal thickness post epithelial removal to post treatment.

3.4.2 Observations during the digestion process

In the porcine corneas, an approximately 10-fold increase in the thickness of the corneal disk was observed in all cases within 24 hours of submersion in the pepsin digest solution. This increase in corneal thickness occurred as a result of stromal swelling in the posterior-anterior direction (Figure 3.3b). During swelling, the corneal disk assumed a cylindrical shape but after one week of digestion, the anterior portion of each treated and untreated

specimen separated from the posterior portion. Once detached, the posterior stroma was rapidly digested (within 10 days). The anterior stromal disk persisted considerably longer (particularly in the CXL treated corneas) and maintained its form sufficiently to obtain reliable measurements of its changing diameter during the digestion process.

The thickness of the human corneal disks increased about 7-fold within 24 hours of submersion in pepsin digest solution as a result of swelling in the posterior-anterior direction (Figure 3.4). However, unlike the porcine corneas, the swollen human corneal disks assumed a mushroom shape whereby the diameter of the posterior surface of the cornea became notably smaller than that of the anterior. Further to this, the posterior portion of the cornea did not separate from the anterior portion at any stage of the digestion process.

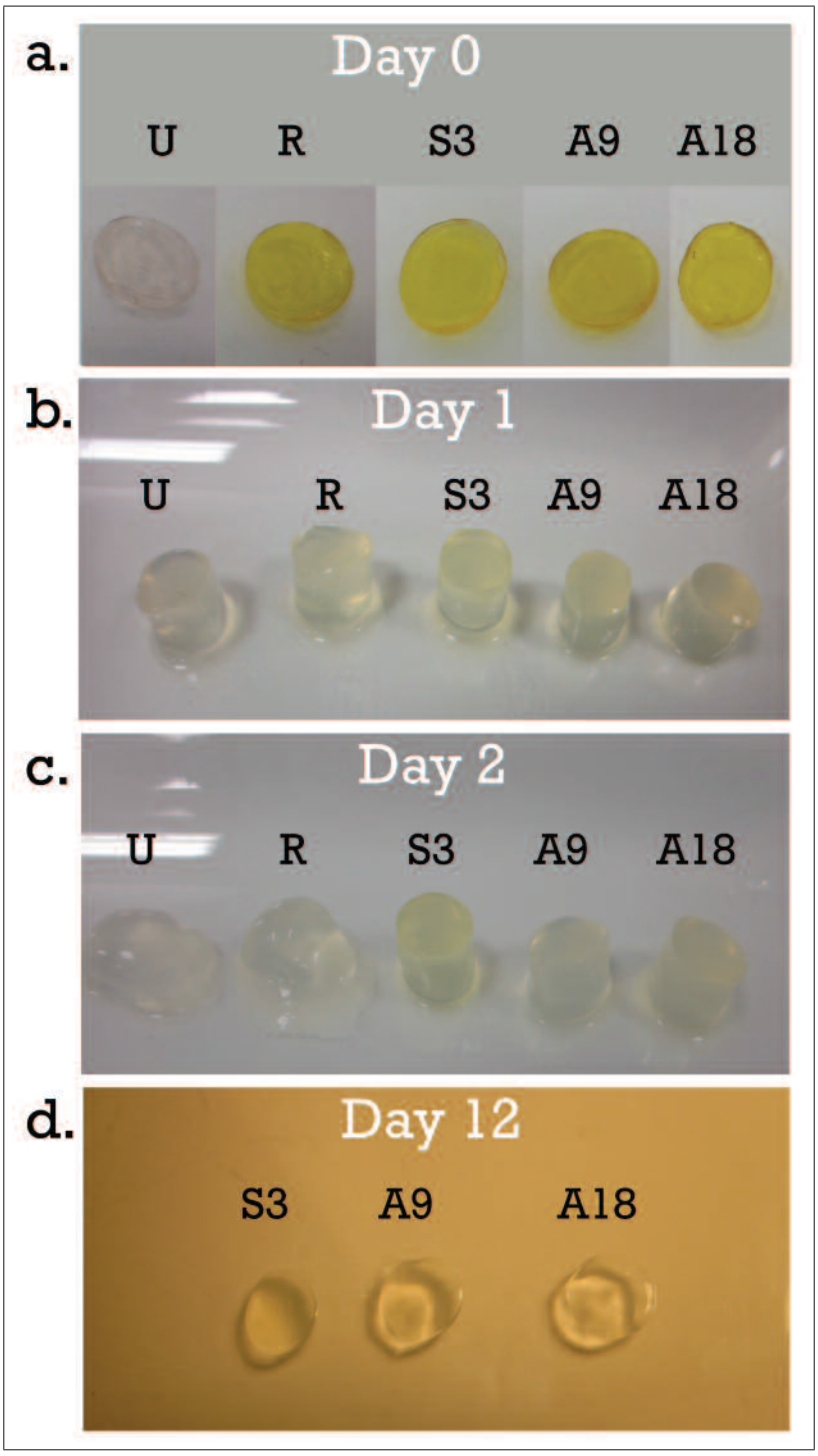

Figure 3.3: Porcine corneal disks at various stages of digestion. Each panel shows photographs of untreated (U), riboflavin-only (R), SCXL 3 mW (S3), ACXL 9 mW (A9), and ACXL 18 mW (A18) treated corneas before (a) and after 1 (b), 2 (c) and 12 (d) days of immersion in pepsin digest solution. All corneal disks are shown to be swollen after 1 day in pepsin digest solution (b). After 2 days of digestion, the anterior curvature has been lost in the untreated corneas but remains intact in the cross-linked corneas (c). After 12 days, all non-irradiated disks have been completely digested and only the anterior portion of the cross-linked corneas remain.

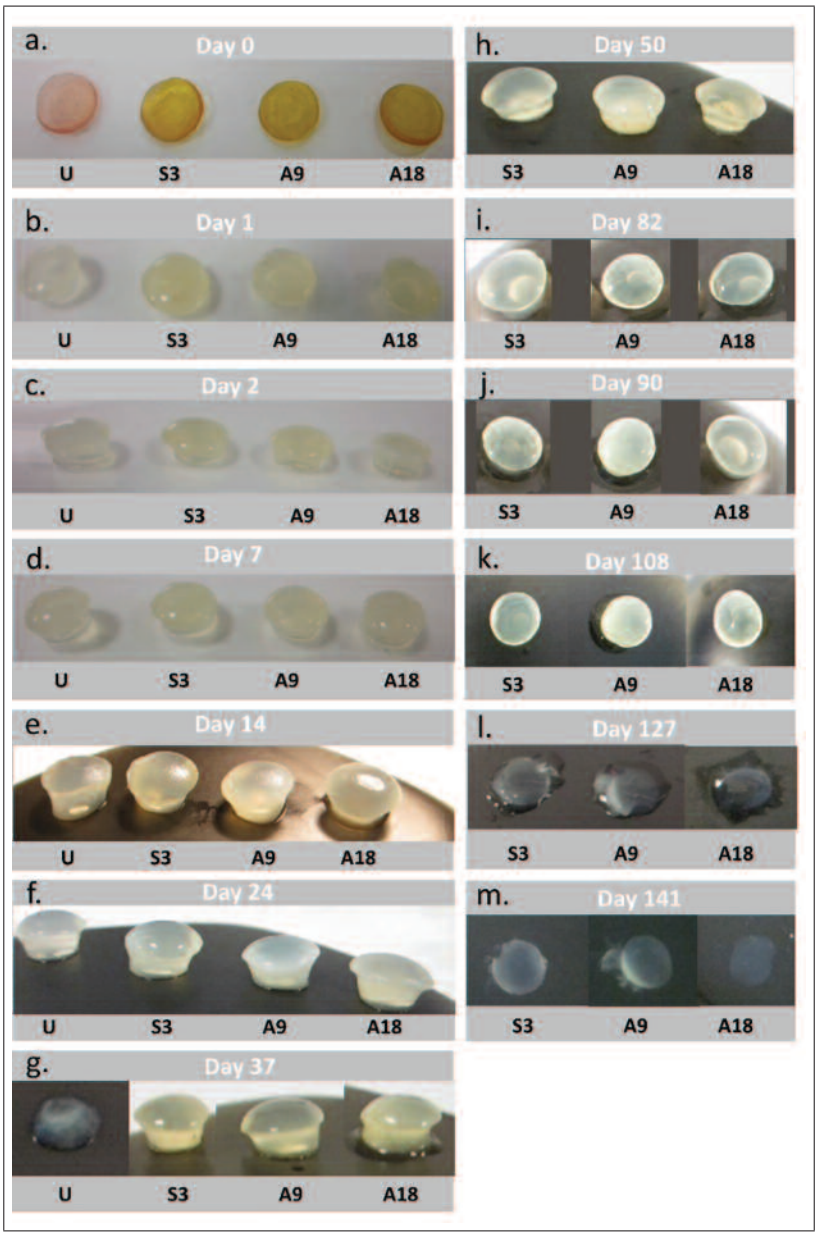

Figure 3.4: Human corneal disks at various stages of digestion. Each panel shows photographs of untreated (U), SCXL 3 mW (S3), ACXL 9 mW (A9), and ACXL 18 mW (A18) treated corneas before (a) and after 1 (b), 2 (c), 7 (d), 14 (e), 24 (f), 37 (g), 50 (h), 82 (i), 90 (j), 108 (k), 127 (l), and 141 (m) days of immersion in pepsin digest solution. All corneal disks are shown to be swollen after 1 day in pepsin digest solution (b). After 37 days, the untreated disks have been almost completely digested and by 50 days they have disappeared, whereas the cross-linked corneas remain intact (h). The anterior and posterior portion of the human corneal disks did not detach, however, the posterior portion digested earlier than anterior and showed almost a complete posterior digestion at the final stages of the digestion process (day 37 in the untreated corneas (g) and day 127 in the cross-linked corneas (l)).

3.4.3 Effect of CXL on enzymatic resistance: rate of digestion and total digestion time

Figure 3.5 shows the summed diameters of eight porcine corneal disks within each treatment group as a function of incubation time in pepsin solution. Statistical analysis revealed no significant difference in either the average porcine corneal disk diameter of non-irradiated specimens (untreated, dextran-only and riboflavin-only) at any time point during digestion or in the time taken for complete digestion to occur (Table 3.5). Similarly, in the irradiated specimens, no significant differences in these parameters were detected between porcine specimens treated with SCXL 3 mW, ACXL 9 mW or ACXL 18 mW. The diameters of the SCXL and ACXL treated corneas were however significantly larger than those of the non-irradiated specimens at all daily time points after day 8 ($p < 0.0001$) (Figure 3.5), and the time required for complete digestion to occur was significantly longer ($p < 0.0001$) (Table 3.5). By day 12, all non-irradiated porcine corneas had been completely digested but the average diameter of the CXL treated porcine eyes had decreased by only 27.2%, 27% and 26.6%, in the SCXL 3 mW, ACXL 9 mW and ACXL 18 mW groups respectively.

Figure 3.6 shows the summed diameters of three human corneal disks within each treatment group as a function of incubation time in pepsin solution. Enzymatic resistance was significantly enhanced in all of the cross-linked human corneas at all daily time points after day 35 compared to the untreated controls ($p < 0.0001$). Complete digestion of all untreated human corneas had occurred by day 46, whereas at this same time point the average diameter of the CXL treated human eyes had decreased by only 23.2%, 22.8% and 27.1%, in the SCXL 3 mW, ACXL 9 mW and ACXL 18 mW groups respectively. However, the SCXL human corneal disks completed their enzymatic digestion 8 days and 10 days later than ACXL 9 mW and ACXL 18 mW, correspondingly. Therefore, the SCXL protocol resulted in a greater increase in enzymatic resistance than the ACXL 9 mW and ACXL 18 mW protocols ($p < 0.0001$).

The untreated human corneas took significantly longer to digest than the untreated

porcine eyes ($p < 0.0001$). In human corneas, the time required for cross-linked specimens to undergo complete digestion was ≈3.5 times longer than their untreated controls, whereas for the porcine corneas the cross-linked specimens took only ≈2.4 times longer to digest than the untreated controls.

Table 3.5: Time taken for the complete digestion of treated and untreated human and porcine corneas.

Type	Time taken for complete digestion (days)			
	Minimum	**Maximum**	**Average (± SD)**	**Normalized digestion time**
Human corneas				
Untreated	45	46	45.5 ± 0.58	0.28
SCXL 3 mW	183	185	184.3 ± 0.96	1.00
ACXL 9 mW	177	178	177.3 ± 0.5	0.96
ACXL 18 mW	175	176	175.5 ± 0.58	0.95
Porcine corneas				
Untreated	10	11	10.5 ± 0.55	0.42
Dextran-only	10	11	10.5 ± 0.55	0.46
Riboflavin-only	9	11	9.83 ± 0.75	0.42
SCXL 3 mW	24	26	24.7 ± 1.03	1.00
ACXL 9 mW	23	26	24.7 ± 1.03	1.00
ACXL 18 mW	24	27	24.8 ± 0.98	1.00

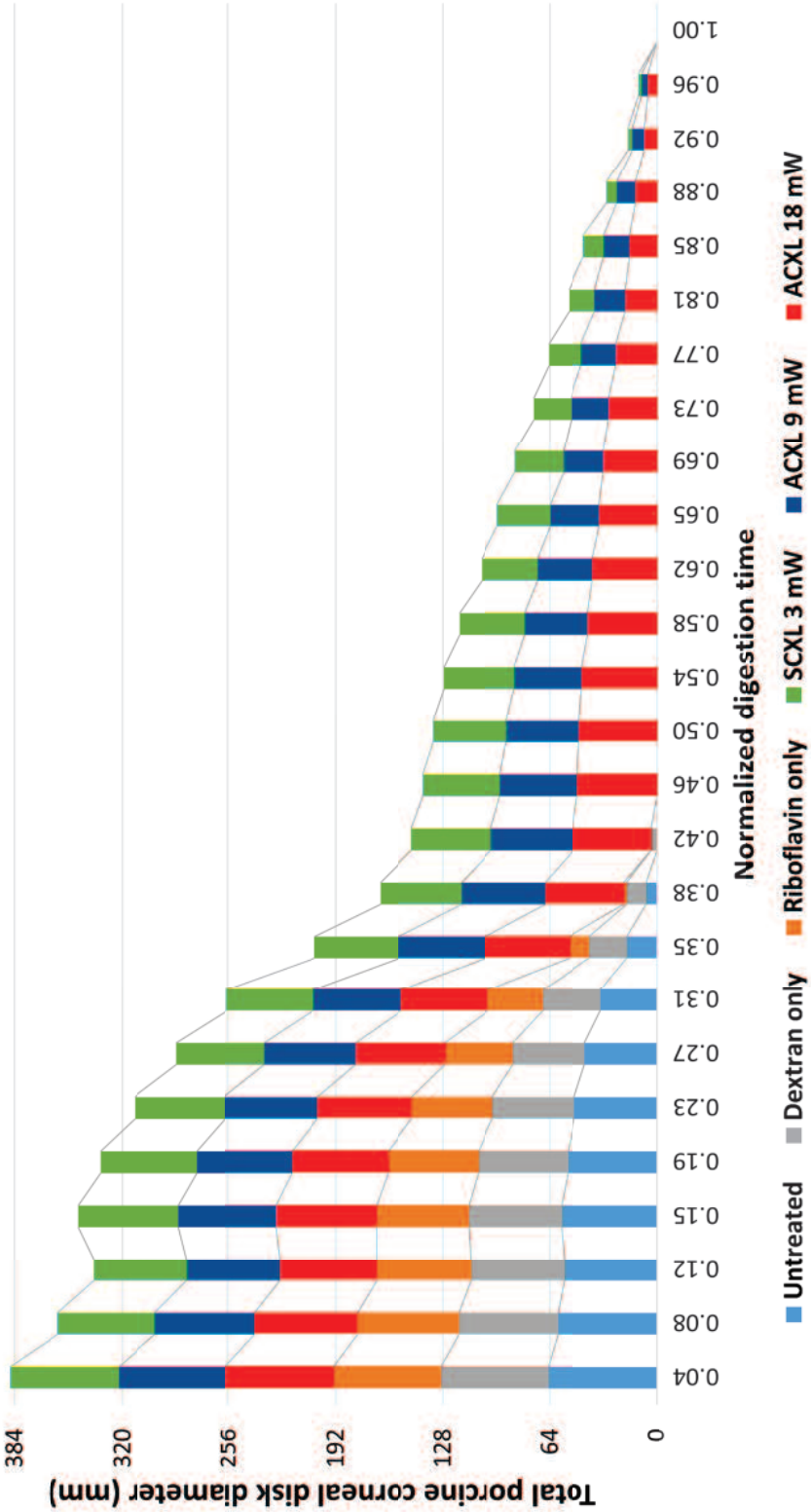

Figure 3.5: Observation during digestion of accelerated CXL treatments on porcine corneas. The summed diameter of all porcine corneal disks (n = 8) within each treatment group shown as a function of time in pepsin digest solution. The digestion time for each treatment group has been normalized against the time taken for the standard SCXL group to undergo complete digestion. Cross-linking treatments: Standard cross-linking (SCXL 3 mW); accelerated cross-linking (ACXL 9 mW and ACXL 18 mW).

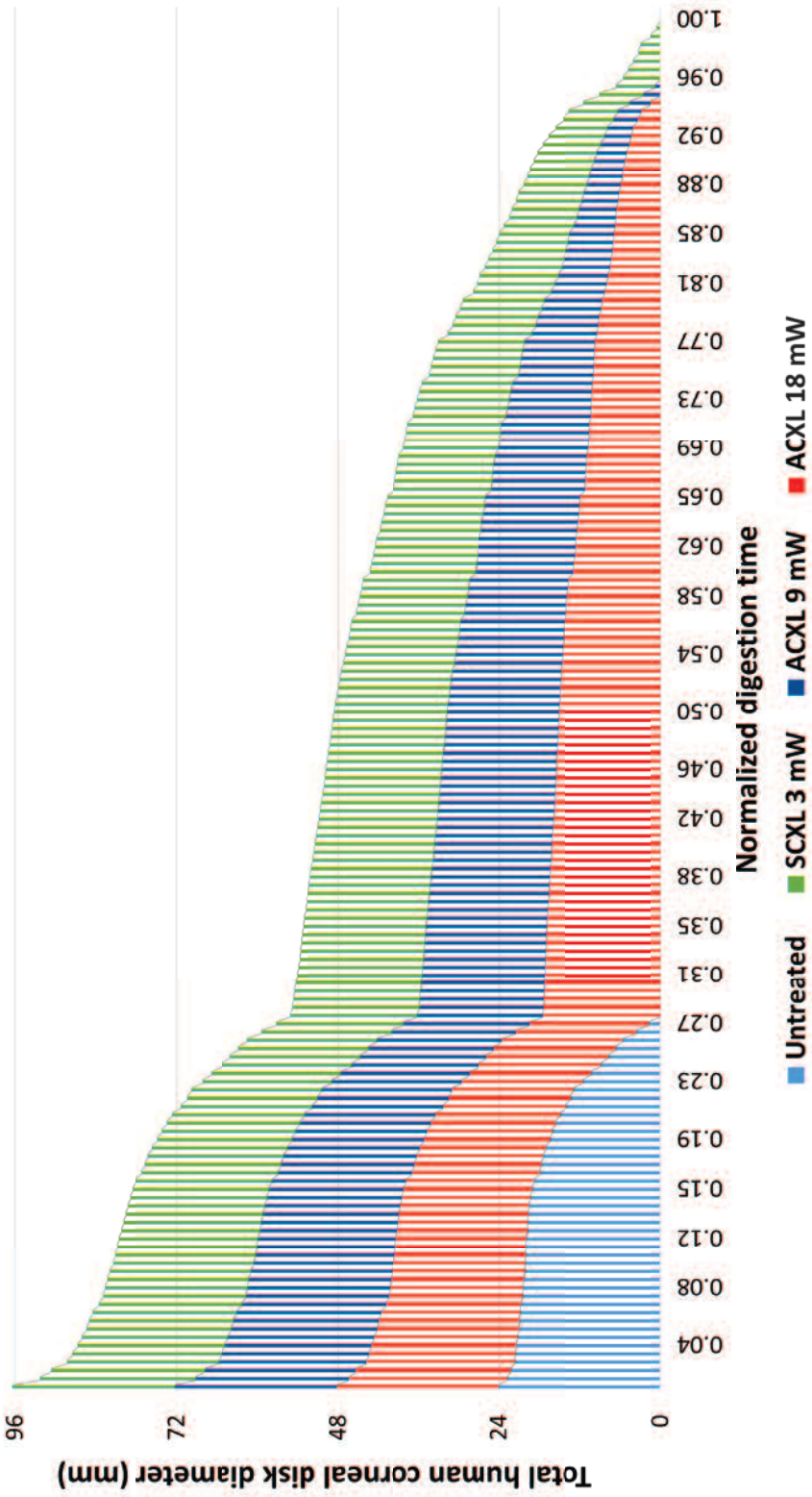

Figure 3.6: Observation during digestion of accelerated CXL treatments on human corneas. The summed diameter of all human corneal disks (n = 3) within each treatment group shown as a function of time in pepsin digest solution. The digestion time for each treatment group has been normalized against the total time of the standard SCXL group. Cross-linking treatments: Standard cross-linking (SCXL 3 mW); accelerated cross-linking (ACXL 9 mW and ACXL 18 mW).

3.4.4 Effect of CXL on enzymatic resistance: residual stromal mass at day 12

At day 12, the non-irradiated porcine corneas had undergone complete digestion, whilst the anterior stroma of the irradiated specimens remained intact. As a result, measurements of corneal disk dry weights at 12 days showed a statically significant difference between the irradiated and non-irradiated specimens ($p < 0.0001$). Further statistical differences were detected between the irradiated corneas treated with SCXL 3 mW, ACXL 9 mW or ACXL 18 mW ($p < 0.0001$) (Figure 3.7). The SCXL 3 mW group had a statistically higher average dry weight than the ACXL 9 mW and ACXL 18 mW groups ($p < 0.0001$), and the ACXL 9 mW group had a higher dry weight than the ACXL 18 mW group ($p < 0.003$).

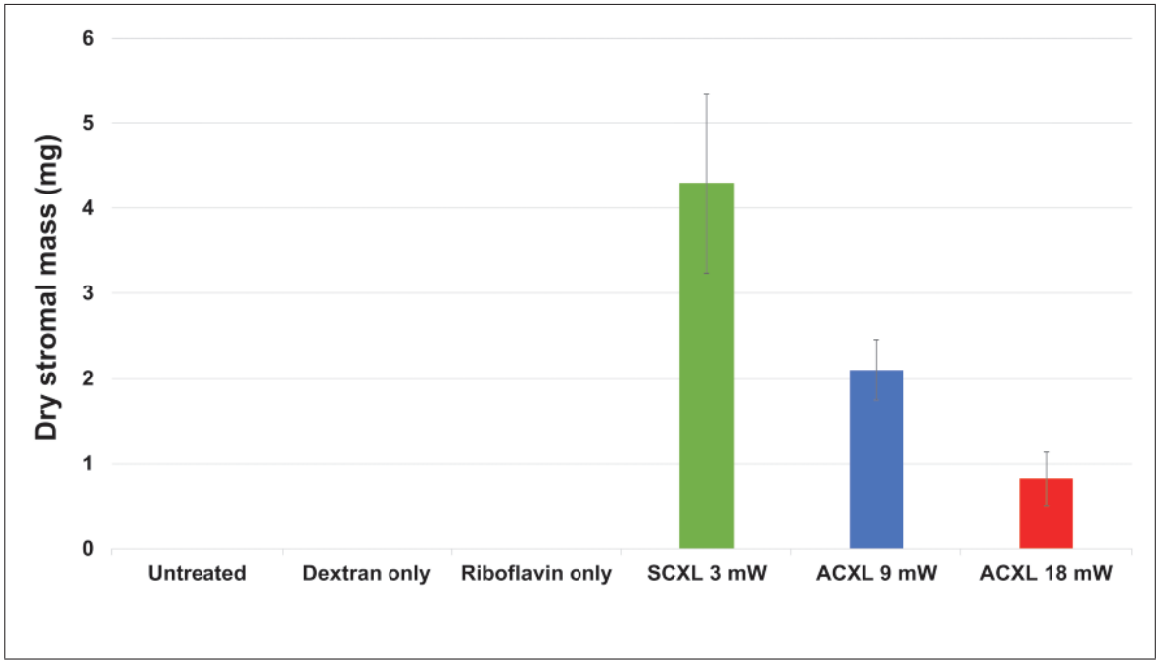

Figure 3.7: Average stromal dry weight of porcine corneal disks treated with SCXL, ACXL 3 mW, ACXL 9 mW and ACXL 18 mW, after 12 days of digestion. Error bars show standard deviation. Cross-linking treatments: Standard cross-linking (SCXL 3 mW); accelerated cross-linking (ACXL 9 mW and ACXL 18 mW).

3.4.5 Extensometry: stress-strain curves

Stress-strain fitted curves were plotted for all control and treatment groups and the general trend of the curves was examined in term of stress/strain ratio (Figure 3.8). Samples that underwent CXL treatment showed a higher average stress:strain ratio than non-cross-linked samples ($p < 0.01$). Although the stress-strain curves showed a negative trend on the curves with increasing UVA light intensity, there was no significant difference between the treated groups. This would imply that these samples had increased in stiffness as a result of their respective treatments to the same extent as the samples treated with the standard procedure.

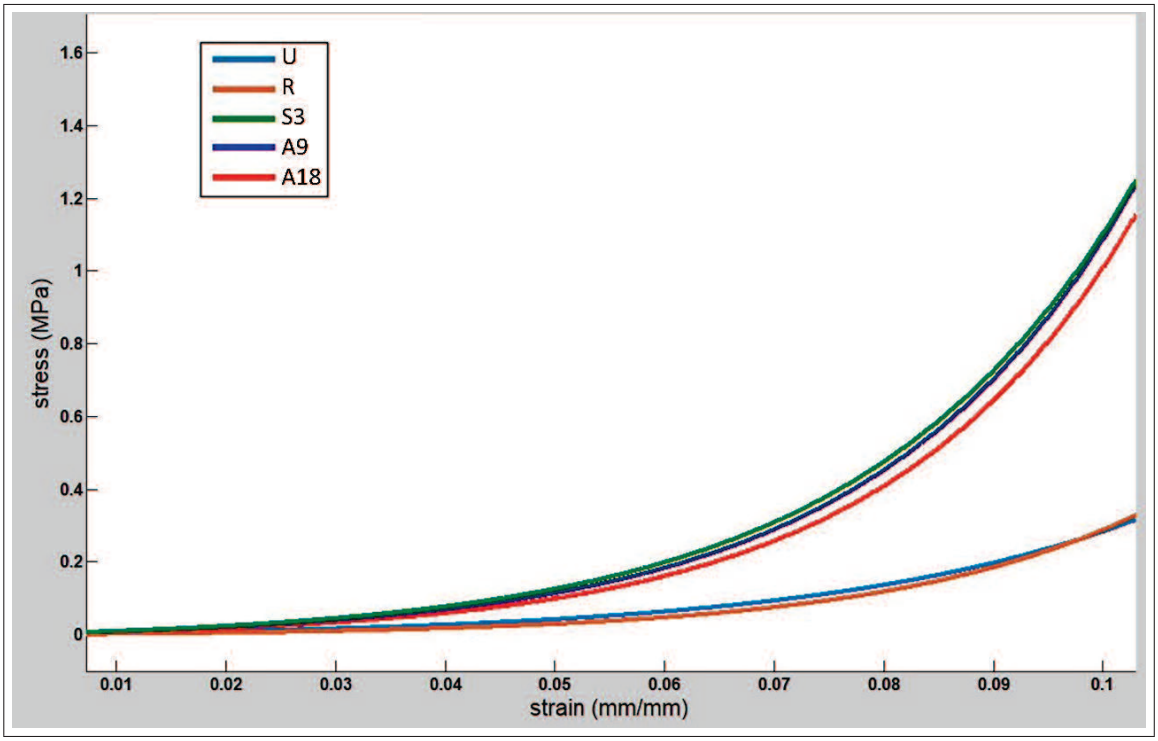

Figure 3.8: Stress-strain behaviour of cross-linked and non-cross-linked corneas. The cross-linked corneas showed a higher stress-strain ratio than the non-cross-linked control groups. Cross-linking treatments: Standard cross-linking with 3 mW UVA (S3), accelerated cross-linking using 9 mW (A9) and 18 mW (A18) UVA. Non-cross-linked controls: untreated (U) and riboflavin-only (R).

Tangent modulus

Bar charts depicting the average tangent modulus for each group at 2%, 4%, 6% and 8% strain are presented in Figure 3.9 a, b, c and d, respectively. At 2% strain a significant

difference in tangent modulus was only evident between the SCXL group and the two controls groups (untreated and riboflavin only) ($p < 0.005$, $p < 0.004$, respectively) (Figure 3.9 a). At 4%, 6% and 8% strain, all SCXL and ACXL treated groups had a significantly higher tangent modulus than the non-cross-linked controls ($p < 0.01$) (Table 3.6 and Figure 3.9 b, c and d). At 6% strain, the average tangent modulus for the SCXL 3 mW, ACXL 9 mW and 18 mW was 4.3, 3.8 or 3.4 times higher respectively than the non-cross-linked controls. However, no significant difference was detected between the SCXL and ACXL groups at any of the measured levels of strain ($p > 0.23$) (Table 3.6 and Figure 3.9).

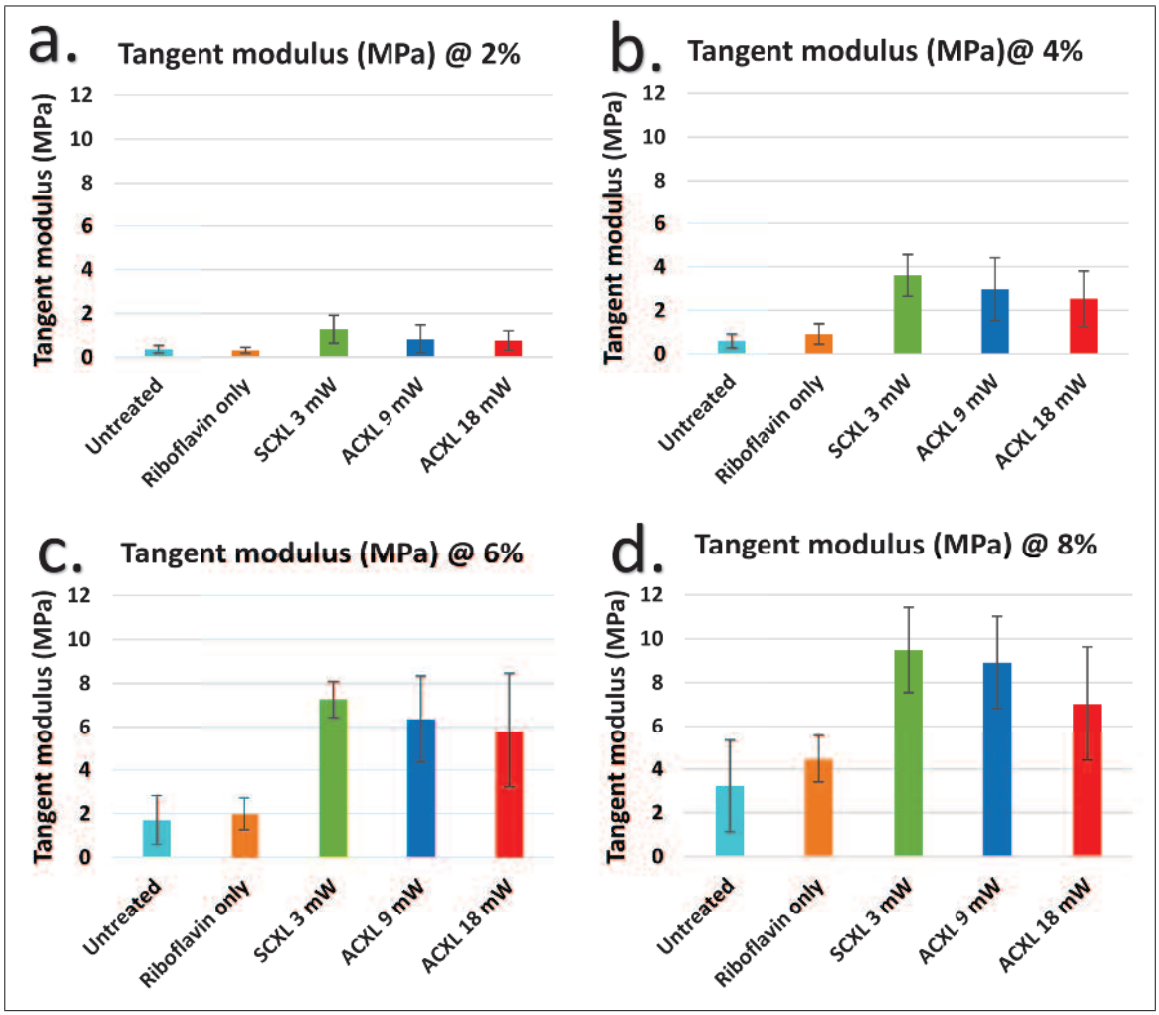

Figure 3.9: Average tangent modulus of cross-linked and non-cross-linked corneas at (a) 2%, (b) 4%, (c) 6% and (d) 8% strain. Error bars show standard deviation. Cross-linking treatments: Standard cross-linking (SCXL 3 mW), accelerated cross-linking (ACXL 9 mW and ACXL 18 mW). Non-cross-linked controls: untreated and riboflavin-only.

Table 3.6: P-values of the tangent modulus at 2%, 4%, 6% and 8% resulting from Bonferroni multiple comparisons between groups. Asterisks indicate where p-values were < 0.05.

P Value	Untreated	Riboflavin only	SCXL 3 mW	ACXL 9 mW
at 2%				
Riboflavin only	1.000			
SCXL 3 mW	0.005*	0.004*		
ACXL 9 mW	0.362	0.274	1.000	
ACXL 18 mW	0.198	0.147	1.000	1.000
at 4%				
Riboflavin only	1.000			
SCXL 3 mW	0.0001*	0.0001*		
ACXL 9 mW	0.0001*	0.001*	1.000	
ACXL 18 mW	0.004*	0.009*	0.792	1.000
at 6%				
Riboflavin only	1.000			
SCXL 3 mW	0.0001*	0.0001*		
ACXL 9 mW	0.0001*	0.0001*	0.838	
ACXL 18 mW	0.0001*	0.001*	0.229	1.000
at 8%				
Riboflavin only	1.000			
SCXL 3 mW	0.0001*	0.0001*		
ACXL 9 mW	0.0001*	0.001*	1.000	
ACXL 18 mW	0.002*	0.010*	0.698	1.000

3.5 Discussion

The SCXL protocol has proven its efficacy and safety to strengthen the cornea and halt the progression of keratoconus and other corneal ectasia diseases (Spoerl et al. 1998). However, more recently, ACXL procedures that are based on the Bunsen-Roscoe law of reciprocity and use higher UVA intensities, have been introduced to reduce the duration of the CXL treatment to one-third or one-sixth of the original procedure time. Despite the promising clinical results of ACXL treatments in the short-term, several publications have warned that the Bunsen-Roscoe law may not be a valid application for the cornea (Mazzotta et al. 2013; Richoz et al. 2013; Wernli et al. 2013) and a comparison of the long-term benefits of SCXL and ACXL treatment protocols has yet to be established. In this *ex vivo* study the enzymatic resistance and biomechanical properties of corneas cross-linked with the standard 3 mW SCXL procedure were compared to those of corneas cross-linked

using 9 mW and 18 mW ACXL procedures. In agreement to other clinical and laboratory based studies (Greenstein et al. 2011; Hassan et al. 2014; Hayes et al. 2013) a significant reduction in corneal thickness was detected following CXL using an isotonic riboflavin solution; as the post-treatment thickness of the irradiated corneas did not differ from that of the non-irradiated riboflavin treated corneas, the corneal thinning detected during CXL and ACXL may be attributed predominantly to the application of riboflavin/dextran solution rather than to the effect of CXL following UVA exposure. The application of riboflavin solution (containing 20% dextran) resulted in a significantly greater reduction in corneal thickness than application of the same concentration of dextran in the absence of any riboflavin. This finding may be the result of riboflavin increasing the ionic strength of the applied solution, as higher ionic strengths are known to be correlated with lower corneal hydrations (Huang et al. 1999) and hence also, decreased corneal thickness.

This study and earlier studies have indicated that a significant stromal swelling occurred (predominantly in the posterior stroma) in all corneal disks during the first 24 hours in pepsin solution (Hayes et al. 2013; Spoerl et al. 2004). This observation can attribute to the negatively charged glycosaminoglycans components of the proteoglycans within the extracellular matrix, which draw the pepsin digest solution into the tissue (Klyce et al. 1988). The higher ratio of keratan sulphate to condroitin sulphate in the posterior stroma compared to the anterior (Castoro et al. 1988) could give a reason for the occurrence of most of the swelling in this area, since keratan sulphate has a higher water affinity than chondroitin sulphate (Bettelheim et al. 1975). Interestingly, the separation of the cornea into anterior and posterior stromal regions during the first week of digestion was observed in all cross-linked and non-cross-linked porcine corneas but did not occur in any of the human corneas. The separation could not therefore be attributed to cross-linking induced changes within the anterior stroma. Instead this phenomenon may be due to the naturally occurring structural differences that exist between the anterior and posterior regions of the human and porcine cornea. This could be related to the higher interlacing of the anterior stroma collagen bundles than the posterior stroma in human cornea (Radner et al. 1998), whereas the porcine corneas show regular interweave of the lamellae over the stromal

depth (Bueno et al. 2011; Tan et al. 2006). In both species, the changes in corneal hydration did not affect the diameter of the anterior portion of the corneal disk and thus formed a more reliable measure of the rate of enzymatic digestion than measurements of corneal thickness. Calculations based on the used sample size and the standard deviation of diameter measurements however, determined that the sensitivity of the technique was such that differences between groups (in terms of the time taken for complete digestion) of less than one day could not be distinguished by this method. Therefore, measurements of corneal disk dry weight, which reflect the mass of undigested corneal tissue, were recorded at day 12 of the digestion process, this allows finer differences in enzymatic resistance between treatment groups to be identified. Measurements of corneal disk diameter provide valuable information on the structural integrity of the most anterior layers of the cornea, whilst the dry weight measurements, representing the total mass of undigested tissue, negate the complications associated with within-sample variations in corneal thickness and between sample differences in hydration and provide information about the effective depth of CXL.

The results indicated an increased resistance to proteinase digestion following SCXL that is in agreement with the findings of other investigators (Hayes et al. 2013; Kissner et al. 2010; Spoerl et al. 2004). However, for the first time it was shown (in both porcine and human corneas) that a similar increase in enzymatic resistance can also be obtained using higher fluences (up to 18 mW/cm^2) and shorter exposure times. Although the diameter measurements recorded from the porcine corneas showed no difference in enzymatic resistance between the CXL protocols used in this study, the average dry weight of corneal tissue after 12 days of protein digestion was found to differ significantly between groups (SCXL 3 mW > ACXL 9 mW > ACXL 18 mW). The greater enzymatic resistance conferred by the 3 mW SCXL protocol compared to the 9 mW and 18 mW protocol was further supported by the slower digestion rate of the SCXL treated human donor corneas compared to the ACXL treated corneas. This postulates that protocols using a higher fluence and shorter exposure time, result in either the most anterior layers of the corneal stroma being cross-linked equally but the effective depth of cross-linking being decreased

or the intensity of cross-linking ,which is known to be depth-dependent (Scarcelli et al. 2013), declining more rapidly as a function of depth. One interesting observation by previous studies is the presence of a shallower demarcation line in ACXL compared to SCXL (Brittingham et al. 2014; Kymionis et al. 2016; Ng et al. 2016; Touboul et al. 2012), suggesting that this may represent a reduced or shallower CXL effect. However, this speculates that the depth of the demarcation line correlates directly with the degree and depth of CXL and currently there is no direct evidence to support this. The so-called stromal demarcation line, first defined by Seiler et al (2006), has been revealed to possibly be shallower in older patients and those with more severe ectatic disease (Yam et al. 2012). It has been shown to be thicker centrally and thinner peripherally (Kymionis et al. 2013) and possibly related to an increased density of the extracellular matrix (Mazzotta et al. 2007). Although a deeper demarcation line has been correlated with a larger reduction in post-CXL corneal thickness (Doors et al. 2009), its depth has not been shown to be associated to either visual or keratometric changes at 6 months post-operatively (Yam et al. 2012). It may simply represent natural wound healing responses rather than describe the true area between cross-linked and un-cross-linked tissue and more research is necessary to determine the true nature of this demarcation line and its relationship to the actual cross-linking process.

The untreated human corneas took significantly longer to digest than the untreated porcine eyes ($p < 0.0001$) which may, to a small extent, be due to differences in the pH of the pepsin digest solution used, which is known to affect the rate of digestion. However, the greater resistance of the human corneas to enzymatic digestion is more likely the result of the natural increase in collagen cross-linking that occurs with age, since the study utilized relatively young pig corneas (< 1 year of age and equivalent to ≈18 human years) and more mature human corneas (mean age of 73 years). The *ex vivo* studies presented in this chapter disclose that the ACXL protocols are equivalent to the SCXL procedure in terms of increasing the stiffness of the cornea. The results, which show that corneal stiffness can be increased by cross-linking, are supported by other publications (Kling et al. 2010; Kohlhaas et al. 2006; Wollensak et al. 2009, 2003). However, the 300-400% increase

in porcine corneal stiffness observed in this study following cross-linking is higher than that published by Wollensak et al, where the increase in stiffness was 180% (Wollensak et al. 2003). This variance can be credited to the slight differences in the way in which the extensometry was performed. The applied stress is very reliant on the experimental procedure, for example, the load on the fixation clamp, the pre-stress power of the machine, and the use of hydration control techniques (Hatami-Marbini et al. 2015). In the current study, the gauge length between the two clamps was much smaller (5×6 mm) than that utilized by Wollensak et al. (5×14 mm), and this may influence the total energy absorbed during the tissue tests.

In agreement with the findings presented in the current study, Wernli et al. showed that there was no significant difference between 3 mW SCXL, 9 mW and 18 mW ACXL treated corneas in terms of their enhanced tissue stiffness (Wernli et al. 2013). Further to this, the stiffening effect was still comparable with ACXL procedures using 40 mW/cm^2 but at very high irradiations of more than 45 mW/cm^2, no corneal cross-linking or enhanced strength was achieved. The failure of the Bunsen-Roscoe law of reciprocity in cases of very high intensity and short illumination time is not yet understood, but may be related to rapid oxygen consumption and subsequent reduced oxygen availability, which has been shown to limit the photochemical cross-linking process (McCall et al. 2010). Oxygen and its vital role in free radical production has been shown to be central in driving the CXL process (McCall et al. 2010). Therefore limitation in availability, due to reduced time to replenish suitable oxygen levels, can theoretically inhibit the photochemical cross-linking process (McCall et al. 2010). The current study results showed a difference in enzymatic resistance, with increasing UVA intensity up to 18 mW/cm^2. Further studies with energies of 30 mW/cm^2 and above are needed to see whether the results of pepsin digestion studies replicate those of extensometry and other mechanical methods.

The results presented here also confirm the findings of other studies which have demonstrated the comparable stiffening effect of SCXL and 9 mW ACXL using extensometry (Schumacher et al. 2011) and a variety of other biomechanical testing techniques, such as surface wave elastometry (Rocha et al. 2008), scanning acoustic microscopy

(Beshtawi et al. 2013) and inflation testing (Bao et al. 2018). However, contrary to this, Hammer et al. (2014) found the stiffening effect to be greater following SCXL than 9 mW ACXL. In addition, the authors reported no significant difference between untreated corneas and those treated with 18 mW ACXL. This finding is clearly at odds with the results of the current study, which demonstrate a similar stiffening effect as a result of SCXL, ACXL 9 mW and ACXL 18 mW. The difference between the two studies might be caused by slight differences in the sample size and the methodologies used, for example, differences in the time-delay between treatment and testing (5 minutes in the present study versus 30 minutes in the Hammer et al. study). Certainty, the ACXL 9 mW protocol provides cross-links to the cornea and clinical validation is required to better understand the findings.

Further clinical studies of ACXL have been discussed in the literature. Researchers validated the effectiveness of ACXL to halt keratoconus progression and improve vision (Alnawaiseh et al. 2015; Kymionis et al. 2014). The equivalence of ACXL and SCXL was pointed out in several clinical trials (Cinar et al. 2014; Kymionis et al. 2014). A significant reduction in topographic keratometry and improvement in corrected distance acuity, comparable to SCXL has been showed post-ACXL treatment using 9 mW/cm^2 for 10 minutes at 6 months follow-up (Cinar et al. 2014). This finding was supported by another clinical study using a similar intensity of ACXL 9 mW that found a significant reduction in keratometry following CXL with no adverse effects in terms of endothelial cell counts at 3 months (Kymionis et al. 2014). In addition, Touboul et al described the superiority of ACXL over the SCXL (Touboul et al. 2012). According to Mazzotta et al (2013) the penetration of ACXL treatment reached the depth of 200 μm in the anterior-mid stroma, compared to 300 μm a maximum depth of SCXL. However, the most vital biomechanical impact identified with cross-linking is located in the front 200 μm of the cornea as reported in the literature (Kohlhaas et al. 2006), so the effect of ACXL might be adequate in terms of biomechanical and biochemical impact (Mazzotta et al. 2013). Clearly, further long-term clinical studies in large cohorts are required to validate the efficacy and safety of this higher intensity procedure.

In conclusion, this study shows that the enhanced tissue stiffness following ACXL (with a UVA intensity of up to 18 mW/cm^2), is comparable to that of SCXL. Although, SCXL resulted in a subtly greater enhancement of enzymatic resistance than the ACXL protocols, the minimum effective amount of cross-linking desired for ectasia stabilization has not yet been established. Previous clinical studies demonstrated that the amount of cross-linking produced by ACXL may indeed be sufficient to stabilize disease progression. The accumulating clinical and laboratory evidence demonstrating the similar efficacy of ACXL (up to 18 mW) and SCXL, the reduced cell toxicity associated with the ACXL technique and the clear benefits of ACXL, in terms of patient and surgeon convenience, support its use. However, longer-term follow-up clinical studies, especially randomized prospective trials, will be necessary to ascertain the clinical safety and efficacy of ACXL. In addition to this, further laboratory studies are needed to determine whether even higher UVA intensity/shorter duration cross-linking procedures can achieve the same level of enzymatic resistance and biomechanical stiffening as that of the SCXL procedure.

CHAPTER 4

AN INVESTIGATION INTO CORNEAL ENZYMATIC RESISTANCE FOLLOWING STANDARD AND TRANS-EPITHELIAL CORNEAL CROSS-LINKING PROCEDURES.

This chapter was published as a laboratory science article in Experimental Eye Research 2016; 153:141–151. Published by Elsevier Ltd.

4.1 Introduction

Riboflavin is a hydrophilic molecule, with a molecular weight of 340 Dalton (Da), while, the corneal epithelium is lipophilic, with a decreasing permeability to molecules over 180 Da (Huang et al. 1989). Hence, the removal of the epithelium from the central corneal is essential to allow adequate stromal absorption of riboflavin prior to UVA irradiation in the "gold-standard" CXL protocol. This requirement was supported by Spoerl et al., who reported no changes in corneal biomechanics when CXL was performed with the epithelium intact (Spoerl et al. 1998). Based on this study, the epithelium was removed in the first published clinical studies (Caporossi et al. 2006; Gkika et al. 2011; O'Brart et al. 2011; Richoz et al. 2013; Wittig-Silva et al. 2014; Wollensak et al. 2003). However, there are some complications associated with the epithelial debridement, including severe ocular pain in the immediate post-operative period, delayed visual rehabilitation, the risks of scarring and infectious and non-infectious keratitis (Evangelista et al. 2017; Koller et al. 2009).

Due to these complications, several trans-epithelial CXL techniques have been proposed. The first epithelium-on CXL (epi-on-CXL) protocols included the use of multiple topical applications of tetracaine 1% to disrupt epithelial tight junctions (Boxer Wachler et al. 2010; Chan et al. 2007) and partial epithelial debridement in a grid pattern (Rechichi et al. 2013). Lately, innovative development of formulations of riboflavin has been introduced to facilitate epi-on-CXL (Alhamad et al. 2012; Kissner et al. 2010; Raiskup et al. 2012). Ambiguous results were demonstrated in clinical studies with such formulations, with some demonstrating similar efficacy to epithelium-off CXL (epi-off-CXL) (Filippello et al. 2012; Magli et al. 2013), and others showing less pronounced effects (Buzzonetti et al. 2012; Kocak et al. 2014; Koppen et al. 2012; Leccisotti et al. 2010). As riboflavin is negatively charged at physiological pH and soluble in water, it is assumed that iontophoresis can be used as a means of enhancing trans-epithelial absorption. In vitro studies of CXL using iontophoresis-assisted delivery (Ion-CXL) of riboflavin 0.1% with a current of 0.5 - 1 mA for 5 to 10 min have been encouraging, demonstrating enhanced

trans-epithelial riboflavin absorption and increased corneal tissue strength (Cassagne et al. 2016; Lombardo et al. 2014; Mastropasqua et al. 2014a; Touboul et al. 2014; Vinciguerra et al. 2014a). Previous clinical studies have stated cessation of progression and improvements in keratometric and visual parameters (Bikbova et al. 2014; Buzzonetti et al. 2015; Vinciguerra et al. 2014b).

Apart from the requirement to remove the epithelium, the current "gold-standard", epi-off-CXL protocol, involves a 30 min application of riboflavin followed by a 30 min irradiation with 370 nm UVA light, with an intensity of 3 mW/cm^2, demanding an hour in treatment time. In an attempt to reduce treatment time, the use of accelerated CXL (ACXL) procedures using the same energy dose but higher UVA intensities and shorter exposure times have been studied. There are a small number of clinical studies of ACXL protocols that are published. Improvements were recorded in corrected distance acuity together with a reduction in topographic keratometry in those using 7 mW for 15 min or 9 mW for 10 min at up to 46 months follow-up with no complications linked with the high fluences used (Cinar et al. 2014; Cummings et al. 2016; Kanellopoulos 2012; Kymionis et al. 2014b; Shetty et al. 2015). As stated in the previous chapter, the 9 mW ACXL for 10 min was found to be as effective as the 3 mW for 30 min, therefore, it was chosen in this study to allow a faster throughput of samples. In recent times, it has also been confirmed that the efficacy of ACXL may be additionally enhanced by increasing the UVA exposure time, and the overall cumulative dosage (Aldahlawi et al. 2016; Kymionis et al. 2014a; Sherif 2014).

4.2 Research aim

To assess the effectiveness of partially disrupted-epithelium CXL (dis-CXL) and various epi-on-CXL protocols at enhancing corneal enzymatic resistance and compare their effectiveness to that of the standard epi-on and epi-off ACXL treatment. This study will examine the effect of using different riboflavin formulations, modes of riboflavin delivery and cumulative UVA energy dose on the enzymatic resistance of cross-linked corneas.

4.3 Materials and methods

4.3.1 Specimen preparation

Fresh porcine cadaver eyes with clear corneas and intact epithelium were purchased from a local European Community licensed abattoir. A total of one hundred and fourteen eyes were retrieved within 6 - 8 hours of death. The study was split into two runs because of the large number of eyes and treatment groups involved. Run 1 examined the effectiveness of dis-CXL and epi-on-CXL protocols (including iontophoretic epi-on-CXL) at increasing corneal enzymatic resistance to digestion with pepsin, whereas run 2 examined the effect on enzymatic resistance of increasing the UVA dosage by 25% from 5.4 J/cm^2 to 6.75 J/cm^2 during iontophoretic epi-on-CXL. Additionally, the usefulness of the epi-off CXL protocol at increasing enzymatic resistance was observed in both runs for comparative purposes. The 11 treatment groups are described below and summarised in Table 4.1.

Table 4.1: Treatment groups.

Group	Abbreviation	Epithelium	Riboflavin formulation	Ionto (1mA)	Ribosoak	Ionto (0.5 mA)	Ribosoak	Saline rinse	9 mW UVA	Applied during irradiation
(1) Epithelium-offnon-irradiated control	Epi-off-ribo	Off	Mediocross D:0.1% Riboflavin, 20%dextran	-	30 min	-	-	-	-	-
(2) Epithelium-offacceleratedCXL	Epi-off-CXL5.4 J/cm^2	Off	Mediocross D	-	30 min	-	-	-	10 min	Mediocross D
(3) Disrupted epithelium non-irradiated control	Dis-ribo	Disrupted	Vitamin B2Streuli: 0.1% riboflavin, saline	-	30 min	-	-	5 min	-	-
(4) Disrupted epithelium CXL	Dis-CXL 5.4 J/cm^2	Disrupted	Vitamin B2Streuli	-	30 min	-	-	5 min	10 min	PBS
(5) Epithelium intact non-irradiated control	Medio-ribo	On	Mediocross TE:0.25% riboflavin, 1.2% HPMC, 0.01% BACS, Pi-water	-	30 min	-	-	5 min	-	-
(6) Epithelium intact highribo flavin concentration CXL	Medio-CXL 5.4 J/cm^2	On	Mediocross TE	-	30 min	-	-	5 min	10 min	PBS
(7) Epithelium intact, highribo flavin concentration andprolonged iontophoresis non-irradiated control	TC-ion-ribo	On	Mediocross TE	5 min	5 min	5 min	5 min	5 min	-	-
(8) Epithelium intact, highribo flavin concentration andprolonged iontophoresis CXL	TC-ion-CXL 5.4 J/cm^2	On	Mediocross TE	5 min	5 min	5 min	5 min	5 min	10 min	PBS
(9) Epithelium intact, highribo flavin concentration, prolonged iontophoresis andhighUVAenergy dose CXL	TC-ion-CXL 6.75 J/cm^2	On	Mediocross TE	5 min	5 min	5 min	5 min	3 min	12 min 30 s	PBS
(10) Epithelium intact, basic iontophoresis protocol	Ion-CXL 5.4 J/cm^2	On	Mediocross M:0.1% riboflavin, 1.0% HPMC	5 min	-	-	-	3 min	10 min	PBS
(11) Epithelium intact, basic iontophoresis protocol withhigh UVAenergy dose	Ion-CXL 6.75 J/cm^2	On	Mediocross M	5 min	-	-	-	3 min	12 min 30 s	PBS

PBS: Phosphate buffered saline

Run 1:

Each treatment group consisted of six eyes.

i) Epi-off protocol (Group 1: Epi-off-ribo; Group 2: Epi-off-CXL)

Using a single-edged razor blade, complete corneal epithelial debridement was accomplished in groups 1 and 2. These eyes then received 0.1% riboflavin eye drops containing 20% dextran T-500 solution (Mediocross D®, Peschke Meditrade, Huenenberg, Switzerland) using corneal annular suction rings for 30 min. The central 9 mm region of the corneas in group 2 were then exposed to 365 nm UVA light with a fluence of CXL 9 mW/cm^2 for 10 min (CCL-365 Vario™ cross-linking system Peschkmed, Huenenberg, Switzerland). The term ACXL (A9) is also described as Epi-off-CXL in this chapter and these terms will be used interchangeably in this study. Using 5 min intervals, riboflavin was re-applied during irradiation. Group 1 served as a non-irradiated control.

ii) Dis-epi protocol (Group 3: Dis-ribo; Group 4: Dis-CXL)

In groups 3 and 4, partial epithelial disruption was performed, by creating 64 full-thickness epithelial punctures with a 25-gauge needle in an 8×8 grid pattern. The corneas were then soaked in riboflavin 0.1% dextran-free solution (Vitamin B2 Streuli, Uznach, Switzerland) using corneal annular suction rings for 30 min and rinsed with phosphate-buffered saline (PBS) for 5 min. 9 mW UVA for 10 min was then irradiated group 4 with PBS applied at 5 min intervals to keep the corneal surface moist. Group 3 served as a non-irradiated control.

iii) Epi-on and high riboflavin concentration protocol (Group 5: Medio-ribo; Group 6: Medio-CXL)

Groups 5 and 6 received 0.25% riboflavin with 1.2% hydroxypropylmethyl cellulose (HPMC) and 0.01% BAC (Mediocross TE®, Peschketrade, Huenenberg, Switzerland) every 5 min for 30 min. After that, they underwent a 5 min rinse with PBS. Group 6 was then irradiated with 9 mW UVA for 10 min with PBS applied at 5 min intervals. Group 5 served as a non-irradiated control.

iv) Epi-on, high riboflavin concentration and prolonged iontophoresis (St. Thomas-Cardiff) protocol (Group 7: TC-ion-ribo; Group 8: TC-ion-CXL)

Groups 7 and 8 received iontophoresis assisted delivery of 0.25% riboflavin with 1.2% HPMC and 0.01% BAC (Mediocross TE®, Peschketrade, Huenenberg, Switzerland) using a current of 1 mA for 5 min. corneas were then soaked with the riboflavin solution for 5 mins, prior to applying iontophoresis with a power of 0.5 mA/min for 5 min and another 5 min riboflavin soak. Ex vivo eyes were treated by the iontophoresis delivery system by connecting the return electrode to a needle inserted into the vitreous chamber; the negative electrode was a steel grid contained in a corneal well applicator which was adhered to the eye by means of a vacuum well system (Figure 4.1). Riboflavin totally covered the steel grid (negative electrode) and the power generator set to the chosen current and duration. During the entire procedure, the steel grid remained covered with riboflavin solution. The applicator was removed from the cornea and the corneas were washed with PBS for 5 min after treatment. Following that, group 8 was then irradiated with 9 mW UVA for 10 min with PBS applied at 5 min intervals. Group 7 served as a non-irradiated control.

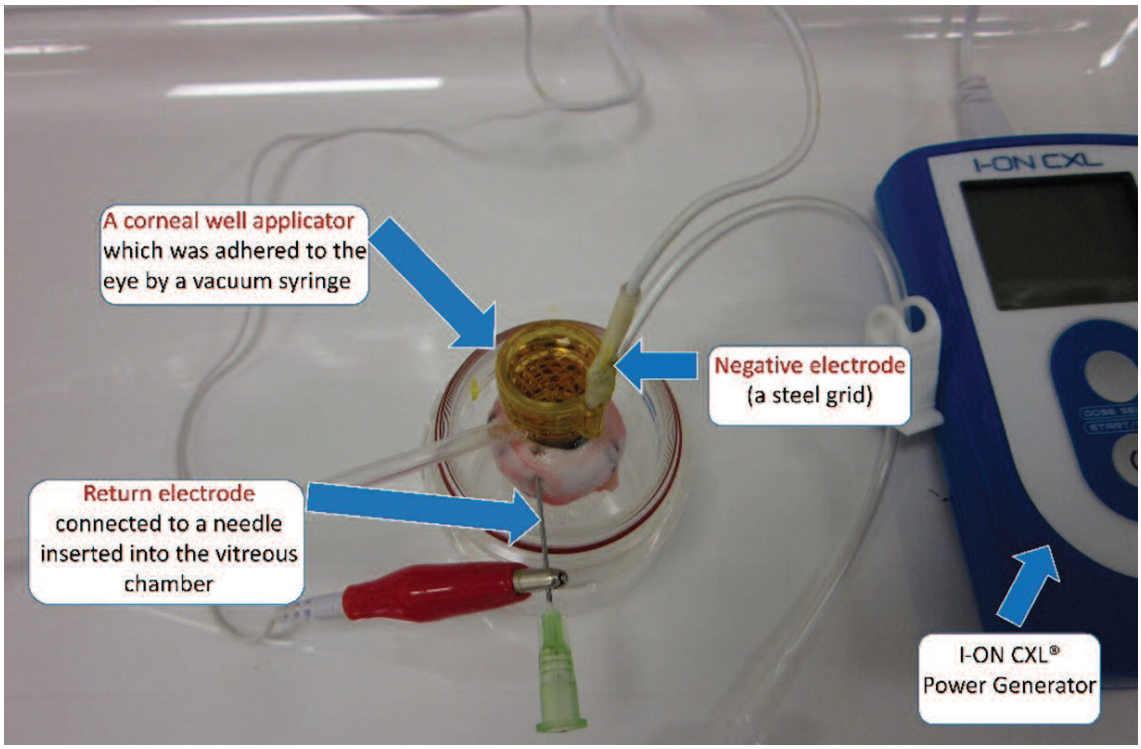

Figure 4.1: Iontophoresis riboflavin delivery system modified for use in ex-vivo eyes.

Run 2:

Each treatment group consisted of 11 eyes.

i) Epi-off protocol (Group 1: Epi-off-ribo; Group 2: Epi-off-CXL 5.4 J/cm^2)

Similar treatment was performed in corneas as shown in groups 1 and 2 in run 1.

ii) Epi-on, high riboflavin concentration and prolonged iontophoresis/St. Thomas-Cardiff protocol (Group 8: TC-ion-CXL 5.4 J/cm^2; Group 9: TC-ion-CXL 6.75 J/cm^2)

Assisted delivery of 0.25% riboflavin with 1.2% HPMC and 0.01% BAC were performed in groups 8 and 9 via iontophoresis (Mediocross TE®, Peschketrade, Huenenberg, Switzerland) using a current of 1 mA for 5 min. Subsequently, the corneas were soaked with riboflavin solution for 5 min before receiving an additional application of iontophoresis with a power of 0.5 mA/min for 5 min and another 5 min riboflavin soak. After a 3 min wash with PBS, the corneas in Group 8 were irradiated with 9 mW UVA for 10 min and those in Group 9 were irradiated with 9 mW UVA for 12 min and 30 sec. PBS drops were applied at 5 min intervals during irradiation to avoid dehydration.

iii) Epi-on basic iontophoresis protocol (Group 10: Ion-CXL 5.4 J/cm^2; Group 11: Ion-CXL 6.75 J/cm^2)

According to the Sooft iontophoresis protocol, groups 10 and 11 underwent iontophoresis assisted riboflavin delivery using an isotonic 0.1% riboflavin solution (Vitamin B2) containing 1.0% HPMC dextran-free solution (Mediocross M®, Peschketrade, Huenenberg, Switzerland) and a 1 mA current (Iontophoresis device, Sooft Italia S.p.A, Italy). The corneas were washed with PBS for 3 min following treatment. Irradiation of group 10 was performed with 9 mW UVA for 10 min and group 11 was irradiated with 9 mW UVA for 12 min and 30 sec. PBS drops were applied at 5 min intervals during irradiation to avoid dehydration.

4.3.2 Measurements of corneal thickness

The central corneal thickness was measured in all eyes prior to treatment, after removal of the epithelium, post application of riboflavin and when applicable, after UVA irradiation. Corneal thickness measurements were made using a Pachette2™ Ultrasonic Pachymetry (DGH Technology, Exton, USA) or a Tomey ultrasound pachymeter (Tomey Corporation, Nuremberg, Germany).

4.3.3 Measurements of enzymatic digestion

Straightway after treatment, a corneo-scleral ring was dissected from each eye, wrapped tightly in ClingfilmTM (to prevent moisture loss) and refrigerated until all treatments were finished. Using a disposable skin biopsy punch, an 8 mm corneal disc was trephined from the centre of each cornea. Then, the corneal discs were submerged into individual plastic tubes, each containing 5 ml of pepsin solution, and immersed in a water bath at a temperature of 23°C. The pepsin solution was made up of 1 g of > 500 U/mg pepsin from porcine gastric mucosa (Sigma-Aldrich, Dorset, UK) in 10 ml 0.1M HCl at pH 1.2. Daily measurements of corneal disc diameter were used to assess the stability of the most anterior layers of the cornea. An electronic digital caliper was used to acquire the measurements, and measurements were made until the point at which the specimen could no longer be differentiated from the surrounding pepsin solution. At this point the tissue was considered to have undergone complete digestion. The total digestion time (in days) was recorded for each cornea. In addition to assessing enzymatic resistance, 5 corneal discs from each of the 6 treatment groups in run 2 were removed from pepsin digest solution after 11 days and transferred to a 60°C oven for a minimum of one week until a constant dry weight was measured. The dry weight of the tissue signifies the total mass of undigested tissue and consequently can be used as an indicator of the effective depth of cross-linking.

4.3.4 Statistical Evaluation

One-way analysis of variance (ANOVA) test was used to statistically analyse measurements of corneal thickness, complete digestion time and tissue dry weight. In order to isolate significant interactions, post hoc Bonferroni comparisons were used. All statistical analyses were performed with the Statistical Package for the Social Sciences (IBM SPSS Statistics 20, New York, USA). P-value < 0.01 was considered to be significant. Data were presented in the results as mean ± standard deviation (SD).

4.4 Results

4.4.1 Corneal thickness

The average corneal thickness pre-treatment, post-riboflavin application and post-irradiation for each treatment group in run 1 and 2 are shown in Figure 4.2. Statistical tests discovered a significant difference in thickness between corneas treated using the epi-off protocol and an iso-osmolar riboflavin solution (groups 1 and 2) and the corneas in all other groups ($p < 0.007$).

4.4.2 Qualitative assessment of riboflavin uptake

As shown in Figure 4.3, the distinctive yellow colouration of riboflavin was most obviously noticeable in the epi-off and TC-ion treated corneas. Even if riboflavin was also seen in corneas from other treatment groups, the colour was notably less intense. A non-homogenous distribution of riboflavin in Ion-CXL treated corneas and a more uniform distribution following epi-off CXL and TC-Ion-CXL were seen in photographs recorded during the irradiation process in run 2.

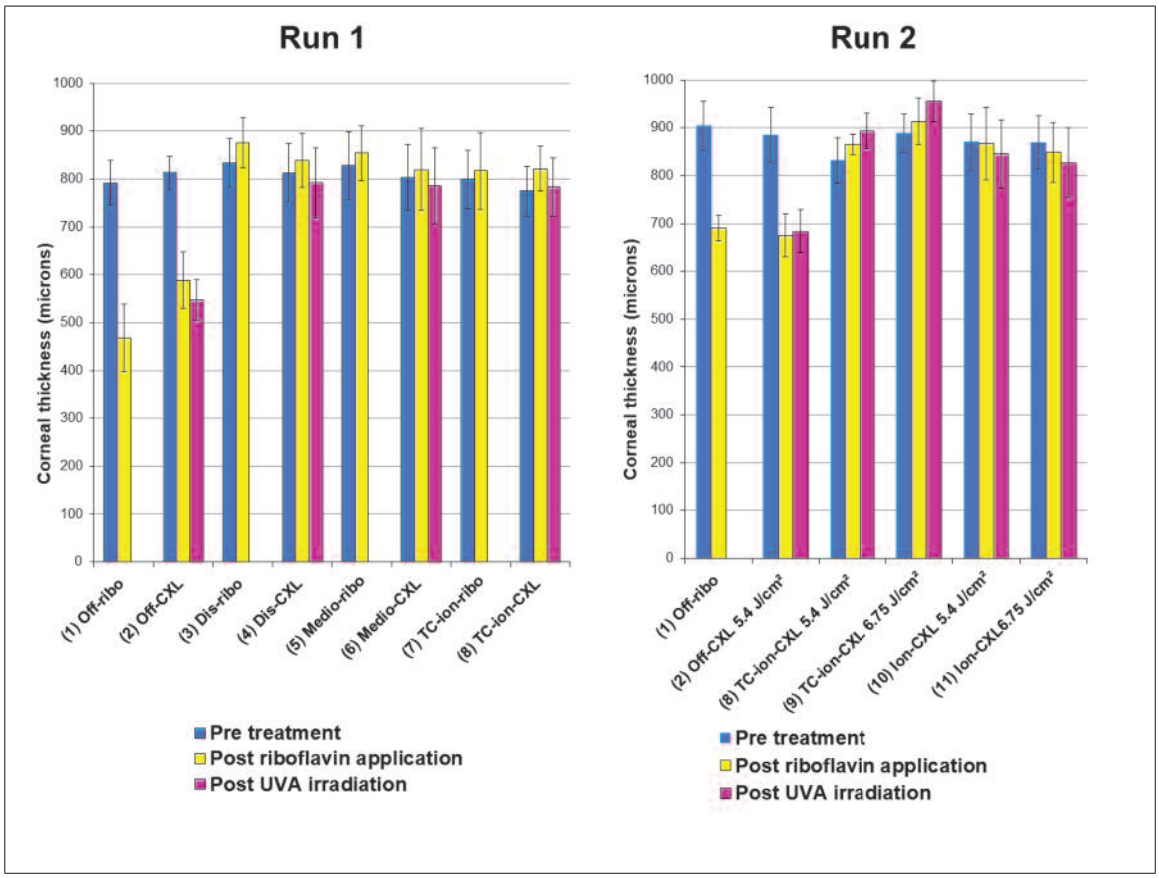

Figure 4.2: Corneal thickness measurements are shown for each group in run 1 and run 2 before treatment, after riboflavin application and where applicable, following UVA irradiation. In groups 1 and 2 the corneal epithelium (measuring 90 μm in thickness) was removed as part of the riboflavin application process.
Cross-linking treatments: (1) Epi-off-ribo (Epithelium-off non-irradiated control); (2) Epi-off-CXL 5.4 J/cm^2 (Epithelium-off standard CXL); (3) Dis-ribo (Disrupted epithelium non-irradiated control); (4) Dis-CXL 5.4 J/cm^2 (Disrupted epithelium CXL); (5) Medio-ribo (Epithelium intact non-irradiated control); (6) Medio-CXL 5.4 J/cm^2 (Epithelium intact high riboflavin concentration CXL); (7) TC-ion-ribo (Epithelium intact, high riboflavin concentration and prolonged iontophoresis non-irradiated control); (8) TC-ion-CXL 5.4 J/cm^2 (Epithelium intact, high riboflavin concentration and prolonged iontophoresis CXL); (9) TC-ion-CXL 6.75 J/cm^2 (Epithelium intact, high riboflavin concentration, prolonged iontophoresis and high UVA energy dose CXL); (10) Ion-CXL 5.4 J/cm^2 (Epithelium intact, basic iontophoresis protocol) and (11) Ion-CXL 6.75 J/cm^2 (Epithelium intact, basic iontophoresis protocol with high UVA energy dose).

4.4.3 Pepsin digestion of corneal disks

The number of days required for complete tissue digestion to occur in each irradiated and non-irradiated treatment group is shown in Table 4.2. Even though the duration of digestion of equivalent non-irradiated (group 1) and cross-linked treatment groups (group 2) varied slightly between runs 1 and 2, the same general trends were observed in both

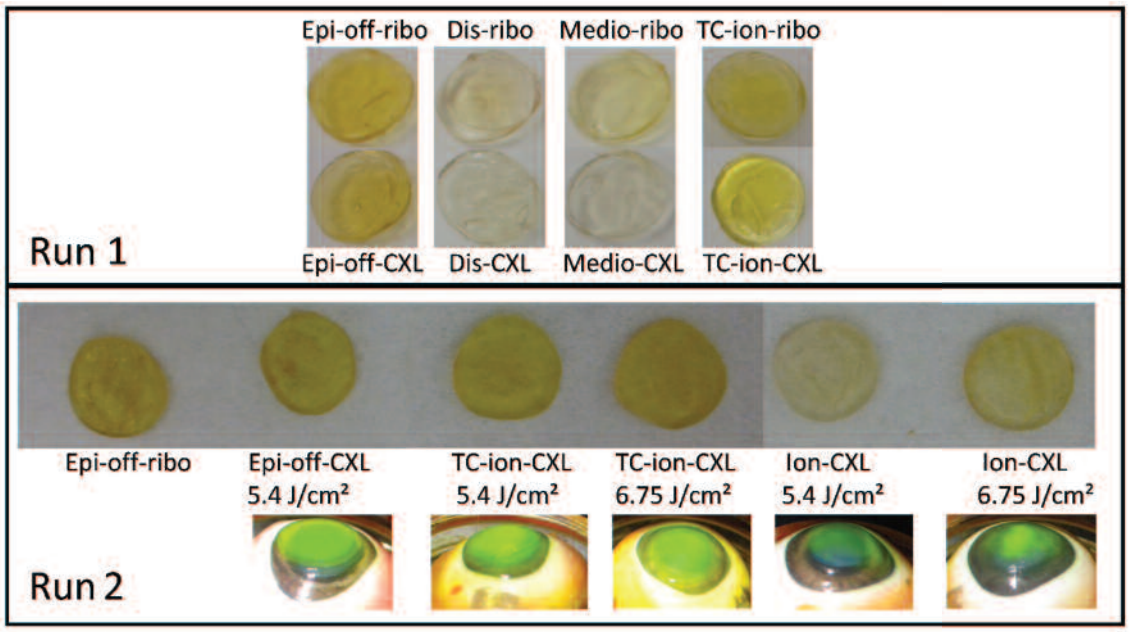

Figure 4.3: Corneal disks from each group in run 1 and 2 are shown immediately post-treatment. The characteristic yellow colour of riboflavin can be seen most clearly in the epithelium-removed, riboflavin treated corneas (epi-off) and in the corneas that received riboflavin via the St Thomas's/Cardiff modified iontophoresis protocol (TC-Ion). Photographs recorded during the irradiation process show a non-homogenous distribution of riboflavin in corneas treated with the basic iontophoresis protocol (Ion-CXL).
Cross-linking treatments: (1) Epi-off-ribo (Epithelium-off non-irradiated control); (2) Epi-off-CXL 5.4 J/cm^2 (Epithelium-off standard CXL); (3) Dis-ribo (Disrupted epithelium non-irradiated control); (4) Dis-CXL 5.4 J/cm^2 (Disrupted epithelium CXL); (5) Medio-ribo (Epithelium intact non-irradiated control); (6) Medio-CXL 5.4 J/cm^2 (Epithelium intact high riboflavin concentration CXL); (7) TC-ion-ribo (Epithelium intact, high riboflavin concentration and prolonged iontophoresis non-irradiated control); (8) TC-ion-CXL 5.4 J/cm^2 (Epithelium intact, high riboflavin concentration and prolonged iontophoresis CXL); (9) TC-ion-CXL 6.75 J/cm^2 (Epithelium intact, high riboflavin concentration, prolonged iontophoresis and high UVA energy dose CXL); (10) Ion-CXL 5.4 J/cm^2 (Epithelium intact, basic iontophoresis protocol) and (11) Ion-CXL 6.75 J/cm^2 (Epithelium intact, basic iontophoresis protocol with high UVA energy dose).

runs. Therefore, the data from each run was normalised against the total digestion time of the epi-off CXL group to permit comparison between the two runs (Figure 4.4 and 4.5).

Cumulative measurements of corneal disk diameter for each irradiated and non-irradiated treatment group throughout the digestion process are shown in figures 4.4 and 4.5. In both runs 1 and 2, the cross-linked groups showed a significantly greater resistance to enzymatic digestion than the non-irradiated groups ($p < 0.0001$). In run 1, by day 13, complete digestion of all non-irradiated corneas had occurred (Table 4.2). At the same time point (normalized digestion time of 0.33), the mean diameter of the epi-off-CXL,

dis-CXL, medio-CXL and TC-ion-CXL groups had only decreased by 39%, 62%, 74%, and 40 %, respectively (Figure 4.4). No significant difference was found between the non-irradiated groups in terms of either the average corneal disc diameter at any time point in the digestion process or in the time required for complete digestion to occur (Figure 4.4). Nevertheless, there were significant differences in the time taken for complete digestion to occur between the cross-linked groups (Figure 4.4). The epi-off-CXL corneas (group 2) took significantly longer to digest than all other cross-linked corneas ($p < 0.0001$). Although less resistant to enzyme digestion than the epi-off CXL corneas, the TC-ion-CXL treated corneas took significantly longer to digest than corneas treated with other dis-CXL or epi-on-CXL protocols ($p < 0.0001$).

In run 2, the non-irradiated corneas were completely digested by day 10 (Table 4.2) which equates to a normalized digestion time of 0.25. At this time point, the mean diameter of corneas in the epi-off-CXL 5.4 J/cm^2, TC-ion-CXL 5.4 J/cm^2, TC-ion-CXL 6.75 J/cm^2, Ion-CXL 5.4 J/cm^2 and Ion-CXL 6.75 J/cm^2 treatment groups had only reduced by 21.4%, 16.2%, 13.4%, 26.7% and 19.4%, respectively (Figure 4.5). After 24 days of digestion (normalised digestion time of 0.6), significant differences in the mean disk diameter in the CXL treatment groups were seen (Figure 4.5). The epi-off-CXL group (group 2) took longer to undergo complete digestion than all other cross-linked groups ($p < 0.0001$). On the other hand, corneas treated with the prolonged, high riboflavin concentration, iontophoresis protocol (TC-ion-CXL) were found to persist in the pepsin digest solution for significantly longer than those treated with the basic Ion-CXL protocol (Figure 4.5). In both the Ion-CXL and TC-ion-CXL treatment groups, a significant increase in the time required for complete digestion to occur ($p < 0.0001$) was observed when the UVA radiance was increased from 5.4 J/cm^2 to 6.75 J/cm^2.

Table 4.2: Time taken for the complete tissue digestion to occur.

Groups	Time taken for complete digestion (in days)			
	Minimum	Maximum	Average (± SD)	Normalised digestion time*
RUN 1				
(1) Epi-off-ribo	11	12	11.5 ± 0.55	0.30
(2) Epi-off-CXL	39	40	39.5 ± 0.55	1.00
(3) Dis-ribo	11	13	11.8 ± 0.75	0.33
(4) Dis-CXL	15	16	15.6 ± 0.52	0.38
(5) Medio-ribo	11	12	11.6 ± 0.51	0.30
(6) Medio-CXL	14	15	14.6 ± 0.52	0.40
(7) TC-ion-ribo	11	12	11.3 ± 0.52	0.30
(8) TC-ion-CXL	32	33	32.2 ± 0.41	0.83
RUN 2				
(1) Epi-off-ribo	9	10	9.5 ± 0.55	0.25
(2) Epi-off-CXL 5.4 J/cm^2	43	44	43.5 ± 0.55	1.00
(8) TC-ion-CXL 5.4 J/cm^2	34	35	34.3 ± 0.52	0.80
(9) TC-ion-CXL 6.75 J/cm^2	41	42	41.7 ± 0.52	0.95
(10) Ion-CXL 5.4 J/cm^2	27	28	27.3 ± 0.52	0.65
(11) Ion-CXL 6.75 J/cm^2	34	35	34.5 ± 0.55	0.80

* The data was normalised against epi-off CXL group.

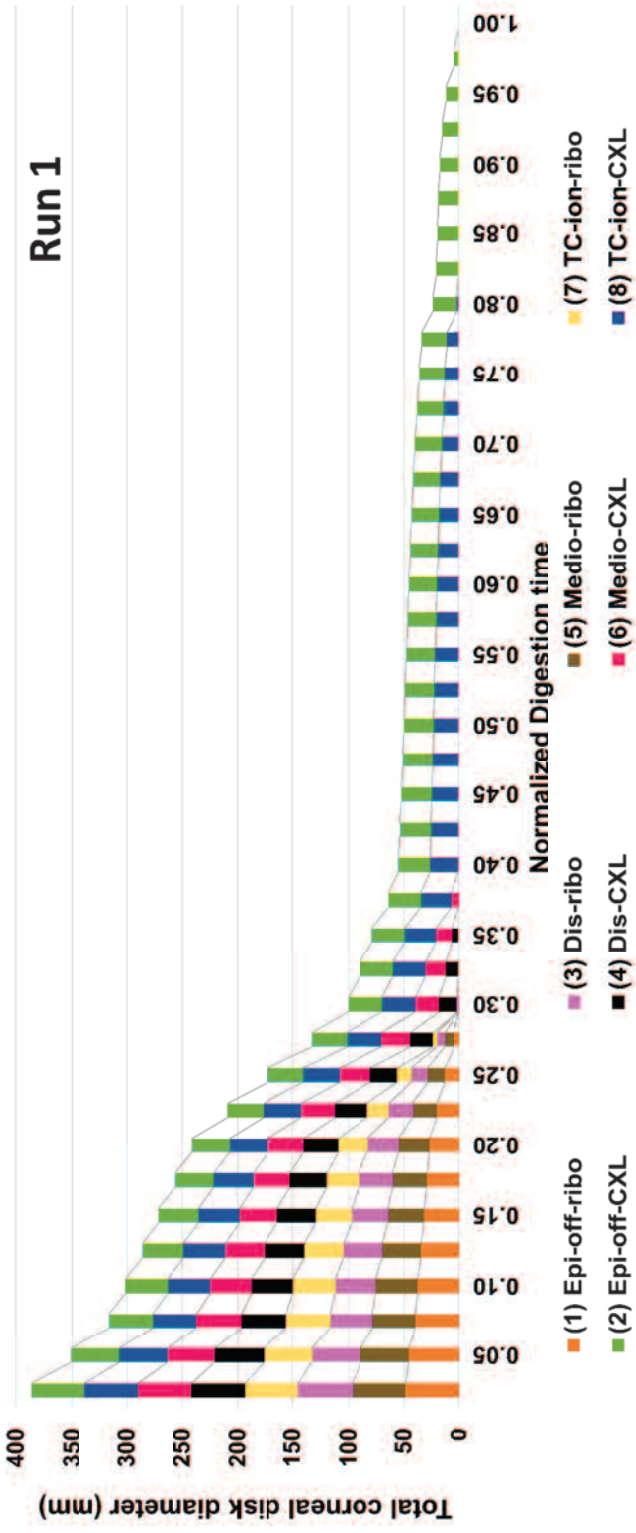

Figure 4.4: The digestion rate of corneal disks treated with Epi-off-ribo, Epi-off-CXL, Dis-ribo, Dis-CXL 5.4 J/cm^2, Medio-ribo, Medio-CXL 5.4 J/cm^2, TC-ion-ribo and TC-ion-CXL 5.4 J/cm^2. The summed diameter of all corneal disks within each treatment group (n = 6) are shown for run 1 as a function of time in pepsin digest solution. The digestion time for each treatment group has been normalised against the total digestion time of the epi-off CXL group.
Cross-linking treatments: (1) Epi-off-ribo (Epithelium-off non-irradiated control); (2) Epi-off-CXL 5.4 J/cm^2 (Epithelium-off standard CXL); (3) Dis-ribo (Disrupted epithelium non-irradiated control); (4) Dis-CXL 5.4 J/cm^2 (Disrupted epithelium CXL); (5) Medio-ribo (Epithelium intact non-irradiated control); (6) Medio-CXL 5.4 J/cm^2 (Epithelium intact high riboflavin concentration CXL); (7) TC-ion-ribo (Epithelium intact, high riboflavin concentration and prolonged iontophoresis non-irradiated control) and (8) TC-ion-CXL 5.4 J/cm^2 (Epithelium intact, high riboflavin concentration and prolonged iontophoresis CXL).

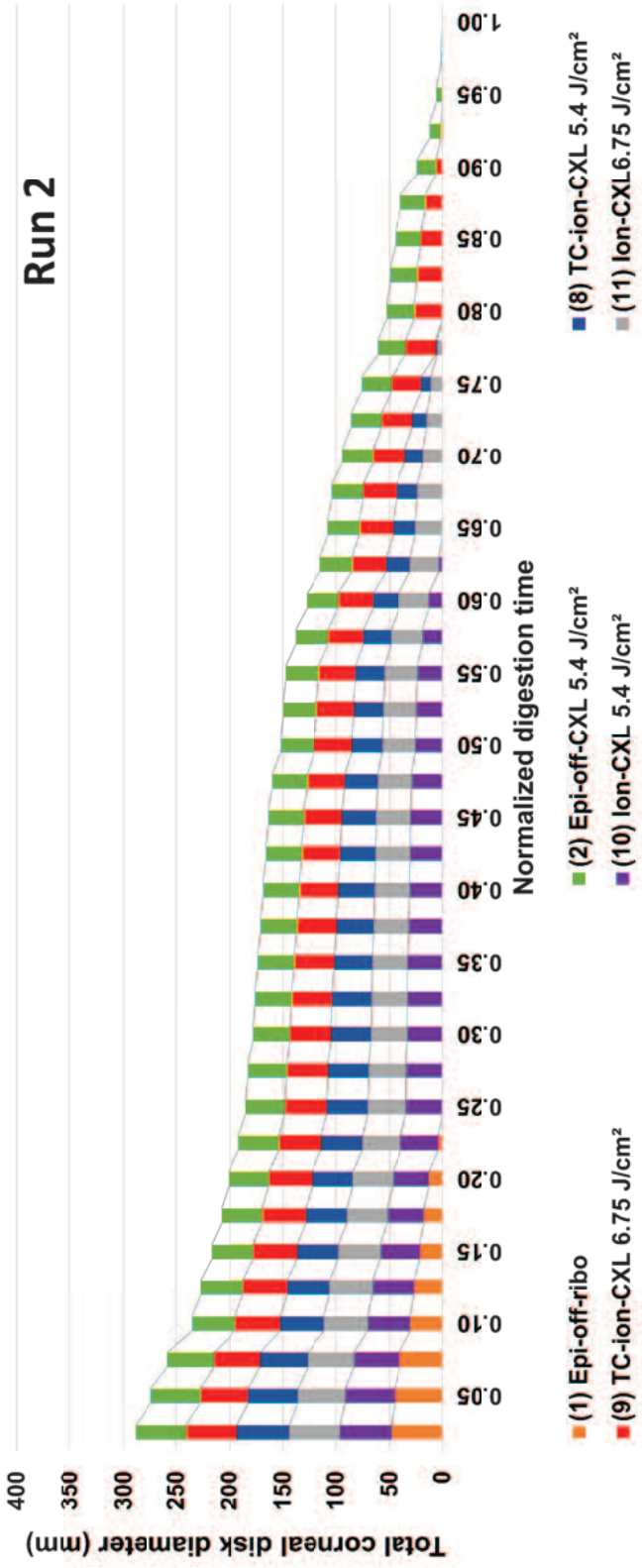

Figure 4.5: The digestion rate of corneal disks treated with Epi-off-ribo, Epi-off-CXL, TC-ion-CXL 5.4 J/cm^2, TC-ion-CXL 6.75 J/cm^2, Ion-CXL 5.4 J/cm^2 and Ion-CXL 6.75 J/cm^2. The summed diameter of all corneal disks within each treatment group (n = 6) are shown for run 2 as a function of time in pepsin digest solution. The digestion time for each treatment group has been normalised against the total digestion time of the epi-off CXL group. (1) Epi-off-ribo (Epithelium-off non-irradiated control); (2) Epi-off-CXL 5.4 J/cm^2 (Epithelium-off standard CXL); (8) TC-ion-CXL 5.4 J/cm^2 (Epithelium intact, high riboflavin concentration and prolonged iontophoresis CXL); (9) TC-ion-CXL 6.75 J/cm^2 (Epithelium intact, high riboflavin concentration, prolonged iontophoresis and high UVA energy dose CXL); (10) Ion-CXL 5.4 J/cm^2 (Epithelium intact, basic iontophoresis protocol) and (11) Ion-CXL 6.75 J/cm^2 (Epithelium intact, basic iontophoresis protocol with high UVA energy dose).

4.4.4 Undigested tissue mass

In run 2, after 11 days in pepsin digest solution only the cross-linked corneas remained (Figure 4.6). At this time point, the average stromal dry weight of the epi-off-CXL 5.4 J/cm^2 treated corneas (group 2) was significantly higher than that of all other treatment groups (groups 8, 10, 11, $p < 0.0001$; group 9, $p < 0.001$). The stromal dry weight did not differ significantly between the Ion-CXL 5.4 J/cm^2 and Ion-CXL 6.75 J/cm^2 treatment groups ($p = 0.32$) or between the TC-ion-CXL 5.4 J/cm^2 and TC-ion-CXL 6.75 J/cm^2 groups ($p = 0.038$). However, corneas treated with the TC-Ion-CXL 6.75 J/cm^2 protocol had a higher stromal dry weight than corneas treated with basic ion-CXL 5.4 J/cm^2 protocol ($p < 0.003$).

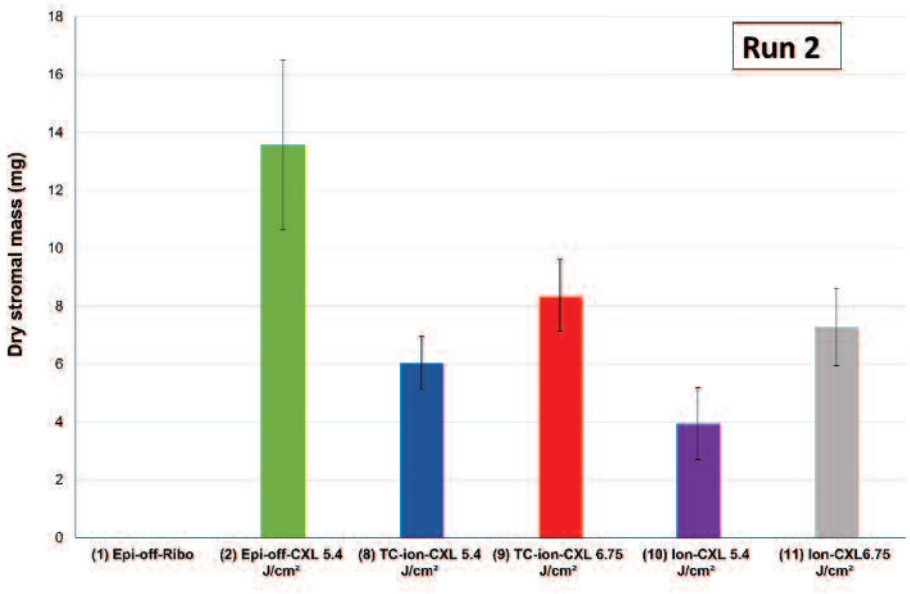

Figure 4.6: Average stromal dry weight of corneal disks treated with Epi-off-ribo, Epi-off-CXL, TC-ion-CXL 5.4 J/cm^2, TC-ion-CXL 6.75 J/cm^2, Ion-CXL 5.4 J/cm^2 and Ion-CXL 6.75 J/cm^2, after 11 days of digestion. Error bars show standard deviation.
Cross-linking treatments: (1) Epi-off-ribo (Epithelium-off non-irradiated control); (2) Epi-off-CXL 5.4 J/cm^2 (Epithelium-off standard CXL); (8) TC-ion-CXL 5.4 J/cm^2 (Epithelium intact, high riboflavin concentration and prolonged iontophoresis CXL); (9) TC-ion-CXL 6.75 J/cm^2 (Epithelium intact, high riboflavin concentration, prolonged iontophoresis and high UVA energy dose CXL); (10) Ion-CXL 5.4 J/cm^2 (Epithelium intact, basic iontophoresis protocol) and (11) Ion-CXL 6.75 J/cm^2 (Epithelium intact, basic iontophoresis protocol with high UVA energy dose).

4.5 Discussion

Achieving sufficient stromal riboflavin concentration is crucial for CXL. Riboflavin acts as a photo-sensitizer for the production of oxygen free radicals, which drive the CXL process (McCall et al. 2010) and consequently, insufficient stromal absorption may cause treatment failure (Wollensak et al. 2009, 2003). Since riboflavin is a hydrophilic molecule that is unable to penetrate epithelial cell membranes and tight junctions, the first riboflavin/UVA CXL protocols required complete central corneal epithelial debridement prior to riboflavin application (Spoerl et al. 1998; Wollensak et al. 2003). Epi-off-CXL is considered to be the gold standard technique as supported by a number of prospective and randomized controlled studies demonstrating its efficacy in relation to cessation of keratoconus progression and improvements in keratometric and visual parameters (Caporossi et al. 2006; Gkika et al. 2011; O'Brart et al. 2011; Richoz et al. 2013; Wittig-Silva et al. 2014; Wollensak et al. 2003). However, new techniques of epi-on-CXL have been considered to eliminate the necessity for epithelial debridement, thus reducing post-operative pain and possible risks of infection (Henriquez et al. 2017; Koller et al. 2009). Moreover, the use of ACXL protocols applying the same energy dose but higher UVA intensities and shorter exposure times to decrease the long treatment times associated with epi-off-CXL with 3 mW/cm^2 UVA irradiation have been proposed (Aldahlawi et al. 2015; Elbaz et al. 2014; Konstantopoulos et al. 2015; Shetty et al. 2015). With the aim of assessing the efficacy of such varying CXL protocols, multiple methodologies, including extensiometry (Cassagne et al. 2016; Kissner et al. 2010; Vinciguerra et al. 2014a; Wollensak et al. 2009), shear wave elastography (Singh et al. 2017; Touboul et al. 2014), Brillouin microscopy (Randleman et al. 2017; Scarcelli et al. 2013) and Scheimpflug air pulse tonometry (Mastropasqua et al. 2014b) have been applied. However, each of these methodologies has their imprecisions and so far, there is no approved best practice for evaluating biomechanical changes following CXL.

Even though the precise aetiology of keratoconus is unidentified (Davidson et al. 2014), an increased activity of protease enzymes and reduced activity of protease inhibitors

has been recognised (Spoerl et al. 2004), with the subsequent increase in stromal protein digestion liable to be a factor in corneal thinning and secondary biomechanical instability (Andreassen et al. 1980). An increase in resistance of stromal tissue to enzymatic digestion following epi-off CXL with a dose response related to the intensity of UVA irradiance was stated by Spoerl et al. (2004). Some researchers replicated this increased resistance to protease digestion following CXL (Aldahlawi et al. 2016; Hayes et al. 2013) and it is thought that this enhanced enzymatic resistance may be a key factor in protection against disease advancement, in light of the known increase in proteinase activity and a reduction in proteinase inhibitor activity in keratoconic corneas (Zhou et al. 1998). In this study, pepsin was selected as the enzyme of choice in preference to collagenase, as it is a non-specific endopeptidase that can break down both collagen and proteoglycan core proteins, and both of these are thought to be sites of riboflavin/UVA induced cross-links (Hayes et al. 2013). Due to the limited availability of human cadaver eyes and rabbit eyes in the UK, porcine eyes were used. The reason is that they were freshly obtainable and in the sufficiently large numbers required for this study. Nevertheless, owing to the porcine cornea having a thicker corneal epithelium than the human cornea, the results have to be regarded as a conservative assessment of the effectiveness of trans-epithelial CXL.

In this study, examination of the enzymatic resistance of corneas to pepsin digestion was used to evaluate the effectiveness of epi-off-CXL, dis-CXL and epi-on-CXL. Despite slight alterations in the rate of enzymatic digestion between similarly treated corneas in runs 1 and 2, perhaps due to variations in the age and breed of the pig eyes in different batches of abattoir tissue, each run exhibited an increased resistance in all of the cross-linked groups in comparison to their non-irradiated controls. Conversely, in agreement with the results of Wollensak et al. (2009), which stated corneal stiffness after epi-on-CXL to be only one fifth of that seen after epi-off-CXL (indicating a reduced crosslinking effect), our study shows enzymatic resistance to be significantly greater in epi-off-CXL treated corneas than in dis-CXL or epi-on-CXL treated corneas. Despite the fact that dis-CXL showed a greater resistance to digestion than the non-irradiated controls, it was not as effective as the other epi-on-CXL protocols, maybe because of the non-homogeneous

uptake of riboflavin which was observed here and documented previously (Alhamad et al. 2012). This finding is supported by a recent, randomized controlled clinical study which showed better corneal flattening with epi-off-CXL than dis-CXL, even though remarkably, dis-CXL lead to enhancement of corrected distance visual acuity at 6 months (Razmjoo et al. 2014).

In this study, it was demonstrated that corneas cross-linked using Mediocross TE® (Medio-CXL protocol) showed a greater resistance to enzymatic digestion than non-irradiated controls and dis-CXL treated corneas. However, the enhanced enzymatic resistance achieved with Medio-CXL was established to be inferior to that of the epi-off and ion-CXL protocols. Mediocross TE® is a hypo-osmolar riboflavin solution that contains 0.01% BAC, a cationic surfactant that can disrupt epithelial tight junctions to increase corneal permeability to riboflavin (Kissner et al. 2010; Raiskup et al. 2012). Preparations with sodium chloride and BAC can facilitate riboflavin transfer through an intact epithelium albeit with significant linked superficial epithelial damage and a lower stromal concentration compared to that achieved with epi-off-CXL (Touboul et al. 2014; Uematsu et al. 2007). A recent study examining the resistance of cross-linked corneas to collagenase showed that an extended penetration time of TE-riboflavin may improve the effect of CXL treatment and make it equivalent to SCXL (Cruzat et al. 2017). Only limited clinical studies using enhanced riboflavin solutions with epithelial penetration enhancers have been published and have given inconsistent results. Some have reported a similar efficacy to epi-off-CXL (Filippello et al. 2012; Magli et al. 2013), however others have shown high rates of treatment failure (Buzzonetti et al. 2012; Kocak et al. 2014; Koppen et al. 2012; Leccisotti et al. 2010). Currently, published randomized, controlled trials comparing epi-off and epi-on-CXL showed similar conclusions, with follow-up times of up to 12 months (Nawaz et al. 2015; Rossi et al. 2015). Contrary to this, another study involving 61 patients, showed epi-on-CXL to be safe but progression of keratoconus was documented in 23% of cases at 12 months follow-up (Soeters et al. 2015). The last study results are consistent with the less pronounced biomechanical alterations detected by laboratory experiments after epi-on-CXL (Wollensak et al. 2009). Moreover, a prospective

study with a follow-up of 12 months demonstrated the safety and efficacy of accelerated epi-on CXL for halting progression of keratoconus (Aixinjueluo et al. 2017).

The use of iontophoresis has been suggested to enhance trans-epithelial riboflavin absorption because riboflavin is negatively charged at physiological pH and soluble in water. Commercially available procedures for iontophoresis utilize 0.1% riboflavin solution and electrical currents of 0.5 - 1 mA for 5 to 10 min (Foschini et al. 2016). On iontophoresis procedure using 1 mA for 5 min, a reduction by two thirds in the stromal riboflavin uptake achieved with epi-off-CXL was documented in treatment of rabbit corneas, nonetheless to produce a similar enhancement in corneal biomechanics (Cassagne et al. 2016). Similar findings were reported in studies on rabbit and human cadaver corneas, with improved riboflavin penetration and increased elastometry measurements acquired with Ion-CXL than with epi-on-CXL (using Ricrolin TE) but less than epi-off-CXL (Vinciguerra et al. 2014a); the same result was found by combining the accelerated 9 mW/cm^2 for 10 min and the iontophoresis technique on human cadaver eyes, and this revealed increased riboflavin penetration and biomechanical resistance (Lanzini et al. 2016). In a human donor eye model, a corneal stiffening effect following Ion-CXL was described by Mastropasqua et al. (2014b) using deformation amplitude index, and inflation tests by Lombardo et al. (2014) reported a similar effect on corneal stiffness to that with epi-off-CXL. Supersonic shear wave elastography has confirmed these findings (Touboul et al. 2014). Moreover, preliminary Ion-CXL clinical studies in prospective case series have stated termination of keratoconus progression with up to 15 months follow-up and some partial progress in keratometric and visual parameters (Bikbova et al. 2014; Buzzonetti et al. 2015; Vinciguerra et al. 2014b). Nevertheless, the relative effectiveness of this technique compared to epi-off-CXL are yet to be confirmed particularly over longer-term follow-up.

It has been established that stromal riboflavin absorption in epithelium-intact corneas can be improved by increasing riboflavin concentration, epithelial contact time and iontophoresis dosage when using spectrophotometry (Hayes et al. 2015), two-photon fluorescence microscopy (Gore et al. 2014) and enzymatic digestion (O'Brart et al. 2018), Based on this work, the basic Sooft italia Ion-CXL protocol (Sooft italia S.p.A, Motegiorgio,

Italy) was modified and the St Thomas's/Cardiff modified iontophoresis protocol (TC-ion-CXL) established. The TC-ion-CXL protocol uses Mediocross TE® in preference to the Ricrolin+® solution used in the Ion-CXL protocol on the basis that the riboflavin concentration of the former is higher (0.25%) and the use of the cationic surfactant BAC has been shown with percutaneous treatment to have synergistic effect with iontophoresis on the transport of anions (Fang et al. 1998). The TC-Ion-CXL protocol also includes an extended riboflavin-epithelial contact period of 5 min after iontophoresis to permit time for the sub-epithelial iontophoretically transported riboflavin to diffuse homogeneously into the stroma, and involves an increased dosage of iontophoresis with a second treatment 5 min after the first. Results from this study have shown that both the basic Ion-CXL and modified TC-ion-CXL protocols result in a greater resistance to enzymatic digestion than all of the other dis-CXL and trans-epithelial CXL protocols examined. Furthermore, this study has shown that the enzymatic resistance of Ion-CXL and TC-ion-CXL treated corneas can be further improved by increasing the UVA energy dose from 5.4 J/cm^2 to 6.75 J/cm^2, presumably by permitting additional type I photochemical cross-linking to happen. The enhancement in enzymatic resistance was evidenced by the Ion-CXL and TC-ion-CXL corneas treated with a total energy dose of 6.75 J/cm^2, persisting for longer in enzyme digest solution than those that received a lower energy dose of 5.4 J/cm^2. The similarity in their dry weights after 11 days of digestion is probably clarified by the fact that at this phase of the digestion process, the rate of digestion was alike for both the 5.4 J/cm^2 and 6.75 J/cm^2 treatment groups and significant differences in average corneal disk diameter were not observed until day 24.

The enzymatic resistance accomplished with the TC-ion-CXL 6.75 J/cm^2 protocol was closest to that of the epi-off-CXL 5.4 J/cm^2 protocol, signifying that this method may be the best trans-epithelial substitute for epi-off-CXL. Its somewhat lower effectiveness compared to epi-off-CXL, as evidenced by measurements of corneal disk diameter and tissue dry weight, may be due to a reduced riboflavin stromal absorption or an accumulation of riboflavin inside the epithelium, which would have the effect of absorbing UVA and shielding the underlying stroma. However, the latter explanation is doubtful as a 3 min

PBS wash of the ocular surface was done before UVA exposure which has been shown by others to successfully remove riboflavin from the epithelium (Gore et al. 2015). Another explanation is that the wash-out period may have been too long and resulted in some loss of riboflavin from the anterior stroma. It is worth stating that excess wash-out could also explain the reduced amount of cross-linking and hence, epithelium riboflavin wash-out times require further optimisation, especially as the human corneal epithelium is thinner and therefore, 3 minutes may wash-out a lot more riboflavin from the human anterior stroma than the porcine anterior stroma. No longer than 1-2 min PBS rinse is highly recommended (E. Spoerl, personal communication, International CXL Experts meeting 2014 in Zurich). One more likely reason of the reduced efficacy could be the oxygen consumption by the epithelium itself (Harvitt et al. 1998), which might lessen the amount of oxygen available to the stroma to drive the CXL process (Friedman et al. 2017; McCall et al. 2010). Additional manipulation of the UVA dosage can overcome such complications, regarding its intensity and duration and/or by increasing oxygen accessibility and necessitate further exploration. Another additional explanation may be the restriction of our porcine model. Due to the porcine cornea having a much thicker corneal epithelium than the human cornea (90 μm and 50 μm, respectively), the results of this study must be observed as a conservative assessment of the efficiency of trans-epithelial CXL. Regrettably, human donor corneas are inappropriate for investigating the effects of CXL on enzymatic resistance as a result of the fact that donors are usually over 60 years old, and the naturally occurring cross-links which increase with age, may disguise the effects of the CXL treatment under investigation. Nevertheless, it would be interesting to replicate our methodology in the rabbit model which has a thinner epithelium (40 μm) and is closer in thickness to that of the human cornea. Such a study would supplement our present conclusions by providing a more generous approximation of the usefulness of trans-epithelial cross-linking.

The present study demonstrated the St Thomas'/Cardiff modified iontophoresis protocol (TC-ion-CXL) to be more effective than other trans-epithelial CXL protocols at increasing the enzymatic resistance of the cornea, backing the concept that iontophoresis-

assisted CXL may, with modifications in terms of riboflavin concentration, duration of iontophoretic treatment, riboflavin soak-time and UVA energy dose, be an effective technique to inhibit the development of keratoconus and avoid the postoperative pain related with epithelial debridement. This technique is predicted to be particularly suitable for eyes that are not suitable for treatment with epi-off-CXL due to minimum corneal thickness values less than 400 μm. Additional laboratory studies to enhance this protocol and randomized, prospective clinical studies to compare its effectiveness with epi-off CXL are required and are presently being commenced (D. O'Brart, personal communication, International Standard Randomized Controlled Trials Number: 04451470).

CHAPTER 5

AN EX VIVO INVESTIGATION INTO THE EFFECT OF ACCELERATED CROSS-LINKING USING PULSED AND CONTINUOUS UVA IRRADIATION MODES ON CORNEAL ENZYMATIC RESISTANCE.

This chapter was published as a laboratory science article in Invest Ophthalmol Vis Sci. 2016; 57:1547–1552. DOI:10.1167/iovs.15-18769.

5.1 Introduction

The exact photochemical mechanism involved in riboflavin/UVA CXL is at present uncertain. Interestingly, however, it has been shown that oxygen is crucial to drive the process and in the absence of oxygen, CXL is impaired (McCall et al. 2010). Not only is oxygen an integral part of the equation, it has also been suggested that higher UVA intensity or so-called 'accelerated' CXL (ACXL) protocols cause a more rapid oxygen depletion thereby reducing efficacy (Brittingham et al. 2014; Touboul et al. 2012). However, it has been shown that when UV irradiation is ceased, oxygen can be restored to its normal level within 3 to 4 minutes (Kamaev et al. 2012). On this basis, it has been advocated that by pulsing the UV light throughout the procedure, oxygen levels may continue to be replenished, so that the CXL process is no longer impaired (Krueger et al. 2014; Mazzotta et al. 2014). Additionally, it has also been postulated that the efficacy of accelerated protocols may be improved by increasing the exposure time by 30 to 40% (Kymionis et al. 2014; Sherif 2014).

5.2 Research aim

In order to further investigate these issues and compare the efficacy of accelerated CXL, extended accelerated CXL and pulsed CXL protocols with the 'gold standard' SCXL protocol, the rate of enzymatic digestion after each CXL protocol was examined in an ex-vivo porcine model.

5.3 Methods

5.3.1 Tissue Preparation and CXL Treatments

A total of 66 enucleated porcine eyes, obtained from a local European Community licensed abattoir, were used within 6 hours of death. All have intact corneal epithelium and

transparent cornea. After a complete debridement of the corneal epithelium using a single-edged razor blade, the eyes were randomly and equally divided into the 6 groups; groups 1 and 2 served as controls. With the exception of group 1, which received no treatment, for the rest of the 5 groups (2, 3, 4, 5 and 6), 0.1% riboflavin solution containing 20% dextran T-500 (Mediocross D®, Peschke Meditrade, Huenenberg, Switzerland) was applied to the anterior corneal surface for 30 minutes, using an annular suction ring (for detail see Chapter 2). Groups 3, 4, 5 and 6 were then irradiated in the manner described in Table 5.1, with Group 3 undergoing the SCXL protocol, Group 4 receiving a 30 mW UVA for 3 min ACXL protocol (with the same total energy dose as that of the SCXL group) and Groups 5 and 6 receiving a high total energy dose protocol (HCXL) comprising 30 mW UVA for 4 min (corresponding to a 25 % increase in the total energy dose compared to the SCXL protocol). In the case of Group 6 only, the UVA light was pulsed during exposure in a cycle of 10-s on and 10-s off.

All of the irradiation protocols were performed using the Phoenix CXL System (Peschke trade GmbH, Huenenberg, Switzerland) with a wavelength of 365 nm, a 50 mm working distance and a 9 mm aperture (Figure 5.1). Measurement of the central corneal thickness was via ultrasound pachymetry (DGH Pachmate 55; DGH Technologies, Exton, PA, USA) (for more details please refer to Chapter 2) pre-treatment (after epithelial debridement), post-riboflavin application and post-UVA exposure.

Following treatment, an 8 mm full-tissue-thickness biopsy was trephined from the centre of each cornea. The corneal disks were placed in individual sealed tubes containing 5 ml of pepsin digest solution (1 g of 600 to1200 U/mg pepsin from porcine gastric mucosa (Sigma-Aldrich, Dorset, UK) in 10 ml 0.1 M HCl at pH 1.2) and incubated in a water bath at 23°C. 5 corneal disks from each group were removed from the pepsin digest solution after 13 days and placed in a 60°C oven until a constant dry weight was obtained. The measurement and calculation used in this chapter were the same as mentioned previously in Chapter 3.

Table 5.1: Irradiation protocols of the six groups of porcine eyes

Groups		Treatment Protocols				
		Riboflavin application	UVA intensity (mW/cm^2)	Duration of UVA exposure (minutes)	Total Energy Dose (J/cm^2)	Frequency of Riboflavin application during UVA exposure
1	Untreated	-	-	-	-	-
2	Riboflavin only (R)	√	-	-	-	-
3	Standard 3mW CXL (**SCXL 5.4** J/cm^2)	√	3	30	5.4	Once at the start and every 5 minutes during (total = 6)
4	Accelerated 30mW CXL (**ACXL 5.4** J/cm^2)	√	30	3	5.4	Once at the start
5	High energy dose accelerated 30mW CXL (**HCXL 7.2** J/cm^2)	√	30	4	7.2	Once at the start
6	High energy dose accelerated pulsed 30mW CXL (**p-HCXL 7.2** J/cm^2)	√	30	8 in a pulsed radiation of 10-s on and 10-s off	7.2	Once at the start and after 5 minutes (total = 2)

5.3.2 Data analysis

Data are shown as mean measurements (± SD) for corneal thickness, dry weight and complete digestion time. Corneal disk diameter is presented as a daily cumulative measurement for each treatment group. Statistical analysis was performed using a one-way ANOVA and Bonferroni multiple comparisons in a depth-wise manner. All statistical analyses were performed with the Statistical Package for the Social Sciences (SPSS Statistics 20; IBM, Armonk, NY, USA), whereby a probability value of $p < 0.05$ was considered significant.

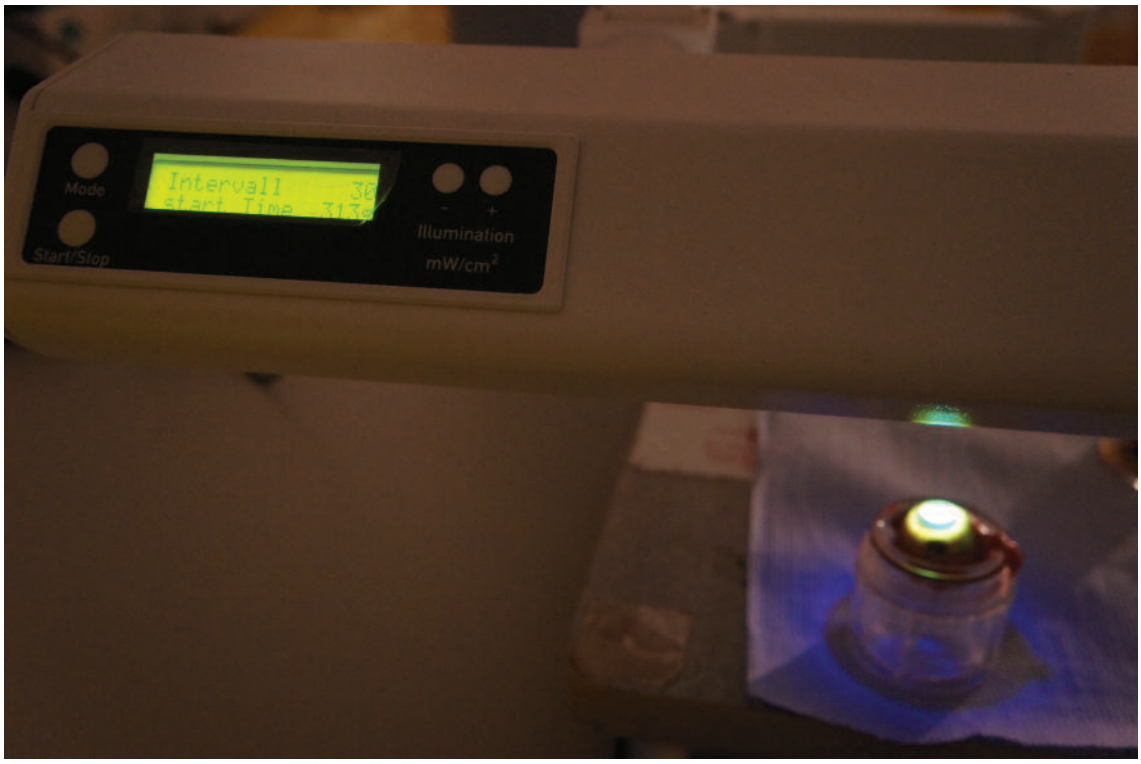

Figure 5.1: The Phoenix CXL System (Peschke trade GmbH, Huenenberg, Switzerland) with a wavelength of 365 nm, a 50 mm working distance and a 9 mm aperture.

5.4 Results

5.4.1 Corneal Thickness

The average stromal thickness at each stage of treatment is shown in Figure 5.2. The average stromal thickness did not differ significantly between groups before treatment. However, a significant decrease in stromal thickness ($p < 0.0001$) was noted after 30-minute application of riboflavin-dextran solution (group 2–6). The subsequent irradiation of corneas in groups 3 to 6 produced no further changes in corneal thickness and the final stromal thickness did not differ significantly between any of the CXL groups.

5.4.2 Time Taken for Complete Digestion

Figure 5.3 shows photographs of a representative corneal disk from each treatment group prior to immersion in pepsin digest solution (day 0) and 1 and 2 days after digestion. As

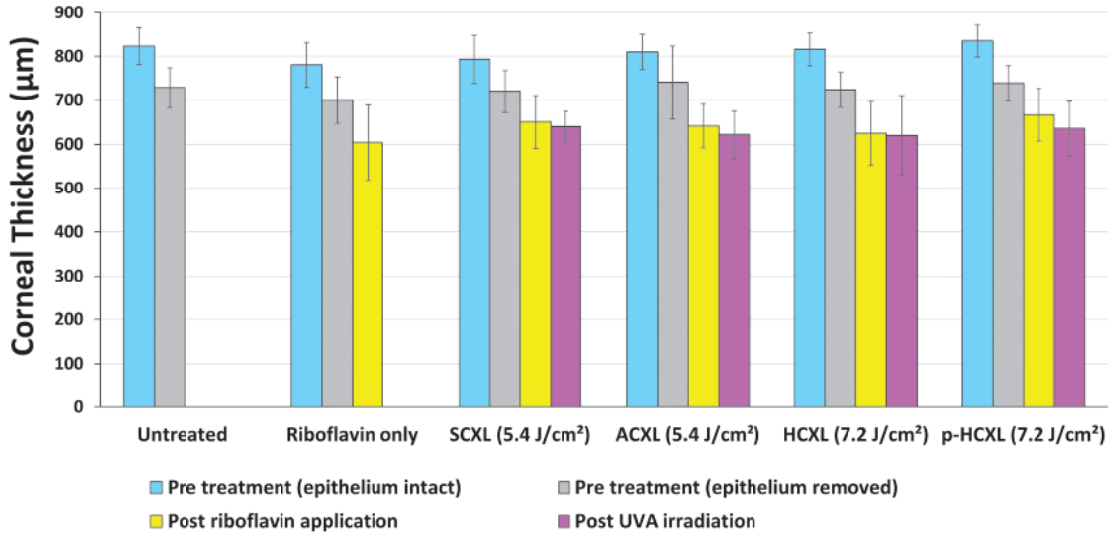

Figure 5.2: Average corneal thickness measured before, during and after treatment. Error bars show standard deviation.
Cross-linking treatments: SCXL 3 mW (5.4 J/cm^2) (standard cross-linking); ACXL 30 mW (5.4 J/cm^2) (accelerated cross-linking); HCXL 30 mW (7.2 J/cm^2) (accelerated, and high energy UVA cross-linking) and p-HCXL 30 mW (7.2 J/cm^2) (pulsed, accelerated and high energy UVA cross-linking).

shown in previous experiments, within 1 day of submersion in pepsin solution, stromal swelling, in a posterior-anterior direction was observed in all corneal disks (Figure 5.3). After 2 days of digestion, a loss of structural integrity was seen in the untreated corneas but the cross-linked corneas remained intact (Figure 5.3).

The cross-linked corneas (groups 3–6) took significantly longer to digest than the non-irradiated specimens (groups 1 and 2) ($p < 0.0001$; Figure 5.4). Complete digestion of non-irradiated corneas was noted after 13 days.

Corneas cross-linked with higher energy dose treatments (7.2 J/cm^2) using continuous (group 5) or pulsed light (group 6) took significantly longer to digest than corneas cross-linked using lower (5.4 J/cm^2) energy dose treatments (groups 3 and 4; $p < 0.0001$). A direct comparison between treatments using the same energy dose revealed that corneas cross-linked using the SCXL 3 mW (5.4 J/cm^2) procedure took longer to digest than corneas cross-linked using the ACXL 30 mW (5.4 J/cm^2) procedure ($p < 0.0001$), and corneas cross-linked using the pulsed irradiation p-HCXL 30 mW (7.2 J/cm^2) procedure

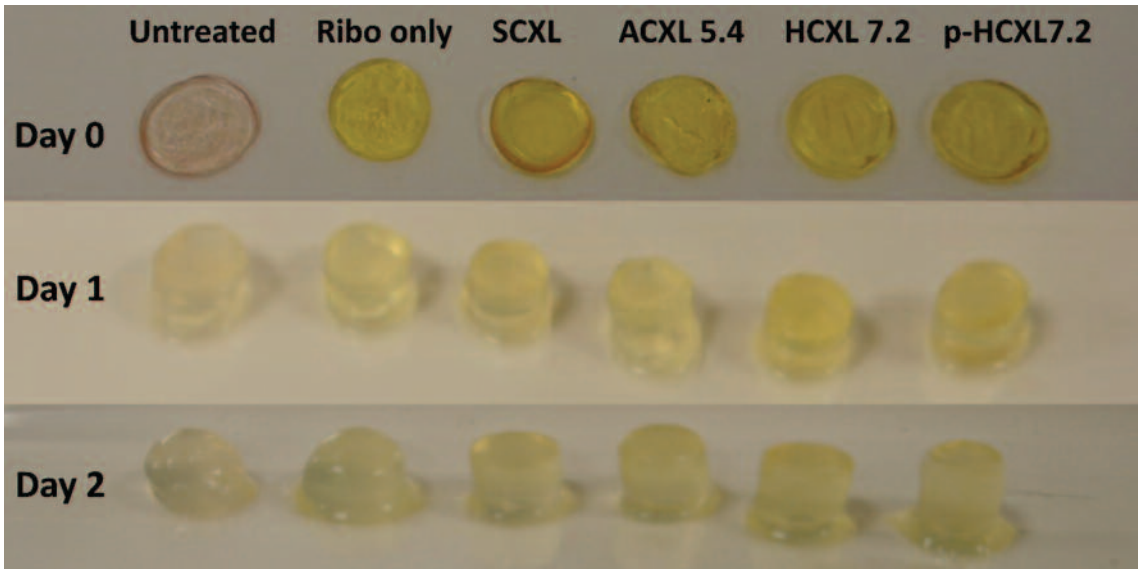

Figure 5.3: Photographs of a representative corneal disk from each treatment group prior to immersion in pepsin digest solution (day 0) and 1 and 2 days after digestion.
Cross-linking treatments: SCXL 3 mW (5.4 J/cm^2) (standard cross-linking); ACXL 30 mW (5.4 J/cm^2) (accelerated cross-linking); HCXL 30 mW (7.2 J/cm^2) (accelerated, and high energy UVA cross-linking) and p-HCXL 30 mW (7.2 J/cm^2) (pulsed, accelerated and high energy UVA cross-linking).

took significantly longer to digest than those treated with the continuous irradiation HCXL 30 mW (7.2 J/cm^2) procedure ($p < 0.0001$). The summed diameter of all corneal disks ($n = 6$) within each cross-linked and non-cross-linked treatment group is shown as a function of time in pepsin digest solution (Figure 5.4). In addition, the average time (± SD) required for complete digestion of each treatment group has been added to the time-line.

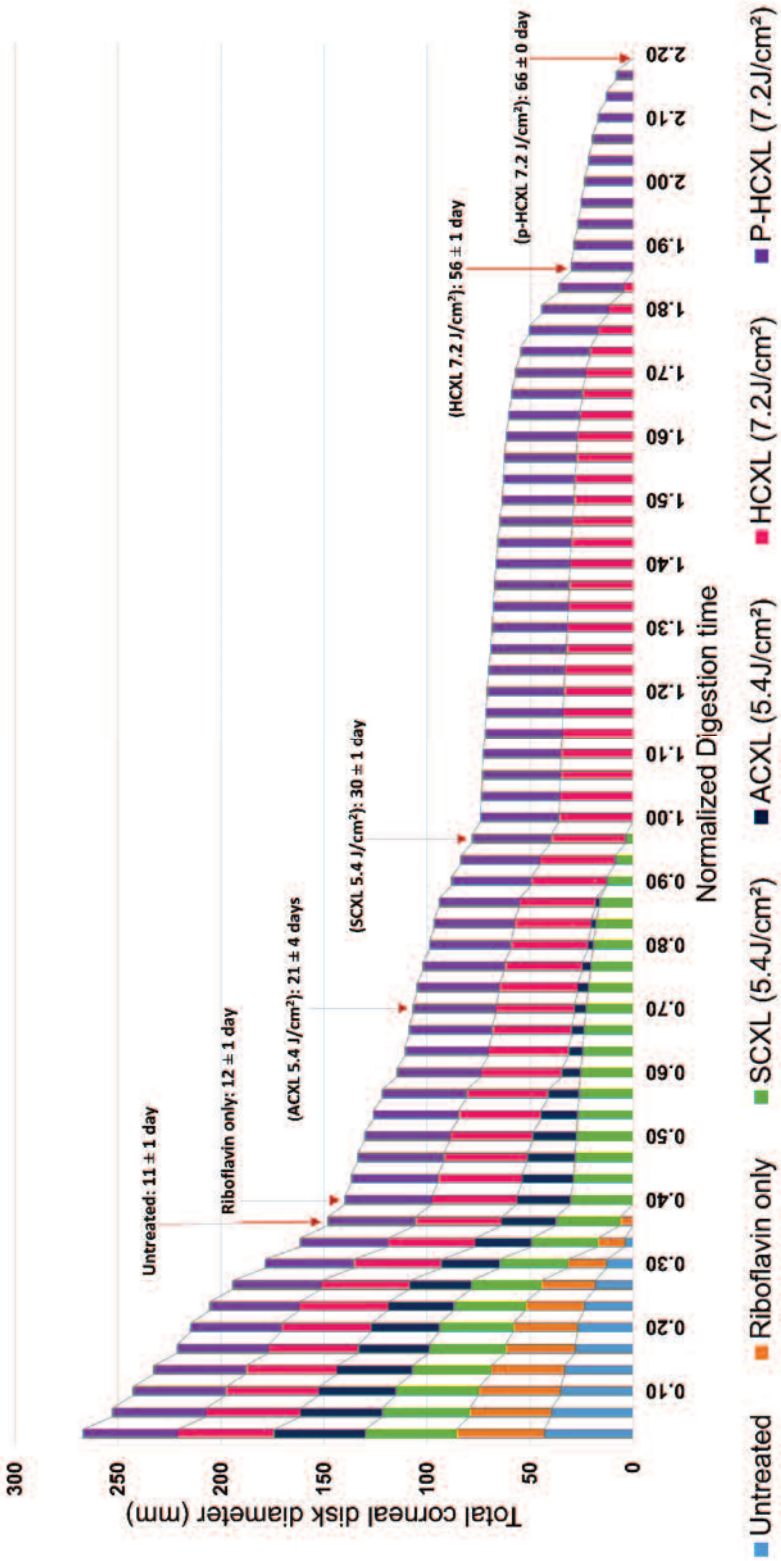

Figure 5.4: The digestion rate of corneal disks treated with control untreated, riboflavin-only, SCXL, ACXL, HCXL and p-HCXL. The summed diameter of all corneal disks (n = 6) within each cross-linked and non-cross-linked treatment group is shown as a function of time in pepsin digest solution) normalised against the standard SCXL.
Cross-linking treatments: SCXL 3 mW (5.4 J/cm^2) (standard cross-linking); ACXL 30 mW (5.4 J/cm^2) (accelerated cross-linking); HCXL 30 mW (7.2 J/cm^2) (accelerated, and high energy UVA cross-linking) and p-HCXL 30 mW (7.2 J/cm^2) (pulsed, accelerated and high energy UVA cross-linking).

5.4.3 Undigested Tissue Mass

Thirteen days following submersion in pepsin digest solution, only the CXL-treated corneas remained (Figure 5.5); corresponds to approximately 0.43 normalized digestion time against the SCXL (Figure 5.4). At this time point, the average corneal disk dry weight of the SCXL (5.4 J/cm^2) treated corneas was significantly higher than that of the ACXL 30 mW (5.4 J/cm^2) ($p < 0.0001$), HCXL 30 mW (7.2 J/cm^2) ($p < 0.001$) and p-HCXL 30 mW (7.2 J/cm^2) treated corneas ($p < 0.05$). Interestingly, there is no significant difference in stromal dry weight between the two higher energy treatment groups which used continuous (HCXL 30 mW (7.2 J/cm^2)) and pulsed (p-HCXL 30 mW (7.2 J/cm^2)) irradiation. The corneas treated with p-HCXL 30 mW (7.2 J/cm^2) had a higher stromal dry weight than the corneas treated with ACXL 30 mW (5.4 J/cm^2) ($p < 0.0001$).

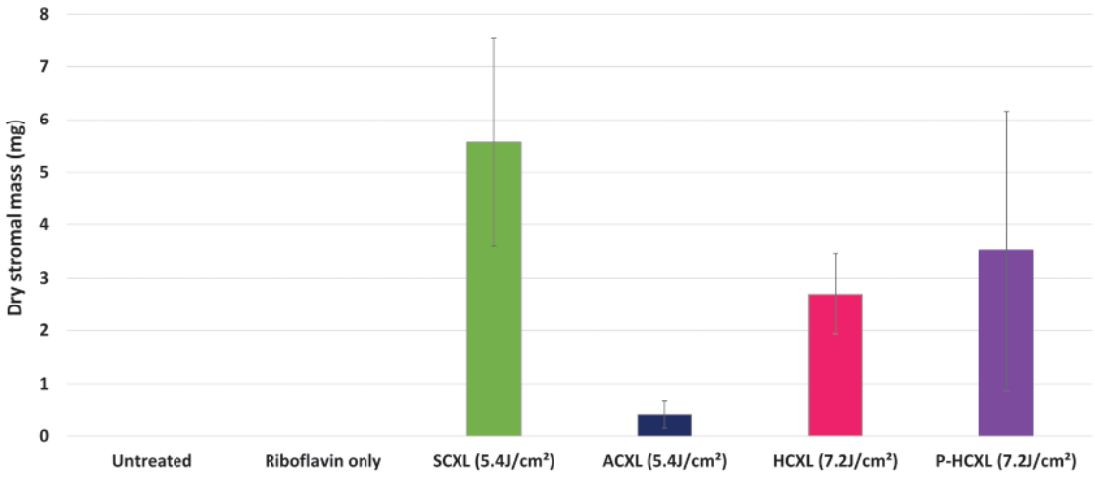

Figure 5.5: Average stromal dry weight of corneal disks treated with control untreated, riboflavin-only, SCXL, ACXL, HCXL and p-HCXL, after 13 days of digestion. Error bars show standard deviation.
Cross-linking treatments: SCXL 3 mW (5.4 J/cm^2) (standard cross-linking); ACXL 30 mW (5.4 J/cm^2) (accelerated cross-linking); HCXL 30 mW (7.2 J/cm^2) (accelerated, and high energy UVA cross-linking) and p-HCXL 30 mW (7.2 J/cm^2) (pulsed, accelerated and high energy UVA cross-linking).

5.5 Discussion

Oxygen is crucial to drive the riboflavin/UVA CXL process; in its absence cross-link formation is impaired (McCall et al. 2010). Reduced efficacy with ACXL protocols has been postulated to be due to more rapid oxygen depletion compared to the more prolonged but less intense UVA exposure in SCXL (Brittingham et al. 2014; Touboul et al. 2012). The actual photochemical mechanisms involved in riboflavin/UVA CXL are uncertain. It has been propounded that under aerobic conditions with a brief type II photochemical reaction, sensitised photooxidation of stromal proteins occurs, mainly by their reaction with photochemically generated reactive oxygen species (Kamaev et al. 2012). After the initial 15 seconds of exposure to UVA, when oxygen becomes depleted, a type I photosensitizing mechanism may then predominate, subsequently producing radical ions that can induce covalent CXL of stromal macromolecules (Friedman et al. 2017; Kamaev et al. 2012). In SCXL, where UVA exposure occurs over 30 minutes, the oxygen concentration in the cornea may slowly increase during the later stages of the treatment to a level at which a type-II mechanism may once again begin (Kamaev et al. 2012). On the basis that oxygen can be restored to its normal tissue levels within 3 to 4 minutes of cessation of UVA radiation (Kamaev et al. 2012). If this is so, then pulsing the UV light could potentially help replenish oxygen levels, so that the CXL process is no longer impaired (Krueger et al. 2014; Mazzotta et al. 2014).

The other method found to improve efficacy of the accelerated CXL protocol is increasing UVA exposure time, and ultimately the overall cumulative dosage, by 30 to 40% (Kymionis et al. 2014; Sherif 2014). In the present study, the aim was to investigate the porcine corneal resistance to enzymatic (pepsin) digestion, utilising a number of these newer commercially available extended and pulsed accelerated protocols.

All the eyes treated in this study received an application of an iso-osmolar riboflavin solution (containing 20% dextran) to the deepithelialised corneal surface. Consistent with earlier studies (Hassan et al. 2014; Hayes et al. 2013), a decrease in corneal thickness was noted. This can be ascribed to the dehydration effect of the dextran and, possibly, to the

existence of riboflavin (Aldahlawi et al. 2015), which has the effect of enhancing the ionic strength of the applied solution and likely cause further reduction of the cornea hydration (Huang et al. 1999).

Corneal thickness measurements were considered to be an unreliable measure of the rate of enzymatic digestion due to treatment-induced variations in corneal thickness and the swelling of the trephined corneal disks (in the posterior-anterior direction) during the first 24 hours of immersion in pepsin digest solution (Aldahlawi et al. 2015). As such, in this current study, daily measurement of the diameter of the anterior corneal surface and the dry weight of the undigested tissue after 13 days of digestion was taken. These measurements provided a more reliable assessment of both the structural integrity of the anterior corneal stroma and the effective depth of CXL following each treatment variation.

Corneas treated with ACXL 30 mW (5.4 J/cm^2) had a lower residual mass after 13 days of digestion, and took less time to undergo complete digestion than SCXL-treated corneas. This may be due to a reduced CXL effect and a failure of the Bunsen-Roscoe law of reciprocity at higher UVA intensities. This idea is supported by the findings of biomechanical studies that report a reduced corneal stiffening effect with increasing UVA intensity up to 18 mW (Hammer et al. 2014), and a sudden decrease in efficacy with very high intensities greater than 45 mW/cm^2 (Wernli et al. 2013). It is thought that the failure of the Brunsen-Roscoe law in cases of very high intensity and short illumination time, may be attributed to inhibition of the CXL process due to a lack of oxygen (McCall et al. 2010) and on this basis the concept of p-HCXL was introduced. However, recent studies comparing the biomechanical changes after p-HCXL and SCXL have reported a reduced corneal stiffening effect with p-HCXL (30 mW/cm^2 for 8 min) compared to SCXL 3 mW (5.4 J/cm^2) (Kling et al. 2017), whereas, another study using uniaxial strip extensiometry demonstrated an equal increase in the stiffening effect following cross-linking with a 45 mW pulsed UVA illumination compared to cross-linking with a 45 mW continuous UVA illumination (Zhang et al. 2017). These findings, along with our results of increased residual mass in p-HCXL treated eyes, lends support to this hypothesis; oxygen availability is greater than in non-pulsed HCXL treatments. It seems that some oxygen replenishment

occurred after each pulse. A longer pulse duration (in excess of 10 s) might be a means of enhancing the cross-linking process further.

The enhanced enzymatic resistance observed with increased exposure time of the cornea to 30 mW UVA from 3 to 4 minutes may be due to the increase in the total energy dose from 5.4 to 7.2 J/cm^2, which allowed additional type I photochemical CXL to take place. It is improbable that the increased CXL effect is due to the extended treatment providing additional time for the oxygen levels to be replenished to a level at which the type II CXL reaction could be restarted as, even when SCXL is performed, the oxygen concentration is thought only to reach adequate levels in the latter half of the 30-minute protocol (Kamaev et al. 2012).

Although the dry weight of the SCXL-treated corneas was higher when measured midway through the digestion process, corneas treated with HCXL and p-HCXL and a total energy dose of 7.2 J/cm^2 were found to persist for longer in enzyme digest solution than SCXL (5.4 J/cm^2) treated corneas. This suggests that differences in the distribution of CXL may occur within the tissue. It can be theorised that CXL using a higher UVA intensity and a greater total energy dose results in superior CXL strength within the most anterior stromal layers and/or the mid-corneal region, leading to longer overall digestion times. However, the depth of CXL may be shallower or there may be a more rapid decrease in the intensity of CXL as a function of depth, compared to SCXL, resulting in a reduced overall mass of cross-linked tissue. It is of interest that Brillouin microscopy studies of SCXL-treated corneas have shown that the intensity of CXL is depth-dependent, with the anterior stroma contributing the most to the increase in mechanical stiffness, and examination of the effect of varying UVA exposure time (0–30 minutes) has shown a dose-dependent tissue stiffening in the anterior third of the cornea (Scarcelli et al. 2013).

The clinical importance of these findings is ambiguous, as the exact amount and location of cross-linked tissue necessary to prevent keratoconic progression has yet to be determined. Clinical studies comparing CXL with accelerated pulsed or continuous UVA CXL protocols are limited and somewhat conflicting. In a clinical study by Tomita

et al comparing the outcomes of SCXL to an ACXL procedure using a UVA exposure of 30 mW/cm^2 for 3 minutes, there was no notable difference in either the visual and topographic indices or the depth of the demarcation line at 6 months (Tomita et al. 2014); however, in a randomized clinical study involving 138 eyes, Shetty et al. reported poorer refractive and tomographic outcomes at 12 months follow-up in the patients treated with a 30 mW/cm^2 for 3 minutes ACXL procedure compared to those treated with SCXL (Shetty et al. 2015). A 1-year follow-up of 20 patients treated with either pulsed or continuous light HCXL 30 mW (7.2 J/cm^2) showed keratoconus stability in both groups, although better functional outcomes and a deeper demarcation line were noted for the pulsed light treatment (Mazzotta et al. 2014) and a 2-year prospective study of 132 eyes showed same results with ACXL pulsed 15 mW/cm^2 for 12 min and a total dose of 5.4 J/cm^2 (Mazzotta et al. 2017). Similarly, in a retrospective study of 60 patients treated with HCXL 30 mW (7.2 J/cm^2), the demarcation line was found to be deeper in patients treated with pulsed rather than continuous light (Moramarco et al. 2015). Peyman et al. (2016) reported also similar results in a clinical study of 70 eyes. However, in a comparative clinical study by Jiang et al. (2017) between pulsed HCXL 30 mW (7.2 J/cm^2) to SCXL, there was statistically greater reduction in maximum and mean keratometry and deeper demarcation lines in SCXL treated eyes. This result endorsed our finding that a higher undigested corneal mass was found in SCXL than p-HCXL 30 mW (7.2 J/cm^2). Clearly further, prolonged clinical studies are needed to compare the outcomes of p-HCXL with SCXL, both of which appear on the basis of this study to offer the best outcomes in terms of resistance to enzyme digestion.

In conclusion, differences in the enzymatic resistance of SCXL, ACXL and HCXL corneas indicate that the intensity and distribution of cross-links differs as a result of the treatment protocol employed. Although the use of an accelerated protocol with a higher energy dose and pulsed UVA (p-HCXL) appears to offer the best results in terms of increased enzymatic resistance, the exact amount of cross-linking needed to prevent disease progression is not yet known.

CHAPTER 6

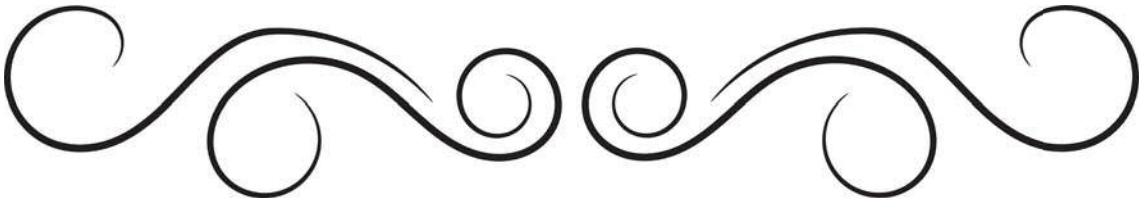

AN IN-VITRO INVESTIGATION OF EPITHELIUM-OFF AND IONTOPHORETIC EPITHELIUM-ON HIGH ENERGY PULSED & PROLONGED RIBOFLAVIN/ULTRAVIOLET CORNEAL CROSS-LINKING PROTOCOLS.

6.6 Introduction

Whilst the clinical outcomes of the SCXL procedure have been very positive, there are number of drawbacks to this treatment, such as the prolonged procedure time (which lasts over an hour) and the postoperative pain/risk of infection associated with debriding the epithelium. These factors have led to an interest in modifying CXL protocols, to overcome these problems. These modifications include (1) reducing the irradiation time, whilst simultaneously increasing the UVA irradiance, to deliver the same (ACXL) or higher (HCXL) energy dose to that of the SCXL technique but over a shorter time-frame (Cinar et al. 2014; Elbaz et al. 2014), (2) pulsed UVA delivery techniques to increase oxygen availability during ACXL and HCXL (Mazzotta et al. 2014; Mencucci et al. 2015) and (3) non-removal of the epithelium and the application of riboflavin solutions with permeation enhancers, either in isolation or in combination with iontophoretic delivery techniques to enhance stromal penetration (Arboleda et al. 2014; Bouheraoua et al. 2014). As described in Chapters 3, 4 and 5, each of these modifications on their own has had varied success to improve the resistance of the cornea to enzymatic digestion.

In vitro studies examining the effectiveness of the basic iontophoresis-assisted, epithelium-on cross-linking protocol, which uses a dextran-free riboflavin solution and a current intensity of 1 mA for 5 min, have been encouraging in that they appear to enhance the penetration of riboflavin across the epithelium (Cassagne et al. 2016). However, the stromal riboflavin concentration remains less than that achieved with epithelium-off riboflavin application (Cassagne et al. 2016). Clinical studies of iontophoresis-assisted cross-linking have shown a cessation of disease progression and improvements in visual parameters in many cases, but the outcomes appear to be inferior to those of SCXL, and the long-term efficacy of the technique is unknown (Mastropasqua et al. 2014a). As demonstrated in Chapter 4, corneal resistance to enzyme digestion can be improved by increasing both the concentration of riboflavin and the duration of iontophoresis and further gains may be achieved through the use of pulsed UVA light and HCXL treatments involving exposure to higher UVA energy doses (Chapter 5). In this study several of

these modifications have been combined in an attempt to find a method of trans-epithelial cross-linking that is equally effective as SCXL but offers the promise of increased patient comfort and a shorter treatment time.

6.7 Research aim

The aim of this study was to compare the efficacy of the gold-standard SCXL protocol to that of a novel epithelium-on CXL protocol that involves the iontophoretic delivery of a high concentration riboflavin solution and exposure to high-energy, pulsed UVA. The efficacy of each protocol is assessed in terms of their ability to enhance the stiffness and enzymatic resistance of the cornea.

6.8 Methods

6.8.1 Sample preparation

Sixty-three fresh porcine eyes, all with transparent corneas and an intact corneal epithelium, were obtained from a local European Community licensed abattoir and used within 6 hours of death. The eyes were divided into the five treatment groups described below and summarised on Table 6.3.

1. Untreated corneas:

The corneal epithelium was removed from 6 eyes. These corneas received no further treatment (no eye drops or UVA exposure).

2. Riboflavin only:

The corneal epithelium was removed from 6 eyes and a 0.1% iso-osmolar riboflavin solution containing 20% dextran T-500 (Mediocross D®, Peschke Meditrade, Huenenberg, Switzerland) was applied to the anterior corneal surface for 30 min.

3. Standard epi-off, low UVA intensity CXL protocol (SCXL 5.4 J/cm^2):

The corneal epithelium was removed from 17 eyes and a 0.1% iso-osmolar riboflavin solution containing 20% dextran T-500 was applied to the anterior corneal surface for 30 min. The cornea was then exposed to 3mW UVA for 30 min (total energy dose of 5.4 J/cm^2), during which time riboflavin was re-applied at 5 min intervals. Total treatment time: 60 min.

4. Epi-off, medium UVA intensity, high energy, pulsed CXL protocol (p-HCXL 7.56 J/cm^2):

The corneal epithelium was removed from 17 eyes and a 0.1% iso-osmolar riboflavin solution containing 20% dextran T-500 was applied to the anterior corneal surface for 30 minutes. The cornea was then exposed to 9 mW UVA for a period of 14 min with regular stops of 15 sec every 1 min (total energy 7.56 J/cm^2). Riboflavin was re-applied every 5 min throughout the course of the treatment. Total treatment time: 47.5 min.

5. Modified trans-epithelial iontophoresis CXL protocol using medium intensity, high energy, pulsed UVA (p-TC-ion-HCXL 7.56 J/cm^2):

Seventeen corneas (with their epithelium intact) had a prolonged iontophoresis (St. Thomas-Cardiff) protocol similar to Chapter 4, which received an iontophoresis assisted delivery of a 0.25% hypo-osmolar riboflavin solution containing 1.2% HPMC and 0.01% BAC (Mediocross TE®, Peschketrade, Huenenberg, Switzerland) using a current of 1 mA for 5 min. After this initial application, the corneas were soaked with this riboflavin solution for 5 min. Following this period of soakage, the corneas received a second iontophoresis assisted delivery of fresh 0.25% hypo-osmolar riboflavin solution using a current of 1 mA for 5 min and a further 5 min of riboflavin soakage. The corneas were then washed with PBS for 1 min to remove riboflavin trapped within the epithelium and irradiated with 9 mW UVA for 14 min with a 15 sec break from irradiation every 1 min (total energy 7.56 J/cm^2). PBS was applied at 5 min intervals throughout to keep the corneal surface moist. Following treatment, the corneal epithelium was debrided to ensure consistency with the other groups. Total treatment time: 38.5 min.

All of the irradiation protocols were performed using 370 nm UVA light delivered via a CCL-365 vario™ cross-linking system (Peschkmed, Huenenberg, Switzerland), with a 50 mm working distance and a 9 mm aperture.

6.8.2 Pachymetry

Central corneal thickness was measured using ultrasound pachymetry (DGH Pachmate 55; DGH Technologies, Exton, PA), at the following experimental stages: immediately pre-treatment (epithelium intact); pre-treatment (epithelium removed) (if applicable); post-riboflavin application and post-UVA exposure (if applicable).

6.8.3 Enzymatic digestion

In this study, 6 riboflavin-only treated corneas and 11 corneas from each of the CXL treatment groups were examined. An 8 mm full-tissue-thickness biopsy was trephined from the centre of each cornea. The corneal disks were placed in individual sealed tubes containing 5 ml of pepsin digest solution (1 g of ≥ 500 U/mg pepsin from porcine gastric mucosa (Sigma-Aldrich, Dorset, UK) in 10 ml 0.1M HCl at pH 1.2) and incubated in a water bath at 23°C. Using electronic digital callipers, the diameter of the anterior surface of each corneal disk was recorded daily. Measurements were continued until the tissue could no longer be distinguished from the surrounding pepsin solution (even under microscopical examination) and was considered to have undergone ‘complete digestion’. The digestion time for each group was normalised against the total digestion time of the SCXL treatment group.

To further assess the effect of each treatment on enzymatic resistance, 5 corneal disks from each group were removed from the pepsin digest solution after 12 days and placed in a 60°C oven until a constant dry weight was obtained. The average corneal dry weight was then calculated for each group.

Table 6.3: A summary of the treatment groups.

Group	Epi.	Riboflavin formulation	Ionto (1 mA)	Ribo soak	Ionto (1 mA)	Ribo soak	Saline rinse	UVA intensity	Duration of CXL	UVA Energy	Applied during irradiation
Untreated	**Off**	-	-	-	-	-	-	-	-	-	-
Riboflavin only	**Off**	**0.1% ribo 20% dextran (Ricrolin)**	-	**30 min**	-	-	-	-			-
SCXL	**Off**	**0.1% ribo 20% dextran (Ricrolin)**	-	**30 min**	-	-	-	**3 mW/cm^2**	**30 min**	**5.4 J/cm^2**	**0.1% ribo 20% dextran (Ricrolin)**
p-HCXL (7.56 J/cm^2)	**Off**	**0.1% ribo 20% dextran (Ricrolin)**	-	**30 min**	-	-	-	**9 mW/cm^2 14 min stop 15 sec every 1 min**	**14 min + 3.5 min stop = total time 17.5 min**	**7.56 J/cm^2**	**0.1% ribo 20% dextran (Ricrolin)**
p-TC-ion-HCXL (7.56 J/cm^2)	**On**	**0.25% Mediocross TE (Mediocross TE)**	**5 min**	**5 min**	**5 min**	**5 min**	**1 min**	**9 mW/cm^2 14 min stop 15 sec every 1 min**	**14 min + 3.5 min stop = total time 17.5 min**	**7.56 J/cm^2**	**Saline rinse**

6.8.4 Biomechanical test

In this study, 6 untreated corneas and 6 corneas from each of the three CXL treated groups were examined. The corneal strip preparation, extensometer set-up and the biomechanical data analysis were exactly the same as described in Chapter 2 and used in Chapter 3 apart from the use of a 10 N load cell and the speed of the tensile test was reduced to 0.1 mm/min to allow the collection of more data points. The testing parameters are summarized in Table 6.4.

Table 6.4: The values required by Nexygen 4.1 to perform a stress–strain test.

Parameter	Logged value
Speed	0.1 mm/min
Specimen dimensions: Gauge length Breadth Thickness	 6 mm 5 mm 0.512 - 0.837 ± 0.115 mm
Maximum force	9.5 N

6.8.5 Data analysis

All data are presented as mean ± SD. Measurements were taken of corneal thickness, dry weight and complete digestion time for the enzymatic digestion experiment. Measurements of corneal disk diameter are presented as the daily cumulative measurement of six samples from each treatment group. For the biomechanical test, measurements were taken of corneal thickness, while specimen strain and force were measured by the extensometry system. The tangent modulus and fitting parameters A, B and AB were calculated from force-extension data (for details see Chapter 2). Statistical analysis for each experiment was performed using a one-way ANOVA and Bonferroni multiple comparisons in a depth-wise manner. All statistical analyses were performed with the Statistical Package for the Social Sciences (IBM SPSS Statistics 20, New York, USA). The statistical significance of difference was taken as $p \leq 0.05$.

6.9 Results

6.9.1 Corneal Pachymetry

Figure 6.7 shows the average corneal thickness measurements recorded for each group during the preparation of the tissue for the enzymatic digestion study (Figure 6.7a) and the extensiometry study (Figure 6.7b). Note that in the p-TC-ion-HCXL (7.56 J/cm^2) group, the epithelium, which constitutes $\approx$75 μm of the total corneal thickness, remained intact during CXL treatment. A significant reduction in corneal thickness occurred immediately after the application of riboflavin-dextran solution (for 30 min) to the de-epithelized corneas (all p-values were < 0.0001). The application of hypo-osmolar riboflavin (riboflavin-dextran free) via the iontophoresis device did not significantly change the corneal thickness from the original thickness ($p = 1.00$). The differences in corneal thickness between the untreated group and both the SCXL (5.4 J/cm^2) and the p-HCXL (7.56 J/cm^2) groups ($p < 0.0001$) are highlighted in Figure 6.7. Further differences were observed between the epi-on, p-TC-ion-HCXL group and both the epi-off, SCXL (5.4 J/cm^2) group and the p-HCXL (7.56 J/cm^2) group ($p < 0.0001$). The treatment-induced changes in corneal thickness may be attributed to both epithelium debridement (which accounts for $\approx$100 μm) and the application of a riboflavin-dextran solution ($p < 0.0001$). As no significant difference in corneal thickness was evident between the two epi-off groups that were treated with the same iso-osmolar riboflavin solution, it seems that the mode of UVA delivery (continuous or pulsed) has no influence on corneal thickness ($p = 1.00$). Furthermore, the extent of corneal thinning following UVA exposure did not differ significantly from that associated with riboflavin-dextran application alone ($p = 0.653$), suggesting that thinning observed after epi-off CXL is solely due to the application of an iso-osmolar solution.

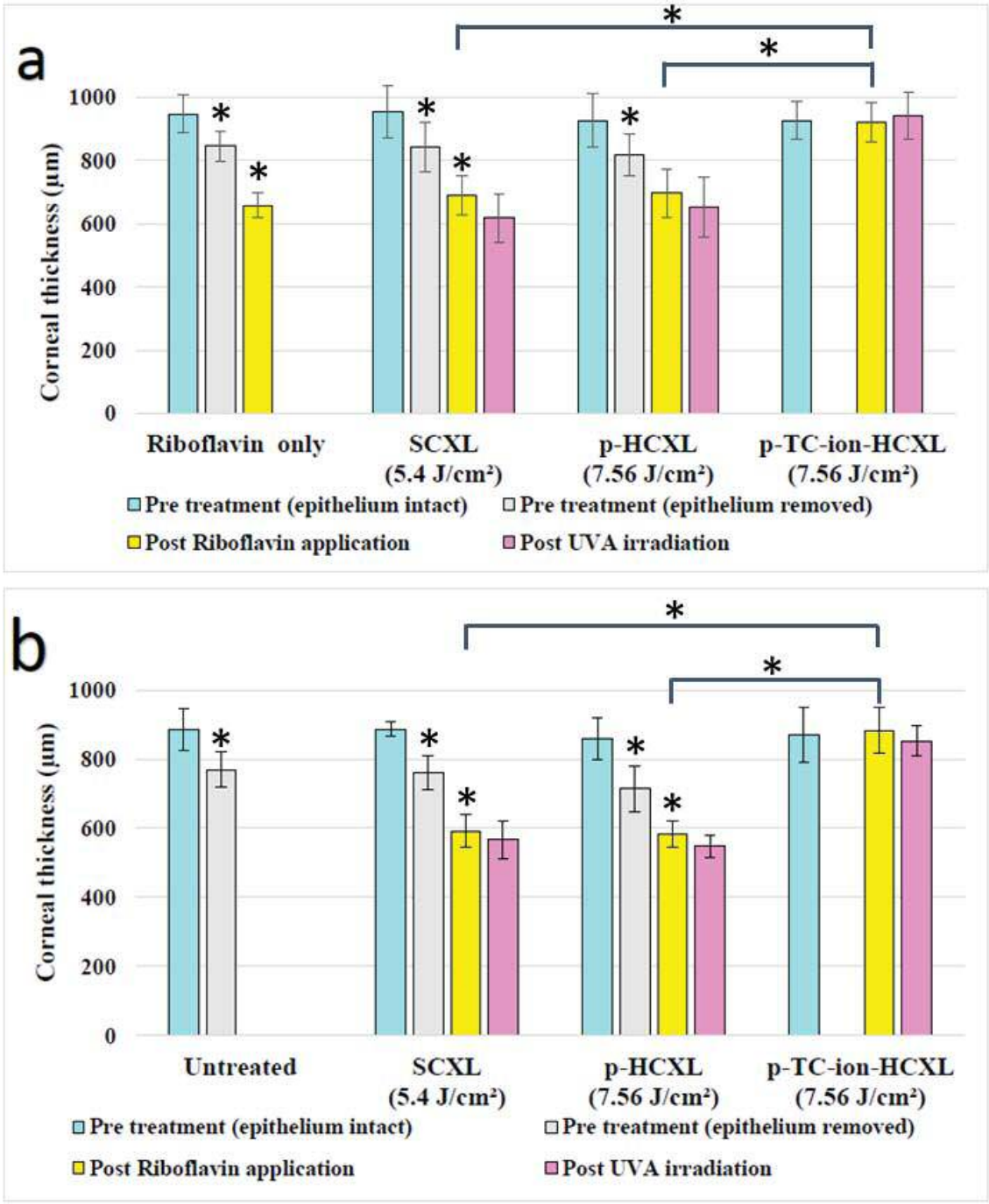

Figure 6.7: Average corneal thickness measurements recorded for each group used in the enzyme digest study (a) and the extensometry study (b). Measurements were recorded at various stages of sample preparation: pre-treatment (epithelium intact), pre-treatment (epithelium removed), post-riboflavin application and post-UVA irradiation. Note that in group 5 (p-TC-ion-HCXL 7.56 J/cm^2) alone, the epithelium, which constitutes ≈75 microns of the total corneal thickness, remained intact during CXL treatment. Error bars show standard deviation.
Cross-linking treatments: SCXL (5.4 J/cm^2) (standard cross-linking); p-HCXL (7.56 J/cm^2) (pulsed, high intensity and high energy UVA cross-linking) and p-TC-ion-HCXL (7.56 J/cm^2) (pulsed, high intensity and high energy UVA cross-linking with iontophoretic riboflavin delivery).

6.9.2 Enzymatic digestion study: Riboflavin uptake

Photographic images of the corneal disks taken immediately after treatment (and after post-treatment epithelial removal in the case of p-TC-ion-HCXL) (7.56 J/cm^2), showed the distinctive yellow colouration of riboflavin within the stroma of all corneas and illustrated the successful trans-epithelial delivery of riboflavin in the p-TC-ion-HCXL (7.56 J/cm^2) treatment group (Figure 6.8).

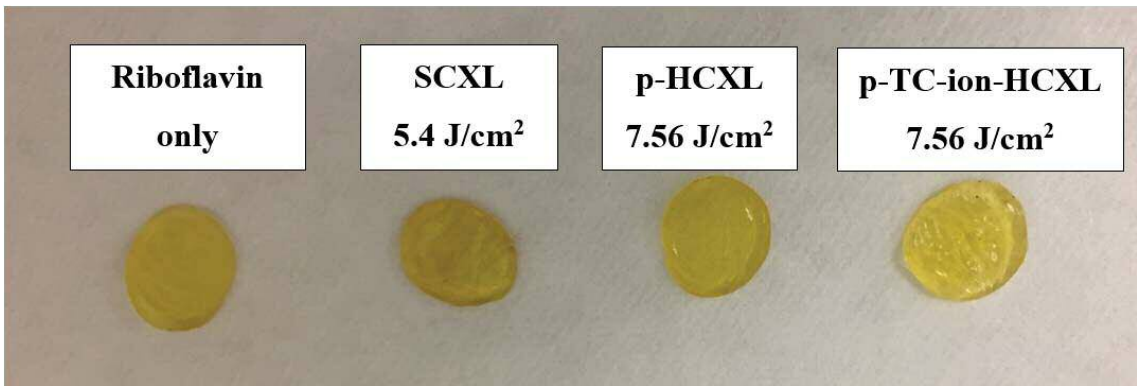

Figure 6.8: Corneal disks from each group are shown immediately after treatment (and prior to enzyme digestion). In each case the epithelium has been removed (either pre- or post- treatment) and the characteristic yellow colour of riboflavin can be seen within the corneal stroma.
Cross-linking treatments: Cross-linking treatments: SCXL (5.4 J/cm^2) (standard cross-linking); p-HCXL (7.56 J/cm^2) (pulsed, high intensity and high energy UVA cross-linking) and p-TC-ion-HCXL (7.56 J/cm^2) (pulsed, high intensity and high energy UVA cross-linking with iontophoretic riboflavin delivery).

6.9.3 Corneal disk diameter measurements during enzymatic digestion

As mentioned earlier (Chapters 3, 4 and 5), posterior-anterior stromal swelling was observed in all samples after 24 hours of pepsin submersion. After one week of digestion the anterior and posterior regions were separated, and the posterior was completely digested by 10 days. The anterior portion of the corneal disks persisted beyond this time point and diminished gradually allowing daily measurements of corneal disk diameter (Figure 6.9).

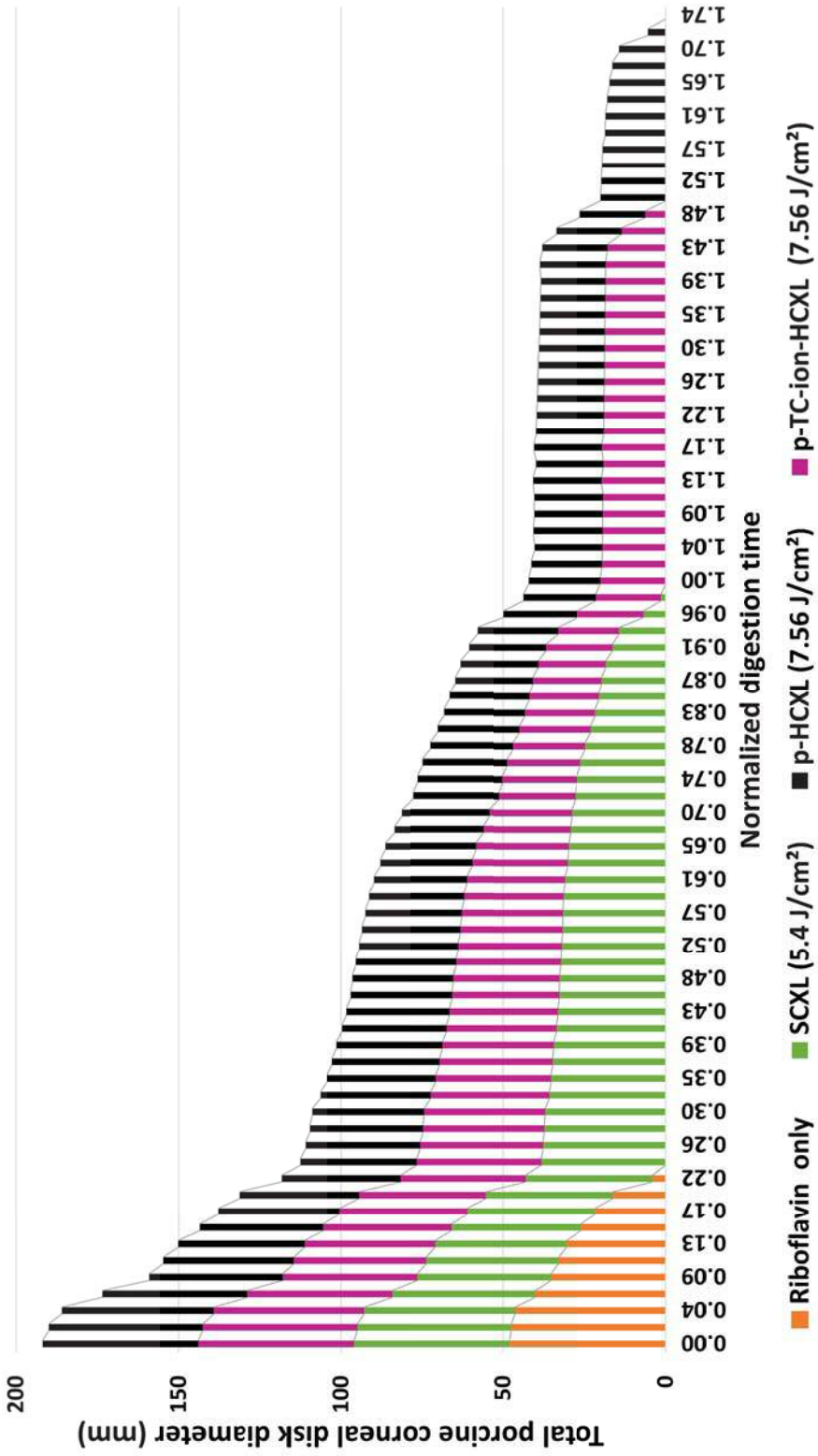

Figure 6.9: The digestion rate of corneal disks treated with riboflavin-only, SCXL, p-HCXL and p-TC-ion-HCXL. The summed diameter of the corneal disks (n = 6) within each treatment group is shown as a function of time in pepsin digest solution. The digestion time for each treatment group has been normalised against the total digestion time of the SCXL treatment group.
Cross-linking treatments: SCXL (5.4 J/cm^2) (standard cross-linking); p-HCXL (7.56 J/cm^2) (pulsed, high intensity and high energy UVA cross-linking) and p-TC-ion-HCXL (7.56 J/cm^2) (pulsed, high intensity and high energy UVA cross-linking with iontophoretic riboflavin delivery).

There was a significantly longer duration required for complete digestion of the CXL treated corneal disks than that required for the riboflavin-only control specimens ($p < 0.0001$) (Figure 6.9, Table 6.5). The corneas in the high energy CXL treatment groups (p-HCXL 7.56 J/cm^2 and p-TC-ion-HCXL 7.56 J/cm^2) took significantly longer to digest than those treated with SCXL ($p < 0.0001$), and the p-HCXL 7.56 J/cm^2 treated corneas took significantly longer to digest than that the p-TC-ion-HCXL 7.56 J/cm^2 treated corneas ($p < 0.0001$) (Figure 6.9, Table 6.5).

Table 6.5: Average time in days taken for complete digest to occur in all groups ± SD.

Group	Time taken for complete digestion to occur (days)	Normalised digestion time*
Riboflavin only	10 ± 0.5	0.24
SCXL (5.4 J/cm²)	45 ± 0.5	1.00
p-HCXL (7.56 J/cm²)	80 ± 0.5	1.74
p-TC-ion-HCXL (7.56 J/cm²)	69 ± 0.5	1.50

*The total digestion time for each control and treatment group was normalised against the total digestion time for the SCXL group.

6.9.4 Dry weights at day 12 of digestion (5 samples/group)

At day 12 (which corresponds to a normalised digestion time of 0.26), all of the CXL-treated corneas were still present but the riboflavin-only treated corneas had undergone complete digestion. No significant differences were found between the average stromal dry weights of the CXL treated groups ($p = 1.0$), however a large variability in stromal mass dry weight was observed within each group (Figure 6.10).

6.9.5 Stress-strain measurements

The averaged stress–strain fitted curves for each group show the typical nonlinear behaviour of a biological tissue (Figure 6.11). The stress-strain fitted data for the untreated group were found to be significantly lower than those for the SCXL (5.4 J/cm^2) group ($p <$

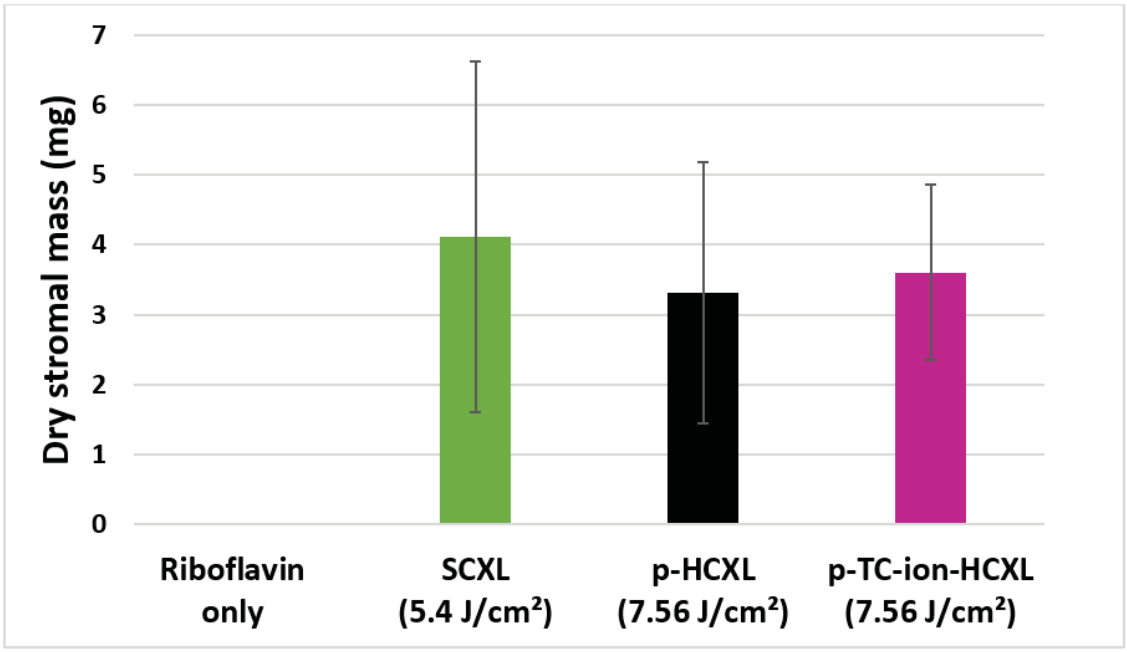

Figure 6.10: Average stromal dry weight of corneal disks treated with SCXL, p-HCXL and p-TC-ion-HCXL, after 12 days of digestion. Error bars show standard deviation. Cross-linking treatments: SCXL (5.4 J/cm^2) (standard cross-linking); p-HCXL (7.56 J/cm^2) (pulsed, high intensity and high energy UVA cross-linking) and p-TC-ion-HCXL (7.56 J/cm^2) (pulsed, high intensity and high energy UVA cross-linking with iontophoretic riboflavin delivery).

0.005). However, the stress–strain fitted data did not reveal any significant differences between the p-HCXL (7.56 J/cm^2), p-TC-ion-HCXL (7.56 J/cm^2) and the untreated group ($p = 1.00$).

6.9.6 Tangent modulus (6 per group)

The average tangent modulus values were obtained by a nonlinear fit of each stress-strain curve for the four groups. Figure 6.12 shows the average of the tangent modulus and standard deviation for each group at 2%, 4%, 6%, 8% and 10% strains. The chart shows that the SCXL protocol yielded the largest increases in tangent modulus and had a significantly higher tangent modulus that that of the untreated corneas at all strains ($p < 0.04$) (Table 6.6). However, despite general trends for the tangent modulus to be higher in the p-HCXL (7.56 J/cm^2) and p-TC-ion-HCXL (7.56 J/cm^2) groups than in the untreated group but lower than that of the SCXL group, no significant difference was

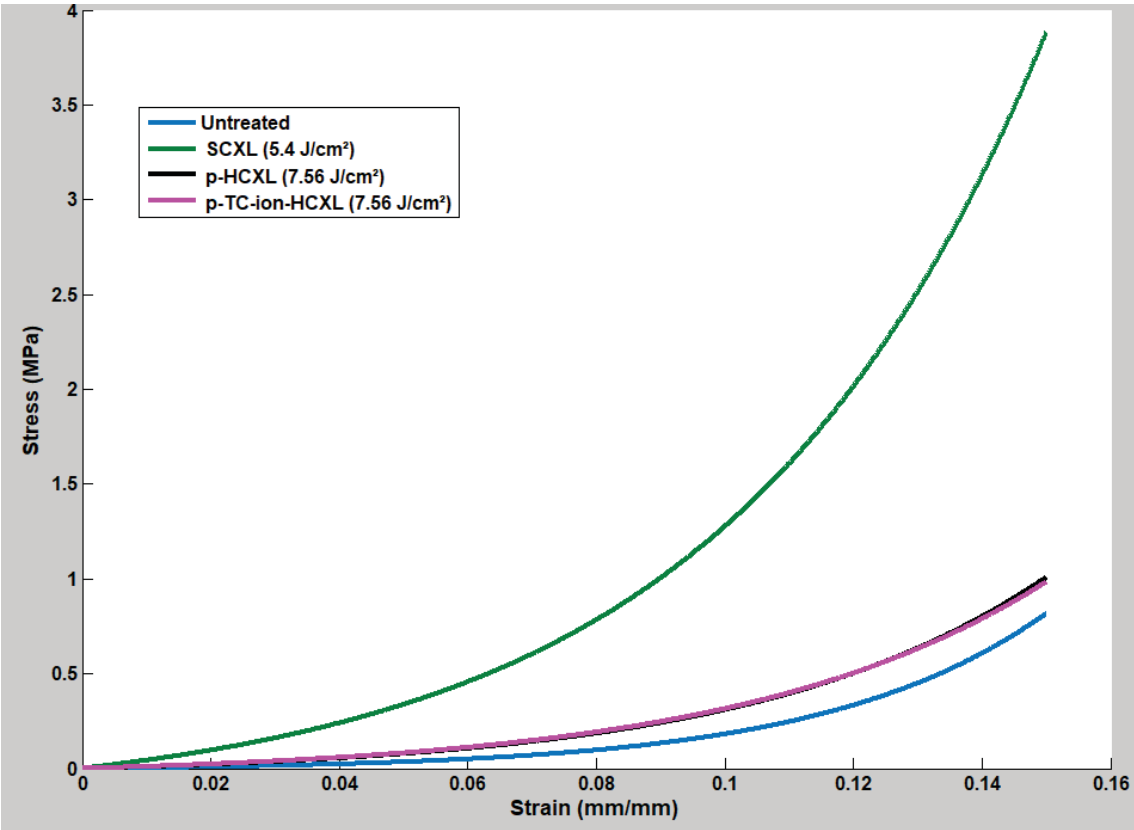

Figure 6.11: Comparison between stress-strain behaviors of untreated, SCXL, p-HCXL and p-TC-ion-HCXL treated corneas.
Cross-linking treatments: SCXL (5.4 J/cm^2) (standard cross-linking); p-HCXL (7.56 J/cm^2) (pulsed, high intensity and high energy UVA cross-linking) and p-TC-ion-HCXL (7.56 J/cm^2) (pulsed, high intensity and high energy UVA cross-linking with iontophoretic riboflavin delivery).

detected at 2 - 8% strain. The average tangent modulus at 6% strain was 0.3×10^6 Pa for the untreated group, 3.3×10^6 for SCXL, 0.9×10^6 Pa for p-HCXL (7.56 J/cm^2), and 1.1×10^6 Pa for p-TC-ion-HCXL (7.56 J/cm^2), thus the stiffness (relative to the untreated cornea) increased by a factor of 9.9, 2.8 and 3.1 for the cross-linked groups, respectively. The 'stiffening factor' decreased slightly with increasing strain from 8% to 10%. For the SCXL at 8% strain, the stiffness of the cornea was 7.6 times greater than that of the untreated corneas, and at 10% strain, the SCXL treated corneas were 6.9 times stiffer than the untreated corneas. Simultaneously, the stiffness increased by a factor of 2.3 at 8% strain and 1.3 at 10% strain for the p-HCXL (7.56 J/cm^2) group. Meanwhile, the stiffness for epi-on p-TC-ion-HCXL (7.56 J/cm^2) treated group raised by the factor of 3.0 at 8% strain and 2.9 at 10% strain. Only at 10% strain was the tangent modulus for the SCXL

group significantly higher than the p-HCXL (7.56 J/cm^2) epi-off treated group (p = 0.025) (Table 6.6).

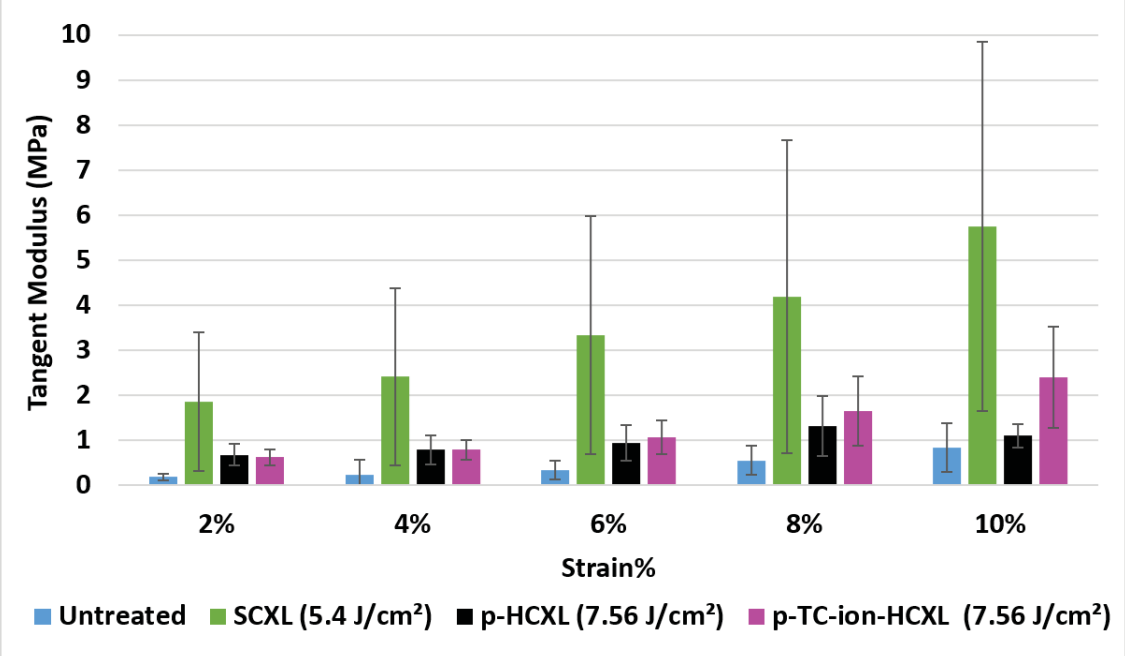

Figure 6.12: Tangent modulus for each treatment group at 2%, 4%, 6%, 8% and 10% strain.
Cross-linking treatments: SCXL (5.4 J/cm^2) (standard cross-linking); p-HCXL (7.56 J/cm^2) (pulsed, high intensity and high energy UVA cross-linking) and p-TC-ion-HCXL (7.56 J/cm^2) (pulsed, high intensity and high energy UVA cross-linking with iontophoretic riboflavin delivery).

Table 6.6: P-values of the tangent modulus at 2%, 4%, 6%, 8% and 10% resulting from Bonferroni multiple comparisons between groups. Asterisks indicate where p-values were < 0.05.

P-Value	Untreated	SCXL (5.4 J/cm²)	p-HCXL (7.56 J/cm²)
at 2%			
SCXL (5.4 J/cm²)	0.015*		
p-HCXL (7.56 J/cm²)	1	0.145	
p-TC-ion-HCXL (7.56 J/cm²)	1	0.113	1
at 4%			
SCXL (5.4 J/cm²)	0.013*		
p-HCXL (7.56 J/cm²)	1	0.094	
p-TC-ion-HCXL (7.56 J/cm²)	1	0.095	1
at 6%			
SCXL (5.4 J/cm²)	0.012*		
p-HCXL (7.56 J/cm²)	1	0.062	
p-TC-ion-HCXL (7.56 J/cm²)	1	0.084	1
at 8%			
SCXL (5.4 J/cm²)	0.040*		
p-HCXL (7.56 J/cm²)	1	0.159	
p-TC-ion-HCXL (7.56 J/cm²)	1	0.282	1
at 10%			
SCXL (5.4 J/cm²)	0.017*		
p-HCXL (7.56 J/cm²)	1	0.025*	
p-TC-ion-HCXL (7.56 J/cm²)	1	0.184	1

6.10 Discussion

Based on evidence from previous studies that iontophoresis delivery techniques using a 5 min riboflavin soak time result in only superficial stromal riboflavin penetration and minimal cross-linking of the tissue (Aldahlawi et al. 2016a; Vinciguerra et al. 2014a), a

modification to the protocol was introduced in this study which aimed to enhance stromal riboflavin penetration (and ultimately the amount of cross-linking). In the modified p-TC-ion-HCXL (7.56 J/cm^2) protocol the riboflavin soak time was extended from 5 min to 20 min to allow more time for riboflavin diffusion. Further to this, a higher concentration riboflavin solution containing BAC was used to help facilitate stromal delivery across the intact epithelium and enhance the cross-linking process. Sufficient riboflavin penetration is a key step in the cross-linking process (Mastropasqua et al. 2014a,b) as the presence of the photosensitiser in the corneal stroma is essential to trigger cross-link formation during UVA irradiation. Riboflavin also allows approximately 95% of the UV light to be absorbed in the cornea, thus protecting the internal ocular structures such as the endothelium, lens, and retina from the UV light (Raiskup et al. 2013; Spoerl et al. 2007; Wollensak et al. 2003b,c).

In this study the effectiveness of a range of epi-off protocols and a novel modified epi-on iontophoretic delivery cross-linking protocol were investigated in terms of their ability to increase both enzymatic resistance and corneal stiffness, thereby providing a more accurate assessment of the effectiveness of each CXL protocol. In order to ensure a fair comparison between the epi-on (p-TC-ion-HCXL (7.56 J/cm^2)) and epi-off treated corneas, the epithelium was removed from the p-TC-ion-HCXL (7.56 J/cm^2) treated corneas immediately prior to commencing the enzyme digest and biomechanical testing procedures. By doing so, any effects that the presence or absence of an intact epithelium might have had on the biomechanical and biochemical properties of the cornea were removed; this allowed the effect of each treatment on the properties of the corneal stroma to be isolated and compared between groups.

Consistent with previous experimental and clinical studies, a significant drop in corneal thickness was recorded during epi-off protocols, which was due to a combination of epithelial removal and application of an iso-osmolar riboflavin solution (containing dextran) (Aldahlawi et al. 2015, 2016a,b; Greenstein et al. 2011; Hassan et al. 2014; Hayes et al. 2013). The corneal thinning can be attributed primarily to the deturgescent effect of the dextran but also, possibly, to the presence of riboflavin (Aldahlawi et al. 2015),

which has the effect of increasing the ionic strength of the applied solution and creating an osmotic imbalance that draws water out of the cornea (Huang et al. 1999). The finding that application of a dextran-free, hypo-osmolar riboflavin solution to epithelium-intact corneas did not result in any change in corneal thickness, is at odds with clinical studies which have shown that the trans-epithelial delivery of hypo-osmolar riboflavin solutions increases the corneal thickness by ≈66 μm (Hafezi 2011; Hafezi et al. 2009; Kymionis et al. 2012; Zhang et al. 2012). This difference is most likely due to the structural differences that exist between human and porcine corneas, in terms of the thickness of the epithelium (Sanchez et al. 2011). However, despite the porcine corneal epithelium presenting a greater barrier to riboflavin penetration than the human cornea, spectrophotometry studies have shown that the modified iontophoresis delivery protocol results in significant stromal riboflavin penetration (Hayes et al. 2015). The current study supports this finding, as visual observation of the treated corneas following epithelium removal, revealed the presence of riboflavin within the stroma of all epi-on and epi-off treated porcine corneas (Figure 6.8). Consistent with other studies, the mode of delivery of UVA (continuous or pulsed) during accelerated CXL had no effect on corneal thickness (Chen et al. 2015; Sherif et al. 2016).

As shown in Chapter 4, the effectiveness of iontophoretic cross-linking (measured in terms of corneal enzymatic resistance post-treatment), can be enhanced by increasing the riboflavin concentration, increasing the duration of the iontophoresis assisted delivery of riboflavin and increasing the riboflavin soakage time. However, despite these modifications, the protocol was found to remain inferior to the SCXL (5.4 J/cm^2) protocol (Aldahlawi et al. 2016a). The current study showed that the further development of the iontophoresis protocol to include the use of pulsed UVA light and a higher energy dose (TC-ion-p-HCXL (7.56 J/cm^2)), resulted in an enhanced corneal enzymatic resistance that was superior to that achievable with the SCXL (5.4 J/cm^2) protocol. However, the epi-off p-HCXL (7.56 J/cm^2) protocol was found to be even more effective than the epi-on TC-ion-p-HCXL (7.56 J/cm^2) at increasing the enzymatic resistance of the cornea. The enhanced efficacy of the epi-off p-HCXL (7.56 J/cm^2) protocol compared to that of the epi-on TC-ion-p-HCXL (7.56 J/cm^2) protocol may be due to the greater stromal riboflavin

uptake in the epi-off treated corneas, which has been previously demonstrated by spectrophotometry (Hayes et al. 2015). It may also be due to some UVA being absorbed by the intact epithelium in the TC-ion-p-HCXL (7.56 J/cm^2) group and thus reducing the amount available for stromal cross-linking.

In the enzyme digest study, measurement of the average dry weight of the tissue during the digestion process (which represents the undigested tissue mass), somewhat surprisingly, showed no significant difference between the cross-linked groups, suggesting an equal proportion of the full-tissue thickness was cross-linked in each case. This appears at first glance to contradict the findings presented in Chapter 5, which showed a significant difference between the dry weights in the SCXL (5.4 J/cm^2) and p-HCXL (7.2 J/cm^2) treatment groups. However, this may be explained by the dry weights in each study being obtained at slightly different stages in the digestion process. Both studies employed the same methological process, with dry weights being obtained on the day following the complete digestion of the untreated corneas; in the present study this led to the dry weights of the CXL-treated corneas being recorded at day 12 of 45, which equates to a normalised digestion time of 0.26, whereas in Chapter 5 the dry weights were obtained at day 13 of 30, which equates to a much later normalised digestion time of 0.4. It is possible therefore that in the current study, differences between the CXL groups were regrettably not detected due to the dry weights being obtained too early in the digestion process. Another possible interpretation is that the slight difference in the energy dose used in the p-HCXL treatments described in this chapter and Chapter 5 (7.2 J/cm^2 and 7.56 J/cm^2 respectively), may have resulted in a different depth of CXL formation. Although, there is no way at present to visualise the precise depth of cross-linking, clinical evidence shows the appearance of a demarcation line at $\approx$ 2 weeks post-treatment which some believe may represent the transition between cross-linked and non-cross-linked tissue (Spadea et al. 2016). It has been shown clinically that an increase in the UVA energy dose results in a deeper demarcation line (Kymionis et al. 2016; Mazzotta et al. 2008), which may indicate a deeper level of cross-linking Moreover, clinical evidence indicates that p-HCXL (7.2 J/cm^2) forms a deeper demarcation line than continuous HCXL (7.2 J/cm^2) (Peyman et al.

2016). Here, the dry weight of the SCXL treated corneas was equal to that of the p-HCXL (7.56 J/cm^2) and TC-ion-p-HCXL (7.56 J/cm^2) treated corneas.

As the chemical bonds formed during collagen cross-linking cannot be directly visualized by staining methods, improvements in corneal biomechanical properties, such as increased tissue rigidity, are frequently used as positive indicators of cross-linking effectiveness (Hammer et al. 2014; Kohlhaas et al. 2006; Schumacher et al. 2011; Studer et al. 2010; Wollensak et al. 2003b). However, most of these studies measure the changes in corneal stiffness following CXL as a bulk of the biomechanical properties of corneal tissue (Beshtawi et al. 2013), even though the SCXL stiffening effect is concentrated in the anterior 200 - 300 μm of the cornea and the effective depth of CXL may differ between treatment protocols (Kohlhaas et al. 2006). In the current study, examination of corneal biomechanical properties demonstrated that the tangent modulus at 8% applied strain was significantly higher in the SCXL treated corneas than in the untreated control group. Although the tangent modulus increased by factors of 7.6, 2.3 and 3.0 for the SCXL, p-HCXL (7.56 J/cm^2), and epi-on p-TC-ion-HCXL (7.56 J/cm^2) treated groups, the two latter groups did not significantly differ from either the untreated corneas or the SCXL treated corneas. This may be due to the within-group variability associated with the biomechanical testing technique and differences in the intensity and effective depth of cross-linking between protocols. For example, based on the results of the enzyme digestion studies, the HCXL (7.56 J/cm^2), and epi-on p-TC-ion-HCXL (7.56 J/cm^2) protocols appear to result in an enhanced cross-linking of the most superficial stromal layers but may show a more rapid decrease in cross-linking intensity with depth compared to the SCXL protocol. As the extensometry technique provides a measurement of the overall stiffness of full-thickness tissue strips, highly localised anterior-posterior differences may therefore not be detected. Indeed, evaluation of anterior and posterior corneal stromal elasticity after corneal collagen cross-linking (CXL) treatment in human cadaver eyes using atomic force microscopy through indentation, has shown that stiffness of the anterior corneal stroma increases significantly after SCXL, while the posterior stroma remains unaffected (Dias et al. 2013).

Some of the extensometry outcomes showed a large amount of variability which might be caused by other limitations of the technique. Past examinations have underlined the limitations of corneal strip extensometry measurements to evaluate biomechanical properties (Elsheikh et al. 2005). These limitations include: the initial straightening of strips that natively followed corneal curvature; cutting significant quantities of collagen during the strip preparation process; and ignoring the meridional differences. Strip extensometry is inherently uniaxial while the native cornea experiences planar forces. Using an inflation technique would overcome to some extent the uniaxial limitation, by reflecting the native mechanical environment of an eyeball where the cornea is intact and loading of posterior pressure could simulate the intraocular pressure. Nevertheless, this technique has its own drawback of producing less accurate measurements of CXL stiffness as only 8 mm of the central cornea is cross-linked and increasing the intraocular pressure could influence the biomechanics measurement. Uniaxial extensometry, despite its many drawbacks, is still the most widely used technique to measure the biomechanical properties of biological tissues, but the results need to be interpreted with great caution. It is possible that other mechanical testing techniques, such as atomic force microscopy or interferometry, may therefore be more suitable than extensometry for identifying differences between CXL protocols.

There are number of factors to consider when using porcine eyes as a model for humans, particularly for trans-epithelial CXL studies. Although it is commonly agreed that the porcine cornea is a suitable model for the human cornea in terms of its mechanical properties (Elsheikh et al. 2008), corneal strip extensometry experiments on human and porcine cross-linked corneas have revealed a superior CXL-induced stiffening effect in human corneas compared to porcine corneas (Elsheikh et al. 2008; Wollensak et al. 2003b; Zeng et al. 2001). This is likely due to differences in the proportion of the tissue that is cross-linked, since cross-linking following SCXL is limited to the anterior 200 - 300 μm of the cornea (Kohlhaas et al. 2006). Based on the typical values of porcine and human corneal thickness, this represents 35% of the total porcine corneal thickness being cross-linked and 54% in humans (Wollensak et al. 2003b). This difference will be even

more pronounced when comparing porcine corneas with keratoconic corneas, which are significantly thinner than their healthy counterparts (Schlatter et al. 2015). Biomechanical evaluation in rabbit studies demonstrated a corneal stiffening effect following standard iontophoresis CXL (Touboul et al. 2014; Vinciguerra et al. 2009, 2014a) and standard iontophoresis CXL with pulsed UVA irradiation of total energy of 7.2 J/cm^2 (Park et al. 2017) but less than the SCXL. The porcine epithelium is much thicker (100 μm) than human (50 μm) (Sanchez et al. 2011), however, it would be interesting to repeat these treatments in the rabbit model which has a slightly thinner epithelium (40 μm) (Li et al. 1997) but closer in thickness to that of the human cornea. Such a study could complement the current results which may allow a more liberal estimate of the effectiveness of trans-epithelial cross-linking.

In conclusion, the results indicated that the outcome of the trans-epithelial corneal cross-linking could be improved by the use of higher concentration of riboflavin, a longer duration of iontophoresis and riboflavin soak time and an increase in the total UVA energy dose. Based on the experimental findings presented in this study, the St Thomas's/Cardiff modified iontophoresis protocol (p-TC-ion-HCXL (7.56 J/cm^2)) may be a promising, less painful but equally effective alternative to SCXL. As the amount of cross-linking of stromal tissue required to stabilize the progression of an ectatic disorder is not yet defined further clinical studies, especially randomized prospective trails, will be necessary to complete the evaluation of this modified cross-linking technique. Meanwhile, the long-term clinical validity of the SCXL protocol remains the gold standard approach.

CHAPTER 7

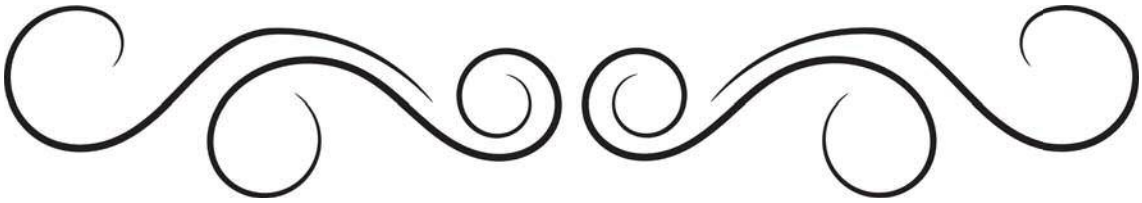

EVALUATION OF THE CHANGES TO CORNEAL ULTRA-STRUCTURE FOLLOWING TREATMENT WITH BACTE-RIOCHLOROPHYLL DERIVATIVE WST-D AND NEAR INFRARED LIGHT.

7.1 Introduction

Although conventional CXL (riboflavin/UVA) therapy has proved to be a highly effective treatment for stabilising keratoconus progression, it requires a minimum corneal thickness of 400 μm after epithelial removal and before riboflavin instillation to ensure the safety of the endothelial cell layer, lens and retina (Spoerl et al. 2007; Wollensak et al. 2003). As a result, very thin keratoconus corneas are not eligible for treatment. Although CXL treatment has a relatively low failure rate (approximately 7.6%) and a complication rate of only 2.8% (Koller et al. 2009), there have been sporadic reports of side-effects such as corneal haze, keratitis and corneal scarring (O'Brart 2014).

To avoid the hazard of corneal endothelial degeneration by UVA, a group of specialists at the Weizmann Institute of Science examined the capability of integrated chemical derivatives of photosynthetic pigments (chlorophylls and bacteriochlorophylls) as a means of stiffening corneas of all thicknesses (Marcovich et al. 2012). The direct application of Bacteriochlorophyll Derivative (Bchl-Ds) or (WST11) to connective tissue followed by non-hazardous spectrum, near infrared (NIR, 755 nm) illumination is expected to initiate collagen cross-linking by the generated oxygen radicals (Hamblin et al. 2013). One role of these photogenerated radicals is thought to be in promoting protein cross-linking (Liu et al. 2004). WST11, or palladium bacteriochlorin 130-(2-sulfoethyl) amide dipotassium salt, is a water-soluble synthesized chemical derivative of a photosynthetic pigment that generates oxygen radicals (O_{2-} and OH) after illumination with non-hazardous NIR (Ashur et al. 2009; Mazor et al. 2005). To avoid endothelium damage, Marcovich et al. mixed the WST11 with high molecular weight dextran T500 (WST-D). This treatment limited the stiffening to the anterior part of the cornea and noticeably decreased post treatment oedema and promoted faster epithelial healing. Histology post WST-D/NIR showed a reduction in keratocyte population in the anterior cornea with no damage to the endothelium (Marcovich et al. 2012). WST-D/NIR treatment also produced biomechanical improvements, which was significantly increase the corneal stiffening at irradiation of 10 mW/cm^2 at different exposure time for 1, 5 and 30 minutes (Brekelmans et al. 2017). Marcovich et al. found that

saturation of the corneal stroma with palladium bacteriochlorin 130-(2-sulfoethyl) amide dipotassium salt (Brandis et al. 2005) in 20% dextran T-500 (WST-D) and subsequent exposure to near infra-red light (NIR) at 755 nm, resulted in a 174% increase in rabbit corneal stiffness with minimal side effects (Marcovich et al. 2012) .

Utilizing both x-ray scattering and electron microscopy, this study analyses the structure of rabbit corneas immediately after treatment with WST-D/NIR and following 30 days of recovery to gain a better understanding of the means by which the corneal stiffening is accomplished. Electron microscopy images give data at a highly-localised level and can enable changes in cell morphology, collagen organisation and collagen D-periodicity to be identified, while small-angle x-ray scattering (SAXS) patterns provide quantitative information about fibril diameter and fibril separation distance as an average throughout the thickness of the cornea, and are thus highly representative of the tissue as a whole (Meek et al. 2001).

7.2 Research aim

The purpose of the current study was to present the first evaluation of ultrastructural changes in the stromal matrix following *in vivo* treatment with bacteriochlorophyll derivative WST-D and near infrared light (WST-D/NIR).

7.3 Methods

7.3.1 Study 1. X-ray scattering studies

Tissue preparation for x-ray scattering studies

At the Weizmann Institute of Science (Rehovot), our collaborators performed unilateral WST-D/NIR treatment on 6 live New Zealand White rabbits (Table 7.1). In each case, the contralateral eyes acted as untreated controls. At all times, the animals were treated in

accordance with the Association for Research in Vision and Ophthalmology Statement for the Use of Animals in Ophthalmic and Vision Research. The animals were anaesthetised using intramuscular (IM) injection of 35mg/kg ketamine (Rhone Merieux, Lyon, France) and 5mg/kg xylazine (Vitamed, Benyamina). In the case of the treated eye, the corneal epithelium was removed and WST-D (containing 20% dextran T-500) was applied to the corneal stroma for 20 minutes by means of 12 mm diameter eye cap. Following saturation of the corneal stroma, the tissue was exposed to NIR (755 nm, 10 mW/cm^2) for a period of 30 minutes (Figure 7.1a). To prevent exposure of the limbal stem cells, the illuminated area was restricted by an aluminium foil mask with an 8 mm diameter central opening. An ophthalmic steroid and antibiotic ointment containing dexamethasone 0.1%, neom cine and pol m i in (a itrol®, lcon, el ium) e es once dail until full and con®rm ed re epit eliali a and t ickness of t e cornea w ere documented at re ula process. portable slit lam p w as used to e aluate t e e blue ®lter, idolon ptical , assec usetts, S), uore follow t e re epit eliali ation (io Glo, P arm aceutica pac m etr w as utili ed to m easure t e cornea l t ickne nc., le eland, S). T w ent ei t da s after t e treatm en and corneo scleral disks w ere rem o ed, placed in sto t e iam ond i t Source (idcot,) for e am ination o T e corneo scleral discs destined for S S studies w e edium a le ( ) bu er w it de tran. T is w as nec durin transportation from e o otto ardi . T e sacri®c to coincide w it t e allocated beam tim e att e s nc rotr onl stored in t e m edium for tw o da s.

furt er tw el e pairs of rabbit e es w ere obtained fr *vivo* w it in tw o ours of deat (i u in *vivo* t e ba) t. e ds ef o r s t o n e e from eac pair underw ent cornea l de epit elialisation w ilst t e contralateral e ser ed as an untreated contr

(wit a mm scleral rim) was wrapped in pol in l c lo
kept in t e dark, and tra s o a re e t te s ecim ens rem aine
transportation to t e iam ond i t Source and were ma
for S S data collection.

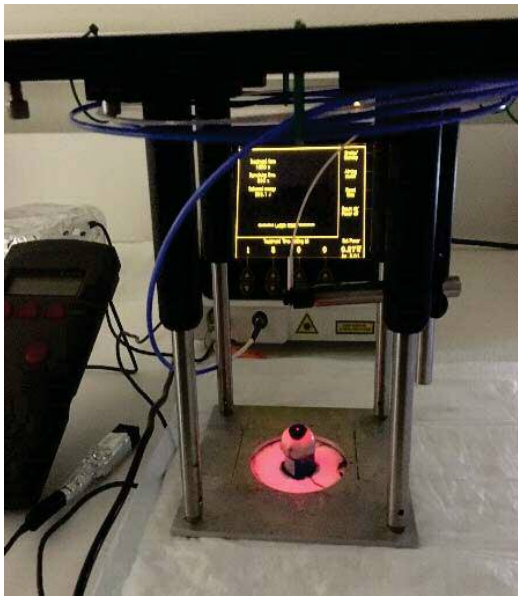

(a) in itro

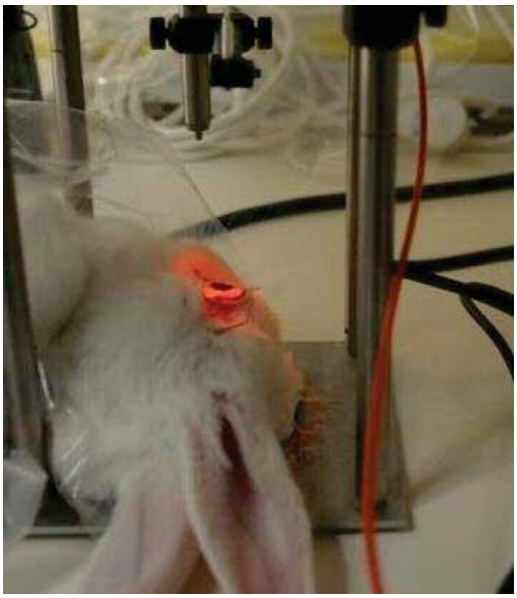

(b) *in vivo*

i ure 7.1: perim ental setu *in vivo* (b) in S Ttro (a) ea adtm ento
rabbit e es. ma e pro ided courtes of Jurriaan rekelm
ei m ann nstitute of S cience (17)

Table 7.1: Specimen treatments and data collection.

Data collection method	44 Rabbit eyes	Tx	n	Epi.	Photosensitising solution	Light intensity	Exposure duration	Energy	Enucleated
Small-angle x-ray scattering	Ex vivo	Untreated	12	intact	-	-	-	-	immediately
		WST-D/NIR	12	off	WST-D/20% dextran (for 20 min)	10 mW/cm^2 NIR	30 min	18 J/cm^2	
	In vivo	Untreated	6	intact	-	-	-	-	1 month
		WST-D/NIR	6	off	WST-D/20% dextran (for 20 min)	10 mW/cm^2 NIR	30 min	18 J/cm^2	
Electron microscopy	In vivo	Untreated	2	intact	-	-	-	-	
		WST-D/NIR	2	off	WST-D/20% dextran (for 20 min)	10 mW/cm^2 NIR	30 min	18 J/cm^2	
		Untreated	2	intact	-	-	-	-	
		riboflavin/UVA	2	off	0.1% Riboflavin/20% dextran (for 30 min)	3 mW/cm^2 UVA	30 min	5.4 J/cm^2	

Small-angle x-ray scattering data collection and analysis

T irt minu tes bef ore data collection, eac *ex vivo* treated (n = 1) and u ntreated (n = 1) corneo scleral disk (w rapped in lin mT) w as t aw ed at room temperatu re. t is notew ort t at f ree in and t aw in (and t e conse u ent f ormation of ice cr stals) does not a ect t e colla en parameters measu red b S S (u llw ood et al. 1). mmediatel bef ore data collection, a mm disk w as t en trep ined f rom t e centre of eac cornea and w ei ed to obtain a 'w et w ei t bef ore data collection (i u re 7.). T e same process w as repeated f or t e pairs of *in vivo* prepared corneas. f ter w ei in , eac corneal disk w as rew rapped in a sin le la er of lin mT and mou nted in a sealed pol met l met acr late c amber (Perspe t eplastics op.co.u k , o entr ,) w it pol ester m w indow s (lar u Pont Tei in, iddlesbrou ,) (i u re 7.). sin le ra scatter pattern w as obtained f rom t e centre of eac corneal disk u sin a . sec e posu re to a 18 × μm ra beam (λ = .8 nm) and recorded on a detector positioned .8 m be ind t e sample.

ollow in data collection, t e corneal disk s w ere placed in a o en f or appro i matel one w eek u ntil a constant 'dr w ei t w as reac ed. T e dration of eac corneal disk w as t en calcu lated u sin t e f ollow in e u ation: dration = (w et w ei t dr w ei t) dr w ei t (apter , u ation .1).

n t e case of 8 *ex vivo* corneal disk s, an additional w et w ei t measu rement w as recorded immediatel f ollow in data collection to assess t e e tent of dr in t at occu rred du rin t e data collection process. s colla en inter brillar spacin is particu larl sensi ti e to c an es in corneal dration (eek et al. 1 1) su c inf ormation is necessar to distin u is betw een dration and treatment indu ced c an es in corneal u ltrastru ctu re.

s described in detail in apter , t e small an le ra scatter patterns w ere calibrated a ainst t e .8 8 nm peak associated w it t e rst order re ection of pow dered sil er be anate, t u s allow in a era e measu rements of colla en period, bril diameter and inter brillar spacin to be ascertained f or eac specimen e amined.

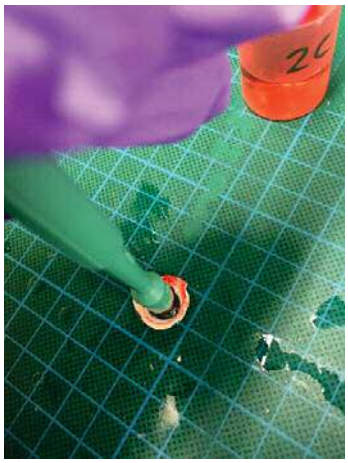

(a)

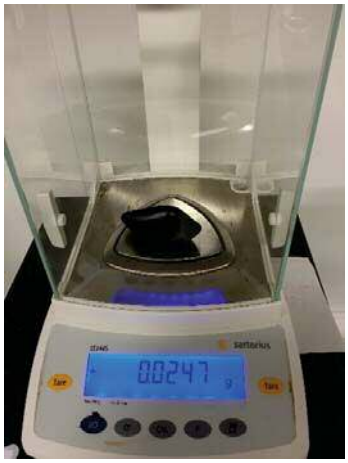

(b)

(c)

i u re 7. : Preparation of corneal tissu e f or ra scatterin data collection. mm disk w as trep ined f rom t e centre of t e cornea (a) and w ei ed (b). T e corneal disk w as t en w rapped in a sin le la er of lin ®lmT and mou nted in a sealed pol met l met acr late c amber w it pol ester ®lm w indow s (c). ra sensiti e paper (reen) w as u sed to determine t e e act position of t e ra beam w it respect to t e sample c amber and allow accu rate positionin of t e sample to ensu re t at t e ra beam passed t rou t e centre of t e corneal disk (c).

7.3.2 Study 2. Electron microscopy studies

Tissue preparation for electron microscopy studies

ou r w eek old (.) f emale, ew ealand ite rabbits w ere anest eti ed as described pre iou sl . T e lef t e e of eac rabbit u nderw ent corneal de epit elialisation. n tw o rabbits, corneal de epit elialisation w as f ollow ed b ST cross link in (as described pre iou sl f or ra scatterin tissu e preparation) w ilst in t e remainin tw o rabbits t e de epit elialised cornea u nderw ent ribo a in cross link in , in ol in a minu tes pre treatment w it a commercial ribo a in solu tion (containin .1 ribo a in and de tran (ediocross, German) f ollow ed b a minu tes il lu mination w it a nm diode at m cmT e ST and ribo a in crosslink ed e es w ere treated w it a itrol (steroid and antibiotic) ointment dail f or w eek s u ntil t e corneal erosion ad f u ll ealed. T e ri t e e in eac rabbit ser ed as an u ntreated control (Table 1). Pac metr w as measu red immediatel bef ore corneal de epit elialisation and a ain af ter treatment. ne mont post treatment t e rabbit e es w ere enu cleated, and t e cornea scleral rims dissected and ® ed in . lu taralde de

and paraf ormalde de (P) in .1 Sorensen p osp ate bu er f or tw o ou rs. T e specimens w ere t en stored in . Sodiu m cacod late bu er (p 7.) u ntil t e w ere re u ired f or transmission electron microscop processin .

Electron microscopy data collection and analysis

orneas w ere w as ed tw ice in .1 Sorensen p osp ate bu er (p 7. 7.) f or ou rs on a rotator and stored o erni t in .1 Sorensen p osp ate bu er at º . Spec imens w ere prepared f or transmission electron microscop b t e f ollow in con entional processin sc edu le. u ll t ick ness corneas w ere cu t into u arters t en into 1 pieces (pie se ments), su c t at t e narrow est point indicated t e corneal centre to aid in orientation f or u ltramicrotom . T ese corneal specimens w ere post ® ed in 1 osmiu m tetro ide in cacod late bu er f or 1 ou r and t en w as ed in distilled w ater. T e specimens w ere t en placed in 1 a u eou s u ran l acetate f or 1 ou r f ollow ed b w as in in distilled w ater. Specimens w ere de drated t rou a raded series of et anol w as es f rom 7 to 1 et anol in f ou r steps o er t e cou rse of one ou r. T e samples w ere t en in®ltrated w it prop lene o ide w it tw o c an es at 1 min inter als, t en into a 1:1 mi tu re of prop lene o ide and raldite resin f or one ou r bef ore pu re resin in®ltration. Si c an es of raldite Y 1 resin, f or abou t tw o ou rs eac , w ere perf ormed, (see apter , section .8 .). T e corneal specimens w ere t en embedded into mou lds su c t at t e centre of t e cornea w as at t e block ed e. T is u aranteed t at sectionin t e block f ace w ou ld produ ce f u l t ick ness (epit eliu m t rou endot eliu m) sections at t e centre of t e cornea. lock s w ere pol meri ed at ° in epo resin o er tw o da s (raldite Y 1 resin, T ab oratories, n land,). eica u ltramicrotome w as u sed to *cut* tt ick w it a lass k nif e, semit in sections w ic w ere t en stained w it tolu idine blu e to identif areas of interest b li t microscop . ltrat in sections (1 nm t ick) w ere t en cu t w it a diamond k nif e f rom t e re ions of interest, collected on eit er copper mes or slot rids (. mm in diameter) and stained w it u ran l acetate and lead citrate f or e amination in a J 1 1 transmission electron microscope operatin at 8 k e (Jeol ( ) td, elw n Garden it ,) (f or more details see apter , section .8 .). Transmission electron

microscop ima es w ere collected f rom t e anterior and posterior re ions of eac cornea. nal sis of t ese ima es in ma e J i i enabled t e a era e diameter of appro imatel 1 ®brils to be calcu lated f or eac re ion (bramo et al.) (f or detail see apter , section .8 .).

Positive staining analysis of fibrils

To a oid o erlappin f rom di erent colla en ®brils la ers and pro ide bandin patterns t at do not cross on top of eac ot er, u ltrat in sections w it 7 nm t ick (sil er interf erence color) w ere cu t w it a diamond k nif e and su pported on copper rids (see apter , section .8 .). T e sections w ere t en positi el stained w it u ran l acetate and lead citrate f or e amination in a J 1 1 transmission electron microscope (Jeol ( ) td, elw n Garden it ,). on itu dinal sections (i.e., parallel to t e ®ber a is) w ere captu red f rom t e anterior and posterior re ions of eac cornea w ×it a ma ni®cation. ata w as e tracted f rom p oto rap s in .dm f ormat to produ ce band intensit plots f or all f easible periods alon eac selected ®bril.

Transmission electron micro rap s of positi el stained rabbit corneal colla en ®brils w ere anal sed u sin ma e anal sis J i i. or positi e stainin anal sis, ®brils w it clear bandin w ere c osen caref u ll . T e positi e stainin bandin pattern w as described earlier (apter 1, section 1. .). T e ob ecti e ere w as to obtain a t pical stain intensit pro®le f rom a i en treatment su c t at direct comparisons cou ld be made betw een specimens to look f or an c an es in stain bindin cau sed b t e presence of cross link s. To e tract t pical band intensit data f or eac period, a rectan le w as draw n o er a selected re ion alon t e ®bril containin se eral w ell stained periods. T e dataset f or t e c osen re ion w as t en e tracted u sin t e “Plot Pro®le” f u nction as described in apter section .8 . .

n t is stu d , onl t ree periods w ere matc ed and a era ed to e alu ate t e positi el stained bandin pattern becau se of t e i noise le el in t e stainin pat terns. T e si nal to noise ratio initiall redu ced, bu t t en increased w en f u rt er scans

w ere added, du e to t e difficu lt in obtainin precise a ial ali nment of t e scans to be a era ed.

7.3.3 Statistical analysis

n t e ra scatterin stu dies, statistical di erences betw een paired samples (treated and u ntreated f ellow e es) and betw een measu rements recorded f rom t e same samples at mu ltiple time points (e. . pac metr measu rements) w ere e alu ated b means of a paired Stu dent t test. di erence betw een an pair of means of reater t an or e u al to t e least si ni®cant di erence at p< . w as considered to be statisticall si ni®cant. alu es presented in t e resu lts are means standard de iation (S).

Statistical anal ses f or t e electron microscop stu dies w ere completed u sin one w a f ollow ed b Sidak post oc test and or onf erroni post oc test. T e data w ere s ow n as mean standard de iation. ll statistical anal ses w ere ac ie ed w it t e Statistical Pack a e f or t e Social Sciences (SPSS Statistics , rmonk , Y, S). probabilit alu e of P . w as considered si ni®cant.

7.4 Results

7.4.1 Clinical observations and pachymetry

si ni®cant decline in corneal t ick ness w as obser ed f ollow in epit elial debridement and ST treatment in t e *ex vivo* treated corneas (p < .) (Table 7. , i u re 7.). sli t reen discolou ration and loss of corneal transparenc w ere seen immediatel f ollow in ST treatment (i u re 7.). T e reenis discolou ration disappeared w it in 1 da s in all corneas. orneal transparenc w as restored w it in da s. mm epit elial erosion w as e ident at da s post treatment bu t w it in 8 da s of treatment, t e epit eliu m ad f u ll reco ered (i u re 7.). t t e time of enu cleation (da s post treatment) t e t ick ness of eac *in vivo* treated ST and ribo a in

treated cornea did not di er si ni®cantl f rom t eir pre treatment alu es (p = .7 and p = .), respecti el (Table 7.).

Table 7. : T ick ness measu rements (*μm*) of *in vivo* and *ex vivo* treated and u ntreated corneas.

Treatment	Pre-treatment	Immediately post-treatment	Day 30 post-treatment
Ex vivo: small angle x-ray scattering studies			
Untreated (n = 12)	383 ± 18	-	-
WST-D/NIR (n = 12)	386 ± 23	364 ± 13	-
In vivo: small angle x-ray scattering studies			
Untreated (n = 6)	368 ± 34	-	386 ± 30
WST-D/NIR (n = 6)	368 ± 34	-	370 ± 20
In vivo: electron microscopy studies			
Untreated (n =2)	383 384	-	387 386
WST-D/NIR (n = 2)	383 380	-	361 377
Untreated (n =2)	398 381	-	375 370
Riboflavin/UVA (n =2)	381 382	-	409 393

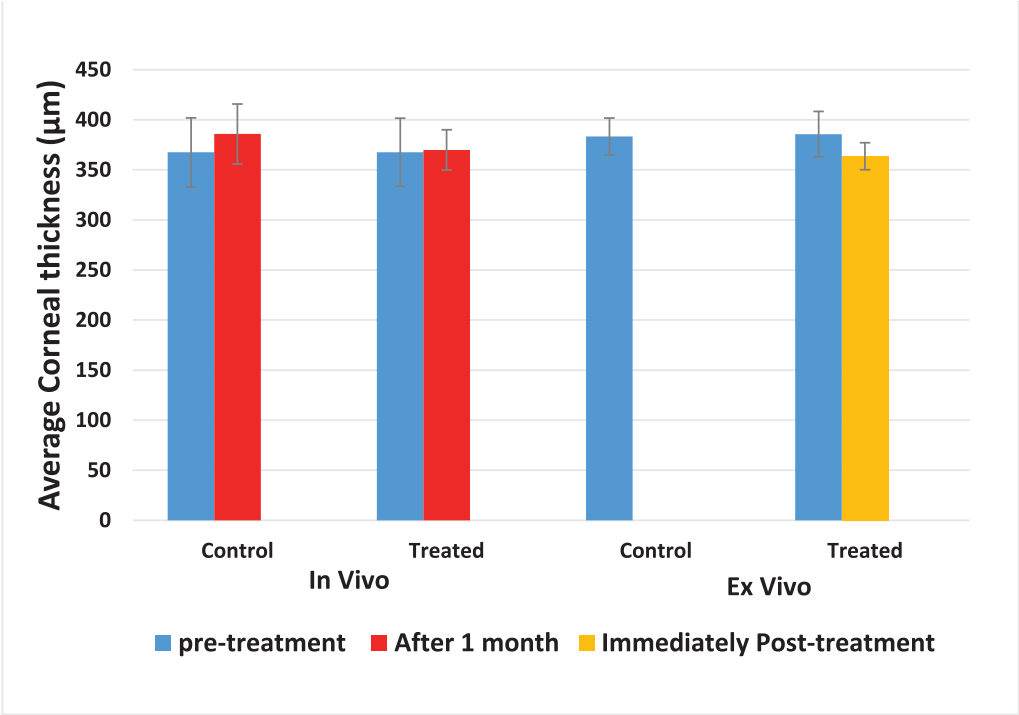

i u re 7. : era e corneal t ick ness pre treatment, immediatel post ST treat ment (*ex vivo*) and da post ST treatment and du rin ealin (*in vivo*) f or S S stu d

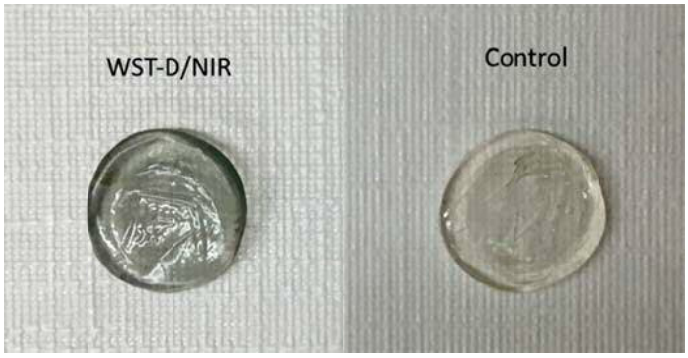

i u re 7. : orneal disk s trep ined immediatel af ter t e treatments. rom lef t to ri t ST (re reen), and u ntreated (clear) disk s. ma e pro ided cou rtes of Ju rriaan rek elmans, w it permission f rom t e ei mann nstitu te of Science (17).

i u re 7. : P otos of rabbit corneas post ST treatment at da , 7 da s and da s. f ter da s t ere w as a mm erosion t at ealed one w eek postoperati el . f ter da s t e cornea w as ealt .

7.4.2 Corneal hydration

et w ei t measu rements recorded f rom 8 of t e 1 pairs of *in vivo* corneal disk s bef ore and af ter S S re ealed no si ni®cant c an e in corneal dration du rin data collection (i u re 7.). it in bot t *in vivo* and *ex vivo* rou ps, t e dration of t e ST treated and u ntreated corneas did not di er si ni®cantl f rom eac ot er.

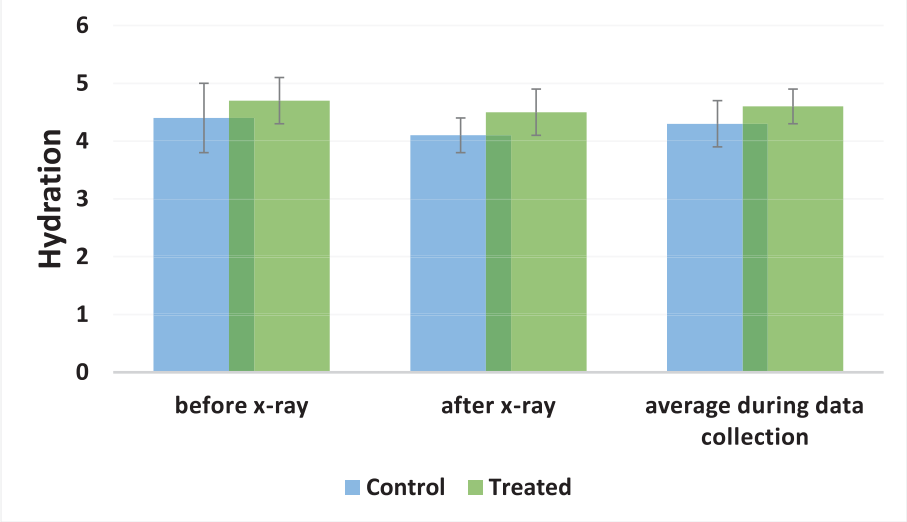

i u re 7. : orneal dration bef ore, af ter and du rin ra data collection.

7.4.3 Collagen interfibrillar spacing, fibril diameter and D-periodicity

Table 7. s ow st e a era e colla en inter®brillar spacin , ®bril diameter and periodicit f or eac treated and u ntreated cornea. o si ni®cant di erence in t ese colla en param eters w ere detected betw een t e ST treated corneas and t eir f ellow u ntreated corneas.

Table 7. : era e colla en inter®brillar spacin , ®bril diameter and periodicit in ST treated and u ntreated corneas.

SAXS	**Ex vivo**		**In vivo**	
	Untreated (n = 12)	WST-D/NIR (n = 12)	Untreated (n = 6)	WST-D/NIR (n = 6)
Interfibrillar Bragg Spacing (nm)	61.7 ± 2.6	62.3 ± 2.8	56.4 ± 0.8	55.3 ± 1.2
Fibril diameter (nm)	39.3 ± 0.6	39.4 ± 0.6	42.0 ± 1.1	41.8 ± 1.5
D-period (nm)	65.9 ± 0.0	65.9 ± 0.0	65.9 ± 0.0	65.9± 0.0

7.4.4 Electron microscopy

lectron microscop ima es obtained f rom t e anterior and posterior stromal re ions of paired ST treated and u ntreated corneas and ribo a in treated and u ntreated corneas s ow ed no ob iou s di erences in t e pack in arran ement of stromal colla en (i u re 7.7). easu rements of a era e ®bril diameter (i u re 7.8) s ow ed t e colla en ®brils to be si ni®cantl narrow er in t e posterior stroma compared to t e anterior stroma in all corneas re ardless of treatment (p< . 1). lt ou statistical anal sis of ®bril diameter measu rements betw een indi idu al rabbits w as not possible du e to t e small sample si e, pair w ise comparisons of ®bril diameter measu rements recorded f rom t e treated and u ntreated cornea of t e same animals re ealed a small increase (.) bu t si ni®cant di erence in ®bril si e betw een t e ST treated cornea and u ntreated cornea in t e anterior stroma (p < . 1) bu t no di erence in t e posterior stroma (p = .). ow e er, t e a era e diameter of ®brils w as f ou nd to be appro imatel w ider in t e anterior stroma and 18 lar er in t e posterior of t e ribo a in treated corneas w en compared w it t eir paired u ntreated corneas (Table 7.).

ibril diameter measu rements of u ntreated and ST treated corneas calcu lated f rom electron microscop ima es (i u re 7.7) w ere f ou nd to be appro imatel smaller t an t ose calcu lated f rom ra scatter patterns (Table 7.), w ereas electron microscop deri ed measu rements of ®bril diameter in t e ribo a in cornea w ere

f ou nd to be onl low er t an ou r pre iou sl reported ra scatterin measu rements f rom similarl treated rabbit corneas (a es et al. 1).

Table 7. : easu rements of ®bril diameter (in nm) made f rom electron microscop ima es of a ST treated cornea, a ribo a in treated cornea and t eir contralateral u ntreated corneas.

Fibril diameter	Untreated	WST-D/NIR	Untreated	Riboflavin/UVA
Anterior	28.3 ± 1.4	29.2 ± 1.9	28.4 ± 1.9	34.0 ± 1.8
Posterior	27.9 ± 2.0	27.7 ± 1.6	27.0 ± 1.6	30.5 ± 2.8

Table 7. : easu rements (in nm) of t e positi el stained bandin pattern made f rom electron microscop ima es of a ST treated cornea, a ribo a in treated cornea and t eir contralateral u ntreated corneas. (T ose indicated in bold s ow statistical si ni®cant resu lts).

D-period	Untreated	WST-D/NIR	Untreated	Ribo/UVA
Anterior	**54.6 ± 1.6**	**58.4 ± 4.4**	57.1 ± 0.6	56.2 ± 1.3
Posterior	54.5 ± 4.3	56.6 ± 1.1	55.2 ± 4.3	56.3 ± 2.5

ort periods measu red f rom t e stain densit pattern alon t e rabbit corneal colla en ®bril s ow ed no si ni®cant di erence betw een t e ribo a in treated and u ntreated corneas. ow e er, t e len t of t e period w as si ni®cantl i er in t e anterior stroma of ST treated corneas compared to t eir contralateral u ntreated corneas ($p < .$. s ow n in bold) (Table 7. and i u re 7.).

T e a ial stain intensit pro®les f or u ntreated and ST treated cornea are s ow n in (i u re 7.1) ac plot represents t e a era e ± standard de iation of t ree period band intensit traces f rom a sin le ®bril f rom one rabbit. T e positi e stainin locations are indicated (i u re 7.1). nl si stainin bands w ere identi®ed in t is stu d (b1 b c d e a). n t e ST treatment, t e trace s apes appear to be di erent to t e correspondin u ntreated control traces, s ow in a di erent pattern of positi e stainin in ariou s locations.

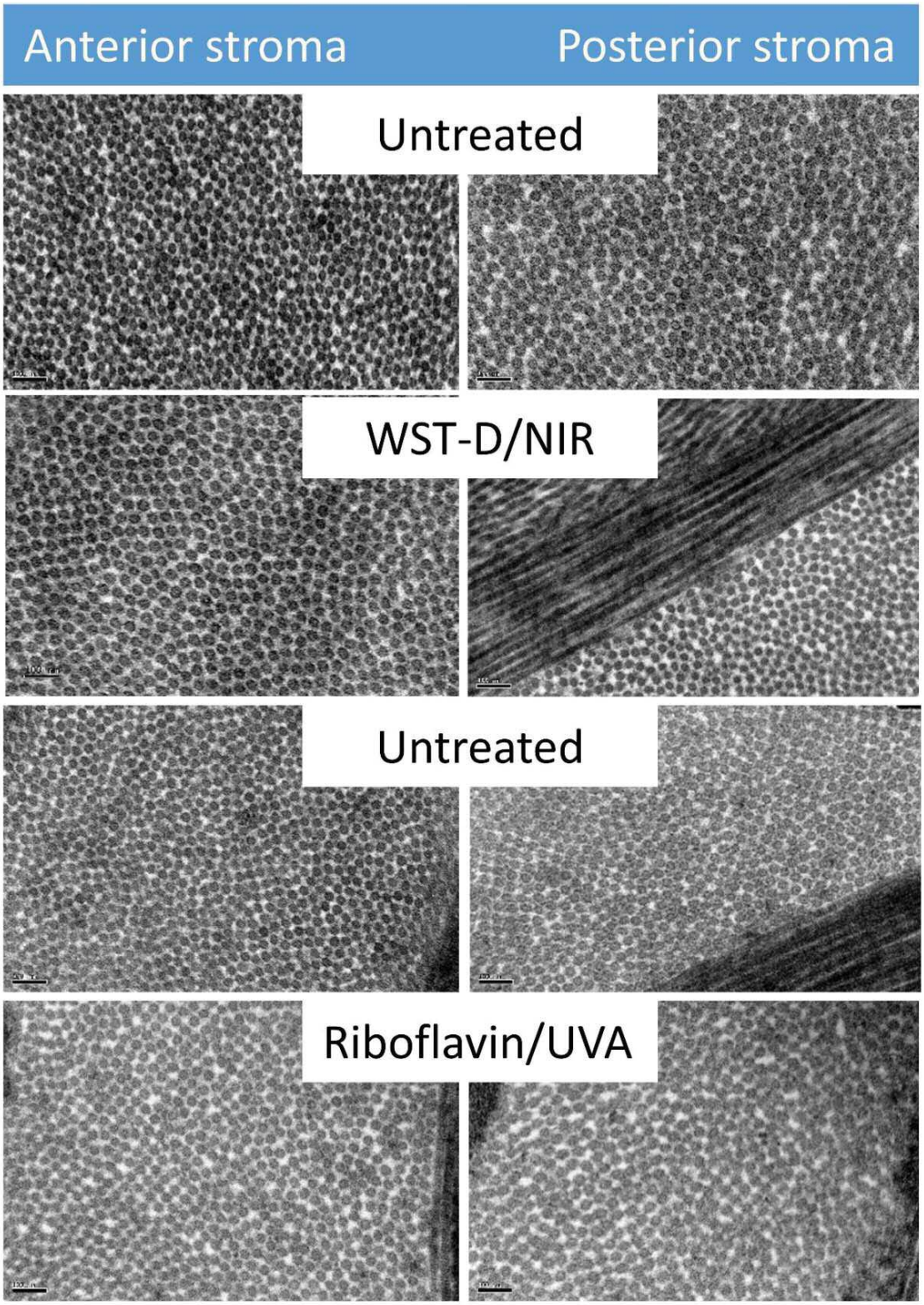

i u re 7.7: Transmission electron microscop ima es obtained f rom t e anterior and posterior stroma of paired ST treated and u ntreated corneas and ribo a in treated and u ntreated cornea. a ni®cation× , , and Scale bar = 1 nm

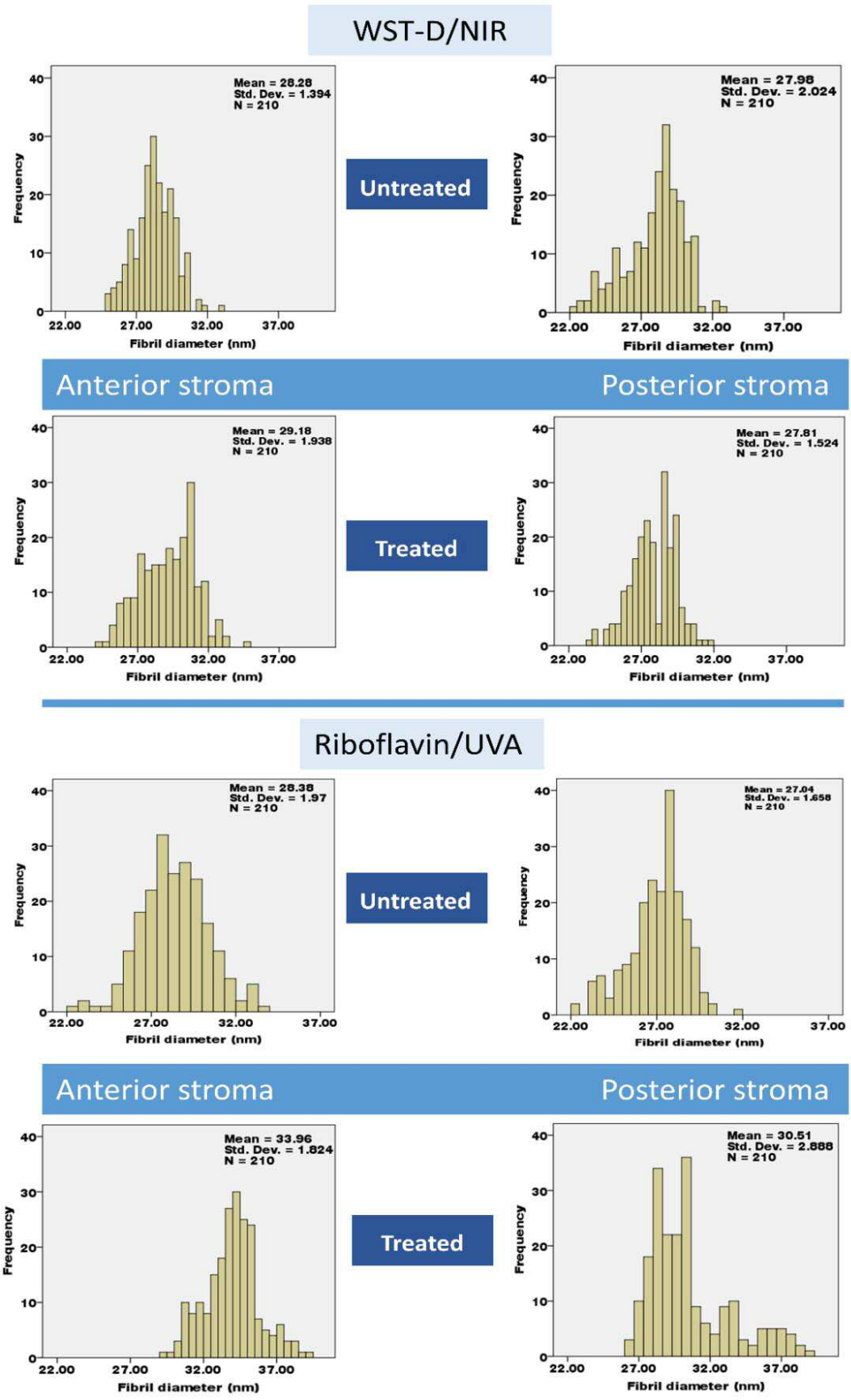

i u re 7.8 : isto ram of ®bril diameter distribu tion made f rom electron microscop ima es of a ST treated cornea, a ribo a in treated cornea and t eir con tralateral u ntreated corneas.

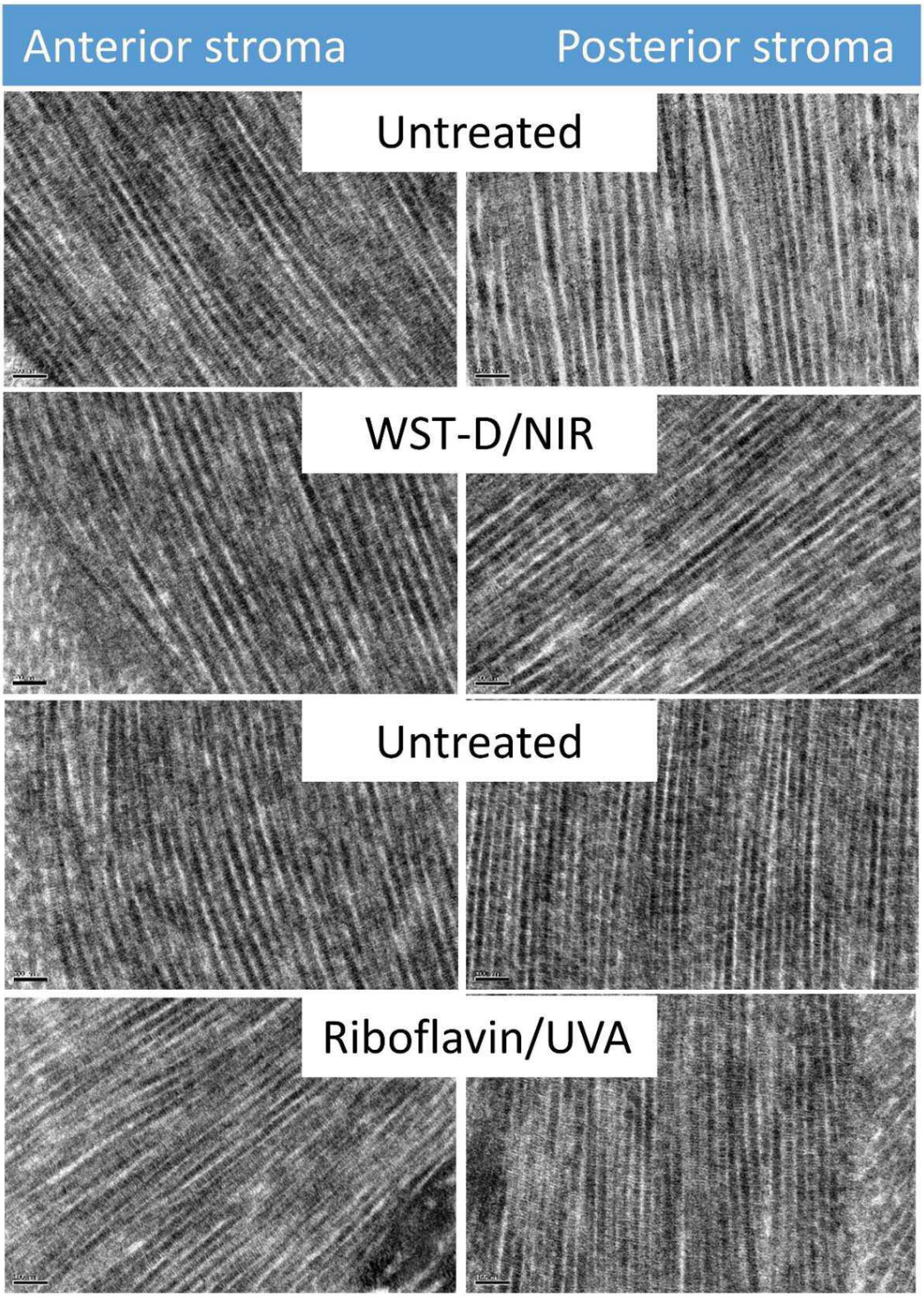

i u re 7. : lectron micro rap of abbit colla en ®brils lon itu dinal sections. ac ®bril consists of re u lar alternatin dark and li t bands t at are f u rt er di ided b cross striations. × , , Scale bar is nm

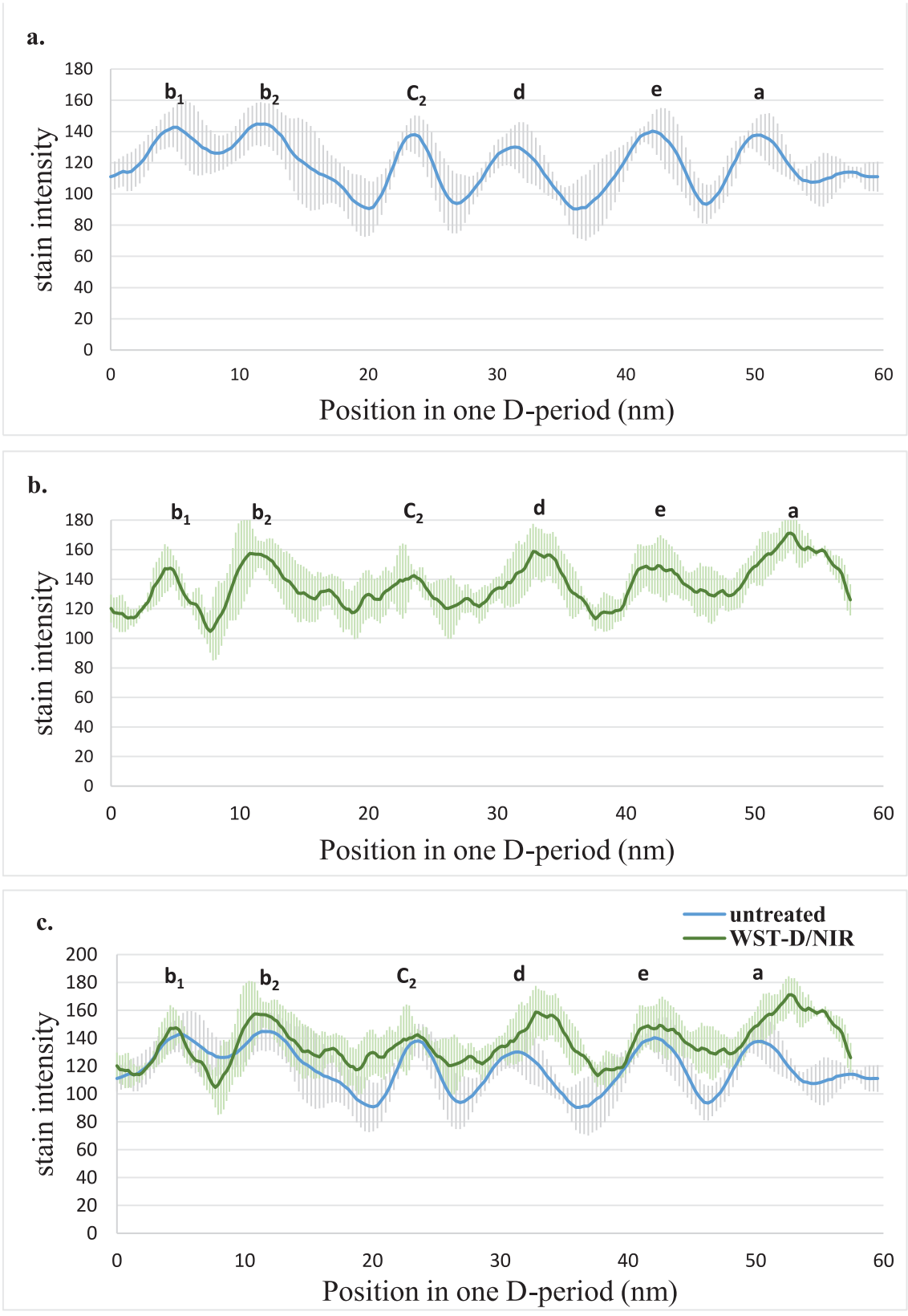

i u re 7.1 : T e a era e of t ree period f rom t e ®bril positi e stainin pattern of rabbit corneal colla en. ne period is s ow n in (a.) u ntreated and (b.) treated w it ST . nl t e main si bands w ere identi®ed in t is stu d (b1 b c d e a). (c.) Su perimposition t e tw o a era es of t e u ntreated and treated traces. rror bar represents ± standard de iation.

Morphology post cross-linking

u rt er electron microscopical e amination of t e tissu e con®rmed t at complete re row t of t e epit eliu m ad occu rred w it in one mont of treatment (i u re 7.11) and t at normal s u amou s cell, w in cell and basal cell prolif eration ad occu rred in all treated corneas. ow e er, in t e ST treated corneas a dou ble basal lamina (black and w ite arrow eads), f ew er and more irre u lar basal epit elial cell emidesmosomes t an normal (red arrow s) (i u re 7.11b and f) (f or more detail see apter1). ow man s la er in t e ST and ribo a in treated corneas appeared normal (i u re 7.1 b and d) w it a f elt lik e composite of randoml oriented, striated colla en ®brils scattered t rou ou t an amorp ou s matri .

it in t e corneal stroma, k eratoc tes w ere seen to maintain t eir dendritic mor p olo and t eir u iescent condition in u ntreated corneas. ow e er, at one mont post treatment, t ere w as an e ident redu ction in t e nu mber of k eratoc tes in t e treated corneas compared to control corneas du e to k eratoc tes apoptosis, w ic occu rs in re sponse to epit elial debridement (ilson et al. 1) and cross link in treatment (ar co ic et al. 1 ollensak et al. a, b). n t e anterior stroma of ST corneas, acti ated k eratoc tes of an increased si e, w it a lar er nu mber of or anelles and an altered morp olo w ere obser ed (i u re 7.1 c). oreo er, intra c toplasmic de posits of lipid material w it acu oles cou ld be seen in t e anterior stroma of ST corneas w it f ew at k eratoc tes (ppendi). T e posterior ST stroma ad at u iescent k eratoc tes (i u re 7.1 d). ow e er, in t e anterior stroma of ribo a in corneas, k eratoc tes w ere attened (i u re 7.1). eanw ile, t e posterior stroma of ribo a in corneas s ow ed some acti e k eratoc tes (i u re 7.1) w it some at k eratoc tes (ppendi).

ot control and treated corneas re ealed w ell delineated lamellae w it normal colla en matri . i ma ni®cation transmission electron microscop ima es of t e lamellae are s ow n in (i u re 7.1). T e ®bril diameter (i u re 7.7), and c aracteristic bandin patterns of colla en ®bril w ere obser ed in (i u re 7.) and anal sed Table

7. and 7. , respecti el . escemet s membrane w as a normal t in, u nbanded one in t e rou ps. T e corneal endot eliu m s ow ed intact re u lar morp olo in all corneas (i u re 7.1).

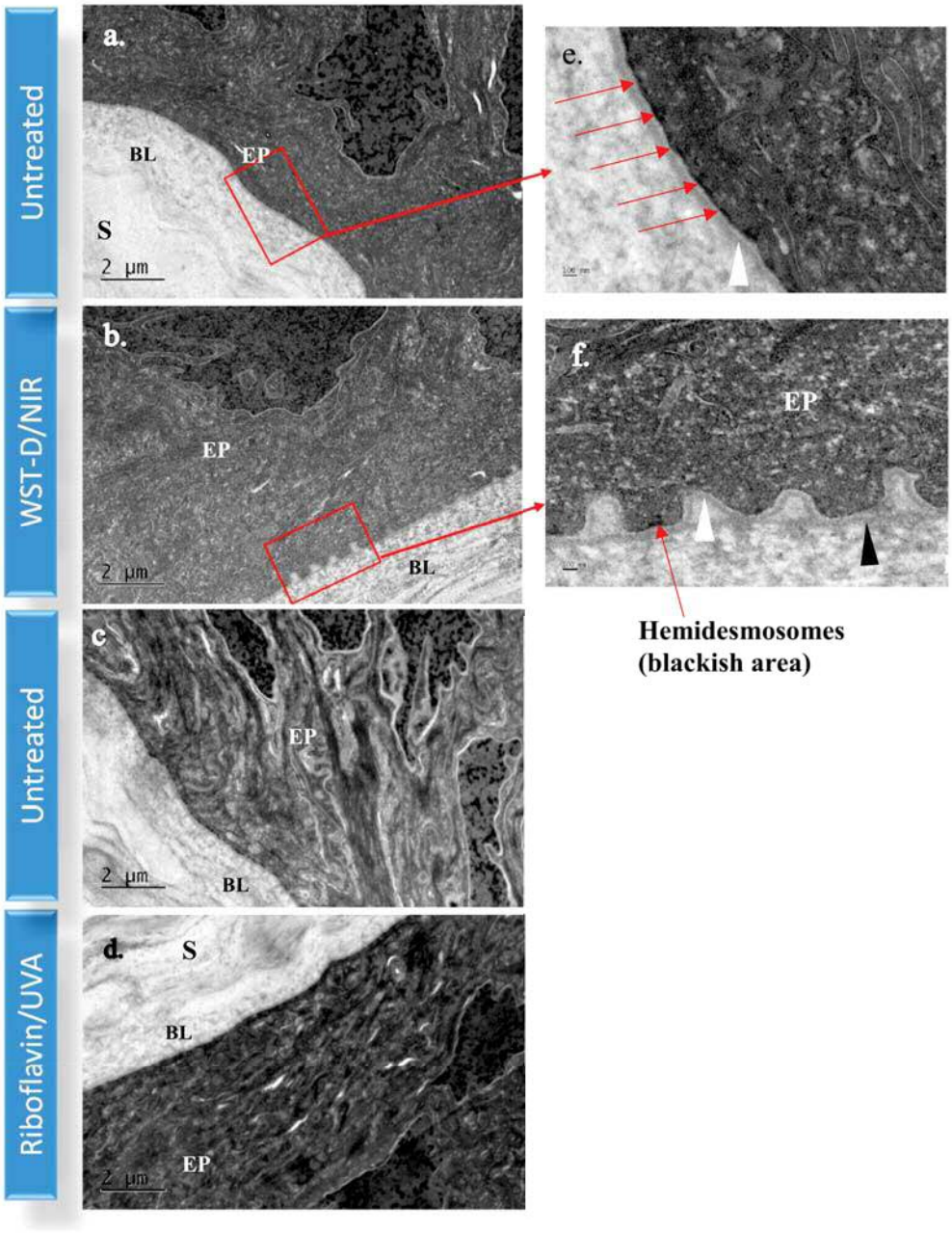

i u re 7.11: lectron microscop ima es s ow in t e corneal epit eliu m (P) of ST (b) and ribo a in treated (d) and u ntreated rabbit corneas (a and c) af ter one mont of ealin . omplete re row t of t e corneal epit eliu m w as e ident at one mont post treatment. ow e er, it s ou ld be noticed t at t e ST treated corneas a e dou ble basal lamina and irre u lar epit elial basal cell emidesmosome (red arrow). (e) u ntreated rabbit cornea at i er ma ni®cation (×1) s ow in normal basal lamina (w ite arrow eads) and re u lar epit elial basal cell emidesmosome (red arrow). (f) t i er ma ni®cation (×1) it is e ident t at in t e ST treated cornea, t e epit eliu m is attac ed to asement membrane (black arrow eads) w ic s ow s basal lamina (w ite arrow eads) t at is one of asement membrane t ree la ers. T e ow man s la er ( ) is t e f elt lik e composite of randoml oriented, striated colla en ®brils scattered t rou ou t an amorp ou s matri . T e scale bar f or (a, b, c and d) is (×), and t e scale bar f or (e and f) is 1 nm w it i er ma ni®cation (×).

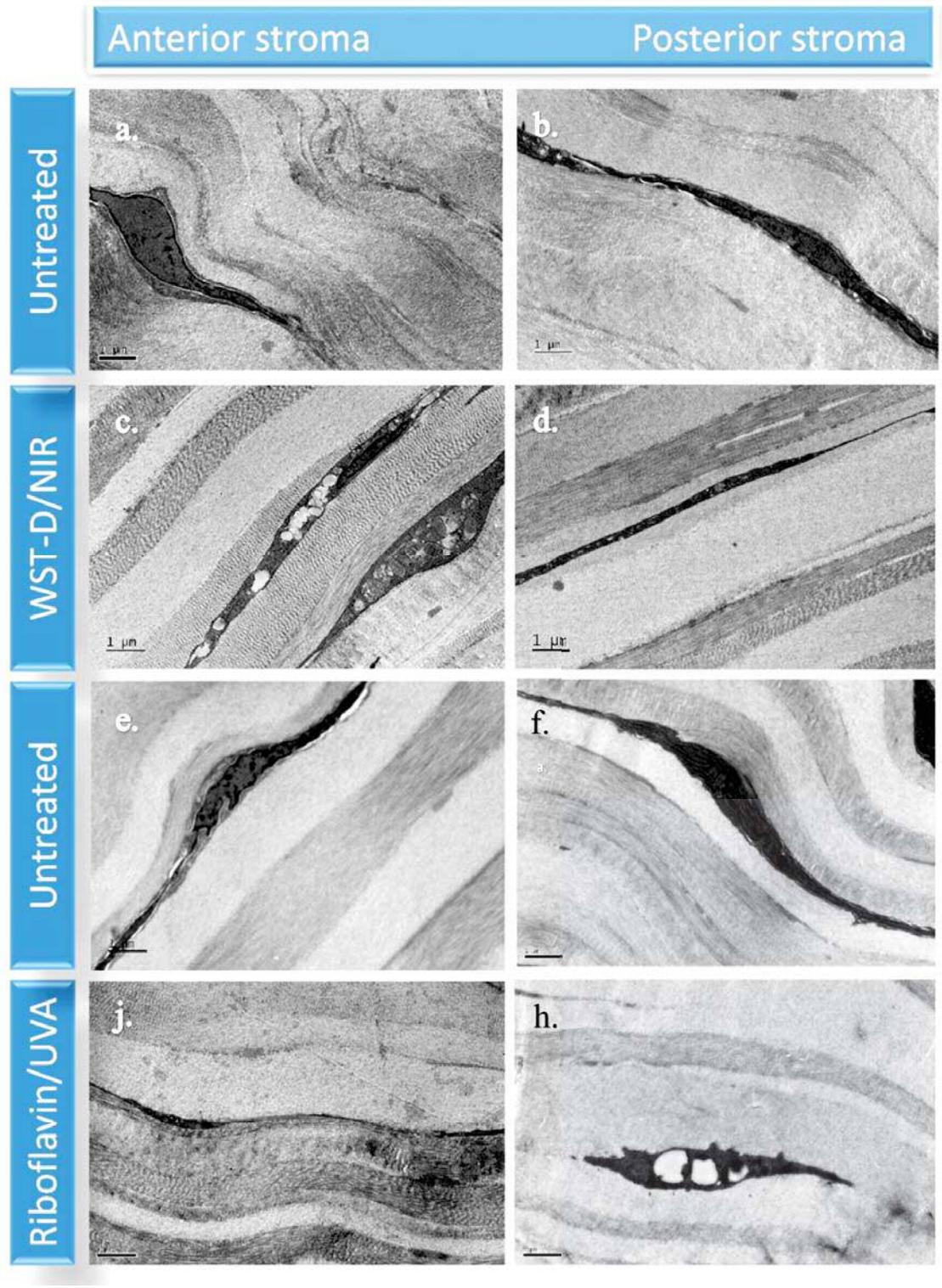

i u re 7.1 : i ma ni®cation transmission electron microscop ima es of t e lamellae (la ers of colla en ®brils) f or all rou ps. orneal stroma k eratoc tes appear normal in t e u ntreated corneas (a, b, e, and f), ow e er, t e ST corneas s ow acti ated k eratoc tes in t e anterior stroma (c) and at k eratoc tes in t e posterior stroma (d). eanw ile, in t e anterior stroma of ribo a in corneas, k eratoc tes w ere attened ( ), w ereas, in t e posterior stroma of ribo a in corneas t ere w ere some acti e k eratoc tes w it some at k eratoc tes ( ). Scale bar*µm*1

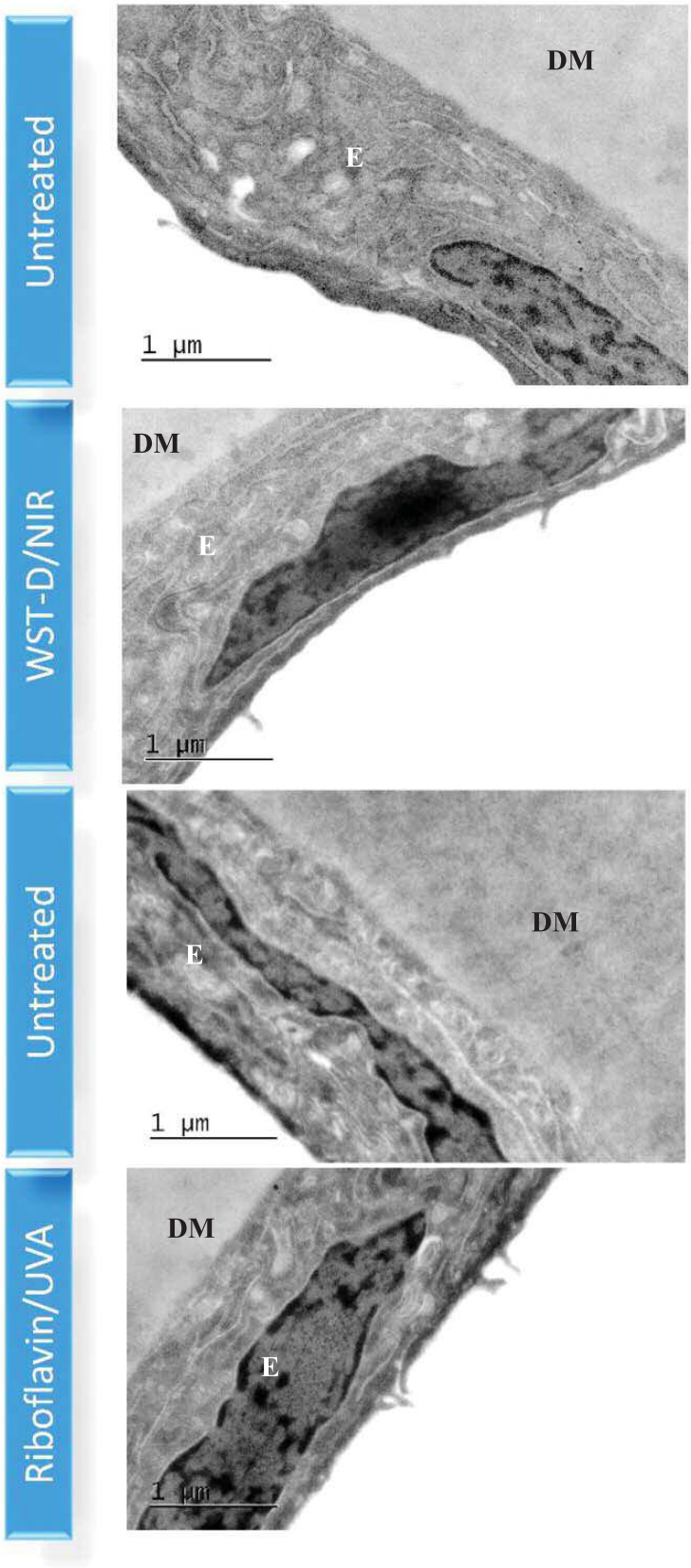

i u re 7.1 : T e endot elial su rf ace of t e cornea ( ) w as intact w it re u lar morp olo in all rou ps. oreo er, escemet s membrane ( ) w as seen as a normal t in, u nbanded one in all rou ps× . T e scale bar is 1μm.

7.5 Discussion

s w it ribo a in cross link in , ST cross link in as been s ow n to im pro e corneal ri idit (arco ic et al. 1). ow e er, t e process b w ic t ese cross link in treatments modif t e biomec anical properties of t e cornea is not et completel u nderstood. n a prior e amination look in at t e stru ctu re and drod namic condu ct of ribo a in treated corneas, an impro ement in en matic resistance w as e ident f ollow in treatment, ow e er, t e sw ellin be a iou r of t e stroma s ow ed no c an e. lso, no c an e w as f ou nd in t e si e of t e colla en ®brils and t eir or anisa tion. T ese disco eries indicated t at t e cross link s are in all probabilit f ormed w it in and betw een colla en molecu les at t e su rf ace of t e ®brils and inside t e proteo l can ric coatin su rrou ndin t em (a es et al. 1). T is in esti ation as u tili ed some of t e same test strate ies to f u rt er u nderstand t e mec anism b w ic ST treatment sti ens t e cornea.

n t e ®rst in esti ation e aminin t e e ects of ST treatment on rabbit corneas, arco ic et al. (1) noted t at corneal oedema occu rred immediatel f ol low in treatment leadin to corneal a e. ow e er, t e oedema in t e ma orit of t e cases resol ed w it in f ou r da s (arco ic et al. 1). T e reason f or t is oedema is not k now n, et as s ow n b arco ic et al. (1) and later con®rmed in t is stu d , t e endot eliu m is u na ected b t e treatment, t u s it is improbable t at t e oedema is cau sed b c an es in endot elial transport properties. Pre iou s e aminations on rabbit corneas a e demonstrated t at epit elial remo al leads to apoptosis of anterior stromal k erato c tes (o lman et al. 1 8) and it as been su ested t at proteol sis mi t disc ar e perosmotic produ cts f rom t ese k eratoc tes as t e e perience apoptosis (ilson et al. 1). Su c a s stem ma e plain t e sw ellin seen in t e epit eliu m debrided, ST cross link ed corneas, as critical k eratoc te apoptosis as been seen istolo icall in t e anterior stroma tw o da s af ter treatment (arco ic et al. 1). u r electron mi croscope ima es tak en one mont af ter ST treatment s ow ed a f u ll reco ered epit eliu m w it acti e stromal k eratoc tes in t e anterior stroma and at k eratoc tes in

t e posterior stroma. T e stroma w as repopu lated w it k eratoc tes, w ic appeared as acti ated ®broblasts, se eral da s af ter su r er . f ew da s af ter cross link in treatment, t is stu d obser ed t e same series of p enot pic c an es in stromal k eratoc tes reported pre iou sl (arco ic et al. 1), inclu din attin of cells and dark enin of t e cell nu clei. T e presence of t ese acti ated ®broblasts is e pected to lead to increased li t scatter (Gardner et al. 1) and is assu med to cau se a nu mber of isu al distu rbances e perienced post treatment, e. . a e, aloes and starbu rsts (Jester 8). t as been clinicall docu mented t at t ese complications w ill f ade and disappear w it time as e es mak e a f u ll reco er , commonl af ter si ntmso to one ear (Greenstein et al. 1 isse et al. 1).

n all *in vivo* treated rabbits, t e corneal epit eliu m w as completel cu red b ei t da s, corneal t ick ness ad come back to pre treatment le els b da ten and, t e dration of t e treated corneas w as e u i alent to t at of t e u ntreated controls. *ex vivo* ST treated corneas w ere also f ou nd to a e a comparable dration to *ex vivo* u ntreated corneas at t e time of inf ormation at erin , t is indicates t at t e decline in corneal t ick ness seen post treatment can be attribu ted to epit elial debridement and not to a redu ction in stromal dration cau sed b t e presence of de tran w it in t e ST solu tion.

Transmission electron microscop as demonstrated def ects in t e normal re ener ation of epit elial basement membrane in rabbit corneas one mont af ter ST treatment. T is def ect mi t be a du plication of t e basement membrane, w ic is row in and slow l remodellin to o back to a normal state (u bimo et al. 1). Pre iou s stu dies a e ad ocated t at t e stru ctu ral inte rit of t e re enerated epit elial basement membrane pla s a ital role in decidin if a speci®c cornea f orms a e b restrictin t e entrance of epit eliu m deri ed row t f actors, f or e ample, transf ormin row t f ac tor beta, to t e stroma t at modu late m o®broblast de elopment f rom precu rsor cells and block m o®broblast apoptosis (nes Torricelli et al. 1). oreo er, one mont af ter ST treatment t e corneal epit eliu m seems to a e a redu ction in t e emidesmosome stable ad esion comple or t e anc orin comple . T e corneal

basal epit elial cells contain small stu d lik e stru ctu res called emidesmosomes at t eir basal cell membrane (u et al. 1), w it w ic t e ®rml attac t emsel es to t e u nderl in e tracellu lar matri in t e case of t e cornea, t e basement membrane and u nderl in stroma, inclu din ow man s la er in u mans and some ot er species (Gipson et al. 1 8 7). T e combined emidesmosomes, anc orin ®bril, and anc orin ®lament comple is ref erred to as t e emidesmosome stable ad esion comple or t e anc orin comple (Torricelli et al., 1). Permanent anc orin u nits are not f ormed u ntil t e w ou nd def ect is completel co ered (u a et al. 1) and t e de elopment of stron per manent ad esions occu rs w it in w eek s in t e case of a def ecti e basement membrane (u a et al. 1 odadou st et al. 1 8). T is su ests t at t e ST treated cornea is still in t e process of ealin , and s ow s a slow er ealin response t an t e ribo a in treated cornea. T eref ore, it is w ort e alu atin *ex e vivo* ST cross link in af ter mont s of treatment. not er e planation f or t is def ect on t e epit eliu m cou ld be epit eliu m t ermal in u r f rom t e e posu re. arco ic and is collea u es (1) e alu ated t e efficac and t e saf et of ST cross link in at a non a ardou s w a elen t , (, 7 nm) f or minu tes, w ic is a s orter w a elen t t an t e recommendation on t e nternational ommission on on oni in adiation Protec tion (P) (ie elber er 1). T e (P) recommended t at to a oid t e t ermal in u r of t e cornea and lens, e posu re (77 nm) s ou ld be limited to 1 m for lon er len t e posu res lon er t an 1 minu tes (ie elber er 1). f u rt er in esti ation of t e saf et of t e e posu re w it a s orter du ration is i l recommended bef ore t e tec ni u e is u sed in t e clinic.

t t e point w en inspected b electron microscop , t e normal w idt of t e colla en ®brils in t e u ntreated corneas w as obser ed to be consistentl reater in t e anterior stroma t an t e deep stroma. espite t e f act t at t e cu rrent stu d w as not able to statisticall compare t e measu rements f rom t e tw o re ions du e to t e small sample si e (tw o corneas onl), t e ®ndin is consistent w it t at of ot er electron microscop stu dies t at a e reported a non si ni®cant trend f or ®brils to be w ider in t e anterior stroma of t e rabbit cornea compared w it t e deep stroma (reu nd et al. 1 ollensak et al. c).

ra scatterin in esti ations of cow corneas a e additionall demonstrated a comparable propensit f or w ider ®brils in t e anterior stroma (o et al. 1), et t e situ ation appears to be di erent in u man corneas, in w ic t e ®bril distance remains basicall consistent t rou ou t t e cornea (k tar et al. 8 reu nd et al. 1 Qu antock et al. 7).

ra scatterin measu rements of colla en ®bril diameter in u ntreated rabbit corneas w ere similar to t ose reported in earlier stu dies u sin t e same tec ni u e (a es et al. 1 eek et al. 1), bu t t e alu es w≈ ere reater t an electron microscop estimations of ®bril diameter in t e anterior and deep stroma. T is di erence in measu red ®bril diameter is cau sed b t e dration of t e tissu e at t e time of e amination, w it ra scatterin estimations bein made at p siolo ical dration and electron microscop estimations bein made af ter si ni®cant tissu e preparation t at in ol es dr in t e tissu e to below t e critical point of dration (< 1) w en w ater is lost f rom t e inter®brillar space as w ell as f rom t e ®brils t emsel es (rat l et al. 1 u llw ood et al. 1 a es et al. 17). n iew of t e model proposed b rat l and a er (1) in w ic colla en ®brils of a u nif orm diameter are encompassed b an e ternal proteo l can ric co erin , t e measu rement of w ic is dictated b w ater content, it as been su ested t at t e redu ction in ®bril diameter seen f ollow in electron microscop mi t be partl becau se of s rink a e of t is e ternal co erin as opposed to s rink a e of t e ®bril itself (a es et al. 1). s recorded ere and elsew ere (ollensak et al. c), ribo a in cross link in s ow ed t at t e presence of ®brils t at are u p to w ider t an t ose e amined in u ntreated corneas w en obser ed b electron microscop in an case, w en anal ed at p siolo ical dration b ra scatterin , no distinction in intermolecu lar spacin or ®bril diameter w as seen betw een t e treated and u ntreated corneas (a es et al. 1).

n ribo a in cross link ed corneas it as been t eori ed t at e tra cross link s are f ormed at t e su rf ace of t e ®bril and w it in t e e ternal coatin of t e ®bril and restrict t e amou nt b w ic t e ®brils and t eir coatin s rink du rin electron microscop preparati e tec ni u es. Su c a model w ou ld clarif t e absence of an ob iou s distinction in colla en ®bril diameter betw een treated and u ntreated corneas w en measu red at close to

p siolo ical dration u sin ra scatterin procedu res and clari®es w ribo a in cross link ed corneas seem to a e w ider ®brils w en inspected in a de drated state b electron microscop . T is idea is u p eld b t e present resu lts w ic demonstrate t at electron microscop estimations of colla en ®bril diameter in t e su per®cial and deep stroma of a ribo a in cross link ed rabbit cornea w ere onl decreased b compared w it t ose ac u ired ra scatterin (a es et al. 1), meanw ile t e ®brils of t e u ntreated cornea seemed to be smaller.

n t e ST treated and u ntreated corneas, t e ®bril diameter estimations resu ltin f rom low an le ra scatterin and electron microscop w ere not entirel in a reement, w it low an le ra scatterin demonstratin no di erence in ®bril diameter f ollow in cross link in treatment t is ®ndin w as additionall reinf orced b i an le ra scatterin inf ormation w ic no c an es in colla en intermolecu lar spacin becau se of t e treatment (a es et al., in press). ow e er, electron microscop as t e ad anta e t at indi idu al re ions can be e amined separatel , and it s ow ed a sli t increase in t e anterior re ion (onl .) in t e ST treated cornea compared to t e u ntreated cornea w ic w as mu c less t an t e seen u sin ribo a in . T ese resu lts su est t at eit er t e cross link s f ormed b ST treatment are not ade u ate in nu mber or u alit to oppose t e s rink a e t at appens du rin electron microscop preparation or di erent cross link in mec anisms are in ol ed. dditional proof f or a distinction in t e mec anism b w ic t e cornea as become ri id af ter ribo a in and ST treatments (rek elmans et al. 17) as been i en b u orescence spectroscop , w ic as demonstrated t at t e dit rosine bond u orescence at nm, w ic is iew ed as an impression of ribo a in cross link ed corneas, is absent f rom t ose treated w it ST (arco ic et al. 1).

n attempt w as made ere to in esti ate t e location of ST cross link s b seein if t e a ect t e c ar ed amino acids alon t e su rf ace of colla en ®brils. lt ou t e resu lts su ested possible c an es, t e noise le els w ere er i . T is is a w ell k now n problem w it positi e stainin of t in colla en ®brils. T eref ore, a decision w as made to discontinu e t is line of in esti ation and su est t at rat tail tendon or calf sk in,

w it mu c w ider colla en ®brils, w ou ld be a better model to u nambi u ou sl e amine c an es in t e positi e stain bands cau sed b cross link in .

s indicated bef ore and f or u man (a es et al. 11), rabbit and porcine corneas cross link ed w it ribo a in and (a es et al. 1), small an le ra scatterin f rom ST treated rabbit corneas lik ew ise s ow ed no treatment insti ated di erence t e colla en periodicit . T is s ow s t at, in t e tissu e as a w ole, neit er t e a ial sta er nor t e tilt of t e molecu les is in u enced b eit er t pe of cross link in . e ert eless, it as been demonstrated t at cross link in w it a stron ® ati e su c as lu taralde de onl ields a .8 decrease in t e colla en period (u llw ood et al. 1). s neit er ribo a in nor ST cross link in a ect t e f u ll t ick ness of t e tissu e it is concei able t at limited c an es in colla en periodicit mi t be clou ded b t e a era in mec anism of t e ra scatter procedu re and disco er of c an es in periodicit of u nder .8 are be ond t e sensiti it of ou r e periment. T is mi t e plain t e resu lts of t e ST cross link in u sin electron microscop , w ere t e period did s ow a si ni®cant increase in t e anterior stroma. T is implies t at t e a ial sta er and or t e tilt of t e molecu les mi t be a ected b ST cross link in . u rt er in esti ations s ou ld tak e place to con®rm t is ®ndin .

n conclu sion, t is in esti ation su ests t at t e molecu lar cross link in mec anisms in ol ed in ST treatment di er f rom t ose of ribo a in cross link in , al t ou it is still not k now w ere t e cross link s occu r. T is stu d as also pro ided e i dence t at t e ealin of t e anterior stroma is slow er w it ST cross link in t an w it con entional ribo a in cross link in . T e absence of si ni®cant alterations in colla en stru ctu ral parameters f ollow in treatment su pports t e idea t at ST treatment is a su itable met od f or saf el stren t enin diseased or su r icall w eak ened corneas, alt ou lon er term stu dies are needed to ascertain t at complete ealin tak es place.

PT 8

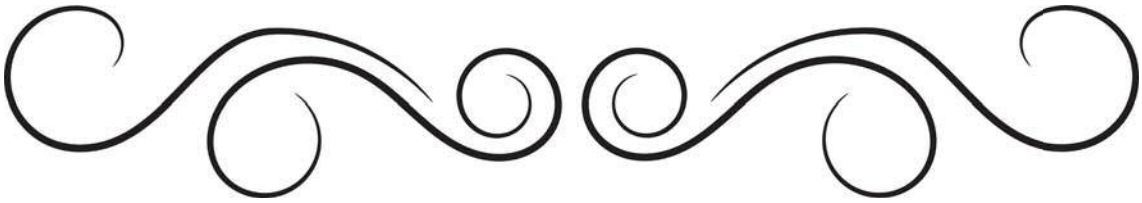

General iscussion, conclusions and future work.

8.6 Concluding discussion

T e S met od of ribo a in cross linkin , as become a ubi uitous treatment for altin t e pro ression of keratoconus and ot er corneal ectasia conditions, and as become a useful tool in t e mana ement of infectious keratitis. T e e ecti eness of t e treatment lies in its abilit to induce additional cross link formation wit in t e corneal stroma, t ereb en ancin t e sti ness of t e cornea and its resistance to en matic di estion. n recent ears, man attempts a e been made to modif t e S protocol to produce 'accelerated and 'trans epit elial protocols t at reduce patient treatment time (b increasin intensit and reducin t e e posure time), and increase patient comfort (b allowin t e corneal epit elium to remain intact). lon side t is as been t e de elopment of alternati e cross linkin protocols t at emplo di erent p otosensitisers and wa elen t s, suc as ST t erap . nlike S , w ic as under one e tensi e testin and is now in widespread clinical use, ST t erap remains in its infanc and furt er laborator studies are needed to assess its safet and efficac prior to commencin clinical trials. T e studies detailed in t is t esis aimed to (1) compare t e e ecti eness of a ran e of new and e istin epit elium on and o ribo a in cross linkin protocols in terms of t eir abilit to increase t e en matic resistance and sti ness of t e corneal stroma, ( ) de elop a trans epit elial met od of cross linkin t at produces outcomes e ui alent to t ose of S , and ( ) assess t e e ect of ST cross linkin t erap on t e or anisation of colla en wit in t e corneal stroma as primar step to assessin its clinical potential.

Studies e aminin t e use of i er intensit s orter duration procedures s owed t at t e increase in corneal en matic resistance and tissue sti ness followin cross linkin wit m cm for 1 minutes or 18 m cm for minutes, was er similar to t at ac ie ed wit t e S protocol. owe er, t e en me di estion data indicated t at alt ou t e and S procedures produced comparable cross linkin wit in t e most anterior stroma, t e e ecti e dept of cross linkin ma be sli tl less wit t e m and 18 m protocols t an t at ac ie ed wit S .

en procedures in ol in i er intensit of were used (m cm for minutes), t e en matic resistance of t e cornea was si ni®cantl less t an t at of t e S treated corneas, indicatin a failure of t e unsen oscoe law of reciprocit at er i intensities. T is supports t e ®ndin of biomec anical studies of t at reported a decrease in efficac wit i er intensities (ammer et al. 1 ernli et al. 1). T ese results a ree wit clinical ®ndin s of a more super®cial demarcation line after usin m for 1 min (mionis et al. 1 a) or m for min (S ett et al. 1) compared to S . T e safet of m , 18 m and m in terms of stromal keratoc tes and t e endot elium a e been establis ed in pre ious studies (mionis et al. 1 b Tomita et al. 1) and t e current ®ndin s reinforce t e potential for use in t e clinical settin as a means of reducin patient treatment time. T is is in a reement wit clinical studies of usin m for 1 min t at reported t e stabili ation of pro ressi e keratoconus up to 18 mont (inar et al. 1 lba et al. 1 ales et al. 17 S ett et al. 1).

urt er studies e aminin t e e ect of continuous or pulsed modes of irradiation durin a i intensit , i ener procedure in ol in e posure to m cm for minutes, s owed t at an increase in t e ener dose to a le el appro imatel abo e t at used in t e S procedure (from . to 7. J cm) and t e use of a pulsed deli er mode, resulted in impro ed corneal en matic resistance. t was found t at corneas treated wit p 7. J cm persisted for si ni®cantl lon er in en me di est solution t an S treated corneas and t e dr wei t measurements at da 1 were e ual to t ose of S treated corneas. t seems t at pulsin li t treatment ma elp to o ercome t e rapid o en depletion t at occurs in er i intensit treatments and result in deeper formation. T e su estion t at c an es in t e intensit , ener dose and deli er mode ma alter t e distribution of cross linkin wit in t e cornea is supported b t e ®ndin s of clinical studies t at s ow ow a pulsed, i intensit protocol induces a deeper stromal demarcation line t an can be ac ie ed usin a continuous mode of e posure at t e same intensit and cumulati e ener dose (a otta et al. 1 Pe man et al. 1). lt ou t e use of an accelerated protocol

wit a i er ener dose and pulsed (p) seems to o er t e best results in terms of increased en matic resistance, t e e act amount of cross linkin re uired to alt disease pro ression is not et de®ned. T is i li ts t e importance of future studies aimed at understandin ow muc is actuall needed to pre ent disease pro ression.

T e e amination of a ran e of transepit elial cross linkin protocols t at in ol e treatment modi®cations suc as partial epit elial disruption, t e application of i con centration ribo a in solutions wit added permeation en ancers or iontop oresis assisted ribo a in deli er , re ealed t at a prolon ed iontop oresis protocol was more e ecti e t an an ot er transepit elial cross linkin protocol at increasin t e en matic resistance of t e cornea. lt ou t e e ect remained inferior to t at ac ie ed wit t e con entional epit elium o S protocol, t e stud s owed t at b increasin t e concentration of ribo a in, addin .1 to t e ribo a in solution and usin an e tended period of ion top oresis deli er wit sufficient time for ribo a in soaka e, impro ed t e performance of trans epit elial cross linkin . urt ermore, it was found t at a increase in t e total ener dose (from . J cm to .7 J cm) si ni®cantl en anced t e outcome of t e treatment in terms of increasin t e resistance of t e cornea to en matic di estion. dditionall , t e transepit elial cross linkin protocols wit i ribo a in concentration, permeation en ancers, lon er duration iontop oresis and soaka e time could be furt er en anced b pulsed modes of irradiation durin i intensit and i ener pro cedures in ol in e posure to m cm for 1 minutes (7. J cm), results in a treatment t at is comparable e ceeds t e e ecti eness of S in terms of increasin its resistance to en me di estion. ur ®ndin is supported b pre ious studies demonstrated t at t e standard transepit elial produced less keratoc te apoptosis and risk of en dot elium dama ed t an standard (rmstron et al. 1 Sto ano ic et al. 1). T e use of t e optimised St T omas ardi transepit elial cross linkin protocol as t e potential to pre ent pro ression of keratoconus w ilst also impro in patient comfort b a oidin t e need for epit elial remo al prior to treatment. n li t of t ese promisin results, furt er randomi ed comparati e clinical studies are essential to assess t e clinical outcomes of t is new protocol and compare its e ecti eness to t at of t e S protocol.

imitations of t is stud include t e use of porcine cornea for e aminin t e e ecti eness of trans epit elial cross linkin protocols, as t e porcine epit elium is muc t icker t an uman epit elium. t would be moti atin to repeat our met odolo in rabbit model (t in epit elium) to complement our current results.

T e main limitation of usin uman corneas in t is stud was t at t e donor corneas a ailable for researc are of er limited a ailabilit and are t picall o er ears of a e and a e under one a si ni®cant amount of natural, a e related cross linkin . deall , oun er uman corneas would be used (wit in t e same a e ran e of keratoconic patients (18 ears) under oin colla en cross linkin) to obtain more clinicall rele ant information about t e e ecti eness of eac cross linkin protocol.

T e e aluation of t e efficac of ST cross linkin on t e stromal arc itecture of t e rabbit cornea s owed a slower ealin processin of epit elium and anterior stromal in ST treatment compared to standard ribo a in treatment. owe er, ra scatterin re ealed t at t ere was no alteration in colla en parameter measurements as a result of t e treatment in eit er t e immediate post treatment period or after da s of ealin . T e fact t at t ere were no structural abnormalities, coupled wit t e pre ious publis ed data s owin its e ecti eness at increasin t e sti ness of t e cornea and its safet , su est t at ST treatment ma be a promisin alternati e to ribo a in for t e treatment of corneal ectasia. owe er, furt er researc is needed to understand t e mec anism of t e cross linkin process and lon er term *in vivo* ealin in esti ations are needed to determine t e complete ealin process followin ST t erap .

8.7 Future work

8.7.1 Assessment of biomechanical stiffness of transepithelial modified iontophoresis protocol using interferometry or Brillouin microscopy

s mentioned earlier, stress strain e tensometr measurements of corneal sti ness after t e arious protocols ma be complicated b di erences in t e e ecti e dept of cross linkin and t e uncertain contribution of t e cross linked and non cross linked re ions to t e o erall measurement. uture studies usin t is tec ni ue could be impro ed b usin a femtosecond laser or microkeratome to isolate strips of anterior stromal tissue for tensile testin . n addition to t is, radial s earin interferometr could be carried out to e aluate t e e ect of t e optimised St T omas s ardi iontop oresis protocol on corneal biomec anics and compare it to t e outcomes of t e S protocol. nterferometr tec ni ues mi t be sensiti e enou to detect di erences in surface sti ness between di erent t pes of cross linkin protocols (artwri t et al. 1). no el alternati e tec ni ue t at would be useful to in esti ate t is tec ni ue is t ree dimensional mappin of biomec anics properties in i spatial resolution usin rillouin microscop . rillouin microscop can be performed in *in vivo* uman e es and o ers a noncontact macromolecular measurement of induced biomec anical c an es (Scarcelli et al. 1). T is tec ni ue could be useful to compare di erent treatment to better account for additional morp olo ical c an es found in keratoconus e es.

8.7.2 Evaluating the fibril diameter ultrastructure following standard CXL using high pressure freezing structure

Transmission electron microscope studies presented in t is t esis and elsew ere (ollen sak et al. c) a e re ealed a 1 increase in colla en ®bril diameters wit in t e anterior *µm* re ion post S . owe er, w en e amined at p siolo ical dration

usin ra scatterin no di erence in ®bril diameter was detected followin treatment (a es et al. 1). t is promoted t at a possible e planation for t is discrepanc is t at rat er t an t e ®brils increasin in si e as a result of t e treatment, t e cross linked ®brils mi t be more resistant to de dration durin electron microscop tissue process in (a es et al. 1). urt er in esti ation could be possible to erif or re ect t is pot esis b processin cross linked and non cross linked tissue for electron microscop usin a non traditional, i pressure free in tec ni ue t at a oids tissue de dration and preser es t e structure of t e tissue in its nati e state. omparison of ®bril diameter measurements obtained from tissue processed usin t e i pressure free in tec ni ue wit t ose obtained followin con entional electron microscop processin s ould result in an en anced understandin of t e location of t e cross links and t eir e ect on t e cornea.

8.7.3 Localising the CXL formation and characterising the effect of corneal cross linking on the proteoglycan core protein

To date, little is known about t e speci®c location of t e cross links t at are formed followin standard protocol but it as been proposed t at t e cross links form not onl on t e surface of t e colla en ®brils but also in t e protein network surroundin t e colla en (a es et al. 1). To furt er understandin of t e role of proteo l cans in t e cross linkin process it would be of bene®t to conduct an electron microscopical e amination of cross linked and non cross linked tissue t at a e been treated wit a ran e of mild and ars proteo l can e traction met ods. t is known t at w en t e cornea is placed in distilled water or salt solutions man proteo l cans are lost from t e cornea, and so if in t e treated corneas additional cross links are formed between colla en ®brils and t e proteo l cans t en it would be e pected t at t ese corneas would s ow a reater presence of proteo l cans t an in t e untreated corneas. espite ma or ad ances in t is ®eld, muc work is t erefore still needed to bot understand t e current met ods and to impro e t e treatment.

References

Abad, J. C. et al. (2008). "Corneal collagen cross-linking induced by UVA and riboflavin (CXL)". In: *Techniques in Ophthalmology* 6.1, pp. 8–12.

Abass, A. et al. (2017). "SAXS4COLL: an integrated software tool for analysing fibrous collagen-based tissues". In: *Journal of Applied Crystallography* 50.Pt 4, pp. 1235–1240.

Abraham, A. et al. (2013). *Clinical Ophthalmology Made Easy*. New Delhi, India: Jaypee Brothers, Medical Publishers.

Abramoff, M. D. et al. (2004). "Image processing with ImageJ". In: *Biophotonics international* 11.7, pp. 36–42.

Aixinjueluo, W. et al. (2017). "Accelerated transepithelial corneal cross-linking for progressive keratoconus: a prospective study of 12 months". In: *British Journal of Ophthalmology* 101.9, pp. 1244–1249.

Akcay, E. K. et al. (2017). "Tear Function and Ocular Surface Alterations After Accelerated Corneal Collagen Cross-Linking in Progressive Keratoconus". In: *Eye & Contact Lens-Science and Clinical Practice* 43.5, pp. 302–307.

Akhtar, S., A. J. Bron, et al. (2008). "Ultrastructural analysis of collagen fibrils and proteoglycans in keratoconus". In: *Acta Ophthalmologica* 86.7, pp. 764–772.

Akhtar, S., B. C. Kerr, et al. (2008). "Immunochemical localization of keratan sulfate proteoglycans in cornea, sclera, and limbus using a keratanase-generated neoepitope monoclonal antibody". In: *Investigative Ophthalmology & Visual Science* 49.6, pp. 2424–2431.

Al Suhaibani, A. H. et al. (2007). "Inverse relationship between age and severity and sequelae of acute corneal hydrops associated with keratoconus". In: *British Journal of Ophthalmology* 91.7, pp. 984–985.

Albert, D.M. et al. (2008). *Albert & Jakobiec's Principles and Practice of Ophthalmology*. Philadelphia, USA: Saunders Elsevier.

Aldahlawi, N. H., S. Hayes, D. P. O'Brart, A. Akhbanbetova, et al. (2016). "Enzymatic Resistance of Corneas Crosslinked Using Riboflavin in Conjunction With Low Energy, High Energy, and Pulsed UVA Irradiation Modes". In: *Investigative ophthalmology & visual science* 57.4, pp. 1547–1552.

Aldahlawi, N. H., S. Hayes, D. P. O'Brart, and K. M. Meek (2015). "Standard versus accelerated riboflavin-ultraviolet corneal collagen crosslinking: Resistance against enzymatic digestion." In: *Journal of Cataract & Refractive Surgery* 41.9, pp. 1989–1996.

— (2016). "An investigation into corneal enzymatic resistance following epithelium-off and epithelium-on corneal cross-linking protocols". In: *Experimental Eye Research* 153, pp. 141–151.

Alhamad, T. A. et al. (2012). "Evaluation of transepithelial stromal riboflavin absorption with enhanced riboflavin solution using spectrophotometry". In: *Journal of Cataract and Refractive Surgery* 38.5, pp. 884–889.

Alio, J. L. (2016). *Keratoconus: Recent Advances in Diagnosis and Treatment*. New York, USA: Springer International Publishing.

Alio, J. L. et al. (2014). "Intrastromal corneal ring segments: How successful is the surgical treatment of keratoconus?" In: *Middle East African Journal of Ophthalmology* 21.1, pp. 3–9.

Alnawaiseh M.and Rosentreter, A. et al. (2015). "Accelerated (18 mW/cm2) corneal collagen cross-linking for progressive keratoconus". In: *Cornea* 34.11, pp. 1427–1431.

Ambrósio Jr, R. et al. (2006). "Corneal-thickness spatial profile and corneal-volume distribution: Tomographic indices to detect keratoconus". In: *Journal of Cataract & Refractive Surgery* 32.11, pp. 1851–1859.

Andreassen, T. T., H. Oxlund, et al. (1988). "The Influence of Non-Enzymatic Glycosylation and Formation of Fluorescent Reaction Products on the Mechanical Properties of Rat Tail Tendons". In: *Connective Tissue Research* 17.1, pp. 1–9.

Andreassen, T. T., A. H. Simonsen, et al. (1980). "Biomechanical properties of keratoconus and normal corneas". In: *Experimental Eye Research* 31.4, pp. 435–441.

Arboleda, A. et al. (2014). "Evaluating In Vivo Delivery of Riboflavin With Coulomb-Controlled Iontophoresis for Corneal Collagen Cross-Linking: A Pilot Study". In: *Investigative Ophthalmology & Visual Science* 55.4, pp. 2731–2738.

Armstrong, B. K. et al. (2013). "Biological and biomechanical responses to traditional epithelium-off and transepithelial riboflavin-UVA CXL techniques in rabbits". In: *Journal of refractive surgery* 29.5, pp. 332–341.

Asgari, S. et al. (2013). "Corneal Refractive Power and Eccentricity in the 40-to 64-Year-Old Population of Shahroud, Iran". In: *Cornea* 32.1, pp. 25–29.

Ashalatha, P. R. et al. (2012). *Textbook of Anatomy and Physiology for Nurses*. New Delhi, India: Jaypee Brothers Medical Publishers.

Ashur, I. et al. (2009). "Photocatalytic generation of oxygen radicals by the water-soluble bacteriochlorophyll derivative WST1l, noncovalently bound to serum albumin". In: *Journal of Physical Chemistry A* 113.28, pp. 8027–8037.

Assiri, A. A. et al. (2005). "Incidence and severity of keratoconus in Asir province, Saudi Arabia". In: *British Journal of Ophthalmology* 89.11, pp. 1403–1406.

Balasubramanian, S. A. et al. (2013). "Effects of eye rubbing on the levels of protease, protease activity and cytokines in tears: relevance in keratoconus". In: *Clinical and Experimental Optometry* 96.2, pp. 214–218.

Bao, F. J. et al. (2018). "Changes in Corneal Biomechanical Properties With Different Corneal Cross-linking Irradiances". In: *Journal of Refractive Surgery* 34.1, pp. 51–58.

Barbara, A. et al. (2011). *Textbook on Keratoconus: New Insights*. New Delhi, India: Jaypee Brothers, Medical Publishers.

Bazzoni, G. et al. (2004). "Endothelial cell-to-cell junctions: Molecular organization and role in vascular homeostasis". In: *Physiological Reviews* 84.3, pp. 869–901.

Behndig, A. et al. (2001). "Superoxide dismutase isoenzymes in the normal and diseased human cornea". In: *Investigative Ophthalmology & Visual Science* 42.10, pp. 2293–2296.

Berlau, J. et al. (2002). "Depth and age-dependent distribution of keratocytes in healthy human corneas: a study using scanning-slit confocal microscopy in vivo1 1None of the authors has a financial or proprietary interest in any product mentioned.Robert C. Drews, MD, helped with the manuscript". In: *Journal of Cataract & Refractive Surgery* 28.4, pp. 611–616.

Beshtawi, I. M., R. Akhtar, et al. (2013). "Biomechanical Properties of Human Corneas Following Low- and High-Intensity Collagen Cross-Linking Determined With Scanning Acoustic Microscopy". In: *Investigative Ophthalmology & Visual Science* 54.8, pp. 5273–5280.

Beshtawi, I. M., C. O'Donnell, et al. (2013). "Biomechanical properties of corneal tissue after ultraviolet-A-riboflavin crosslinking". In: *Journal of Cataract and Refractive Surgery* 39.3, pp. 451–462.

Bettelheim, F. A. et al. (1975). "The hydration of proteoglycans of bovine cornea". In: *Biochimica Et Biophysica Acta* 381.1, pp. 203–214.

Bikbova, G. et al. (2014). "Transepithelial corneal collagen cross-linking by iontophoresis of riboflavin". In: *Acta Ophthalmologica* 92.1, E30–E34.

Birk, D. E., J. M. Fitch, J. P. Babiarz, K. J. Doane, et al. (1990). "Collagen fibrillogenesis in vitro: interaction of types I and V collagen regulates fibril diameter". In: *Journal of cell science* 95.4, pp. 649–657.

Birk, D. E., J. M. Fitch, J. P. Babiarz, and T. F. Linsenmayer (1988). "Collagen type-I and type-V are present in the same fibril in the avian corneal stroma". In: *Journal of Cell Biology* 106.3, pp. 999–1008.

Birk, D. E., J. M. Fitch, and T. F. Linsenmayer (1986). "Organization of collagen type-I and type-V in the embryonic chicken cornea". In: *Investigative Ophthalmology & Visual Science* 27.10, pp. 1470–1477.

Bisceglia, L. et al. (2005). "VSX1 mutational analysis in a series of Italian patients affected by keratoconus: Detection of a novel mutation". In: *Investigative Ophthalmology & Visual Science* 46.1, pp. 39–45.

Boote, C., S. Dennis, and K. M. Meek (2004). "Spatial mapping of collagen fibril organisation in primate cornea - an X-ray diffraction investigation". In: *Journal of Structural Biology* 146.3, pp. 359–367.

Boote, C., S. Dennis, R. H. Newton, et al. (2003). "Collagen fibrils appear more closely packed in the prepupillary cornea: Optical and biomechanical implications". In: *Investigative Ophthalmology and Visual Science* 44.7, pp. 2941–2948.

Boote, C., E. P. Dooley, et al. (2013). "Quantification of Collagen Ultrastructure after Penetrating Keratoplasty - Implications for Corneal Biomechanics". In: *Plos One* 8.7.

Boote, C., S. Hayes, et al. (2006). "Mapping collagen organization in the human cornea: Left and right eyes are structurally distinct". In: *Investigative Ophthalmology & Visual Science* 47.3, pp. 901–908.

Bouheraoua, N. et al. (2014). "Optical Coherence Tomography and Confocal Microscopy Following Three Different Protocols of Corneal Collagen Crosslinking in Keratoconus". In: *Investigative Ophthalmology & Visual Science* 55.11, pp. 7601–7609.

Bourne, W. M. et al. (1997). "Central corneal endothelial cell changes over a ten-year period". In: *Investigative Ophthalmology & Visual Science* 38.3, pp. 779–782.

Boxer Wachler, B. S. et al. (2010). "Safety and efficacy of transepithelial crosslinking (C3-R/CXL)". In: *Journal of Cataract and Refractive Surgery* 36.1, pp. 186–188.

Brandis, A. et al. (2005). "Novel water-soluble bacteriochlorophyll derivatives for vascular-targeted photodynamic therapy: Synthesis, solubility, phototoxicity and the effect of serum proteins". In: *Photochemistry and Photobiology* 81.4, pp. 983–993.

Brekelmans, J. et al. (2017). "Corneal Stiffening by a Bacteriochlorophyll Derivative With Dextran and Near-Infrared Light: Effect of Shortening Irradiation Time up to 1 Minute". In: *Cornea* 36.11, pp. 1395–1401.

Brittingham, S. et al. (2014). "Corneal Cross-Linking in Keratoconus Using the Standard and Rapid Treatment Protocol: Differences in Demarcation Line and 12-Month Outcomes". In: *Investigative Ophthalmology & Visual Science* 55.12, pp. 8371–8376.

Bron, A. J. (2001). "The architecture of the corneal stroma". In: *British Journal of Ophthalmology* 85.4, pp. 379–381.

Bueno, J. M. et al. (2011). "Analysis of Corneal Stroma Organization With Wavefront Optimized Nonlinear Microscopy". In: *Cornea* 30.6, pp. 692–701.

Bunsen, R. W. et al. (1862). "Photochemical Researches.–Part V. On the Measurement of the Chemical Action of Direct and Diffuse Sunlight". In: *Proceedings of the Royal Society of London* 12, pp. 306–312.

Burdon, K. P. et al. (2013). "Insights into keratoconus from a genetic perspective". In: *Clinical and Experimental Optometry* 96.2, pp. 146–154.

Bureau, J. et al. (1993). "Modification of prostaglandin E2 and collagen synthesis in keratoconus fibroblasts, associated with an increase of interleukin 1α receptor number". In: *Comptes Rendus de l'Academie des Sciences - Series III* 316.4, pp. 425–430.

Burns, D. M. et al. (2004). "Keratoconus: an analysis of corneal asymmetry". In: *The British Journal of Ophthalmology* 88.10, pp. 1252–1255.

Buzzonetti, L. and G. Petrocelli (2012). "Transepithelial Corneal Cross-linking in Pediatric Patients: Early Results". In: *Journal of Refractive Surgery* 28.11, pp. 763–767.

Buzzonetti, L., G. Petrocelli, et al. (2015). "Iontophoretic Transepithelial Corneal Cross-linking to Halt Keratoconus in Pediatric Cases: 15-Month Follow-up". In: *Cornea* 34.5, pp. 512–515.

Bykhovskaya, Y. et al. (2016). "Genetics in Keratoconus: where are we?" In: *Eye and Vision* 3.1, pp. 16–25.

Cantemir, A. et al. (2017). "Iontophoretic collagen cross-linking versus epithelium-off collagen cross-linking for early stage of progressive keratoconus-3years follow-up study". In: *Acta Ophthalmologica* 95.7, E649–E655.

Caporossi, A., S. Baiocchi, et al. (2006). "Parasurgical therapy for keratoconus by rib oflavin-ultraviolet type A rays induced cross-linking of corneal collagen - Preliminary refractive results in an Italian study". In: *Journal of Cataract and Refractive Surgery* 32.5, pp. 837–845.

Caporossi, A., C. Mazzotta, et al. (2010). "Long-term Results of Riboflavin Ultraviolet A Corneal Collagen Cross-linking for Keratoconus in Italy: The Siena Eye Cross Study". In: *American Journal of Ophthalmology* 149.4, pp. 585–593.

Cartwright, N. E. K. et al. (2012). "In Vitro Quantification of the Stiffening Effect of Corneal Cross-linking in the Human Cornea Using Radial Shearing Speckle Pattern Interferometry". In: *Journal of Refractive Surgery* 28.7, pp. 503–507.

Cassagne, M. et al. (2016). "Iontophoresis Transcorneal Delivery Technique for Transepithelial Corneal Collagen Crosslinking With Riboflavin in a Rabbit Model". In: *Investigative ophthalmology & visual science* 57.2, pp. 594–603.

Castoro, J. A. et al. (1988). "Water gradients across bovine cornea". In: *Investigative Ophthalmology & Visual Science* 29.6, pp. 963–968.

Chan, C. C. K. et al. (2007). "Effect of inferior-segment Intacs with and without C3-R on keratoconus". In: *Journal of Cataract and Refractive Surgery* 33.1, pp. 75–80.

Chang, C. et al. (2008). "Acute Wound Healing in the Human Central Corneal Epithelium Appears to Be Independent of Limbal Stem Cell Influence". In: *Investigative Ophthalmology & Visual Science* 49.12, pp. 5279–5286.

Chapman, J. A. et al. (1990). "The collagen fibril – a model system for studying the staining and fixation of a protein". In: *Electron Microscopy Reviews* 3.1, pp. 143–182.

Charulatha, V. et al. (1997). "Crosslinking density and resorption of dimethyl suberimidate treated collagen". In: *Journal of Biomedical Materials Research* 36.4, pp. 478–486.

Chen, X. et al. (2015). "Corneal collagen cross-linking (CXL) in thin corneas". In: *Eye and Vision* 2, pp. 15–21.

Cheng, X. et al. (2015). "A structural model for the in vivo human cornea including collagen-swelling interaction". In: *Journal of the Royal Society Interface* 12.109.

Cheung, I. M. Y. et al. (2013). "A new perspective on the pathobiology of keratoconus: interplay of stromal wound healing and reactive species-associated processes". In: *Clinical and Experimental Optometry* 96.2, pp. 188–196.

Cinar, Y. et al. (2014). "Accelerated corneal collagen cross-linking for progressive keratoconus". In: *Cutaneous and ocular toxicology* 33.2, pp. 168–71.

Cingu, A. K. et al. (2014). "Transient corneal endothelial changes following accelerated collagen cross-linking for the treatment of progressive keratoconus". In: *Cutaneous and ocular toxicology* 33.2, pp. 127–31.

Connon, C. J. et al. (2003). "Persistent haze and disorganization of anterior stromal collagen appear unrelated following phototherapeutic keratectomy". In: *Journal of Refractive Surgery* 19.3, pp. 323–332.

Croxatto, J. O. et al. (2010). "Sequential in vivo confocal microscopy study of corneal wound healing after cross-linking in patients with keratoconus". In: *Journal of Refractive Surgery* 26.9, pp. 638–645.

Cruzat, A. et al. (2017). "Ex Vivo Study of Transepithelial Corneal Cross-linking". In: *Journal of Refractive Surgery* 33.3, pp. 171–177.

Cummings, A. B. et al. (2016). "Optimizing Corneal Cross-Linking in the Treatment of Keratoconus: A Comparison of Outcomes After Standard- and High-Intensity Protocols." In: *Cornea* 35.6, pp. 814–822.

Davidson, A. E. et al. (2014). "The pathogenesis of keratoconus". In: *Eye* 28.2, pp. 189–195.

Dejana, E. et al. (1995). "Endothelial cell-to-cell junctions". In: *Faseb Journal* 9.10, pp. 910–918.

DelMonte, D. W. et al. (2011). "Anatomy and physiology of the cornea". In: *Journal of Cataract and Refractive Surgery* 37.3, pp. 588–598.

Dhaliwal, J. S. et al. (2009). "Corneal Collagen Cross-Linking: A Confocal, Electron, and Light Microscopy Study of Eye Bank Corneas". In: *Cornea* 28.1, pp. 62–67.

Dhawan, S. et al. (2011). "Complications of Corneal Collagen Cross-Linking". In: *Journal of Ophthalmology* 2011, p. 869015.

Dias, J. et al. (2013). "Anterior and posterior corneal stroma elasticity after corneal collagen crosslinking treatment". In: *Experimental eye research* 116, pp. 58–62.

Dijk, K. van et al. (2014). "Midstromal isolated bowman layer graft for reduction of advanced keratoconus: A technique to postpone penetrating or deep anterior lamellar keratoplasty". In: *JAMA Ophthalmology* 132.4, pp. 495–501.

Dohlman, C. H., A. R. Gasset, et al. (1968). "Effect of absence of corneal epithelium or endothelium on stromal keratocytes". In: *Investigative Ophthalmology* 7.5, pp. 520–534.

Dohlman, C. H., B. O. Hedbys, et al. (1962). "The Swelling Pressure of the Corneal Stroma". In: *Investigative Ophthalmology & Visual Science* 1.2, pp. 158–162.

Dong, Z. X. et al. (2011). "Collagen Cross-Linking With Riboflavin in a Femtosecond Laser-Created Pocket in Rabbit Corneas: 6-Month Results". In: *American Journal of Ophthalmology* 152.1, pp. 22–27.

Doors, M. et al. (2009). "Use of anterior segment optical coherence tomography to study corneal changes after collagen cross-linking". In: *American journal of ophthalmology* 148.6, 844–851.e2.

Doughty, M. J. (2016). "Corneal Surface and Superficial Cells as Viewed by Scanning Electron Microscopy and Impression Cytology Sampling". In: *Cornea* 35.2, pp. 243–248.

Dua, H. S., L. A. Faraj, M. J. Branch, et al. (2014). "The collagen matrix of the human trabecular meshwork is an extension of the novel pre-Descemet's layer (Dua's layer)". In: *British Journal of Ophthalmology* 98.5, pp. 691–697.

Dua, H. S., L. A. Faraj, D. G. Said, et al. (2013). "Human Corneal Anatomy Redefined A Novel Pre-Descemet's Layer (Dua's Layer)". In: *Ophthalmology* 120.9, pp. 1778–1785.

Dua, H. S., J. A. Gomes, et al. (1994). "Corneal epithelial wound healing". In: *The British Journal of Ophthalmology* 78.5, pp. 401–408.

Dua, H. S., L. Mastropasqua, et al. (2015). "Big bubble deep anterior lamellar keratoplasty: the collagen layer in the wall of the big bubble is unique". In: *Acta Ophthalmologica* 93.5, pp. 427–430.

Dua, H. S. and D. G. Said (2016). "Clinical evidence of the pre-Descemets layer (Dua's layer) in corneal pathology". In: *Eye* 30.8, pp. 1144–1145.

Dykstra, M. J. (2012). *Biological Electron Microscopy: Theory, Techniques, and Troubleshooting*. New York, USA: Springer US.

Eberwein, P. et al. (2008). "Corneal melting after cross-linking and deep lamellar keratoplasty in a keratokonus patient". In: *Klinische Monatsblatter Fur Augenheilkunde* 225.1, pp. 96–98.

Efron, N. et al. (2008). "New perspectives on keratoconus as revealed by corneal confocal microscopy". In: *Clinical and Experimental Optometry* 91.1, pp. 34–55.

Elbaz, U., C. Shen, et al. (2014). "Accelerated (9-mW/cm^2) Corneal Collagen Crosslinking for Keratoconus—A 1-Year Follow-up". In: *Cornea* 33.8, pp. 769–773.

Elbaz, U., S. N. Yeung, et al. (2014). "Collagen crosslinking after radial keratotomy". In: *Cornea* 33.2, pp. 131–136.

Elsheikh, A., D. Alhasso, et al. (2008). "Biomechanical properties of human and porcine corneas". In: *Experimental Eye Research* 86.5, pp. 783–790.

Elsheikh, A. and K. Anderson (2005). "Comparative study of corneal strip extensometry and inflation tests". In: *Journal of the Royal Society Interface* 2.3, pp. 177–185.

Ertan, A. et al. (2009). "Location of Steepest Corneal Area of Cone in Keratoconus Stratified by Age Using Pentacam". In: *Journal of Refractive Surgery* 25.11, pp. 1012–1016.

Evangelista, C. B. et al. (2017). "Corneal Collagen Cross-Linking Complications". In: *Seminars in ophthalmology*, pp. 29–35.

Evans, D. J. et al. (2013). "Why Does the Healthy Cornea Resist Pseudomonas aeruginosa Infection?" In: *American Journal of Ophthalmology* 155.6, 961–970.e2.

Fadlallah, A. et al. (2016). "Corneal Resistance to Keratolysis After Collagen Crosslinking With Rose Bengal and Green Light". In: *Investigative Ophthalmology & Visual Science* 57.15, pp. 6610–6614.

Fang, J. Y. et al. (1998). "Development and evaluation on transdermal delivery of enoxacin via chemical enhancers and physical iontophoresis". In: *Journal of Controlled Release* 54.3, pp. 293–304.

Feizi, S. et al. (2014). "Central and Peripheral Corneal Thickness Measurement in Normal and Keratoconic Eyes Using Three Corneal Pachymeters". In: *Journal of Ophthalmic & Vision Research* 9.3, pp. 296–304.

Filippello, M. et al. (2012). "Transepithelial corneal collagen crosslinking: Bilateral study". In: *Journal of Cataract & Refractive Surgery* 38.2, pp. 283–291.

Foschini, F. et al. (2016). "Cross-linking composition delivered by iontophoresis, useful for the treatment of keratoconus". Patentus US9439908 B2.

Franch, A. et al. (2015). "Evaluation of Intrastromal Riboflavin Concentration in Human Corneas after Three Corneal Cross-Linking Imbibition Procedures: A Pilot Study". In: *Journal of Ophthalmology*.

Fratzl, P. et al. (1993). "Structural transformation of collagen fibrils in corneal stroma during drying. An x-ray scattering study". In: *Biophysical Journal* 64.4, pp. 1210–1214.

Freund, D. E. et al. (1995). "Ultrastructure in anterior and posterior stroma of perfused human and rabbit corneas - relation to transparency". In: *Investigative Ophthalmology & Visual Science* 36.8, pp. 1508–1523.

Friedman, M. D. et al. (2017). "Systems and methods for corneal cross-linking with pulsed light". Patentus US9707126 B2.

Fuentes-Páez, G. et al. (2012). "Corneal cross-linking in patients with radial keratotomy: short-term follow-up". In: *Cornea* 31.3, pp. 232–235.

Fukuchi, T. et al. (1994). "Lysosomal enzyme activities in conjunctival tissues of patients with keratoconus". In: *Archives of Ophthalmology* 112.10, pp. 1368–1374.

Fullwood, N. J. and K. M. Meek (1993). "A Synchrotron X-ray Study of the Changes Occurring in the Corneal Stroma during Processing for Electron-Microscopy". In: *Journal of Microscopy-Oxford* 169, pp. 53–60.

— (1994). "An ultrastructural, time-resolved study of freezing in the corneal stroma". In: *Journal of Molecular Biology* 236.3, pp. 749–758.

Fullwood, N. J., S. J. Tuft, et al. (1992). "Synchrotron x-ray diffraction studies of keratoconus corneal stroma". In: *Investigative Ophthalmology & Visual Science* 33.5, pp. 1734–1741.

Galvis, V. et al. (2015). “Keratoconus: An inflammatory disorder?” In: *Eye (Basingstoke)* 29.7, pp. 843–859.

Gardner, S. J. et al. (2015). “Measuring the Refractive Index of Bovine Corneal Stromal Cells Using Quantitative Phase Imaging”. In: *Biophysical Journal* 109.8, pp. 1592–1599.

Garg, P. et al. (2017). “Collagen Cross-linking for Microbial Keratitis”. In: *Middle East African Journal of Ophthalmology* 24.1, pp. 18–23.

Georgiou, T. et al. (2004). “Influence of ethnic origin on the incidence of keratoconus and associated atopic disease in Asians and white patients”. In: *Eye* 18.4, pp. 379–383.

Gharaibeh, A. M. et al. (2012). “KeraRing Intrastromal Corneal Ring Segments for Correction of Keratoconus”. In: *Cornea* 31.2, pp. 115–120.

Ghosh, A. et al. (2013). “Proteomic and gene expression patterns of keratoconus”. In: *Indian Journal of Ophthalmology* 61.8, pp. 389–391.

Gipson, I. K. et al. (1987). “Anchoring fibrils form a complex network in human and rabbit cornea”. In: *Investigative Ophthalmology & Visual Science* 28.2, pp. 212–220.

Gkika, M. et al. (2011). “Corneal collagen cross-linking using riboflavin and ultraviolet-A irradiation: a review of clinical and experimental studies”. In: *International Ophthalmology* 31.4, pp. 309–319.

Godefrooij, D. A. et al. (2016). “Nationwide reduction in the number of corneal transplantations for keratoconus following the implementation of cross-linking”. In: *Acta Ophthalmologica* 94.7, pp. 675–678.

Gokhale, N. S. (2013). “Epidemiology of keratoconus”. In: *Indian Journal of Ophthalmology* 61.8, pp. 382–383.

Gondhowiardjo, T. D. et al. (1993). “Corneal aldehyde dehydrogenase, glutathione reductase, and glutathione S-transferase in pathologic corneas”. In: *Cornea* 12.4, pp. 310–314.

Gonzalez, V. et al. (1992). “Computer-assisted corneal topography in parents of patients with keratoconus”. In: *Archives of ophthalmology* 110.10, pp. 1413–4.

Goodson, Simon J. (2013). “An investigation into effects of in vitro glycation on type I collagen fibrillar structure and related biochemistry”. Thesis.

Gordon-Shaag, A. et al. (2015). “The genetic and environmental factors for keratoconus”. In: *BioMed research international* 2015, pp. 795738–795738.

Gore, D., A. Margineanu, et al. (2014). “Two-Photon Fluorescence Microscopy of Corneal Riboflavin Absorption”. In: *Investigative Ophthalmology & Visual Science* 55.4, pp. 2476–2481.

Gore, D., D. P. O’Brart, et al. (2015). “A Comparison of Different Corneal Iontophoresis Protocols for Promoting Transepithelial Riboflavin Penetration Comparison of Corneal Iontophoresis Protocols”. In: *Investigative ophthalmology & visual science* 56.13, pp. 7908–7914.

Gorskova, E. N. et al. (1998). “Epidemiology of keratoconus in the Urals”. In: *Vestnik oftalmologii* 114.4, pp. 38–40.

Greenstein, S. A., K. L. Fry, J. Bhatt, et al. (2010). “Natural history of corneal haze after collagen crosslinking for keratoconus and corneal ectasia: Scheimpflug and biomicroscopic analysis”. In: *Journal of Cataract & Refractive Surgery* 36.12, pp. 2105–2114.

Greenstein, S. A., K. L. Fry, M. J. Hersh, et al. (2012). "Higher-order aberrations after corneal collagen crosslinking for keratoconus and corneal ectasia". In: *Journal of Cataract and Refractive Surgery* 38.2, pp. 292–302.

Greenstein, S. A., K. L. Fry, and P. S. Hersh (2011). "Corneal Collagen Crosslinking Outcomes With and Without Stromal Swelling with Hypotonic Riboflavin". In: *ARVO Annual Meeting Abstract Search and Program Planner* 2011, pp. 5195–5195.

Greenstein, S. A., V. P. Shah, et al. (2011). "Corneal thickness changes after corneal collagen crosslinking for keratoconus and corneal ectasia: One-year results". In: *Journal of Cataract and Refractive Surgery* 37.4, pp. 691–700.

Grosvenor, T. (2007). *Primary Care Optometry*. Philadelphia, USA: Butterworth-Heinemann/Elsevier.

Grünauer-Kloevekorn, C. et al. (2006). "Keratoconus: Epidemiology, risk factors and diagnosis". In: *Klinische Monatsblatter fur Augenheilkunde* 223.6, pp. 493–502.

Hafezi, F. (2011). "Limitation of collagen cross-Linking with hypoosmolar riboflavin solution: Failure in an extremely thin cornea". In: *Cornea* 30.8, pp. 917–919.

Hafezi, F., A. J. Kanellopoulos, et al. (2007). "Corneal collagen crosslinking with riboflavin and ultraviolet A to treat induced keratectasia after laser in situ keratomileusis". In: *Journal of Cataract and Refractive Surgery* 33.12, pp. 2035–2040.

Hafezi, F., M. Mrochen, et al. (2009). "Collagen crosslinking with ultraviolet-A and hypoosmolar riboflavin solution in thin corneas". In: *Journal of Cataract & Refractive Surgery* 35.4, pp. 621–624.

Hamada, S. et al. (2017). "Corneal cross-linking in children". In: *Corneal Collagen Cross Linking*. New York, USA: Springer, pp. 229–268.

Hamblin, M. R. et al. (2013). *Handbook of Photomedicine*. Boca raton, florida, USA: Taylor & Francis.

Hammer, A. et al. (2014). "Corneal Biomechanical Properties at Different Corneal Cross-Linking (CXL) Irradiances". In: *Investigative ophthalmology & visual science* 55.5, pp. 2881–2884.

Harvitt, D. M. et al. (1998). "Oxygen consumption of the rabbit cornea." In: *Investigative Ophthalmology & Visual Science* 39.2, pp. 444–448.

Hashemi, H. et al. (2015). "Long-term Results of an Accelerated Corneal Crosslinking Protocol (18 mW/cm2) fortheTreatment of Progressive Keratoconus". In: *American Journal of Ophthalmology* 160.6, 1164–1170.e1.

Hassan, Z. et al. (2014). "Intraoperative and postoperative corneal thickness change after collagen crosslinking therapy". In: *European Journal of Ophthalmology* 24.2, pp. 179–185.

Hayat, M.A. (2000). *Principles and Techniques of Electron Microscopy: Biological Applications*. Cambridge, UK: Cambridge University Press.

Hayes, S., C. Boote, et al. (2011). "Riboflavin/UVA Collagen Cross-Linking-Induced Changes in Normal and Keratoconus Corneal Stroma". In: *Plos One* 6.8.

Hayes, S., C. S. Kamma-Lorger, et al. (2013). "The Effect of Riboflavin/ UVA Collagen Cross-linking Therapy on the Structure and Hydrodynamic Behaviour of the Ungulate and Rabbit Corneal Stroma". In: *Plos One* 8.1, e52860.

Hayes, S., S. R. Morgan, et al. (2015). "A study of stromal riboflavin absorption in ex vivo porcine corneas using new and existing delivery protocols for corneal cross-linking". In: *Acta Ophthalmologica* 94.2, E109–E117.

Hayes, S., D. P. O'Brart, et al. (2008). "Effect of complete epithelial debridement before riboflavin-ultraviolet-A corneal collagen crosslinking therapy". In: *Journal of Cataract and Refractive Surgery* 34.4, pp. 657–661.

Hayes, S., T. White, et al. (2017). "The structural response of the cornea to changes in stromal hydration". In: *Journal of the Royal Society Interface* 14.131, p. 20170062.

He, J. C. et al. (2010). "Scheimpflug image–processing method for accurate measurement of ocular surfaces". In: *Journal of Cataract & Refractive Surgery* 36.5, pp. 838–842.

Henriquez, M. A. et al. (2017). "Accelerated Epi-On Versus Standard Epi-Off Corneal Collagen Cross-Linking for Progressive Keratoconus in Pediatric Patients". In: *Cornea* 36.12, pp. 1503–1508.

Heon, E. et al. (2002). "VSX1: A gene for posterior polymorphous dystrophy and keratoconus". In: *Human Molecular Genetics* 11.9, pp. 1029–1036.

Hirata, H. et al. (2017). "Acute corneal epithelial debridement unmasks the corneal stromal nerve responses to ocular stimulation in rats: implications for abnormal sensations of the eye". In: *Journal of Neurophysiology* 117.5, pp. 1935–1947.

Ho, L. T. Y. et al. (2014). "A comparison of glycosaminoglycan distributions, keratan sulphate sulphation patterns and collagen fibril architecture from central to peripheral regions of the bovine cornea". In: *Matrix Biology* 38, pp. 59–68.

Hodge, A. J. (1963). "Recent studies with the electron microscope on ordered aggregates of the tropocollagen macromolecule". In: *Aspects of protein structure*, pp. 289–300.

Hoeltzel, D. A. et al. (1992). "Strip extensiometry for comparison of the mechanical response of bovine, rabbit, and human corneas". In: *Journal of Biomechanical Engineering-Transactions of the Asme* 114.2, pp. 202–215.

Holland, E. J. et al. (2013). *Ocular Surface Disease: Cornea, Conjunctiva and Tear Film*. Philadelphia, USA: Elsevier Health Sciences.

Huang, A. J. W. et al. (1989). "Paracellular permeability of corneal and conjunctival epithelia". In: *Investigative Ophthalmology and Visual Science* 30.4, pp. 684–689.

Huang, Y. F. and K. M. Meek (1999). "Swelling studies on the cornea and sclera: The effects of pH and ionic strength". In: *Biophysical Journal* 77.3, pp. 1655–1665.

Huang, Y. F., K. M. Meek, et al. (2001). "Anaylsis of birefringence during wound healing and remodeling following alkali burns in rabbit cornea". In: *Experimental Eye Research* 73.4, pp. 521–532.

Hynes, R. O. (2009). "Extracellular matrix: not just pretty fibrils". In: *Science (New York, N.Y.)* 326.5957, pp. 1216–1219.

Ihalainen, A. (1986). "Clinical and epidemiological features of keratoconus genetic and external factors in the pathogenesis of the disease". In: *Acta ophthalmologica. Supplement* 178, pp. 1–64.

Jester, J. V. (2008). "Corneal crystallins and the development of cellular transparency". In: *Seminars in Cell and Developmental Biology* 19.2, pp. 82–93.

Jester, J. V., Y. Ghee Lee, et al. (2001). "Measurement of corneal sublayer thickness and transparency in transgenic mice with altered corneal clarity using in vivo confocal microscopy". In: *Vision Research* 41.10–11, pp. 1283–1290.

Jester, J. V., T. Møller-Pedersen, et al. (1999). "The cellular basis of corneal transparency: evidence for 'corneal crystallins'". In: *Journal of Cell Science* 112.5, pp. 613–622.

Jester, J. V., C. J. Murphy, et al. (2013). "Lessons in Corneal Structure and Mechanics to Guide the Corneal Surgeon". In: *Ophthalmology* 120.9, pp. 1715–1717.
Jiang, L. Z. et al. (2017). "Conventional vs. pulsed-light accelerated corneal collagen cross-linking for the treatment of progressive keratoconus: 12-month results from a prospective study". In: *Experimental and Therapeutic Medicine* 14.5, pp. 4238–4244.
John, T. (2010). *Corneal Endothelial Transplant: (DSAEK, DMEK & DLEK)*. New Delhi, India: Jaypee Brothers, Medical Publishers.
Jonas, J. B. et al. (2009). "Prevalence and Associations of Keratoconus in Rural Maharashtra in Central India: The Central India Eye and Medical Study". In: *American Journal of Ophthalmology* 148.5, pp. 760–765.
Kamaev, P. et al. (2012). "Photochemical Kinetics of Corneal Cross-Linking with Riboflavin". In: *Investigative Ophthalmology & Visual Science* 53.4, pp. 2360–2367.
Kanellopoulos, A. J. (2009). "Collagen Cross-linking in Early Keratoconus With Riboflavin in a Femtosecond Laser-created Pocket: Initial Clinical Results". In: *Journal of Refractive Surgery* 25.11, pp. 1034–1038.
— (2012). "Long term results of a prospective randomized bilateral eye comparison trial of higher fluence, shorter duration ultraviolet A radiation, and riboflavin collagen cross linking for progressive keratoconus". In: *Clinical ophthalmology (Auckland, N.Z.)* 6, pp. 97–101.
Kanellopoulos, A. J. et al. (2016). "Cross-Linking Biomechanical Effect in Human Corneas by Same Energy, Different UV-A Fluence: An Enzymatic Digestion Comparative Evaluation". In: *Cornea* 35.4, pp. 557–561.
Kao, W. W. Y. et al. (2003). "Roles of lumican and keratocan on corneal transparency". In: *Glycoconjugate Journal* 19.4-5, pp. 275–285.
Karimian, F. et al. (2008). "Topographic evaluation of relatives of patients with keratoconus". In: *Cornea* 27.8, pp. 874–878.
Kaufman, H. E. et al. (1998). *The Cornea*. Oxford, UK: Butterworth-Heinemann Limited.
Kenney, C. M. et al. (2003). "The cascade hypothesis of keratoconus". In: *Contact lens & anterior eye : the journal of the British Contact Lens Association* 26.3, pp. 139–46.
Khodadoust, A. A. et al. (1968). "Adhesion of Regenerating Corneal Epithelium". In: *American Journal of Ophthalmology* 65.3, pp. 339–348.
Kim, W. J. et al. (1999). "Keratocyte apoptosis associated with keratoconus". In: *Experimental Eye Research* 69.5, pp. 475–481.
Kissner, A. et al. (2010). "Pharmacological Modification of the Epithelial Permeability by Benzalkonium Chloride in UVA/Riboflavin Corneal Collagen Cross-Linking". In: *Current Eye Research* 35.8, pp. 715–721.
Kling, S. and F. Hafezi (2017). "An Algorithm to Predict the Biomechanical Stiffening Effect in Corneal Cross-linking". In: *Journal of Refractive Surgery* 33.2, pp. 128–137.
Kling, S., L. Remon, et al. (2010). "Corneal Biomechanical Changes after Collagen Cross-Linking from Porcine Eye Inflation Experiments". In: *Investigative Ophthalmology & Visual Science* 51.8, pp. 3961–3968.
Klyce, S. D. et al. (1988). *Structure and function of the cornea*. The Cornea. New York, USA: Churchill Livingstone.

Kocak, I. et al. (2014). "Comparison of transepithelial corneal collagen crosslinking with epithelium-off crosslinking in progressive keratoconus". In: *Journal Francais D Ophtalmologie* 37.5, pp. 371–376.

Koch, M. et al. (2001). "alpha 1(XX) collagen, a new member of the collagen subfamily, fibril-associated collagens with interrupted triple helices". In: *Journal of Biological Chemistry* 276.25, pp. 23120–23126.

Kohlhaas, M., E. Spoerl, T. Schilde, et al. (2006). "Biomechanical evidence of the distribution of cross-links in corneas treated with riboflavin and ultraviolet A light". In: *Journal of Cataract and Refractive Surgery* 32.2, pp. 279–283.

Kohlhaas, M., E. Spoerl, A. Speck, et al. (2005). "A new treatment of keratectasia after LASIK with riboflavin/UVA light cross-linking". In: *Klinische Monatsblatter Fur Augenheilkunde* 222.5, pp. 430–436.

Koller, T. et al. (2009). "Complication and failure rates after corneal crosslinking". In: *Journal of Cataract & Refractive Surgery* 35.8, pp. 1358–1362.

Komai, Y. et al. (1991). "The three-dimensional organization of collagen fibrils in the human cornea and sclera". In: *Investigative Ophthalmology and Visual Science* 32.8, pp. 2244–2258.

Konstantopoulos, A. et al. (2015). "Conventional Versus Accelerated Collagen Cross-Linking for Keratoconus". In: *Eye & Contact Lens-Science and Clinical Practice* 41.2, pp. 65–71.

Koppen, C. et al. (2012). "Refractive and topographic results of benzalkonium chloride–assisted transepithelial crosslinking". In: *Journal of Cataract & Refractive Surgery* 38.6, pp. 1000–1005.

Krachmer, J. H., R. S. Feder, et al. (1984). "Keratoconus and related noninflammatory corneal thinning disorders". In: *Survey of Ophthalmology* 28.4, pp. 293–322.

Krachmer, J. H. et al. (2005). *Cornea*. Maryland Heights, Missouri, USA: Mosby/Elsevier.

— (2011). *Cornea*. Maryland Heights, Missouri, USA: Mosby/Elsevier.

Krueger, R. R., S. Herekar, et al. (2014). "First Proposed Efficacy Study of High Versus Standard Irradiance and Fractionated Riboflavin/ Ultraviolet A Cross-Linking With Equivalent Energy Exposure". In: *Eye & Contact Lens-Science and Clinical Practice* 40.6, pp. 353–357.

Krueger, R. R., J. C. Ramos-Esteban, et al. (2008). "Staged intrastromal delivery of riboflavin with UVA cross-linking in advanced bullous keratopathy: Laboratory investigation and first clinical case". In: *Journal of Refractive Surgery* 24.7, S730–S736.

Krumeich, J. H. et al. (2009). "Circular Keratotomy to Reduce Astigmatism and Improve Vision in Stage I and II Keratoconus". In: *Journal of Refractive Surgery* 25.4, pp. 357–365.

Ku, Judy Y. F. et al. (2008). "Laser scanning in vivo confocal analysis of keratocyte density in keratoconus". In: *Ophthalmology* 115.5, pp. 845–850.

Kymionis, G. D., M. A. Grentzelos, V. P. Kankariya, et al. (2014). "Safety of high-intensity corneal collagen crosslinking". In: *Journal of cataract and refractive surgery* 40.8, pp. 1337–1340.

Kymionis, G. D., M. A. Grentzelos, G. A. Kounis, et al. (2010). "Intraocular pressure measurements after corneal collagen crosslinking with riboflavin and ultraviolet A in eyes with keratoconus". In: *Journal of Cataract & Refractive Surgery* 36.10, pp. 1724–1727.

Kymionis, G. D., M. A. Grentzelos, A. D. Plaka, et al. (2013). "Evaluation of the Corneal Collagen Cross-Linking Demarcation Line Profile Using Anterior Segment Optical Coherence Tomography". In: *Cornea* 32.7, pp. 907–910.

Kymionis, G. D., G. A. Kontadakis, et al. (2017). "Accelerated versus conventional corneal crosslinking for refractive instability: an update". In: *Current Opinion in Ophthalmology* 28.4, pp. 343–347.

Kymionis, G. D., D. M. Portaliou, D. I. Bouzoukis, et al. (2007). "Herpetic keratitis with iritis after corneal crosslinking with riboflavin and ultraviolet A for keratoconus". In: *Journal of Cataract & Refractive Surgery* 33.11, pp. 1982–1984.

Kymionis, G. D., D. M. Portaliou, V. F. Diakonis, et al. (2012). "Corneal collagen cross-linking with riboflavin and ultraviolet-a irradiation in patients with thin corneas". In: *American Journal of Ophthalmology* 153.1, pp. 24–28.

Kymionis, G. D., K. I. Tsoulnaras, et al. (2014). "Evaluation of corneal stromal demarcation line depth following standard and a modified-accelerated collagen cross-linking protocol". In: *American Journal of Ophthalmology* 158.4, pp. 671–675.

Kymionis, G. D., K. Tsoulnaras, M. A. Grentzelos, et al. (2014). "Corneal stroma demarcation line after standard and high-intensity collagen crosslinking determined with anterior segment optical coherence tomography". In: *Journal of Cataract and Refractive Surgery* 40.5, pp. 736–740.

Kymionis, G. D., K. Tsoulnaras, D. Liakopoulos, et al. (2016). "Corneal Stromal Demarcation Line Depth Following Standard and a Modified High Intensity Corneal Cross-linking Protocol." In: *J Refract Surg* 32, pp. 218–222.

Land, M. F. (2014). *The Eye: A Very Short Introduction*. Oxford, UK: OUP Oxford.

Lanzini, M. et al. (2016). "Confocal microscopy evaluation of stromal fluorescence intensity after standard and accelerated iontophoresis-assisted corneal cross-linking". In: *International Ophthalmology*, pp. 1–9.

Leccisotti, A. et al. (2010). "Transepithelial Corneal Collagen Cross-linking in Keratoconus". In: *Journal of Refractive Surgery* 26.12, pp. 942–948.

Lema, I. et al. (2009). "Unilateral keratoconus: Videokeratography and Orbscan study - Optical correction". In: *Eye and Contact Lens* 35.1, pp. 15–19.

Lens, A. et al. (2008). *Ocular Anatomy and Physiology*. New Jersey, USA: SLACK.

Lewis, P. N., C. Pinali, et al. (2010). "Structural Interactions between Collagen and Proteoglycans Are Elucidated by Three-Dimensional Electron Tomography of Bovine Cornea". In: *Structure* 18.2, pp. 239–245.

Lewis, P. N., T. L. White, et al. (2016). "Three-dimensional arrangement of elastic fibers in the human corneal stroma()". In: *Experimental Eye Research* 146, pp. 43–53.

Li, H. F. et al. (1997). "Epithelial and corneal thickness measurements by in vivo confocal microscopy through focusing (CMTF)". In: *Current Eye Research* 16.3, pp. 214–221.

Li, J., H. Ma, et al. (2014). "Deep anterior lamellar keratoplasty using precut anterior lamellar cap for herpes simplex keratitis: a long-term follow-up study". In: *British Journal of Ophthalmology* 98.4, pp. 448–453.

Li, J., Y. Xiao, et al. (2017). "Identification for Differential Localization of Putative Corneal Epithelial Stem Cells in Mouse and Human". In: *Scientific Reports* 7.1, p. 5169.

Li, X. H. et al. (2004). "Longitudinal study of the normal eyes in unilateral keratoconus patients". In: *Ophthalmology* 111.3, pp. 440–446.
Lim, N. et al. (2002). "Characteristics and functional outcomes of 130 patients with keratoconus attending a specialist contact lens clinic". In: *Eye* 16.1, pp. 54–59.
Liskova, P. et al. (2010). "Evidence for Keratoconus Susceptibility Locus on Chromosome 14 A Genome-wide Linkage Screen Using Single-Nucleotide Polymorphism Markers". In: *Archives of Ophthalmology* 128.9, pp. 1191–1195.
Liu, K. et al. (2004). "Superoxide, hydrogen peroxide and hydroxyl radical in D1/D2/cytochrome b-559 Photosystem II reaction center complex". In: *Photosynthesis Research* 81.1, pp. 41–47.
Ljubimov, A. V. et al. (2015). "Progress in corneal wound healing". In: *Progress in retinal and eye research* 49, pp. 17–45.
Lombardo, M. et al. (2014). "Biomechanical changes in the human cornea after transepithelial corneal crosslinking using iontophoresis". In: *Journal of Cataract & Refractive Surgery* 40.10, pp. 1706–1715.
Määttä, M., R. Heljasvaara, et al. (2006). "Differential expression of collagen types XVIII/endostatin and XV in normal, keratoconus, and scarred human corneas". In: *Cornea* 25.3, pp. 341–349.
Määttä, M., T. Väisänen, et al. (2006). "Altered expression of type XIII collagen in keratoconus and scarred human cornea: Increased expression in scarred cornea is associated with myofibroblast transformation". In: *Cornea* 25.4, pp. 448–453.
Mackiewicz, Z. et al. (2006). "Collagenolytic proteinases in keratoconus". In: *Cornea* 25.5, pp. 603–610.
Macsai, M. S. et al. (1990). "Development of keratoconus after contact lens wear. Patient characteristics". In: *Archives of Ophthalmology* 108.4, pp. 534–538.
Magli, A. et al. (2013). "Epithelium-Off Corneal Collagen Cross-linking Versus Transepithelial Cross-linking for Pediatric Keratoconus". In: *Cornea* 32.5, pp. 597–601.
Maharana, P. K. et al. (2013). "Acute corneal hydrops in keratoconus". In: *Indian Journal of Ophthalmology* 61.8, pp. 461–464.
Makdoumi, K. et al. (2016). "Photodynamic UVA-riboflavin bacterial elimination in antibiotic-resistant bacteria". In: *Clinical and Experimental Ophthalmology* 44.7, pp. 582–586.
Males, J. J. et al. (2017). "Comparative study of long-term outcomes of accelerated and conventional collagen crosslinking for progressive keratoconus". In: *Eye* 32.1, pp. 32–38.
Manetti, M. et al. (2017). "A case of in vivo iontophoresis-assisted corneal collagen cross-linking for keratoconus: An immunohistochemical study". In: *Acta Histochemica* 119.3, pp. 343–347.
Marchini, M. et al. (1986). "Differences in the Fibril Structure of Corneal and Tendon Collagen. An Electron Microscopy and X-Ray Diffraction Investigation". In: *Connective Tissue Research* 15.4, pp. 269–281.
Marcovich, A. L. et al. (2012). "Stiffening of rabbit corneas by the bacteriochlorophyll derivative WST11 using near infrared light". In: *Investigative Ophthalmology and Visual Science* 53.10, pp. 6378–6388.
Mastropasqua, L., M. Lanzini, et al. (2014). "Structural Modifications and Tissue Response After Standard Epi-Off and Iontophoretic Corneal Crosslinking With

Different Irradiation Procedures". In: *Investigative Ophthalmology & Visual Science* 55.4, pp. 2526–2533.

Mastropasqua, L., M. Nubile, et al. (2014). "Corneal Cross-linking: Intrastromal Riboflavin Concentration in Iontophoresis-Assisted Imbibition Versus Traditional and Transepithelial Techniques". In: *American Journal of Ophthalmology* 157.3, 623–630.e1.

Mathew, J. H. et al. (2008). "Fine structure of the interface between the anterior limiting lamina and the anterior stromal fibrils of the human cornea". In: *Investigative ophthalmology & visual science* 49.9, pp. 3914–3918.

Mazor, O. et al. (2005). "WST11, A Novel Water-soluble Bacteriochlorophyll Derivative; Cellular Uptake, Pharmacokinetics, Biodistribution and Vascular-targeted Photodynamic Activity Using Melanoma Tumors as a Model". In: *Photochemistry and Photobiology* 81.2, pp. 342–351.

Mazzotta, C., S. Baiocchi, S. A. Bagaglia, et al. (2017). "Accelerated 15 mW pulsed-light crosslinking to treat progressive keratoconus: Two-year clinical results". In: *Journal of Cataract and Refractive Surgery* 43.8, pp. 1081–1088.

Mazzotta, C., S. Baiocchi, R. Denaro, et al. (2011). "Corneal collagen cross-linking to stop corneal ectasia exacerbated by radial keratotomy". In: *Cornea* 30.2, pp. 225–228.

Mazzotta, C., A. Balestrazzi, et al. (2007). "Treatment of progressive keratoconus by riboflavin-UVA-induced cross-linking of corneal collagen: Ultrastructural analysis by Heidelberg retinal tomograph II in vivo confocal microscopy in humans". In: *Cornea* 26.4, pp. 390–397.

Mazzotta, C., AL Paradiso, et al. (2013). "Qualitative Investigation of Corneal Changes after Accelerated Corneal Collagen Cross-linking (A-CXL) by In vivo Confocal Microscopy and Corneal OCT". In: *Journal of Clinical & Experimental Ophthalmology* 4.6.

Mazzotta, C., C. Traversi, S. Baiocchi, et al. (2008). "Corneal healing after riboflavin ultraviolet-A collagen cross-linking determined by confocal laser scanning microscopy in vivo: Early and late modifications". In: *American Journal of Ophthalmology* 146.4, pp. 527–533.

Mazzotta, C., C. Traversi, S. Caragiuli, et al. (2014). "Pulsed vs continuous light accelerated corneal collagen crosslinking: in vivo qualitative investigation by confocal microscopy and corneal OCT". In: *Eye* 28.10, pp. 1179–1183.

Mazzotta, C., C. Traversi, A. L. Paradiso, et al. (2014). "Pulsed Light Accelerated Crosslinking versus Continuous Light Accelerated Crosslinking: One-Year Results". In: *Journal of Ophthalmology* 2014, pp. 6–12.

McCall, A. S. et al. (2010). "Mechanisms of Corneal Tissue Cross-linking in Response to Treatment with Topical Riboflavin and Long-Wavelength Ultraviolet Radiation (UVA)". In: *Investigative Ophthalmology & Visual Science* 51.1, pp. 129–138.

McLaughlin, C. R. et al. (2008). "Regeneration of corneal cells and nerves in an implanted collagen corneal substitute". In: *Cornea* 27.5, pp. 580–589.

McMahon, T. T. et al. (2006). "Longitudinal changes in corneal curvature in keratoconus". In: *Cornea* 25.3, pp. 296–305.

McMonnies, C. W. (2014). "Corneal endothelial assessment with special references to keratoconus". In: *Optometry and vision science : official publication of the American Academy of Optometry* 91.6, e124–134.

McMonnies, C. W. (2015). “Inflammation and Keratoconus”. In: *Optometry and Vision Science* 92.2, E35–E41.

Meek, K. M. and C. Boote (2009). “The use of X-ray scattering techniques to quantify the orientation and distribution of collagen in the corneal stroma”. In: *Progress in Retinal and Eye Research* 28.5, pp. 369–392.

Meek, K. M., J. A. Chapman, et al. (1979). “The staining pattern of collagen fibrils. Improved correlation with sequence data”. In: *Journal of Biological Chemistry* 254.21, pp. 10710–10714.

Meek, K. M., N. J. Fullwood, et al. (1991). “Synchrotron X-ray-Diffraction Studies of the Cornea, with Implications for Stromal Hydration”. In: *Biophysical Journal* 60.2, pp. 467–474.

Meek, K. M. and D. F. Holmes (1983). “Interpretation of the electron microscopical appearance of collagen fibrils from corneal stroma”. In: *International Journal of Biological Macromolecules* 5.1, pp. 17–25.

Meek, K. M. and C. Knupp (2015). “Corneal structure and transparency”. In: *Progress in Retinal and Eye Research* 49.Supplement C, pp. 1–16.

Meek, K. M. and D. W. Leonard (1993). “Ultrastructure of the corneal stroma: a comparative study”. In: *Biophysical journal* 64.1, pp. 273–280.

Meek, K. M. and A. J. Quantock (2001). “The Use of X-ray Scattering Techniques to Determine Corneal Ultrastructure”. In: *Progress in Retinal and Eye Research* 20.1, pp. 95–137.

Meek, K. M., S. J. Tuft, et al. (2005). “Changes in collagen orientation and distribution in keratoconus corneas”. In: *Investigative Ophthalmology & Visual Science* 46.6, pp. 1948–1956.

Mencucci, R., M. Marini, et al. (2010). “Effects of riboflavin/UVA corneal cross-linking on keratocytes and collagen fibres in human cornea”. In: *Clinical and Experimental Ophthalmology* 38.1, pp. 49–56.

Mencucci, R., C. Mazzotta, et al. (2015). “In Vivo Thermographic Analysis of the Corneal Surface in Keratoconic Patients Undergoing Riboflavin-UV-A Accelerated Cross-Linking”. In: *Cornea* 34.3, pp. 323–327.

Michelacci, Y. M. (2003). “Collagens and proteoglycans of the corneal extracellular matrix”. In: *Brazilian Journal of Medical and Biological Research* 36.8, pp. 1037–1046.

Mita, M. et al. (2014). “High-irradiance accelerated collagen crosslinking for the treatment of keratoconus: Six-month results”. In: *Journal of cataract and refractive surgery* 40.6, pp. 1032–1040.

Moramarco, A. et al. (2015). “Corneal stromal demarcation line afteraccelerated crosslinking using continuous and pulsed light”. In: *Journal of Cataract & Refractive Surgery* 41.11, pp. 2546–2551.

Motooka, D. et al. (2012). “The triple helical structure and stability of collagen model peptide with 4(s)-hydroxyprolyl-pro-gly units”. In: *Biopolymers* 98.2, pp. 111–121.

Nakamura, K. (2003). “Interaction between injured corneal epithelial cells and stromal cells”. In: *Cornea* 22.7, S35–S47.

Nawaz, S. et al. (2015). “Trans-epithelial versus conventional corneal collagen crosslinking: A randomized trial in keratoconus”. In: *Oman journal of ophthalmology* 8.1, pp. 9–13.

Ng, A. L. K. et al. (2016). "Conventional versus accelerated corneal collagen cross-linking in the treatment of keratoconus". In: *Clinical and Experimental Ophthalmology* 44.1, pp. 8–14.

Nielsen, K. et al. (2007). "Incidence and prevalence of keratoconus in Denmark". In: *Acta Ophthalmologica Scandinavica* 85.8, pp. 890–892.

Nottingham, J. (1854). *Practical observations on conical cornea: and on the short sight, and other defects of vision connected with it*. London, UK: John Churchill.

O'Brart, D. P. (2014). "Corneal collagen cross-linking: A review". In: *Journal of optometry* 7.3, pp. 113–24.

O'Brart, D. P. et al. (2011). "A randomised, prospective study to investigate the efficacy of riboflavin/ultraviolet A (370 nm) corneal collagen cross-linkage to halt the progression of keratoconus". In: *British Journal of Ophthalmology* 95.11, pp. 1519–1524.

O'Brart, N. L. et al. (2018). "An Investigation of the Effects of Riboflavin Concentration on the Efficacy of Corneal Cross-Linking Using an Enzymatic Resistance Model in Porcine Corneas". In: *Investigative ophthalmology & visual science* 59.2, pp. 1058–1065.

Orgel, J. P. et al. (2000). "The in situ conformation and axial location of the intermolecular cross-linked non-helical telopeptides of type I collagen". In: *Structure with Folding & Design* 8.2, pp. 137–142.

Ortiz, S. et al. (2012). "In vivo human crystalline lens topography". In: *Biomedical Optics Express* 3.10, pp. 2471–2488.

Owens, H. et al. (2003). "A profile of keratoconus in New Zealand". In: *Cornea* 22.2, pp. 122–125.

Özertürk, Y. et al. (2012). "Comparison of deep anterior lamellar keratoplasty and intrastromal corneal ring segment implantation in advanced keratoconus". In: *Journal of Cataract & Refractive Surgery* 38.2, pp. 324–332.

Park, Y. M. et al. (2017). "Comparison of 2 Different Methods of Transepithelial Corneal Collagen Cross-Linking: Analysis of Corneal Histology and Hysteresis". In: *Cornea* 36.7, pp. 860–865.

Pearson, A. R. et al. (2000). "Does ethnic origin influence the incidence or severity of keratoconus?" In: *Eye* 14.4, pp. 625–628.

Perez-Santonja, J. J. et al. (2009). "Microbial keratitis after corneal collagen crosslinking". In: *Journal of Cataract and Refractive Surgery* 35.6, pp. 1138–1140.

Perry, H. D. et al. (1980). "Round and oval cones in keratoconus". In: *Ophthalmology* 87.9, pp. 905–909.

Peyman, A. et al. (2016). "Stromal Demarcation Line in Pulsed Versus Continuous Light Accelerated Corneal Crosslinking for Keratoconus". In: *Journal of Refractive Surgery* 32.3, pp. 206–208.

Polack, F. M. (1976). "Contributions of electron microscopy to the study of corneal pathology". In: *Survey of Ophthalmology* 20.6, pp. 375–414.

Pollhammer, M. et al. (2009). "Bacterial keratitis early after corneal crosslinking with riboflavin and ultraviolet-A". In: *Journal of Cataract & Refractive Surgery* 35.3, pp. 588–589.

Popescu, I. D. et al. (2014). "Potential serum biomarkers for glioblastoma diagnostic assessed by proteomic approaches". In: *Proteome Science* 12.1.

Potapenko, A. Y. et al. (1991). "Photohemolysis sensitized by psoralen: reciprocity law is not fulfilled". In: *Photochemistry and Photobiology* 54.3, pp. 375–379.

Pron, G. et al. (2011). "Collagen Cross-Linking Using Riboflavin and Ultraviolet-A for Corneal Thinning Disorders: An Evidence-Based Analysis". In: *Ontario Health Technology Assessment Series* 11.5, pp. 1–89.

Quantock, A. J. et al. (2007). "Small-angle fibre diffraction studies of corneal matrix structure: a depth-profiled investigation of the human eye-bank cornea". In: *Journal of Applied Crystallography* 40, S335–S340.

Rabinowitz, Y. S. (1998). "Keratoconus". In: *Survey of Ophthalmology* 42.4, pp. 297–319.

Rabinowitz, Y. S. et al. (1992). "Molecular genetic-analysis in autosomal dominant keratoconus". In: *Cornea* 11.4, pp. 302–308.

Radner, W. et al. (1998). "Interlacing and cross-angle distribution of collagen lamellae in the human cornea". In: *Cornea* 17.5, pp. 537–543.

Rahman, W. et al. (2006). "An unusual case of keratoconus". In: *Journal of Pediatric Ophthalmology & Strabismus* 43.6, pp. 373–375.

Raiskup, F., Anne Hoyer, et al. (2009). "Permanent Corneal Haze After Riboflavin-UVA-induced Cross-linking in Keratoconus". In: *Journal of Refractive Surgery* 25.9, S824–S828.

Raiskup, F., R. Pinelli, et al. (2012). "Riboflavin Osmolar Modification for Transepithelial Corneal Cross-Linking". In: *Current Eye Research* 37.3, pp. 234–238.

Raiskup, F. and E. Spoerl (2011). "Corneal cross-linking with hypo-osmolar riboflavin solution in thin keratoconic corneas". In: *American Journal of Ophthalmology* 152.1, pp. 28–32.

— (2013). "Corneal Crosslinking with Riboflavin and Ultraviolet A. I. Principles". In: *The Ocular Surface* 11.2, pp. 65–74.

Raiskup-Wolf, F. et al. (2008). "Collagen crosslinking with riboflavin and ultraviolet-A light in keratoconus: Long-term results". In: *Journal of Cataract and Refractive Surgery* 34.5, pp. 796–801.

Ramselaar, J. A. M. et al. (1988). "Corneal epithelial permeability after instillation of ophthalmic solutions containing local anaesthetics and preservatives". In: *Current Eye Research* 7.9, pp. 947–950.

Randleman, J. B. et al. (2017). "Biomechanical Changes After LASIK Flap Creation Combined With Rapid Cross-Linking Measured With Brillouin Microscopy". In: *Journal of Refractive Surgery* 33.6, pp. 408–414.

Rao, S. K. (2013). "Collagen cross linking: Current perspectives". In: *Indian Journal of Ophthalmology* 61.8, pp. 420–421.

Rapuano, C. J. (2012). *Wills Eye Institute - Cornea*. Philadelphia, USA: Wolters Kluwer Health.

Razmjoo, H. et al. (2014). "Corneal haze and visual outcome after collagen crosslinking for keratoconus: A comparison between total epithelium off and partial epithelial removal methods". In: *Advanced biomedical research* 3, pp. 221–221.

Rechichi, M. et al. (2013). "Epithelial-disruption collagen crosslinking for keratoconus: One-year results". In: *Journal of Cataract and Refractive Surgery* 39.8, pp. 1171–1178.

Rehnman, J. B. et al. (2011). "Spatial distribution of corneal light scattering after corneal collagen crosslinking". In: *Journal of Cataract and Refractive Surgery* 37.11, pp. 1939–1944.

Reinhard, T. et al. (2010). *Cornea and External Eye Disease: Corneal Allotransplantation, Allergic Disease and Trachoma*. New York, USA: Springer.

Remington, L. A. (2011). *Clinical Anatomy and Physiology of the Visual System*. St. Louis, Missouri, USA: Elsevier/Butterworth-Heinemann.

Richoz, O., A. Hammer, et al. (2013). "The Biomechanical Effect of Corneal Collagen Cross-Linking (CXL) With Riboflavin and UV-A is Oxygen Dependent". In: *Translational Vision Science & Technology* 2.7, pp. 6–10.

Richoz, O., S. Kling, et al. (2014). "Antibacterial Efficacy of Accelerated Photoactivated Chromophore for Keratitis-Corneal Collagen Cross-linking (PACK-CXL)". In: *Journal of Refractive Surgery* 30.12, pp. 850–854.

Richoz, O., N. Mavrakanas, et al. (2013). "Corneal Collagen Cross-Linking for Ectasia after LASIK and Photorefractive Keratectomy Long-Term Results". In: *Ophthalmology* 120.7, pp. 1354–1359.

Rocha, K. M. et al. (2008). "Comparative study of riboflavin-UVA cross-linking and "Flash-Linking" using surface wave elastometry". In: *Journal of Refractive Surgery* 24.7, S748–S751.

Romero-Jimenez, M. et al. (2010). "Keratoconus: A review". In: *Contact Lens & Anterior Eye* 33.4, pp. 157–166.

Romppainen, T. et al. (2007). "Effect of Riboflavin-UVA–Induced Collagen Cross-linking on Intraocular Pressure Measurement". In: *Investigative Ophthalmology & Visual Science* 48.12, pp. 5494–5498.

Rosenfield, M. et al. (2009). *Optometry: Science, Techniques and Clinical Management*. Second. St. Louis, Missouri, USA: Elsevier/Butterworth-Heinemann.

Rossi, S. et al. (2015). "Standard versus trans-epithelial collagen cross-linking in keratoconus patients suitable for standard collagen cross-linking". In: *Clinical Ophthalmology* 9, pp. 503–509.

Ruberti, J. W. et al. (2011). "Corneal Biomechanics and Biomaterials". In: *Annual Review of Biomedical Engineering* 13.1, pp. 269–295.

Saee-Rad, S. et al. (2011). "Mutation analysis of VSX1 and SOD1 in Iranian patients with keratoconus". In: *Molecular Vision* 17.336-37, pp. 3128–3136.

Samaras, K. et al. (2009). "Effect of Epithelial Retention and Removal on Riboflavin Absorption in Porcine Corneas". In: *Journal of Refractive Surgery* 25.9, pp. 771–775.

Sanchez, I. et al. (2011). "The parameters of the porcine eyeball". In: *Graefes Archive for Clinical and Experimental Ophthalmology* 249.4, pp. 475–482.

Sandberg-Lall, M. et al. (2000). "Type XIII collagen is widely expressed in the adult and developing human eye and accentuated in the ciliary muscle, the optic nerve and the neural retina". In: *Experimental Eye Research* 70.4, pp. 401–410.

Sandner, D. et al. (2004). "Collagen crosslinking by combined Riboflavin/Ultraviolet-A (UVA) - Treatment can stop the progression of keratoconus". In: *Investigative Ophthalmology & Visual Science* 45.13, pp. 2887–2887.

Sarezky, D. et al. (2017). "Trends in Corneal Transplantation in Keratoconus". In: *Cornea* 36.2, pp. 131–137.

Savini, G., P. Barboni, et al. (2013). "Comparison of methods to measure corneal power for intraocular lens power calculation using a rotating Scheimpflug camera". In: *Journal of Cataract & Refractive Surgery* 39.4, pp. 598–604.

Savini, G., K. J. Hoffer, et al. (2013). "Influence of axial length and corneal power on the astigmatic power of toric intraocular lenses". In: *Journal of Cataract & Refractive Surgery* 39.12, pp. 1900–1903.

Sawaguchi, S., S. S. Twining, et al. (1990). "Alpha-1 proteinase-inhibitor levels in keratoconus". In: *Experimental Eye Research* 50.5, pp. 549–554.
Sawaguchi, S., Byjt Yue, et al. (1994). "Lysosomal-enzyme and inhibitor levels in the human trabecular meshwork". In: *Investigative Ophthalmology & Visual Science* 35.1, pp. 251–261.
Saxena, S. (2011). *Clinical Ophthalmology*. Second. New Delhi, India: Jaypee Brothers, Medical Publishers.
Scarcelli, G. et al. (2013). "Brillouin Microscopy of Collagen Crosslinking: Noncontact Depth-Dependent Analysis of Corneal Elastic Modulus". In: *Investigative Ophthalmology & Visual Science* 54.2, pp. 1418–1425.
Schegg, B. et al. (2009). "Core Glycosylation of Collagen Is Initiated by Two β (1-O)Galactosyltransferases". In: *Molecular and Cellular Biology* 29.4, pp. 943–952.
Schlatter, B. et al. (2015). "Evaluation of scleral and corneal thickness in keratoconus patients". In: *Journal of Cataract and Refractive Surgery* 41.5, pp. 1073–1080.
Schnitzler, E. et al. (2000). "Crosslinking of the corneal collagen by UV-radiation with Riboflavin for the mode of treatment melting ulcera of the cornea, first results of four patients". In: *Klinische Monatsblatter Fur Augenheilkunde* 217.3, pp. 190–193.
Schumacher, S., M. Mrochen, et al. (2012). "Optimization Model for UV-Riboflavin Corneal Cross-linking". In: *Investigative Ophthalmology & Visual Science* 53.2, pp. 762–769.
Schumacher, S., L. Oeftiger, et al. (2011). "Equivalence of Biomechanical Changes Induced by Rapid and Standard Corneal Cross-linking, Using Riboflavin and Ultraviolet Radiation". In: *Investigative Ophthalmology & Visual Science* 52.12, pp. 9048–9052.
Seal, D. V. et al. (2007). *Ocular Infection: Investigation and Treatment in Practice*. Boca raton, florida, USA: Taylor & Francis.
Seiler, T. G. et al. (2014). "Intrastromal Application of Riboflavin for Corneal Crosslinking". In: *Investigative Ophthalmology & Visual Science* 55.7, pp. 4261–4265.
Seiler, T. et al. (2006). "Corneal cross-linking-induced stromal demarcation line". In: *Cornea* 25.9, pp. 1057–1059.
Sharma, N. et al. (2010). "Pseudomonas keratitis after collagen crosslinking for keratoconus: Case report and review of literature". In: *Journal of Cataract and Refractive Surgery* 36.3, pp. 517–520.
Sherif, A. M. (2014). "Accelerated versus conventional corneal collagen cross-linking in the treatment of mild keratoconus: A comparative study". In: *Clinical Ophthalmology* 8, pp. 1435–1440.
Sherif, A. M. et al. (2016). "Intraoperative Corneal Thickness Changes during Pulsed Accelerated Corneal Cross-Linking Using Isotonic Riboflavin with HPMC". In: *Journal of ophthalmology* 2016, pp. 1471807–1471807.
Sherwin, T. and N. H. Brookes (2004). "Morphological changes in keratoconus: pathology or pathogenesis". In: *Clinical and Experimental Ophthalmology* 32.2, pp. 211–217.
Sherwin, T., N. H. Brookes, et al. (2002). "Cellular incursion into Bowman's membrane in the peripheral cone of the keratoconic cornea". In: *Experimental Eye Research* 74.4, pp. 473–482.

Shetty, R. et al. (2015). "Current Protocols of Corneal Collagen Cross-Linking: Visual, Refractive, and Tomographic Outcomes". In: *American Journal of Ophthalmology* 160.2, pp. 243–249.

Shneor, E. et al. (2013). "Characteristics of 244 patients with keratoconus seen in an optometric contact lens practice". In: *Clinical and Experimental Optometry* 96.2, pp. 219–224.

Sideroudi, H. et al. (2013). "Repeatability, reliability and reproducibility of posterior curvature and wavefront aberrations in keratoconic and cross-linked corneas". In: *Clinical and Experimental Optometry* 96.6, pp. 547–556.

Singh, M. et al. (2017). "Quantifying the effects of UV-A/riboflavin crosslinking on the elastic anisotropy and hysteresis of the porcine cornea by noncontact optical coherence elastography". In: *Optical Elastography and Tissue Biomechanics Iv*. Ed. by K. V. Larin et al. Vol. 10067. Proceedings of SPIE, p. 100670D.

Smolin, G., C.S. Foster, et al. (2005). *Smolin and Thoft's The Cornea: Scientific Foundations and Clinical Practice*. Philadelphia, USA: Lippincott Williams & Wilkins.

Smolin, G. and R.A. Thoft (1994). *The Cornea: scientific foundations and clinical practice*. Third. New York, USA: Little, Brown.

Snellman, A. et al. (2000). "A short sequence in the N-terminal region is required for the trimerization of type XIII collagen and is conserved in other collagenous transmembrane proteins". In: *Embo Journal* 19.19, pp. 5051–5059.

Soeters, N. et al. (2015). "Transepithelial Versus Epithelium-off Corneal Crosslinking for the Treatment of Progressive Keratoconus: A Randomized Controlled Trial". In: *American Journal of Ophthalmology* 159.5, 821–828.e3.

Spadea, L. et al. (2016). "Corneal stromal demarcation line after collagen crosslinking in corneal ectatic diseases: a review of the literature". In: *Clinical Ophthalmology (Auckland, N.Z.)* 10, pp. 1803–1810.

Spoerl, E., M. Huhle, et al. (1998). "Induction of Cross-links in Corneal Tissue". In: *Experimental Eye Research* 66.1, pp. 97–103.

Spoerl, E., M. Mroehen, et al. (2007). "Safety of UVA-riboflavin cross-linking of the cornea". In: *Cornea* 26.4, pp. 385–389.

Spoerl, E., G. Wollensak, et al. (2004). "Increased resistance of crosslinked cornea against enzymatic digestion". In: *Current Eye Research* 29.1, pp. 35–40.

Stabuc-Silih, M. et al. (2010). "Genetics and clinical characteristics of keratoconus". In: *Acta dermatovenerologica Alpina, Pannonica, et Adriatica* 19.2, pp. 3–10.

Stojanovic, A. et al. (2012). "Safety and Efficacy of Epithelium-On Corneal Collagen Cross-Linking Using a Multifactorial Approach to Achieve Proper Stromal Riboflavin Saturation". In: *Journal of Ophthalmology* 2012.

Studer, H. et al. (2010). "Biomechanical model of human cornea based on stromal microstructure". In: *Journal of Biomechanics* 43.5, pp. 836–842.

Sturbaum, C. W. et al. (1993). "Pathology of corneal endothelium in keratoconus". In: *Ophthalmologica* 206.4, pp. 192–208.

Sugar, J. et al. (2012). "What causes keratoconus?" In: *Cornea* 31.6, pp. 716–719.

Sundaram, V. et al. (2009). *Training in Ophthalmology*. Oxford, UK: OUP Oxford.

Szczotka, L. B. et al. (2001). "A summary of the findings from the Collaborative Longitudinal Evaluation of Keratoconus (CLEK) Study". In: *Optometry* 72.9, pp. 574–587.

Tabibian, D., O. Richoz, and F. Hafezi (2015). "PACK-CXL: Corneal cross-linking for treatment of infectious keratitis". In: *Journal of Ophthalmic and Vision Research* 10.1, pp. 77–80.

Tabibian, D., O. Richoz, Arnaud Riat, et al. (2014). "Accelerated Photoactivated Chromophore for Keratitis-Corneal Collagen Cross-linking as a First-line and Sole Treatment in Early Fungal Keratitis". In: *Journal of Refractive Surgery* 30.12, pp. 855–857.

Takahashi, A. et al. (1990). "[Quantitative analysis of collagen fiber in keratoconus]". In: *Nippon Ganka Gakkai zasshi* 94.11, pp. 1068–1073.

Tan, H. Y. et al. (2006). "Multiphoton fluorescence and second harmonic generation imaging of the structural alterations in keratoconus ex vivo". In: *Investigative Ophthalmology & Visual Science* 47.12, pp. 5251–5259.

Tanwar, M. et al. (2010). "VSX1 gene analysis in keratoconus". In: *Molecular Vision* 16.257, pp. 2395–2401.

Tomita, M. et al. (2014). "Accelerated versus conventional corneal collagen crosslinking". In: *Journal of cataract and refractive surgery* 40.6, pp. 1013–1020.

Torricelli, A. A. M., V. Singh, V. Agrawal, et al. (2013). "Transmission Electron Microscopy Analysis of Epithelial Basement Membrane Repair in Rabbit Corneas With Haze". In: *Investigative Ophthalmology & Visual Science* 54.6, pp. 4026–4033.

Torricelli, A. A. M., V. Singh, M. R. Santhiago, et al. (2013). "The Corneal Epithelial Basement Membrane: Structure, Function, and Disease". In: *Investigative Ophthalmology & Visual Science* 54.9, pp. 6390–6400.

Touboul, D., N. Efron, et al. (2012). "Corneal Confocal Microscopy Following Conventional, Transepithelial, and Accelerated Corneal Collagen Cross-linking Procedures for Keratoconus". In: *Journal of Refractive Surgery* 28.11, pp. 769–775.

Touboul, D., J. Gennisson, et al. (2014). "Supersonic Shear Wave Elastography for the In Vivo Evaluation of Transepithelial Corneal Collagen Cross-Linking". In: *Investigative Ophthalmology & Visual Science* 55.3, pp. 1976–1984.

Tzaphlidou, M. et al. (1982). "A study of positive staining for electron-microscopy using collagen as a model system .2. Staining by uranyl ions". In: *Micron* 13.2, pp. 133–145.

Ucakhan, O. O. et al. (2006). "In vivo confocal microscopy findings in keratoconus". In: *Eye & contact lens* 32.4, pp. 183–91.

Uematsu, M. et al. (2007). "Acute corneal epithelial change after instillation of benzalkonium chloride evaluated using a newly developed in vivo corneal transepithelial electric resistance measurement method". In: *Ophthalmic Research* 39.6, pp. 308–314.

Vega-Estrada, A. et al. (2016). "The use of intracorneal ring segments in keratoconus". In: *Eye and Vision* 3.1, pp. 8–14.

Vinciguerra, P., E. Albè, A. M. Mahmoud, et al. (2010). "Intra- and postoperative variation in ocular response analyzer parameters in keratoconic eyes after corneal cross-linking". In: *Journal of Refractive Surgery* 26.9, pp. 669–676.

Vinciguerra, P., E. Albè, S. Trazza, et al. (2009). "Refractive, Topographic, Tomographic, and Aberrometric Analysis of Keratoconic Eyes Undergoing Corneal Cross-Linking". In: *Ophthalmology* 116.3, pp. 369–378.

Vinciguerra, P., R. Mencucci, et al. (2014). "Imaging Mass Spectrometry by Matrix-Assisted Laser Desorption/Ionization and Stress-Strain Measurements in Ion-

tophoresis Transepithelial Corneal Collagen Cross-Linking". In: *Biomed Research International*.

Vinciguerra, P., J. B. Randleman, et al. (2014). "Transepithelial Iontophoresis Corneal Collagen Cross-linking for Progressive Keratoconus: Initial Clinical Outcomes". In: *Journal of Refractive Surgery* 30.11, pp. 747–754.

Wagner, H. et al. (2007). "Collaborative Longitudinal Evaluation of Keratoconus (CLEK) Study: methods and findings to date". In: *Contact lens & anterior eye : the journal of the British Contact Lens Association* 30.4, pp. 223–32.

Wang, M. X. et al. (2008). *Irregular Astigmatism: Diagnosis and Treatment*. New Jersey, USA: SLACK, p. 295.

— (2010). *Keratoconus & Keratoectasia: Prevention, Diagnosis, and Treatment*. New Jersey, USA: SLACK.

Waszczykowska, A. et al. (2015). "Two-year accelerated corneal cross-linking outcome in patients with progressive keratoconus". In: *BioMed research international* 2015, pp. 325157–325157.

Weed, K. H., C. J. MacEwen, A. Cox, et al. (2007). "Quantitative analysis of corneal microstructure in keratoconus utilising in vivo confocal microscopy". In: *Eye* 21.5, pp. 614–623.

Weed, K. H., C. J. MacEwen, T. Giles, et al. (2008). "The Dundee University Scottish Keratoconus study: demographics, corneal signs, associated diseases, and eye rubbing". In: *Eye* 22.4, pp. 534–541.

Weed, K. H., C. J. MacEwen, and C. N. J. McGhee (2007). "The Dundee University Scottish Keratoconus Study II: a prospective study of optical and surgical correction". In: *Ophthalmic and Physiological Optics* 27.6, pp. 561–567.

Wernli, J. et al. (2013). "The Efficacy of Corneal Cross-Linking Shows a Sudden Decrease with Very High Intensity UV Light and Short Treatment Time". In: *Investigative Ophthalmology & Visual Science* 54.2, pp. 1176–1180.

West-Mays, J. A. et al. (2006). "The keratocyte: Corneal stromal cell with variable repair phenotypes". In: *International Journal of Biochemistry & Cell Biology* 38.10, pp. 1625–1631.

Williamson, J. R. et al. (1986). "Islet transplants in diabetic Lewis rats prevent and reverse diabetes-induced increases in vascular permeability and prevent but do not reverse collagen solubility changes". In: *Diabetologia* 29.6, pp. 392–396.

Wilson, S. E., Y. G. He, et al. (1996). "Epithelial injury induces keratocyte apoptosis: Hypothesized role for the interleukin-1 system in the modulation of corneal tissue organization and wound healing". In: *Experimental Eye Research* 62.4, pp. 325–337.

Wilson, S. E. and J. W. Hong (2000). "Bowman's layer structure and function - Critical or dispensable to corneal function? A hypothesis". In: *Cornea* 19.4, pp. 417–420.

Wisse, R. P. L. et al. (2016). "Higher-order aberrations 1 year after corneal collagen crosslinking for keratoconus and their independent effect on visual acuity". In: *Journal of Cataract and Refractive Surgery* 42.7, pp. 1046–1052.

Wittig-Silva, C. et al. (2014). "A Randomized, Controlled Trial of Corneal Collagen Cross-Linking in Progressive Keratoconus Three-Year Results". In: *Ophthalmology* 121.4, pp. 812–821.

Wojcik, K. A., J. Blasiak, et al. (2014). "Role of biochemical factors in the pathogenesis of keratoconus". In: *Acta Biochimica Polonica* 61.1, pp. 55–62.

Wojcik, K. A., A. Kaminska, et al. (2013). "Oxidative Stress in the Pathogenesis of Keratoconus and Fuchs Endothelial Corneal Dystrophy". In: *International Journal of Molecular Sciences* 14.9, pp. 19294–19308.
Wollensak, G. (2006). "Crosslinking treatment of progressive keratoconus: new hope". In: *Current Opinion in Ophthalmology* 17.4, pp. 356–360.
— (2010). "Histological changes in human cornea after cross-linking with riboflavin and ultraviolet A". In: *Acta Ophthalmologica* 88.2, e17–e18.
Wollensak, G., H. Aurich, et al. (2007). "Hydration behavior of porcine cornea crosslinked with riboflavin and ultraviolet A". In: *Journal of Cataract and Refractive Surgery* 33.3, pp. 516–521.
Wollensak, G. and E. Iomdina (2009). "Long-term biomechanical properties of rabbit cornea after photodynamic collagen crosslinking". In: *Acta Ophthalmologica* 87.1, pp. 48–51.
Wollensak, G., E. Spoerl, F. Reber, et al. (2004). "Keratocyte cytotoxicity of riboflavin/UVA-treatment in vitro". In: *Eye* 18.7, pp. 718–722.
Wollensak, G., E. Spoerl, and T. Seiler (2003a). "Riboflavin/ultraviolet-A-induced collagen crosslinking for the treatment of keratoconus". In: *American Journal of Ophthalmology* 135.5, pp. 620–627.
— (2003b). "Stress-strain measurements of human and porcine corneas after riboflavin-ultraviolet-A-induced cross-linking". In: *Journal of Cataract and Refractive Surgery* 29.9, pp. 1780–1785.
Wollensak, G., M. Wilsch, et al. (2004). "Collagen fiber diameter in the rabbit cornea after collagen crosslinking by riboflavin/UVA". In: *Cornea* 23.5, pp. 503–507.
Wollensak, G. et al. (2003). "Endothelial cell damage after riboflavin-ultraviolet-A treatment in the rabbit". In: *Journal of Cataract and Refractive Surgery* 29.9, pp. 1786–1790.
— (2004). "Keratocyte apoptosis after corneal collagen cross-linking using riboflavin/UVA treatment". In: *Cornea* 23.1, pp. 43–49.
Xu, J. et al. (2010). "Ocular manifestations of Alport syndrome". In: *International Journal of Ophthalmology* 3.2, pp. 149–151.
Yam, J. C. S. et al. (2012). "Corneal collagen cross-linking demarcation line depth assessed by Visante OCT after CXL for keratoconus and corneal ectasia". In: *Journal of Refractive Surgery* 28.7, pp. 475–481.
Yamamoto, S. et al. (1999). "Three-dimensional appearance of Bowman's layer after radial keratotomy". In: *Journal of Cataract & Refractive Surgery* 25.3, pp. 363–367.
Yuksel, N. et al. (2016). "Comparison of Aqueous Humor Nitric Oxide Levels After Different Corneal Collagen Cross-Linking Methods". In: *Current Eye Research* 41.12, pp. 1539–1542.
Zaki, A. A. et al. (2015). "Deep anterior lamellar keratoplasty-triple procedure: a useful clinical application of the pre-Descemet's layer (Dua's layer)". In: *Eye* 29.3, pp. 323–326.
Zavala, J. et al. (2013). "Corneal endothelium: developmental strategies for regeneration". In: *Eye* 27.5, pp. 579–588.
Zeng, Y. et al. (2001). "A comparison of biomechanical properties between human and porcine cornea". In: *Journal of Biomechanics* 34.4, pp. 533–537.

Zhang, X. Y. et al. (2017). "Biomechanical and Histopathologic Effects of Pulsed-Light Accelerated Epithelium-On/-Off Corneal Collagen Cross-Linking". In: *Cornea* 36.7, pp. 854–859.

Zhang, X. et al. (2017). "Dry Eye Management: Targeting the Ocular Surface Microenvironment". In: *International Journal of Molecular Sciences* 18.7, p. 1398.

Zhang, Y. et al. (2011). "Effects of Ultraviolet-A and Riboflavin on the Interaction of Collagen and Proteoglycans during Corneal Cross-linking". In: *Journal of Biological Chemistry* 286.15, pp. 13011–13022.

Zhang, Z. Y. et al. (2012). "Corneal collagen cross-linking with Riboflavin and ultraviolet-A irradiation in patients with thin corneas". In: *American Journal of Ophthalmology* 153.5, p. 1002.

Zhou, L. et al. (1998). "Expression of degradative enzymes and protease inhibitors in corneas with keratoconus". In: *Investigative Ophthalmology and Visual Science* 39.7, pp. 1117–1124.

Zhou, W. et al. (2014). "Comparison of Corneal Epithelial and Stromal Thickness Distributions between Eyes with Keratoconus and Healthy Eyes with Corneal Astigmatism >= 2.0 D". In: *Plos One* 9.1, e85994.

Zhu, Y. et al. (2017). "High-intensity corneal collagen crosslinking with riboflavin and UVA in rat cornea". In: *Plos One* 12.6, e0179580.

Ziegelberger, G. (2013). "ICNIRP guidelines on limits of exposure to incoherent visible and infrared radiation". In: *Health Physics* 105.1, pp. 74–96.

Zotta, P. G. et al. (2017). "Long-term outcomes of corneal cross-linking for keratoconus in pediatric patients". In: *Journal of American Association for Pediatric Ophthalmology and Strabismus* 21.5, pp. 397–401.

Appendix A: List of publications and congress contributions that arose out of the work associated with this research project

List of publications

- Aldahlawi, N. H., S. Hayes, D. P. S. O'Brart and K. M. Meek (2015). "Standard versus accelerated riboflavin-ultraviolet corneal collagen crosslinking: Resistance against enzymatic digestion." Journal of Cataract & Refractive Surgery, 41(9): 1989-1996.

- Aldahlawi, N. H., S. Hayes, D. P. S. O'Brart, A. Akhbanbetova, S. L. Littlechild and K. M. Meek (2016). "Enzymatic resistance of corneas crosslinked using riboflavin in conjunction with low energy, high energy, and pulsed UVA irradiation modes." Investigative ophthalmology & visual science, 57(4): 1547-1552.

- Aldahlawi, N. H., S. Hayes, D. P. S. O'Brart, N. D. L. O'Brart and K. M. Meek (2016). "An investigation into corneal enzymatic resistance following epithelium-off and epithelium-on corneal cross-linking protocols." Experimental Eye Research, 153, 141-151.

- O'Brart, N. A. L., D. P. S. O'Brart, N. H Aldahlawi, S. Hayes, and K. M. Meek (2018). An investigation of the effects of riboflavin concentration on the efficacy of corneal cross-linking using an enzymatic resistance model in porcine corneas." Investigative ophthalmology & visual science, 59(2): 1058-1065.

- Hayes, S., N. H. Aldahlawi, A. L. Marcovich, J. Brekelmans, A. Goz, A. Scherz, R. D. Young, N. Terrill, T. Sorensen, D. P. S. O'Brart, RMMA Nuijts, K. M. Meek (2018), The effect of bacteriochlorophyll derivative WST-D and near infrared light on the molecular and fibrillar architecture of the corneal stroma (Manuscript submitted).

- Aldahlawi, N. H., S. Hayes, D. P. S. O'Brart and K. M. Meek (2018). An in-vitro investigation of epithelium-off and iontophoretic epithelium-on high energy pulsed and prolonged riboflavin/ultraviolet corneal cross-linking protocols. (Manuscript in preparation).

List congress contributions that arose out of the work associated with this research project

1. Presented in the Association for Research in Vision and Ophthalmology (ARVO) meeting, 1st -5th May 2016, Seattle, USA.
2. Participation in the 9th Saudi Students Conference which was sponsored by Umm Al-Qura University, that took place at the University of Birmingham, United Kingdom from 13-14th Feb, 2016.
3. Presented in the Young Vision Researchers' Colloquium in Queen's Buildings, School of Computer Science & Informatics and School of Engineering, Cardiff University on 23rd June, 2016.
4. Presented in the British Congress of Optometry and Visual Science (BCOV) meeting, City University London, 7-8th September 2015.
5. Presented in the 3rd South West Regional Regenerative Medicine Meeting Doubletree by Hilton Cadbury House, Bristol, 22nd - 23rd September 2015.
6. Presented in the Association for Research in Vision and Ophthalmology ARVO 3rd - 7th May 2015, Denver, USA
7. Presented in the 8th Saudi Students Conference was sponsored by the Saudi Ministry of Higher Education and King Abdullah University of Science and Technology (KAUST). That took place at the hosting university, Imperial College London, United Kingdom from January 31st - February 1st, 2015
8. Presented and Won the poster prize in the 10th international congress of Corneal Cross-Linking, Communicating and understanding cross-linking technology in Zurich, Switzerland 5 - 6th Dec 2014
9. Presented in the British Congress of Optometry and Visual Science (BCOV) meeting, 8 - 9th Sep 2014, in Cardiff, at School of Optometry and Vision Sciences.
10. Presented in Cardiff Institute of Tissue Engineering and Repair (CITER) Annual Scientific Meeting, 2014 CITER Annual Scientific Meeting, 17 - 18th August 2014, Stradey Park Hotel, Llanelli, Uk.

Appendix B: Published work

Standard versus accelerated riboflavin–ultraviolet corneal collagen crosslinking: Resistance against enzymatic digestion

Nada H. Aldahlawi, MSc, Sally Hayes, PhD, David P.S. O'Brart, MD, FRCS, FRCOphth, Keith M. Meek, DSc

PURPOSE: To examine the effect of standard and accelerated corneal collagen crosslinking (CXL) on corneal enzymatic resistance.

SETTING: School of Optometry and Vision Sciences, Cardiff University, Cardiff, United Kingdom.

DESIGN: Experimental study.

METHODS: Sixty-six enucleated porcine eyes (with corneal epithelium removed) were assigned to 6 groups. Group 1 remained untreated, group 2 received dextran eyedrops, and groups 3 to 6 received riboflavin/dextran eyedrops. Group 4 had standard CXL (3 mW/cm^2 ultraviolet-A for 30 minutes), whereas groups 5 and 6 received accelerated CXL (9 mW/cm^2 for 10 minutes and 18 mW/cm^2 for 5 minutes, respectively). Trephined central 8.0 mm buttons from each cornea underwent pepsin digestion. Corneal diameter was measured daily, and the dry weight of 5 samples from each group was recorded after 12 days of digestion.

RESULTS: All CXL groups (4 to 6) took longer to digest and had a greater dry weight at 12 days ($P < .0001$) than the nonirradiated groups (1 to 3) ($P < .0001$). The time taken for complete digestion to occur did not differ between the standard and accelerated CXL groups, but the dry weights at 12 days showed significant differences between treatments: standard CXL 3 mW > accelerated CXL 9 mW > accelerated CXL 18 mW ($P < .0001$).

CONCLUSIONS: Standard and accelerated CXL both increased corneal enzymatic resistance; however, the amount of CXL might be less when accelerated CXL is used. The precise amount of CXL needed to prevent disease progression is not yet known.

Financial Disclosure: No author has a financial or proprietary interest in any material or method mentioned.

J Cataract Refract Surg 2015; 41:1989–1996 © 2015 The Authors. Published by Elsevier Inc. on behalf of ASCRS and ESCRS. This is an open access article under the CC BY license (http://creativecommons.org/licenses/by/4.0/).

Riboflavin–ultraviolet-A (UVA) corneal collagen crosslinking (CXL) is the first treatment modality shown to halt the progression of keratoconus[1–4] and other corneal ectatic disorders.[4–6] The standard treatment protocol, which was first tested clinically by Wollensak et al.,[1] involves the debridement of the central 7.0 mm of the cornea, followed by the application of riboflavin and a 30-minute exposure to 370 nm UVA at an energy of 3 mW/cm^2. At this fluence, the procedure appears to be safe in terms of endothelial toxicity, provided the stromal corneal thickness is greater than 400 μm.[7] In addition, beneficial clinical outcomes in terms of cessation of disease progression and improvements in visual and topographic parameters are consistently achieved,[1–6,8] with reported follow-up of 4 to 6 years.[9] However, the UVA exposure time required to achieve the wanted clinical effect,[10] coupled with the need to instill riboflavin eyedrops

for at least 20 to 30 minutes before irradiation (to achieve a homogeneous stromal uptake of riboflavin[11]), results in operative times in excess of 1 hour.

Recently, in an attempt to reduce patient treatment time, accelerated CXL protocols using higher fluences and shorter exposure times have been postulated. The envisaged safe and effective use of accelerated CXL is based on the Bunsen-Roscoe law of reciprocity,[12] which predicts that the same subthreshold total cytotoxic corneal endothelial UVA dosage can be administered by increasing UVA fluence while simultaneously reducing exposure time. At present, published clinical studies of patients treated with accelerated CXL protocols are few; however, they report no adverse effects associated with accelerated treatment and a significant reduction in both topographic keratometry and corrected distance visual acuity at up to 46 months of follow-up.[13,14]

Spoerl et al.[15] demonstrated an increased resistance of the corneal stroma to enzymatic digestion after standard CXL, and this has since been replicated by others.[16,17] Because increased activity of proteinase enzymes and reduced activity of proteinase inhibitors have been identified in keratoconic corneas,[18,19] this increased resistance to proteinase digestion is liable to be an important factor in the protection against ectatic progression.[15,17] Therefore, to complement previously published studies focusing solely on the biomechanical changes in the cornea after CXL,[20,21] this study investigated the efficacy of standard and accelerated CXL protocols in terms of their ability to increase the resistance of the cornea against enzymatic digestion. Our previous studies have indicated that riboflavin–UVA causes the formation of crosslinks not only at the collagen fibril surface but also in the protein network surrounding the collagen.[16] For this reason, pepsin was selected for this particular study because it is a nonspecific endopeptidase that can break down collagens and proteoglycan core proteins.

Submitted: February 10, 2015.
Final revision submitted: April 10, 2015.
Accepted: April 27, 2015.

From the Structural Biophysics Research Group (Aldahlawi, Hayes, Meek), School of Optometry and Vision Sciences, Cardiff University, Cardiff, and the Keratoconus Research Institute (O'Brart), Department of Ophthalmology, St Thomas Hospital, London, United Kingdom.

Supported by the Medical Research Council, London, United Kingdom (programme grant 503626), and King Saud University, Riyadh, Saudi Arabia (R1269). Veni Vidi, Halifax, United Kingdom, provided the riboflavin for this study.

Corresponding author: Keith M. Meek, DSc, School of Optometry and Vision Sciences, Cardiff University, Maindy Road, Cathays, Cardiff CF24 4HQ, United Kingdom. E-mail: meekkm@cardiff.ac.uk.

MATERIALS AND METHODS

Sixty-six porcine eyes with clear intact corneas were obtained from a local European Community–licensed abattoir within 6 to 8 hours postmortem. By using a single-edged razor blade, the entire corneal epithelium was carefully removed from each eye. A detailed visual inspection was performed to confirm that the debridement technique had resulted in complete removal of the epithelium without damage to the underlying stroma. The central corneal thickness (CCT) of each eye was measured before and after epithelial debridement using a Pachette2 ultrasonic pachymeter (DGH Technology, Inc.). The 66 eyes were randomly and equally divided into the 6 treatment groups:

Group 1: Untreated controls receiving no eyedrops and no UVA exposure.

Group 2: Dextran-only controls receiving 20% dextran T500 eyedrops (Pharmacosmos A/S) every 5 minutes for 30 minutes and no UVA exposure.

Group 3: Riboflavin-only controls receiving riboflavin eyedrops (0.1% solution riboflavin-5-phosphate in 20% dextran T-500 solution, Mediocross D, Peschke Meditrade GmbH) every 5 minutes for 30 minutes and no UVA exposure.

Group 4: "Standard" 3 mW/cm^2 CXL protocol (standard CXL 3 mW) receiving riboflavin 0.1% eyedrops in 20% dextran T-500 every 5 minutes for 30 minutes before exposure of the central 9.0 mm region of the cornea to UVA light with a fluence of 3 mW/cm^2 for 30 minutes (CCL-365 Vario crosslinking system, Peschke Trade GmbH). Riboflavin eyedrops were reapplied at 5-minute intervals throughout the period of irradiation.

Group 5: Accelerated 9 mW/cm^2 CXL protocol (accelerated CXL 9 mW) receiving riboflavin 0.1% eyedrops in 20% dextran T-500 every 5 minutes for 30 minutes, followed by a 10-minute exposure of the central 9.0 mm region to UVA light with a fluence of 9 mW/cm^2 and reapplied riboflavin eyedrops at 5-minute intervals during the exposure.

Group 6: Accelerated 18 mW/cm^2 CXL protocol (accelerated CXL 18 mW) receiving riboflavin 0.1% eyedrops in 20% dextran T-500 every 5 minutes for 30 minutes, followed by a 5-minute exposure of the central 9.0 mm region to UVA light with a fluence of 18 mW/cm^2.

Immediately after treatment, the CCT was again measured. The cornea with a 4.0 to 5.0 mm scleral rim was then dissected from each globe, wrapped tightly in Clingfilm (to prevent moisture loss), and refrigerated until all treatments were complete. An 8.0 mm corneal button was trephined from the center of each cornea using a disposable skin biopsy punch (ref BP-80F, Kai Europe GmbH). The corneal buttons were weighed, then placed in individual plastic tubes, each containing 5 mL of pepsin solution, and incubated in a water bath (VwB6, VWR International bvba) at a temperature of 23°C. The pepsin solution was made of 1 g of 600 to 1200 U/mg pepsin from porcine gastric mucosa (Sigma-Aldrich Co. LLC) in 10 mL 0.1 M hydrochloric acid at pH 1.4. Previous studies[15] have shown that changes in corneal disk thickness are not a reliable indicator

of the rate of enzymatic digestion because of the considerable stromal swelling that occurs in the vertical direction within 24 hours of immersion in pepsin digest solution. Because the diameter of the anterior surface of each corneal button is unaffected by changes in stromal hydration,[15] this parameter was used to monitor the rate of enzymatic digestion in 6 of the corneas from each treatment group. Measurements of anterior surface diameter were made using an electronic digital caliper (model CM145 4500360, Clarke International) at 24 hourly intervals until complete digestion had occurred. Because the diameter was found to vary slightly between different meridians of an individual specimen, the average of the major axis and minor axis diameter of each corneal button was recorded at each time point and statistically evaluated. The definition of complete digestion was the point at which the specimen could no longer be distinguished from the surrounding pepsin solution, even under microscopic examination.

To further assess the effect of each treatment on enzymatic resistance, 5 corneal disks from each group were removed from the pepsin digest solution after 12 days and placed in a 60°C oven until a constant dry weight was obtained. The average corneal dry weight (which represents the mass of undigested tissue) was calculated for each group.

Statistical Analysis

Measurements of corneal thickness (before and after treatment), corneal disk diameter, dry weight, and complete digestion time were statistically analyzed using a 1-way analysis of variance test. Post hoc Bonferroni comparisons were used to isolate significant interactions. All statistical analyses were performed with Statistical Package for the Social Sciences software (SPSS Statistics 20, International Business Machines Corp.). A P value less than 0.01 was considered to be significant. Data are presented in the results as the mean ± standard deviation. The observed power computed using α equal to 0.05 was 1, demonstrating that the sample size was sufficient.

RESULTS

Measurements of CCT before and after epithelial removal and after each stage of treatment are shown in Table 1. No statistically significant differences in corneal thickness were observed between the groups either before or after epithelial removal. However, there was a significant reduction in corneal thickness after administration of dextran-containing solutions in both group 2 (20% dextran) and group 3 (riboflavin 0.1%–dextran 20%) ($P < .0001$). Application of the riboflavin solution (containing dextran) to the deepithelialized cornea (group 3) resulted in a significantly greater reduction in corneal thickness than application of the dextran-only solution (group 2) ($P < .001$). A significant reduction in corneal thickness was observed after CXL in groups 4, 5, and 6 ($P < .0001$). Because the post-treatment thickness of the irradiated corneas (groups 4, 5, and 6) did not differ from that of the nonirradiated riboflavin–treated corneas (group 3), the corneal thinning in CXL may be attributed to the application of riboflavin rather than to UVA exposure.

An approximately 10-fold increase in the thickness of the corneal disk, as a result of stromal swelling in the posterior–anterior direction, was observed in all corneal buttons within 24 hours of submersion in pepsin digest solution (Figure 1). After 1 week of digestion, the anterior portion of each treated and untreated corneal button had separated from the posterior portion. Once detached, the posterior stroma was rapidly digested (within 10 days); however, the anterior stromal button persisted considerably longer and maintained its form sufficiently to obtain reliable measurements of its changing diameter during the digestion process.

Figure 2 shows the summed diameters of 6 corneal disks within each treatment group as a function of incubation time in pepsin solution. Statistical analysis revealed no significant difference in either the mean corneal button diameter of nonirradiated specimens (groups 1, 2, and 3) at any timepoint during digestion or in the time taken for complete digestion to occur (Table 2). Similarly, in the irradiated specimens, no significant difference in these parameters was detected

Table 1. Central corneal thickness before and after epithelial removal and after treatment.*

Groups	Central Corneal Thickness			
	Before Epithelial Removal (μm)*	After Epithelial Removal (μm)*	Posttreatment (μm)*	Change (%)†
Untreated	830 ± 46	739 ± 45	NA	NA
Dextran only	821 ± 41	721 ± 39	602 ± 41	−17
Riboflavin–dextran only	775 ± 45	676 ± 45	508 ± 39	−24.9
SCXL 3 mW	792 ± 48	694 ± 50	494 ± 28	−28.8
ACXL 9 mW	820 ± 38	716 ± 40	514 ± 31	−28.1
ACXL 18 mW	807 ± 32	706 ± 34	495 ± 34	−29.9

ACXL = accelerated crosslinking; NA = not applicable; SCXL = standard crosslinking
*Data are given as mean ± standard deviation.
†Percentage change from corneal thickness postepithelial removal to posttreatment

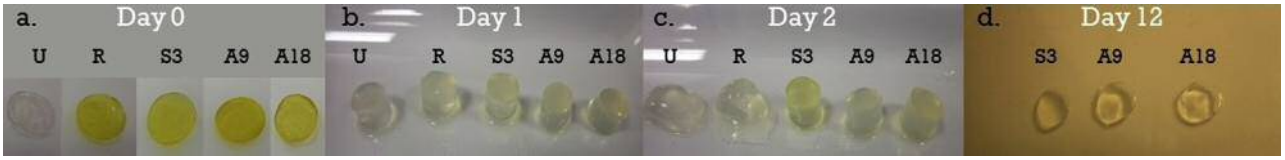

Figure 1. Corneal disks from left to right: untreated (*U*), riboflavin–dextran only (R), standard CXL 3 mW (S3), accelerated CXL 9 mW (A9), and accelerated CXL 18 mW (A18) before (*a*) and after 1 day (*b*), 2 days (*c*), and 12 days (*d*) of immersion in pepsin digest solution. All corneal buttons are swollen after 1 day in pepsin digest solution (*b*). After 2 days of digestion, the anterior curvature has been lost in the untreated corneas but remains intact in the crosslinked corneas (*c*). After 12 days, all nonirradiated buttons have been completely digested and only the anterior portion of the crosslinked corneas remain.

between specimens treated with standard CXL (group 4) or accelerated CXL (groups 5 and 6). The diameter of the corneal disks in the CXL-treated groups (4, 5, and 6) was, however, significantly higher than that in the nonirradiated specimens (groups 1, 2, and 3) at all daily timepoints after 8 days ($P < .0001$) (Figure 2), and the time required for complete digestion to occur was significantly longer ($P < .0001$) (Table 2). By 12 days all nonirradiated corneas had been completely digested, but the mean diameter of the CXL-treated eyes (groups 4, 5, and 6) had decreased by only 27.2%, 27.0%, and 26.6% in the standard CXL 3mW, accelerated CXL 9mW, and accelerated CXL 18 mW groups, respectively.

At day 0, there was no significant difference between the mean wet weight of corneal disks in groups 1, 3, 4, 5, and 6 ($P > .14$). However, the mean wet weight of the dextran-only treated corneas (group 2) was significantly higher than that of the 3 mW standard CXL (group 4) ($P < .03$) and 9 mW accelerated CXL treated corneas (group 5) ($P < .03$) (Table 3).

Measurements of corneal disk dry weight after 12 days of digestion showed a statically significant difference between irradiated and nonirradiated corneas ($P < .0001$) and between irradiated corneas treated with 3 mW, 9 mW, or 18 mW accelerated CXL ($P < .0001$) (Table 3). The standard CXL 3 mW-treated corneas had a statistically higher mean dry weight than the 9 mW and 18 mW accelerated CXL-treated corneas ($P < .0001$) and the 9 mW accelerated CXL group had a higher dry weight than the 18 mW accelerated CXL group ($P < .003$) (Table 3).

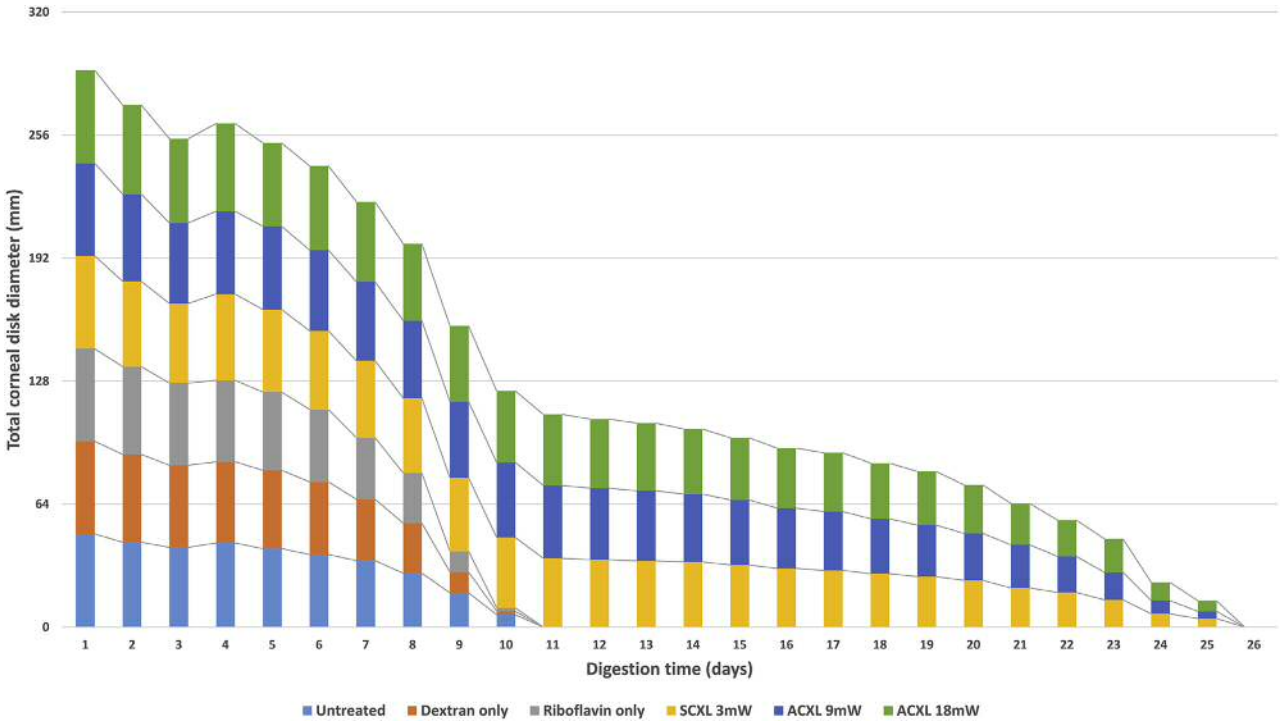

Figure 2. The summed diameter of all corneal disks (n = 8) in each treatment group shown as a function of time in pepsin digest solution (ACXL = accelerated crosslinking; SCXL = standard crosslinking).

Table 2. Time taken for the complete digestion of treated and untreated corneal buttons.

Group	Time Taken for Complete Digestion (Days)		
	Minimum	Maximum	Mean ± SD
Untreated	10	11	10.5 ± 0.55
Dextran only	10	11	10.5 ± 0.55
Riboflavin–dextran only	9	11	9.83 ± 0.75
SCXL 3 mW	24	26	24.7 ± 1.03
ACXL 9 mW	23	26	24.7 ± 1.03
ACXL 18 mW	24	27	24.8 ± 0.98

ACXL = accelerated crosslinking; SCXL = standard crosslinking

Table 3. Corneal disk weight before and after 12 days of pepsin digestion.

Group	Day 0 (Wet Weight) (g)*	Day 12 (Dry Weight) (g)*
Untreated	0.0540 ± 0.0050	0 ± 0
Dextran only	0.0563 ± 0.0055	0 ± 0
Riboflavin–dextran only	0.0477 ± 0.0047	0 ± 0
SCXL 3 mW	0.0438 ± 0.0032	0.0041 ± 0.0013
ACXL 9 mW	0.0440 ± 0.0038	0.0020 ± 0.0005
ACXL 18 mW	0.0445 ± 0.0018	0.0008 ± 0.0003

ACXL = accelerated crosslinking; SCXL = standard crosslinking
*Data are given as mean ± standard deviation.

DISCUSSION

Although the precise etiology of keratoconus is unknown,[22] an increased activity of proteinase enzymes and a reduced activity of protease inhibitors have been identified in keratoconic corneas.[18] This increased stromal protein digestion is thought to be an important factor in the resultant corneal thinning and biomechanical instability seen in keratoconic eyes.[19] Spoerl et al.[15] demonstrated an increased resistance of corneal stromal tissue to enzymatic digestion after CXL, with irradiances of 2 mW/cm^2 and 3 mW/cm^2 UVA. This increased resistance to proteinase digestion after CXL has been replicated by others[16,17] and is likely to be an important factor in preventing disease progression.[15,19]

In this study, the enzymatic resistance of nonirradiated-treated porcine corneas was compared with that of standard CXL- and accelerated CXL-treated corneas. Similar to other clinical- and laboratory-based studies,[16,23,24] a significant reduction in corneal thickness was observed after CXL using an isotonic riboflavin solution. Because the posttreatment thickness of the irradiated corneas did not differ from that of the nonirradiated riboflavin-treated corneas, the corneal thinning observed during CXL and accelerated CXL may be attributed predominantly to the application of riboflavin–dextran solution rather than to the effect of CXL after UVA exposure. The application of riboflavin solution (containing 20% dextran) resulted in a significantly greater reduction in corneal thickness than the application of the same concentration of dextran in the absence of any riboflavin. This finding may be the result of riboflavin increasing the ionic strength of the applied solution, because higher ionic strengths are known to be associated with lower corneal hydrations[25] and reduced corneal thickness.

As described previously,[15,16] significant stromal swelling occurred (predominantly in the posterior stroma) in all corneal buttons during the first 24 hours in pepsin solution. This observation can be attributed to the negatively charged glycosaminoglycan components of the proteoglycans within the extracellular matrix, which result in the pepsin digest solution being drawn into the tissue.[26] The higher ratio of keratan sulfate to chondroitin sulfate in the posterior stroma compared with the anterior[27] may explain why most of the swelling occurred in this region because keratan sulfate has a higher water affinity than chondroitin sulfate.[28] Interestingly, the separation of the cornea into anterior and posterior stromal regions during the first week of digestion was observed in all treated and untreated corneas. The separation of the corneal buttons cannot, therefore, be attributed to CXL-induced changes within the anterior stroma but must instead be the result of naturally occurring structural differences that exist between the anterior and posterior regions. The diameter of the anterior portion of the corneal button was unaffected by the changes in corneal hydration and, therefore, formed a much more reliable measure of the rate of enzymatic digestion than measurements of corneal thickness. However, calculations based on the sample size used and the standard deviation of diameter measurements confirmed that the sensitivity of the technique was such that differences between groups (in terms of the time taken for complete digestion) of less than 1 day could not be detected by this method. For this reason, measurements of corneal disk dry weight (which reflect the mass of undigested corneal tissue) were recorded at day 12 of the digestion process to allow more subtle differences in enzymatic resistance between treatment groups to be identified.

Our results showed an increased resistance to proteinase digestion after standard CXL that is in agreement with the findings of other investigators.[15–17] However, for the first time, we have shown that a similar increase in enzymatic resistance can also be

achieved using higher fluences (up to 18 mW/cm^2) and shorter exposure times. Although the diameter measurements detected no difference in enzymatic resistance between the CXL protocols used in this study, the mean dry weight of corneal tissue after 12 days of protein digestion was found to differ significantly between groups (3 mW accelerated CXL > 9 mW accelerated CXL > 18 mW accelerated CXL). Measurements of corneal dry weight, which represent the total mass of undigested tissue and negate the complications associated with within-sample variations in corneal thickness and between-sample differences in hydration, provide a more accurate means of assessing the relative efficacy of CXL procedures at increasing corneal enzymatic resistance. Our findings suggest that in protocols that use a higher fluence and shorter exposure time, either the most anterior layers of the corneal stroma may be crosslinked equally and the effective depth of CXL is reduced or the intensity of CXL (which is known to be depth dependent[29]) decreases more rapidly as a function of depth. One interesting observation in previous studies is the presence of a shallower demarcation line in accelerated CXL compared with standard CXL,[30,31] suggesting that this may represent a reduced or shallower CXL effect. However, this assumes that the depth of the demarcation line correlates directly with the degree and depth of CXL, and currently there is no direct evidence to support this. The so-called stromal demarcation line, first described by Seiler and Hafezi,[32] has been shown to possibly be shallower in older patients and those with more severe ectatic disease.[33] It has been found to be thicker centrally and thinner peripherally[34] and possibly related to an increased density of the extracellular matrix.[35] Although a deeper demarcation line has been associated with a larger decrease in corneal thickness,[36] its depth has not been shown to be correlated to either visual or keratometric changes 6 months postoperatively.[33] It may simply represent natural wound-healing responses rather than delineate the true area between crosslinked and uncrosslinked tissue, and more research is required to ascertain the true nature of this demarcation line and its relationship to the actual CXL process.

Other studies have concentrated on comparing the biomechanical changes after CXL and accelerated CXL using methods such as scanning acoustic microscopy and extensiometry. Hammer et al.[37] reported a reduced corneal stiffening effect with increasing UVA intensity (up to 18 mW); however, others have shown similar biomechanical changes after both standard 3 mW/cm^2 CXL and 9 to 10 mW/cm^2 accelerated CXL,[20,21] but a sudden decrease in efficacy with high intensities (greater than 45 mW/cm^2).[38] The failure of the Bunsen-Roscoe law[12] of reciprocity in cases of high intensity and short illumination time is not yet understood but may be related to rapid oxygen consumption and subsequent reduced oxygen availability, which has been shown to limit the photochemical CXL process.[39] Oxygen and its vital role in free radical production has been shown to be central in driving the CXL process.[39] Therefore, limitations in availability because of reduced time to replenish suitable oxygen levels can theoretically inhibit the photochemical CXL process.[39] In our study, we found only subtle differences in enzymatic resistance, with increasing UVA intensity up to 18 mW/cm^2. Further studies with energies of 30 mW/cm^2 and above are indicated to see whether the results of pepsin digestion studies replicate those of extensometry and other mechanical methods.

Even though most laboratory results are supportive of accelerated CXL, published clinical studies of the technique are limited. A significant reduction in topographic keratometry and improvement in corrected distance acuity, comparable to standard CXL, have been reported at the 6-month follow-up.[13] In a randomized prospective study comparing a fluence of 7 mW/cm^2 for 15 minutes with 3 mW/cm^2 for 30 minutes,[14] similar clinical results for ectasia stabilization were reported after each treatment protocol, and neither treatment resulted in any adverse effects. Similarly, clinical studies using 9 mW/cm^2 for 10 minutes have shown a significant reduction in keratometry after CXL, with no adverse effects in terms of endothelial cell counts at 3 months.[40] More recently, it was shown that accelerated CXL with an irradiance of 30 mW/cm^2 for 3 minutes resulted in a significant improvement in uncorrected distance visual acuity and a reduction in keratometry at 6 months.[41] This finding was supported by a nonrandomized study comparing standard CXL with 30 mW/cm^2 accelerated CXL, which found no difference in visual, refractive, keratometric, or biomechanical parameters between the 2 treatments at the 12-month follow-up.[42]

Although our studies have indicated that the amount of CXL may be less with accelerated CXL, the minimum effective amount of CXL needed for ectasia stabilization has not yet been established. The success of the clinical studies described previously indicates that the amount of CXL produced by accelerated CXL may be sufficient to prevent keratoconus progression. Clearly, further clinical studies, especially randomized prospective trials, will be necessary to ascertain the clinical safety and efficacy of accelerated CXL. But thus far, the accumulating clinical and laboratory evidence demonstrates its similar efficacy to standard CXL, and its clear benefits in terms of patient and surgeon convenience support its use.

WHAT WAS KNOWN

- Standard riboflavin–UVA CXL increases both the strength of the cornea and its resistance to enzymatic digestion and has proved to be successful in halting keratoconus progression. The effect of accelerated CXL protocols on corneal enzymatic resistance is currently unknown.

WHAT THIS PAPER ADDS

- Both standard and accelerated riboflavin–UVA corneal CXL protocols (up to 18 mW) resulted in an increase in corneal enzymatic resistance.
- Differences in enzymatic resistance suggest that the accelerated protocols result in less CXL than the standard treatment.

REFERENCES

1. Wollensak G, Spoerl E, Seiler T. Riboflavin/ultraviolet-A–induced collagen crosslinking for the treatment of keratoconus. Am J Ophthalmol 2003; 135:620–627. Available at: http://grmc.ca/assets/files/collagen_crosslinking_2003_wollensak.pdf. Accessed July 26, 2015
2. Caporossi A, Baiocchi S, Mazzotta C, Traversi C, Caporossi T. Parasurgical therapy for keratoconus by riboflavin-ultraviolet type A rays induced cross-linking of corneal collagen; preliminary refractive results in an Italian study. J Cataract Refract Surg 2006; 32:837–845
3. O'Brart DPS, Chan E, Samaras K, Patel P, Shah SP. A randomised, prospective study to investigate the efficacy of riboflavin/ultraviolet A (370 nm) corneal collagen cross-linkage to halt the progression of keratoconus. Br J Ophthalmol 2011; 95:1519–1524. Available at: http://bjo.bmj.com/content/95/11/1519.full.pdf?sid=a585cf27-23ec-4a1a-be48-cdf9597f5584. Accessed July 26, 2015
4. Wittig-Silva C, Chan E, Islam FMA, Wu T, Whiting M, Snibson GR. A randomized, controlled trial of corneal collagen cross-linking in progressive keratoconus; three-year results. Ophthalmology 2014; 121:812–821
5. Hafezi F, Kanellopoulos J, Wiltfang R, Seiler T. Corneal collagen crosslinking with riboflavin and ultraviolet A to treat induced keratectasia after laser in situ keratomileusis. J Cataract Refract Surg 2007; 33:2035–2040
6. Spadea L. Corneal collagen cross-linking with riboflavin and UVA irradiation in pellucid marginal degeneration. J Refract Surg 2010; 26:375–377
7. Spoerl E, Mrochen M, Sliney D, Trokel S, Seiler T. Safety of UVA–riboflavin cross-linking of the cornea. Cornea 2007; 26:385–389
8. O'Brart DPS. Corneal collagen cross linking: a review. J Optom 2014; 7:113–124. Available at: http://www.journalofoptometry.org/en/pdf/S1888429613000824/S300/. Accessed July 26, 2015
9. O'Brart DPS, Kwong TQ, Patel P, McDonald RJ, O'Brart NA. Long-term follow-up of riboflavin/ultraviolet A (370 nm) corneal collagen cross-linking to halt the progression of keratoconus. Br J Ophthalmol 2013; 97:433–437. Available at: http://bjo.bmj.com/content/97/4/433.full.pdf. Accessed July 26, 2015
10. Spoerl E, Huhle M, Seiler T. Induction of cross-links in corneal tissue. Exp Eye Res 1998; 66:97–103
11. Gore DM, Margineanu A, French P, O'Brart D, Dunsby C, Allan DB. Two-photon fluorescence microscopy of corneal riboflavin absorption. Invest Ophthalmol Vis Sci 2014; 55:2476–2481. Available at: http://iovs.arvojournals.org/article.aspx?articleid=2190107. Accessed July 26, 2015
12. Bunsen RW, Roscoe HE. Photochemical researches – Part V. On the measurement of the chemical action of direct and diffuse sunlight. Proc R Soc Lond 1862; 12:306–312. Available at: http://rspl.royalsocietypublishing.org/content/12/306.full.pdf
13. Çınar Y, Cingü AK, Turkcu FM, Yüksel H, Şahin A, Yıldırım A, Caca I, Çınar T. Accelerated corneal collagen cross-linking for progressive keratoconus. Cutan Ocul Toxicol 2014; 33:168–171
14. Kanellopoulos AJ. Long term results of a prospective randomized bilateral eye comparison trial of higher fluence, shorter duration ultraviolet A radiation, and riboflavin collagen cross linking for progressive keratoconus. Clin Ophthalmol 2012; 6:97–101. Available at: http://www.ncbi.nlm.nih.gov/pmc/articles/PMC3261695/pdf/opth-6-097.pdf. Accessed July 26, 2015
15. Spoerl E, Wollensak G, Seiler T. Increased resistance of cross-linked cornea against enzymatic digestion. Curr Eye Res 2004; 29:35–40
16. Hayes S, Kamma-Lorger CS, Boote C, Young RD, Quantock AJ, Rost A, Khatib Y, Harris J, Yagi N, Terrill N, Meek KM. The effect of riboflavin/UVA collagen cross-linking therapy on the structure and hydrodynamic behaviour of the ungulate and rabbit corneal stroma. PLoS One 2013; 8(1):e52860. Available at: http://www.ncbi.nlm.nih.gov/pmc/articles/PMC3547924/pdf/pone.0052860.pdf. Accessed July 26, 2015
17. Kissner A, Spoerl E, Jung R, Spekl K, Pillunat LE, Raiskup F. Pharmacological modification of the epithelial permeability by benzalkonium chloride in UVA/riboflavin corneal collagen cross-linking. Curr Eye Res 2010; 35:715–721
18. Zhou L, Sawaguchi S, Twining SS, Sugar J, Feder RS, Yue BYJT. Expression of degradative enzymes and protease inhibitors in corneas with keratoconus. Invest Ophthalmol Vis Sci 1998; 39:1117–1124. Available at: http://iovs.arvojournals.org/article.aspx?articleid=2161735. Accessed July 26, 2015
19. Andreassen TT, Simonsen AH, Oxlund H. Biomechanical properties of keratoconus and normal corneas. Exp Eye Res 1980; 31:435–441
20. Beshtawi IM, Akhtar R, Hillarby MC, O'Donnell C, Zhao X, Brahma A, Carley F, Derby B, Radhakrishnan H. Biomechanical properties of human corneas following low- and high-intensity collagen cross-linking determined with scanning acoustic microscopy. Invest Ophthalmol Vis Sci 2013; 54:5273–5280. Available at: http://iovs.arvojournals.org/article.aspx?articleid=2127902. Accessed July 26, 2015
21. Schumacher S, Oeftiger L, Mrochen M. Equivalence of biomechanical changes induced by rapid and standard corneal cross-linking, using riboflavin and ultraviolet radiation. Invest Ophthalmol Vis Sci 2011; 52:9048–9052. Available at: http://iovs.arvojournals.org/article.aspx?articleid=2187529. Accessed July 26, 2015
22. Davidson AE, Hayes S, Hardcastle AJ, Tuft SJ. The pathogenesis of keratoconus. Eye 2014; 28:189–195. Available at: http://www.nature.com/eye/journal/v28/n2/pdf/eye2013278a.pdf. Accessed July 26, 2015
23. Greenstein SA, Shah VP, Fry KL, Hersh PS. Corneal thickness changes after corneal collagen crosslinking for keratoconus and corneal ectasia: One-year results. J Cataract Refract Surg 2011; 37:691–700

24. Hassan Z, Modis L Jr, Szalai E, Berta A, Nemeth G. Intraoperative and postoperative corneal thickness change after collagen crosslinking therapy. Eur J Ophthalmol 2014; 24:179–185
25. Huang Y, Meek KM. Swelling studies on the cornea and sclera: The effects of pH and ionic strength. Biophys J 1999; 77:1655–1665. Available at: http://www.ncbi.nlm.nih.gov/pmc/articles/PMC1300453/pdf/10465776.pdf. Accessed July 26, 2015
26. Klyce SD, Beuerman RW. Structure and function of the cornea. In: Kaufman HE, McDonald MB, Barron BA, Waltman SR, eds, The Cornea. New York, NY, Churchill Livingstone, 1988; 3–54
27. Castoro JA, Bettelheim AA, Bettelheim FA. Water gradients across bovine cornea. Invest Ophthalmol Vis Sci 1988; 29:963–968. Available at: http://iovs.arvojournals.org/article.aspx?articleid=2159998. Accessed July 26, 2015
28. Bettelheim FA, Plessy B. The hydration of proteoglycans of bovine cornea. Biochim Biophys Acta 1975; 381:203–214
29. Scarcelli G, Kling S, Quijano E, Pineda R, Marcos S, Yun SH. Brillouin microscopy of collagen crosslinking: Noncontact depth-dependent analysis of corneal elastic modulus. Invest Ophthalmol Vis Sci 2013; 54:1418–1425. Available at: http://iovs.arvojournals.org/article.aspx?articleid=2128290. Accessed July 26, 2015
30. Touboul D, Efron N, Smadja D, Praud D, Malet F, Colin J. Corneal confocal microscopy following conventional, transepithelial, and accelerated corneal collagen cross-linking procedures for keratoconus. J Refract Surg 2012; 28:769–776
31. Kymionis GD, Tsoulnaras KI, Grentzelos MA, Plaka AD, Mikropoulos DG, Liakopoulos DA, Tsakalis NG, Pallikaris IG. Corneal stroma demarcation line after standard and high-intensity collagen crosslinking determined with anterior segment optical coherence tomography. J Cataract Refract Surg 2014; 40:736–740
32. Seiler T, Hafezi F. Corneal cross-linking-induced stromal demarcation line. Cornea 2006; 25:1057–1059
33. Yam JCS, Chan CWN, Cheng ACK. Corneal collagen cross-linking demarcation line depth assessed by Visante OCT after CXL for keratoconus and corneal ectasia. J Refract Surg 2012; 28:475–481
34. Kymionis GD, Grentzelos MA, Plaka AD, Stojanovic N, Tsoulnaras KI, Mikropoulos DG, Rallis KI, Kankariya VP. Evaluation of the corneal collagen cross-linking demarcation line profile using anterior segment optical coherence tomography. Cornea 2013; 32:907–910
35. Mazzotta C, Balestrazzi A, Traversi C, Baiocchi S, Caporossi T, Tommasi C, Caporossi A. Treatment of progressive keratoconus by riboflavin-UVA–induced cross-linking of corneal collagen; ultrastructural analysis by Heidelberg Retinal Tomograph II in vivo confocal microscopy in humans. Cornea 2007; 26:390–397
36. Doors M, Tahzib NG, Eggink FA, Berendschot TTJM, Webers CAB, Nuijts RMMA. Use of anterior segment optical coherence tomography to study corneal changes after collagen cross-linking. Am J Ophthalmol 2009; 148:844–851
37. Hammer A, Richoz O, Arba Mosquera S, Tabibian D, Hoogewoud F, Hafezi F. Corneal biomechanical properties at different corneal cross-linking (CXL) irradiances. Invest Ophthalmol Vis Sci 2014; 55:2881–2884. Available at: http://iovs.arvojournals.org/article.aspx?articleid=2128027. Accessed July 26, 2015
38. Wernli J, Schumacher S, Spoerl E, Mrochen M. The efficacy of corneal cross-linking shows a sudden decrease with very high intensity UV light and short treatment time. Invest Ophthalmol Vis Sci 2013; 54:1176–1180. Available at: http://iovs.arvojournals.org/article.aspx?articleid=2127751. Accessed July 26, 2015
39. McCall AS, Kraft S, Edelhauser HF, Kidder GW, Lundquist RR, Bradshaw HE, Dedeic Z, Dionne MJC, Clement EM, Conrad GW. Mechanisms of corneal tissue cross-linking in response to treatment with topical riboflavin and long-wavelength ultraviolet radiation (UVA). Invest Ophthalmol Vis Sci 2010; 51:129–138. Available at: http://iovs.arvojournals.org/article.aspx?articleid=2185576. Accessed July 26, 2015
40. Kymionis GD, Grentzelos MA, Kankariya VP, Liakopoulos DA, Portaliou DM, Tsoulnaras KI, Karavitaki AE, Pallikaris AI. Safety of high-intensity corneal collagen crosslinking. J Cataract Refract Surg 2014; 40:1337–1340
41. Mita M, Waring GO IV, Tomita M. High-irradiance accelerated collagen crosslinking for the treatment of keratoconus: six-month results. J Cataract Refract Surg 2014; 40:1032–1040
42. Tomita M, Mita M, Huseynova T. Accelerated versus conventional corneal collagen crosslinking. J Cataract Refract Surg 2014; 40:1013–1020

First author:
Nada H. Aldahlawi, MSc

School of Optometry and Vision Sciences, Cardiff University, Cardiff, United Kingdom

Experimental Eye Research 153 (2016) 141–151

Contents lists available at ScienceDirect

Experimental Eye Research

journal homepage: www.elsevier.com/locate/yexer

Research article

An investigation into corneal enzymatic resistance following epithelium-off and epithelium-on corneal cross-linking protocols

Nada H. Aldahlawi [a], Sally Hayes [a], David P.S. O'Brart [b], Naomi D. O'Brart [a], Keith M. Meek [a, *]

[a] Structural Biophysics Research Group, School of Optometry and Vision Sciences, Cardiff University, Maindy Road, Cardiff, CF24 4HQ, UK
[b] Keratoconus Research Institute, Department of Ophthalmology, St Thomas Hospital, London, SE1 7EH, UK

ARTICLE INFO

Article history:
Received 9 June 2016
Received in revised form
10 October 2016
Accepted in revised form 14 October 2016
Available online 17 October 2016

Keywords:
Keratoconus
Cornea
Cross-linking
Epithelium-off
Epithelium-on
CXL
Enzymatic digestion

ABSTRACT

The aim of this study was to investigate corneal enzymatic resistance following epithelium off and on riboflavin/UVA cross-linking (CXL). One hundred and fourteen porcine eyes were divided into four non-irradiated control groups and seven CXL groups. The latter comprised; (i) epithelium-off, 0.1% iso-osmolar riboflavin, 9 mW UVA irradiation for 10 min, (ii) disrupted epithelium, 0.1% hypo-osmolar riboflavin, 9 mW UVA for 10 min, (iii) epithelium-on, 0.25% hypo-osmolar riboflavin with 0.01% benzylalkonium chloride (BACS), 9 mW UVA for 10 min, (iv) epithelium-on, 5 min iontophoresis at 0.1 mA for 5 min with 0.1% riboflavin solution, 9 mW UVA for 10 min or (v) 12.5 min, (vi) epithelium-on, prolonged iontophoresis protocol of 25 min with 1.0 mA for 5 min and 0.5 mA for 5 min with 0.25% riboflavin with 0.01% BACS, 9 mW UVA for 10 min or (vii) 12.5 min. Enzymatic resistance was assessed by daily measurement of a corneal button placed in pepsin solution and measurement of corneal button dry weight after 11 days of digestion. This study revealed that the enzymatic resistance was greater in CXL corneas than non-irradiated corneas ($p < 0.0001$). Epithelium-off CXL showed the greatest enzymatic resistance ($p < 0.0001$). The prolonged iontophoresis protocol was found to be superior to all other trans-epithelial protocols ($p < 0.0001$). A 25% increase in UVA radiance significantly increased corneal enzymatic resistance ($p < 0.0001$). In conclusion, although epithelium-on CXL appears to be inferior to epithelium-off CXL in terms of enzymatic resistance to pepsin digestion, the outcome of epithelium-on CXL may be significantly improved through the use of higher concentrations of riboflavin solution, a longer duration of iontophoresis and an increase in UVA radiance.

1. Introduction

Over the past decade, riboflavin/UVA corneal cross-linking (CXL) has become an established treatment to halt the progression of keratoconus and other corneal ectasias. Riboflavin is a hydrophilic molecule, with a molecular weight of 340 Da, while, the corneal epithelium is lipophyllic, with a decreasing permeability to molecules over 180 Da (Huang et al., 1989). Therefore in the "gold-standard" CXL protocol the epithelium is removed from the central corneal to allow adequate stromal absorption of riboflavin prior to UVA irradiation. Spoerl et al. confirmed this need for epithelial removal, reporting no changes in corneal biomechanics when CXL was performed with the epithelium intact (Spoerl et al., 1998). On this basis, the epithelium was removed in the first published clinical studies (Caporossi et al., 2006; Gkika et al., 2011; O'Brart et al., 2011; Richoz et al., 2013; Wittig-Silva et al., 2014; Wollensak et al., 2003). However, epithelial debridement is associated with a number of adverse events, including severe ocular pain in the immediate post-operative period, delayed visual rehabilitation and the risks of scarring, infectious and non-infectious keratitis (Koller et al., 2009).

As a result of such considerations, a number of trans-epithelial CXL techniques have been postulated. The first epithelium-on CXL (epi-on-CXL) protocols included the use of multiple topical applications of tetracaine 1% to disrupt epithelial tight junctions (Boxer Wachler et al., 2010; Chan et al., 2007) and partial epithelial debridement in a grid pattern (Rechichi et al., 2013). More recently, novel formulations of riboflavin have been developed to facilitate

* Corresponding author. School of Optometry and Vision Sciences, Cardiff University, Maindy Road, Cathays, Cardiff CF24 4HQ, UK.
E-mail address: MeekKM@cardiff.ac.uk (K.M. Meek).

http://dx.doi.org/10.1016/j.exer.2016.10.014

epi-on-CXL. Laboratory studies have shown that riboflavin preparations in which trometamol (Tris-hydroxymethyl-aminometane) and sodium ethylenediaminetetraacetic acid (EDTA) have been added facilitate stromal absorption when used in conjunction with superficial/grid pattern epithelial trauma (Alhamad et al., 2012). Similarly, preparations without dextran but with sodium chloride 0.44% and benzalkonium chloride (BAC) have been shown to facilitate trans-epithelial riboflavin stromal absorption (Kissner et al., 2010; Raiskup et al., 2012). Clinical studies with such formulations have demonstrated equivocal results with some suggesting similar efficacy to epithelium-off CXL (epi-off-CXL) (Filippello et al., 2012; Magli et al., 2013), and others showing less pronounced effects (Buzzonetti and Petrocelli, 2012; Kocak et al., 2014; Koppen et al., 2012; Leccisotti and Islam, 2010). As riboflavin is negatively charged at physiological pH and soluble in water, iontophoresis as a means of enhancing trans-epithelial absorption has also been postulated. In vitro studies of CXL using iontophoresis-assisted delivery (Ion-CXL) of riboflavin 0.1% with a current of 0.5–1 mA for 5–10 min have been encouraging, demonstrating enhanced trans-epithelial riboflavin absorption and corneal tissue biomechanics (Cassagne et al., 2016; Lombardo et al., 2014; Mastropasqua et al., 2014; Touboul et al., 2014; Vinciguerra et al., 2014a). Early clinical studies have reported cessation of progression and improvements in keratometric and visual parameters (Bikbova and Bikbov, 2014; Buzzonetti et al., 2015; Vinciguerra et al., 2014b).

In addition to the desire to keep the epithelium intact, the current "gold-standard", epi-off-CXL protocol, involves a 30 min application of riboflavin followed by a 30 min irradiation with 370 nm UVA light, with an intensity of 3 mW/cm^2, necessitating in excess of one hour treatment time. In an attempt to reduce treatment times, the use of accelerated CXL (A-CXL) procedures using the same energy dose but higher UVA intensities and shorter exposure times have been investigated. Published clinical studies of A-CXL protocols are relatively few. However, those using 7 mW for 15 min or 9 mW for 10 min have reported improvements in corrected distance acuity and a reduction in topographic keratometry at up to 46 months follow-up with no adverse events associated with the high fluences used (Cinar et al., 2014; Cummings et al., 2016; Kanellopoulos, 2012; Kymionis et al., 2014a; Shetty et al., 2015). More recently, it has also been demonstrated that the efficacy of A-CXL may be further improved by increasing the UVA exposure time and the overall cumulative dosage (Aldahlawi et al., 2016; Kymionis et al., 2014b; Sherif, 2014).

Increased resistance of the corneal stroma to enzymatic digestion following standard (Hayes et al., 2013; Spoerl et al., 2004) and accelerated (Aldahlawi et al., 2015) epi-off-CXL has been demonstrated by a number of investigators. It is likely that the improved enzymatic resistance is an important factor in protection against disease progression, since an increase in proteinase activity and a reduction in proteinase inhibitor activity has been identified in keratoconic corneas (Zhou et al., 1998). In order to investigate the efficacy of a number of different epi-on-CXL protocols, we compared the enzymatic resistance of corneal tissue cross-linked using epi-off-CXL with that of corneas treated with partially disrupted-epithelium CXL (dis-CXL), existing epi-on-CXL protocols (involving different riboflavin formulations and modes of delivery) and a prolonged iontophoresis CXL protocol with 0.25% riboflavin (TC-ion-CXL) that we have recently developed. In addition to this we examined the effect of increasing the cumulative UVA dosage on the enzymatic resistance of corneas treated with iontophoresis-assisted epi-on-CXL. Pepsin was selected as the enzyme of choice for this study in favour of collagenase, as it is a non-specific endopeptidase that can break down both collagen and proteoglycan core proteins, both of which are believed to be sites of riboflavin/UVA induced cross-links (Hayes et al., 2013). Porcine eyes were used as, unlike human cadaver eyes and rabbit eyes which are of limited availability in the UK, they were readily available in the fresh state and in the large numbers required for this study. However, due to the porcine cornea having a thicker epithelium than the human cornea, the results presented herein should be regarded as a conservative assessment of the effectiveness of trans-epithelial CXL.

2. Materials and methods

2.1. Specimen preparation

A total of one hundred and fourteen fresh porcine cadaver eyes with clear corneas and intact epithelium were retrieved from a local European Community licensed abattoir within 6–8 h of death. Due to the large number of eyes and treatment groups involved, it was necessary to split the study into two runs. Run 1 examined the effectiveness of dis-CXL and epi-on-CXL protocols at increasing corneal enzymatic resistance to digestion with pepsin, whilst run 2 examined the effect on enzymatic resistance of increasing the UVA dosage by 25% from 5.4 J/cm^2 to 6.75 J/cm^2 during iontophoretic epi-on-CXL. In both runs, the effectiveness of the standard epi-off CXL protocol at increasing enzymatic resistance was also examined for comparative purposes. The 11 treatment groups are described below and summarised in Table 1.

Run 1:

Each treatment group consisted of six eyes.

i) Epi-off standard protocol (Group 1: Epi-off-ribo; Group 2: Epi-off-CXL)

Complete corneal epithelial debridement was performed in groups 1 and 2 using a single edged razor blade. These eyes then received 0.1% riboflavin eye drops containing 20% dextran T-500 solution (Mediocross D®, Peschke Meditrade, Huenenberg, Switzerland) every 5 min for 30 min. The central 9 mm region of corneas in group 2 was then exposed to 365 nm UVA light with a fluence of CXL 9 mW/cm^2 for 10 min using a CCL-365 Vario™ cross-linking system (Peschkmed, Huenenberg, Switzerland). During irradiation, riboflavin was re-applied at 5 min intervals. Group 1 served as a non-irradiated control.

ii) Epi-disrupted protocol (Group 3: Dis-ribo; Group 4: Dis-CXL)

Partial epithelial disruption was performed in groups 3 and 4, by making 64 full-thickness epithelial punctures with a 25 gauge needle in an 8 × 8 grid pattern. The corneas were then soaked in riboflavin 0.1% dextran-free solution (Vitamin B2 Streuli, Uznach, Switzerland) for 30 min and rinsed with phosphate-buffered saline (PBS) for 5 min. Group 4 was then irradiated with 9 mW UVA for 10 min with PBS applied at 5 min intervals to keep the corneal surface moist. Group 3 served as a non-irradiated control.

iii) Epi-on and high riboflavin concentration protocol (Group 5: Medio-ribo; Group 6: Medio-CXL)

Groups 5 and 6 received 0.25% riboflavin with 1.2% hydroxypropylmethyl cellulose (HPMC) and 0.01% BAC (Mediocross TE®, Peschketrade, Huenenberg, Switzerland) every 5 min for 30 min. This was followed by a 5 min rinse with PBS. Group 6 was then irradiated with 9 mW UVA for 10 min with PBS applied at 5 min intervals. Group 5 served as a non-irradiated control.

iv) Epi-on, high riboflavin concentration and prolonged iontophoresis (St. Thomas-Cardiff) protocol (Group 7: TC-ion-ribo; Group 8: TC-ion-CXL)

Groups 7 and 8 received iontophoresis assisted delivery of 0.25% riboflavin with 1.2% HPMC and 0.01% BAC (Mediocross TE®, Peschketrade, Huenenberg, Switzerland) using a current of 1 mA for 5 min. The corneas were then soaked with this riboflavin

Table 1
Treatment groups.

Group	Abbreviation	Epithelium	Riboflavin formulation	Ionto (1 mA)	Ribo soak	Ionto (0.5 mA)	Ribo soak	Saline rinse	9 mW UVA	Applied during irradiation
(1)Epithelium-off non-irradiated control	Epi-off-ribo	Off	Mediocross D: 0.1% Riboflavin, 20% dextran	–	30 min	–	–	–	–	–
(2) Epithelium-off standard CXL	Epi-off-CXL 5.4 J/cm^2	Off	Mediocross D	–	30 min	–	–	–	10 min	Mediocross D
(3) Disrupted epithelium non-irradiated control	Dis-ribo	Disrupted	Vitamin B2 Streuli: 0.1% riboflavin, saline	–	30 min	–	–	5 min	–	–
(4) Disrupted epithelium CXL	Dis-CXL 5.4 J/cm^2	Disrupted	Vitamin B2 Streuli	–	30 min	–	–	5 min	10 min	PBS
(5) Epithelium intact non-irradiated control	Medio-ribo	On	Mediocross TE: 0.25% riboflavin, 1.2% HPMC, 0.01% BACS, Pi-water	–	30 min	–	–	5 min	–	–
(6) Epithelium intact high riboflavin concentration CXL	Medio-CXL 5.4 J/cm^2	On	Mediocross TE	–	30 min	–	–	5 min	10 min	PBS
(7) Epithelium intact, high riboflavin concentration and prolonged iontophoresis non-irradiated control	TC-ion-ribo	On	Mediocross TE	5 min	5 min	5 min	5 min	5 min	–	–
(8) Epithelium intact, high riboflavin concentration and prolonged iontophoresis CXL	TC-ion-CXL 5.4 J/cm^2	On	Mediocross TE	5 min	5 min	5 min	5 min	5 min	10 min	PBS
(9) Epithelium intact, high riboflavin concentration, prolonged iontophoresis and high UVA energy dose CXL	TC-ion-CXL 6.75 J/cm^2	On	Mediocross TE	5 min	5 min	5 min	5 min	3 min	12 min 30 s	PBS
(10) Epithelium intact, basic iontophoresis protocol	Ion-CXL 5.4 J/cm^2	On	Mediocross M: 0.1% riboflavin, 1.0% HPMC	5 min	–	–	–	3 min	10 min	PBS
(11) Epithelium intact, basic iontophoresis protocol with high UVA energy dose	Ion-CXL 6.75 J/cm^2	On	Mediocross M	5 min	–	–	–	3 min	12 min 30 s	PBS

solution for 5 min before a further application of iontophoresis with a power of 0.5 mA/min for 5 min and another 5 min riboflavin soak. The iontophoresis delivery system was used to treat ex vivo eyes by connecting the return electrode to a needle inserted into the vitreous chamber; the negative electrode was a steel grid contained in a corneal well applicator which was adhered to the eye by means of a vacuum well system (Fig. 1). The steel grid (negative electrode) was completely covered with riboflavin and the power generator set to the desired current and duration. The steel grid remained covered with riboflavin solution for the entire procedure. After treatment the applicator was removed from the cornea and the corneas were washed with PBS for 5 min. Group 8 was then irradiated with 9 mW UVA for 10min with PBS applied at 5 min intervals. Group 7 served as a non-irradiated control.

Run 2:

Each treatment group consisted of 11 eyes.

i) Epi-off standard protocol (Group 1: Epi-off-ribo; Group 2: Epi-off-CXL 5.4 J/cm^2)

Corneas were treated as described for groups 1 and 2 in run 1.

ii) Epi-on, high riboflavin concentration and prolonged iontophoresis (St. Thomas-Cardiff) protocol (Group 8: TC-ion-CXL 5.4 J/cm^2; Group 9: TC-ion-CXL 6.75 J/cm^2)

Groups 8 and 9 received iontophoresis assisted delivery of 0.25% riboflavin with 1.2% HPMC and 0.01% BAC (Mediocross TE®, Peschketrade, Huenenberg, Switzerland) using a current of 1 mA for 5min. The corneas were then soaked with this riboflavin solution for 5 min before a further application of iontophoresis with a power of 0.5 mA/min for 5 min and another 5 min riboflavin soak. Following a 3 min wash with PBS, the corneas in Group 8 were irradiated with 9 mW UVA for 10 min and those in Group 9 were irradiated with 9 mW UVA for 12min and 30 s. During irradiation, PBS was applied to all corneas at 5 min intervals.

iii) Epi-on basic iontophoresis protocol (Group 10: Ion-CXL 5.4 J/cm^2; Group 11: Ion-CXL 6.75 J/cm^2)

Groups 10 and 11 underwent iontophoresis assisted riboflavin delivery using an isotonic 0.1% riboflavin solution (Vitamin B2) containing 1.0% HPMC dextran-free solution (Mediocross M®, Peschketrade, Huenenberg, Switzerland) and a 1 mA current (Iontophoresis device, Sooft Italia S.p.A, Italy). After treatment the corneas were washed with PBS for 3 min. Group 10 was then irradiated with 9 mW UVA for 10min and group 11 was irradiated with 9 mW UVA for 12 min and 30 s. During irradiation, PBS was applied to all corneas at 5 min intervals.

2.2. Measurements of corneal thickness

Using a Pachette2™ Ultrasonic Pachymeter (DGH Technology, Exton, USA), the central corneal thickness was measured in all eyes prior to treatment and where applicable after removal of the epithelium, application of riboflavin and UVA irradiation.

2.3. Measurements of enzymatic digestion

A corneo-scleral ring was dissected from each eye immediately following treatment, wrapped tightly in Clingfilm™ (to prevent moisture loss) and refrigerated until all treatments were complete. An 8 mm corneal button was trephined from the centre of each cornea using a disposable skin biopsy punch. The corneal buttons were then immersed into individual plastic tubes, each containing 5 ml of pepsin solution, and incubated in a water bath at a temperature of 23 °C. The pepsin solution was made up of 1 g of >500 U/mg pepsin from porcine gastric mucosa (Sigma-Aldrich, Dorset, UK) in 10 ml 0.1 M HCL at pH 1.2. The structural integrity of the most anterior layers of the cornea was assessed by means of daily measurements of corneal button diameter. The measurements, which were made using an electronic digital caliper, continued until the specimen could no longer be distinguished from the surrounding pepsin solution. At this point the tissue was considered to have undergone complete digestion.

As an additional means of assessing enzymatic resistance, 5 corneal buttons from each of the 6 treatment groups in run 2 were removed after 11 days in pepsin digest solution and placed in a 60 °C oven until a constant dry weight was obtained. The dry weight of the tissue represents the total mass of undigested tissue and can therefore be used as an indicator of the effective depth of cross-linking.

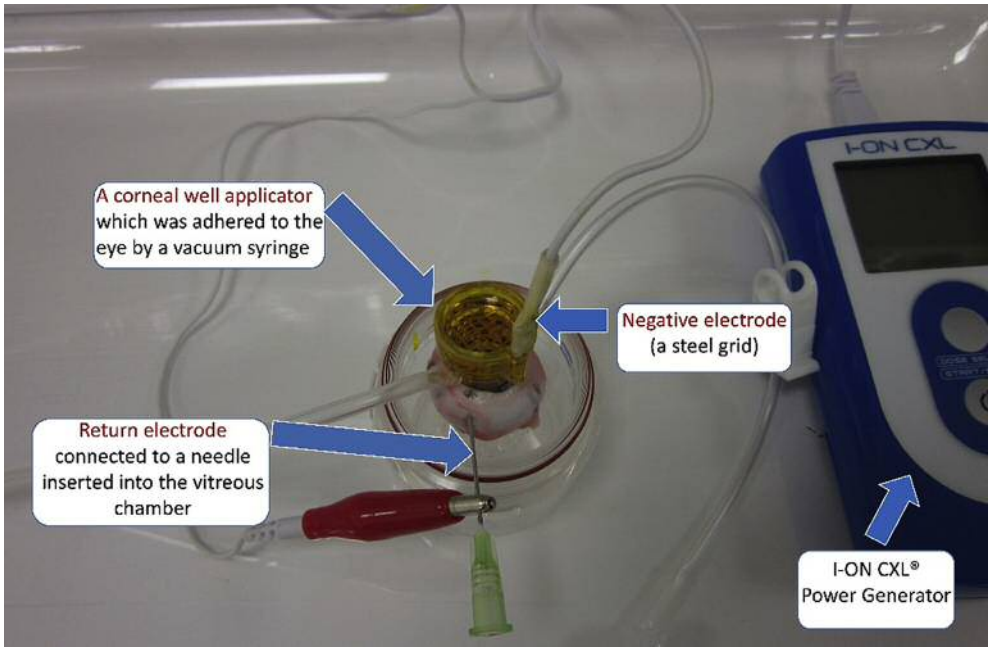

Fig. 1. Iontophoresis riboflavin delivery system modified for use in ex-vivo eyes.

2.4. Statistical evaluation

Measurements of corneal thickness, complete digestion time and tissue dry weight were statistically analysed using a one-way analysis of variance (ANOVA) test. Post hoc Bonferroni comparisons were used to isolate significant interactions. All statistical analyses were performed with the Statistical Package for the Social Sciences (IBM SPSS Statistics 20, New York, USA). $P < 0.01$ was considered significant. Data were presented in the results as mean ± standard deviation (SD).

3. Results

3.1. Corneal thickness

Fig. 2 shows the average corneal thickness pre-treatment, post-riboflavin application and post-irradiation for each treatment group in runs 1 and 2. Statistical tests revealed that corneas treated using the standard, epi-off protocol and an iso-osmolar riboflavin solution (groups 1 and 2) were significantly thinner than the corneas in all other groups ($p < 0.007$).

3.2. Qualitative assessment of riboflavin uptake

As shown in Fig. 3, the distinctive yellow colouration of riboflavin was most clearly visible in the epi-off and TC-ion treated corneas. Although riboflavin was also seen in corneas from other treatment groups, the colour was notably less intense. Photographs recorded during the irradiation process in run 2 showed a non-homogenous distribution of riboflavin in Ion-CXL treated corneas and a more uniform distribution following epi-off CXL and TC-Ion-CXL.

3.3. Pepsin digestion of corneal buttons

Table 2 shows the number of days required for complete tissue digestion to occur in each irradiated and non-irradiated treatment group. Although the digestion times of equivalent non-irradiated (group 1) and cross-linked treatment groups (group 2) were seen to vary slightly between runs 1 and 2, possibly as a result of differences in the breed and age of the pig eyes, the overall trends were consistent between the two runs. For this reason the data from each run was normalized against the total digestion time of the standard epi-off CXL group to facilitate comparison between the two runs (Figs. 4 and 5).

Figs. 4 and 5 show cumulative measurements of corneal disk diameter for each irradiated and non-irradiated treatment group throughout the digestion process. In both runs 1 and 2, the cross-linked groups showed a significantly greater resistance to enzymatic digestion than the non-irradiated groups ($p < 0.0001$). In run 1, complete digestion of all non-irradiated corneas had occurred by day 13 (Table 2). At the same time point (normalized digestion time of 0.33), the mean diameter of the epi-off-CXL, dis-CXL, medio-CXL and TC-ion-CXL groups had only decreased by 39%, 62%, 74%, and 40% respectively (Fig. 4). No significant difference was found between the non-irradiated groups in terms of either the average corneal button diameter at any time point in the digestion process or in the time required for complete digestion to occur (Fig. 4).

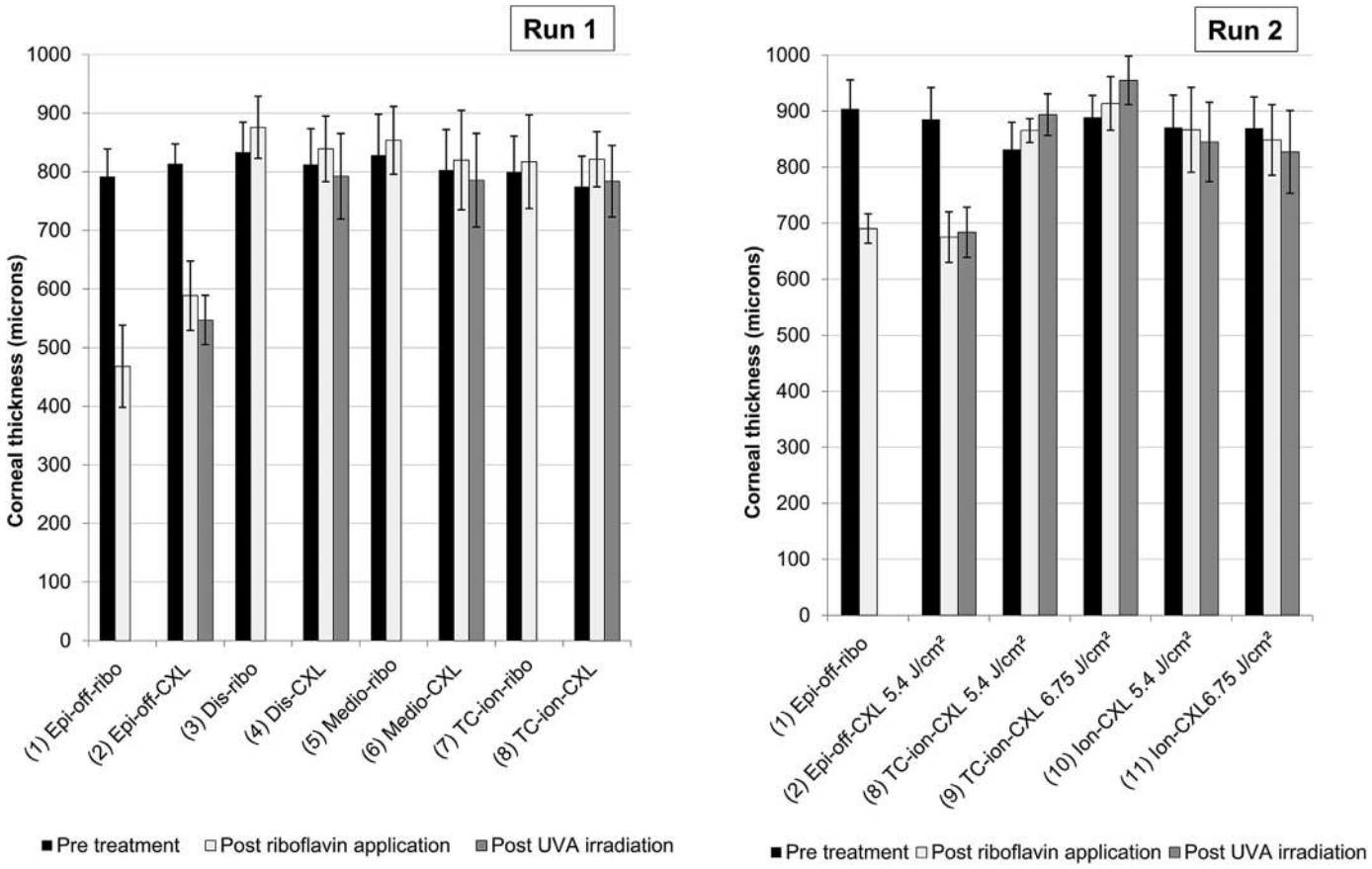

Fig. 2. Corneal thickness measurements are shown for each group in run 1 and run 2 before treatment, after riboflavin application and where applicable, following UVA irradiation.
*In groups 1 and 2 the corneal epithelium (measuring ~90 μm in thickness) was removed as part of the riboflavin application process.

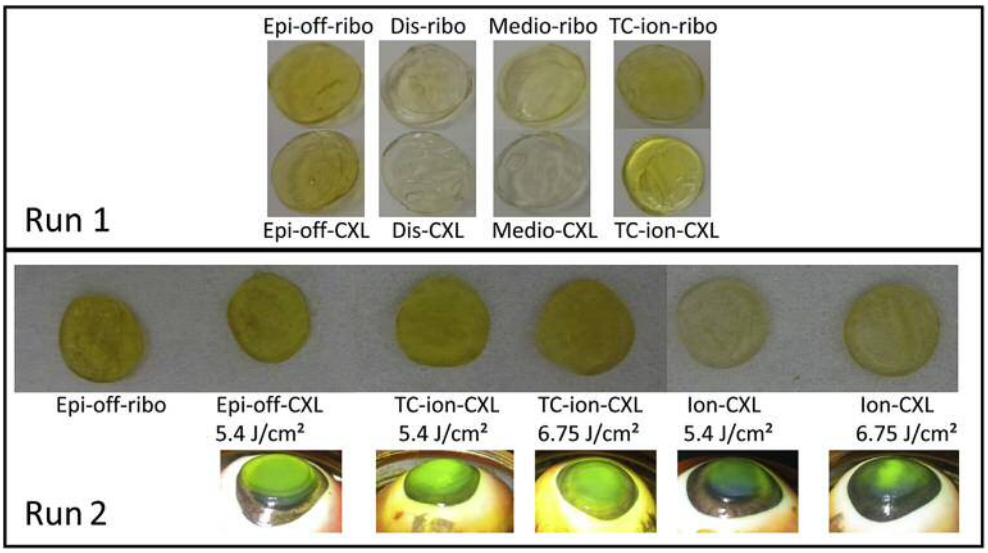

Fig. 3. Corneal buttons from each group in run 1 and 2 are shown immediately post-treatment. The characteristic yellow colour of riboflavin can be seen most clearly in the epithelium-removed, riboflavin treated corneas (epi-off) and in the corneas that received riboflavin via the St Thomas's/Cardiff modified iontophoresis protocol (TC-Ion). Photographs recorded during the irradiation process show a non-homogenous distribution of riboflavin in corneas treated with the basic iontophoresis protocol (Ion-CXL).

Table 2
Time taken for the complete tissue digestion to occur.

Groups	Time taken for complete digestion (in days)		
	Minimum	Maximum	Average (±SD)
RUN 1			
(1) Epi-off-ribo	11	12	11.5 ± 0.55
(2) Epi-off-CXL 5.4 J/cm^2	39	40	39.5 ± 0.55
(3) Dis-ribo	11	13	11.8 ± 0.75
(4) Dis-CXL 5.4 J/cm^2	15	16	15.6 ± 0.52
(5) Medio-ribo	11	12	11.6 ± 0.51
(6) Medio-CXL 5.4 J/cm^2	14	15	14.6 ± 0.52
(7) TC-ion-ribo	11	12	11.3 ± 0.52
(8) TC-ion-CXL 5.4 J/cm^2	32	33	32.2 ± 0.41
RUN 2			
(1) Epi-off-ribo	9	10	9.5 ± 0.55
(2) Epi-off-CXL 5.4 J/cm^2	43	44	43.5 ± 0.55
(8) TC-ion-CXL 5.4 J/cm^2	34	35	34.3 ± 0.52
(9) TC-ion-CXL 6.75 J/cm^2	41	42	41.7 ± 0.52
(10) Ion-CXL 5.4 J/cm^2	27	28	27.3 ± 0.52
(11) Ion-CXL 6.75 J/cm^2	34	35	34.5 ± 0.55

There were however significant differences between the cross-linked groups in term of the time taken for complete digestion to occur (Fig. 4). The conventionally treated, epi-off-CXL corneas (group 2) took significantly longer to digest than all other cross-linked corneas ($p < 0.0001$). Although less resistant to enzyme digestion than the epi-off-CXL corneas, the TC-ion-CXL treated corneas (group 8) took significantly longer to digest than corneas treated with other disrupted epithelium (dis-CXL) or epi-on-CXL protocols ($p < 0.0001$).

In run 2, the non-irradiated corneas were completely digested by day 10 (Table 2). At this same time point, which corresponds to a normalized digestion time of 0.25, the mean diameter of corneas in the epi-off-CXL 5.4 J/cm^2, TC-ion-CXL 5.4 J/cm^2, TC-ion-CXL 6.75 J/cm^2, Ion-CXL 5.4 J/cm^2 and Ion-CXL 6.75 J/cm^2 treatment groups had reduced by 21.4%, 16.2%, 13.4%, 26.7% and 19.4% respectively (Fig. 5). Significant differences in the mean disk diameter of the CXL treatment groups were only apparent after 24 days of digestion (corresponding to a normalized digestion time of 0.6 in Fig. 5). The epi-off-CXL group (group 2) took longer to undergo complete digestion than all other cross-linked groups ($p < 0.0001$) but corneas treated with the prolonged, high riboflavin concentration, iontophoresis protocol (TC-ion-CXL) were found to persist in the pepsin digest solution for significantly longer than those treated with the basic Ion-CXL protocol (Fig. 5). In both the Ion-CXL and TC-ion-CXL treatment groups, an increase in UVA radiance from 5.4 J/cm^2 to 6.75 J/cm^2 resulted in a significant increase in the time required for complete digestion to occur ($P < 0.0001$).

3.4. Undigested tissue mass

In run 2, only the cross-linked corneas remained after 11 days in pepsin digest solution (Fig. 6). At this time point, the average stromal dry weight of the epi-off-CXL 5.4 J/cm^2 treated corneas (group 2) was significantly higher than that of all other treatment groups (groups 8, 10, 11, $P < 0.0001$; group 9, $P < 0.001$). The stromal dry weight did not differ significantly between the Ion-CXL 5.4 J/cm^2 and Ion-CXL 6.75 J/cm^2 treatment groups ($p = 0.32$) or between the TC-ion-CXL 5.4 J/cm^2 and TC-ion-CXL 6.75 J/cm^2 groups ($p = 0.038$). However, corneas treated with the TC-Ion-CXL 6.75 J/cm^2 protocol had a higher stromal dry weight than corneas treated with basic ion-CXL 5.4 J/cm^2 protocol ($p < 0.003$).

4. Discussion

Attaining adequate stromal riboflavin concentration is essential for CXL. Riboflavin acts as a photo-sensitizer for the production of oxygen free radicals, which drive the CXL process (McCall et al., 2010) and as a result insufficient stromal absorption may result in treatment failure (Wollensak et al., 2003; Wollensak and Iomdina, 2009). As riboflavin is a hydrophilic molecule which cannot penetrate epithelial cell membranes and tight junctions, the first riboflavin/UVA CXL protocols required complete central corneal epithelial debridement prior to riboflavin application (Spoerl et al., 1998; Wollensak et al., 2003). Although epi-off-CXL is considered to be the gold standard procedure, with multiple prospective and randomized controlled studies demonstrating its efficacy in terms of cessation of keratoconus progression and improvements in keratometric and visual parameters (Caporossi et al., 2006; Gkika et al., 2011; O'Brart et al., 2011; Richoz et al., 2013; Wittig-Silva et al., 2014; Wollensak et al., 2003), new methods of epi-on-CXL

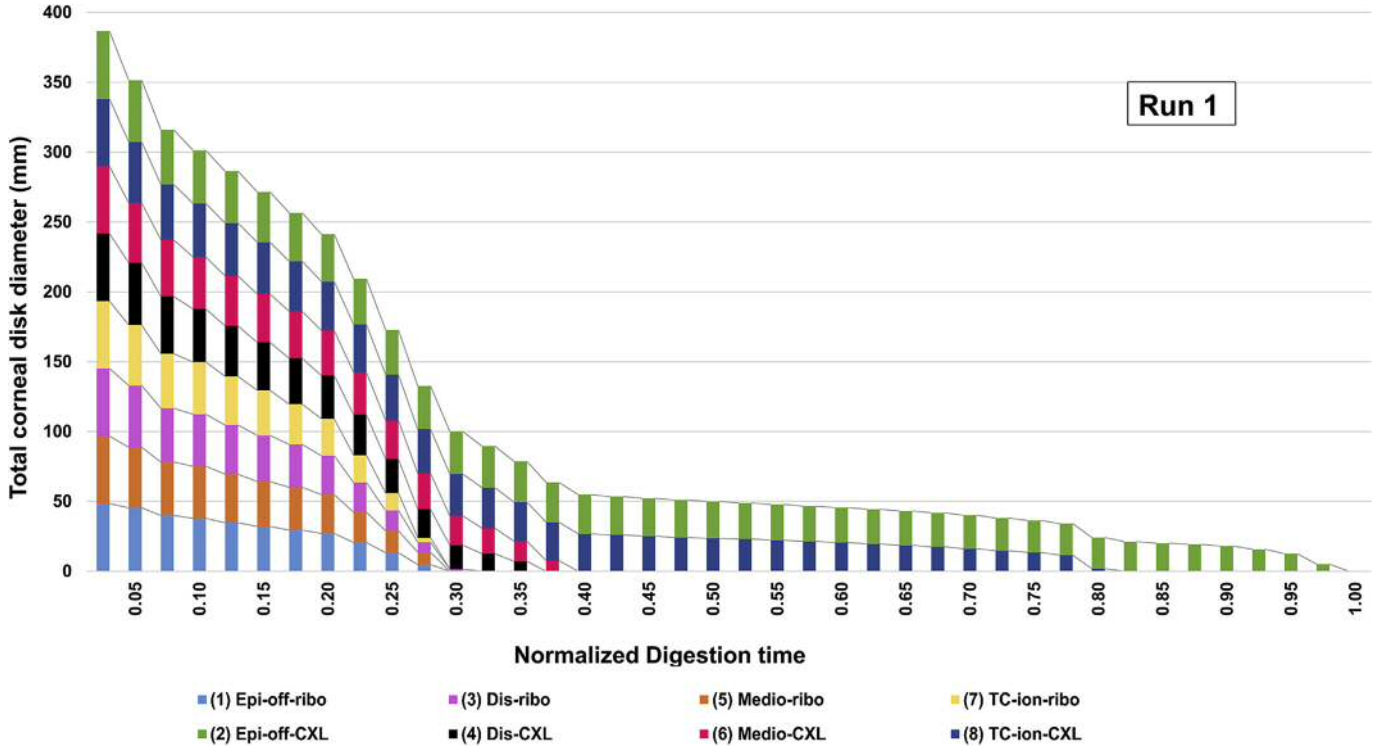

Fig. 4. The summed diameter of all corneal disks within each treatment group (n = 6) are shown for run 1 as a function of time in pepsin digest solution. The digestion time for each treatment group has been normalized against the total digestion time of the standard epi-off CXL group.

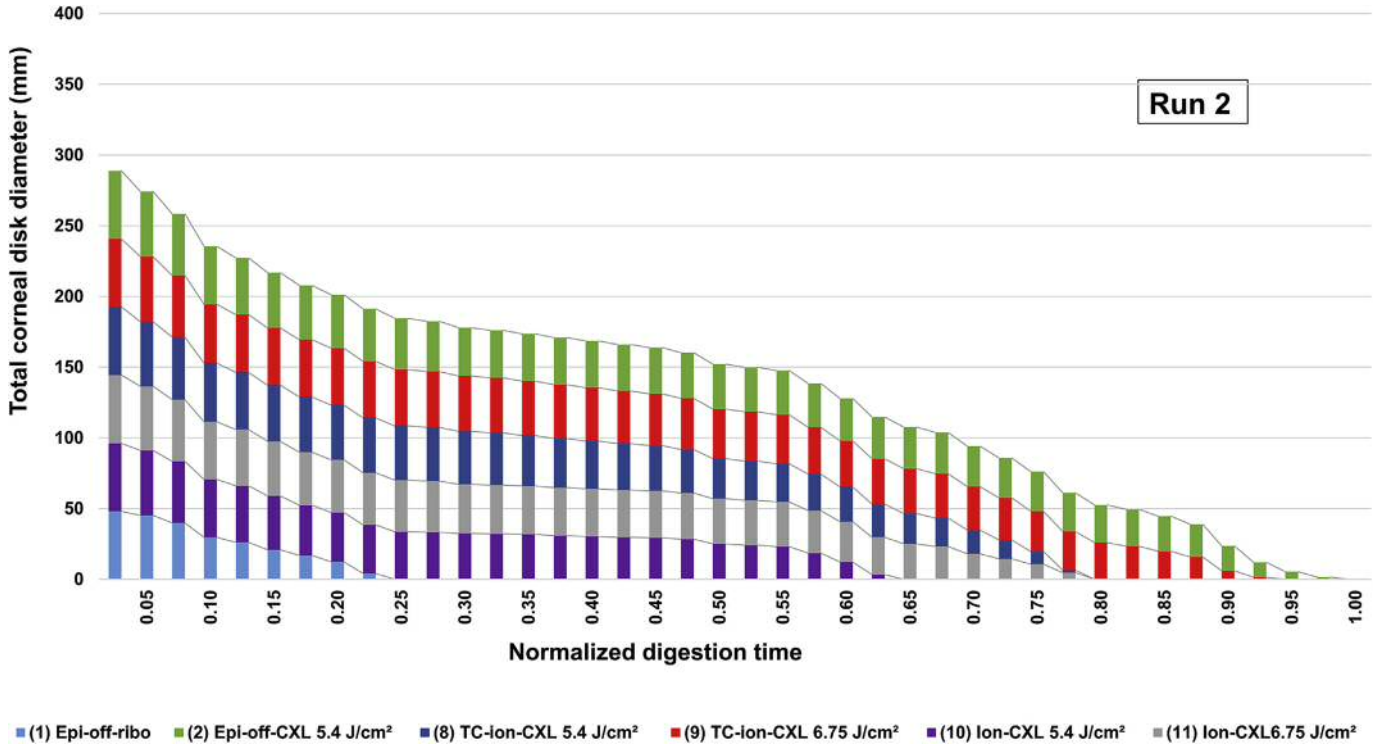

Fig. 5. The summed diameter of all corneal disks within each treatment group (n = 6) are shown for run 2 as a function of time in pepsin digest solution. The digestion time for each treatment group has been normalized against the total digestion time of the standard epi-off CXL group.

have been postulated to remove the need for epithelial debridement, thereby alleviating post-operative pain and potential risks of infection (Koller et al., 2009). In addition, to reduce the long treatment times associated with epi-off-CXL with 3mw/cm^2 UVA irradiation, the use of A-CXL protocols using the same energy dose but higher UVA intensities and shorter exposure times have been

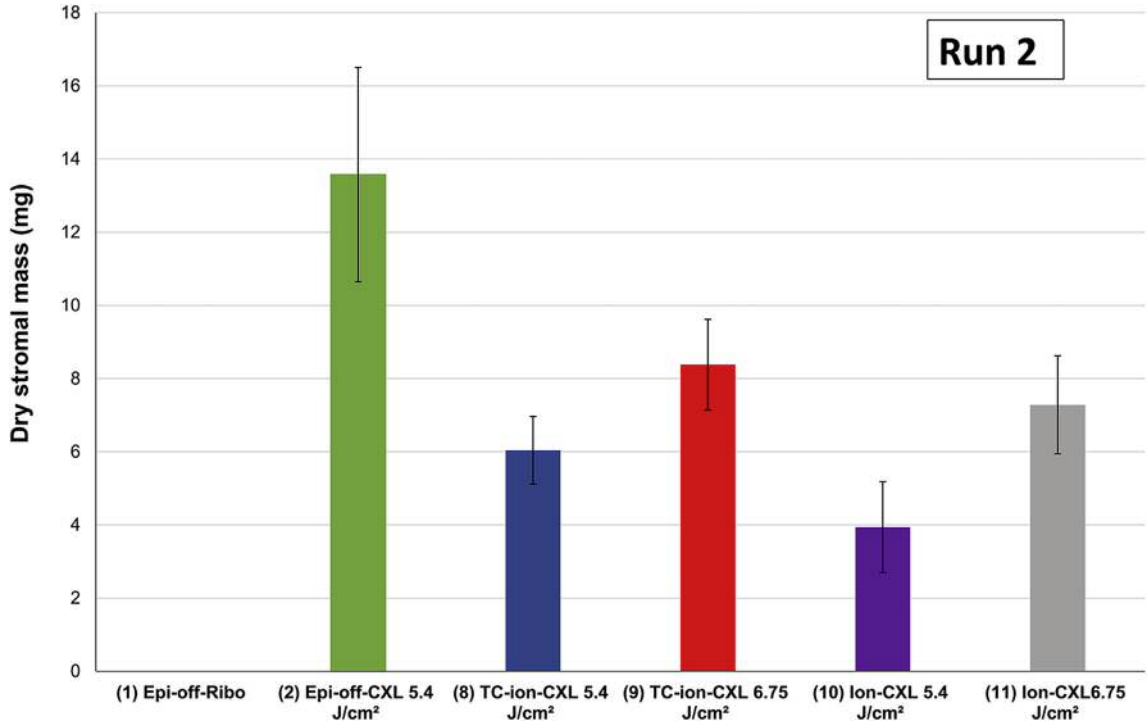

Fig. 6. Corneal button dry weight after 11 days of digestion. Error bars show standard deviation.

advocated. In order to evaluate the efficacy of such differing CXL protocols, multiple methodologies, including extensiometry (Cassagne et al., 2016; Kissner et al., 2010; Vinciguerra et al., 2014a; Wollensak and Iomdina, 2009), shear wave elastography (Touboul et al., 2014), Brillouin microscopy (Scarcelli et al., 2013) and Scheimpflug air pulse tonometry (Mastropasqua et al., 2014) have been employed. However each of these methodologies have their inherent inaccuracies and as yet there is no agreed best practice for assessing biomechanical changes following CXL.

Although the precise aetiology of keratoconus is unknown (Davidson et al., 2014), an increased activity of protease enzymes and reduced activity of protease inhibitors has been identified (Spoerl et al., 2004), with the resultant increase in stromal protein digestion liable to be a factor in corneal thinning and secondary biomechanical instability (Andreassen et al., 1980). Spoerl et al. (2004) reported increased resistance of stromal tissue to enzymatic digestion following epi-off CXL with a dose response related to the intensity of UVA irradiance. This increased resistance to protease digestion following CXL has been replicated by others (Hayes et al., 2013; Aldahlawi et al., 2016) and is thought to be an important factor in preventing disease progression. In this study we utilized enzymatic resistance to pepsin digestion to evaluate the effects of epi-off-CXL, dis-CXL and epi-on-CXL. Although minor differences in the rate of enzymatic digestion were seen between similarly treated corneas in runs 1 and 2, possibly due to variations in the age and breed of the pig eyes in different batches of abattoir tissue, each run showed an increased resistance in all of the cross-linked groups compared to their non-irradiated controls. However, in accordance with the findings of Wollensak and Iomdina (2009), which reported corneal stiffness after epi-on-CXL to be only one fifth of that seen after epi-off-CXL (indicating a reduced cross-linking effect), we found enzymatic resistance to be significantly greater with epi-off-CXL than with dis-CXL or epi-on-CXL. Whilst dis-CXL showed a greater resistance to digestion than the non-irradiated controls, it was not as effective as the other epi-on-CXL protocols tested, possibly due to the non-homogeneous uptake of riboflavin that we have documented previously (Alhamad et al., 2012). Such observations are supported by a recently published, randomized controlled study which showed better corneal flattening with epi-off-CXL than dis-CXL, although interestingly, dis-CXL resulted in better improvement of corrected distance visual acuity at 6 months (Razmjoo et al., 2014).

In this study we showed that corneas cross-linked using Mediocross TE® (Medio-CXL protocol) showed a greater resistance to enzymatic digestion than non-irradiated controls and dis-CXL treated corneas. However, the enhanced enzymatic resistance achieved with Medio-CXL was found to be inferior to that of the epi-off and ion-CXL protocols. Mediocross TE® is a hypo-osmolar riboflavin solution that contains 0.01% BAC, a cationic surfactant that can disrupt epithelial tight junctions to increase corneal permeability to riboflavin (Kissner et al., 2010; Raiskup et al., 2012). Laboratory studies have shown that preparations with sodium chloride and BAC can facilitate riboflavin transfer through an intact epithelium albeit in a reduced concentration compared to the epi-off-CXL (Touboul et al., 2014), and with significant associated superficial epithelial damage (Uematsu et al., 2007). Published clinical studies using enhanced riboflavin solutions with epithelial penetration enhancers are limited and have produced equivocal results. Some have reported similar efficacy to epi-off-CXL (Filippello et al., 2012; Magli et al., 2013), while others have demonstrated less pronounced effects with high rates of treatment failure (Buzzonetti and Petrocelli, 2012; Kocak et al., 2014; Koppen et al., 2012; Leccisotti and Islam, 2010). There are currently only three published randomized, controlled trials comparing epi-off and epi-on-CXL. Two of the studies, with follow-up times of up to 12 months, reported similar outcomes (Nawaz et al., 2015; Rossi et al., 2015). However, the third study, showed epi-on-CXL to be safe but demonstrated continued progression of keratoconus in 23% of cases at 12 month follow-up (Soeters et al., 2015). The latter result is consistent with the less pronounced biomechanical changes

observed experimentally following epi-on-CXL (Wollensak and Iomdina, 2009).

As riboflavin is negatively charged at physiological pH and soluble in water, the use of iontophoresis has been postulated to enhance trans-epithelial absorption. Commercially recommended protocols for iontophoresis utilize 0.1% riboflavin solution and electrical currents of 0.5–1 mA for 5–10 min. Treatment of rabbit corneas by this means has been shown to reduce the stromal riboflavin uptake achieved with epi-off-CXL by two thirds, but to produce a similar improvement in corneal biomechanics (Cassagne et al., 2016). Studies on rabbit and human cadaver corneas have demonstrated similar findings, with better riboflavin penetration and increased elastometry measurements obtained with Ion-CXL than with epi-on-CXL (using Ricrolin TE) but less than epi-off-CXL (Vinciguerra et al., 2014a). In a human donor eye model, Mastropasqua et al. demonstrated a corneal stiffening effect following Ion-CXL (Mastropasqua et al., 2014), with Lombardo et al. (2014) reporting an almost comparable effect on corneal stiffness to that with epi-off-CXL. These findings have been confirmed by supersonic shear wave elastography (Touboul et al., 2014). Furthermore, initial clinical studies in prospective case series have reported cessation of keratoconus progression with up to 15 month follow-up and some limited improvements in keratometric and visual parameters (Bikbova and Bikbov, 2014; Buzzonetti et al., 2015; Vinciguerra et al., 2014b). However, the relative efficacy of this technique compared to epi-off-CXL remains to be determined especially over longer term follow-up.

Using spectrophotometry (Hayes et al., 2015) and two-photon fluorescence microscopy (Gore et al., 2014), we have found that stromal riboflavin absorption in epithelium-intact corneas can be improved by increasing riboflavin concentration, epithelial contact time and iontophoresis dosage. Based on this work, we have modified the basic Sooft italia Ion-CXL protocol (Sooft italia S.p.A, Motegiorgio, Italy) and developed the St Thomas's/Cardiff modified iontophoresis protocol (TC-ion-CXL) which uses Mediocross TE® as the iontophoretic solution instead of Ricrolin+®, as the riboflavin concentration of the former is higher (0.25%) and the use of the cationic surfactant BAC has been shown with percutaneous treatment to have synergistic effect with iontophoresis on the transport of anions (Fang et al., 1998). In addition to using this formulation, the modified protocol employed a riboflavin-epithelial contact period of 5 min after iontophoresis to allow time for the sub-epithelial iontophoretically delivered riboflavin to diffuse homogeneously into the stroma, as well as an increased dosage of iontophoresis with a second treatment 5 min after the first. Results from the present study demonstrated that both the basic Ion-CXL and modified TC-ion-CXL protocols resulted in a greater resistance to enzymatic digestion than all other dis-CXL and trans-epithelial CXL protocols tested. Furthermore, as we have demonstrated previously for epi-off CXL treated corneas (Aldahlawi et al., 2016), we have now shown that the enzymatic resistance of Ion-CXL and TC-ion-CXL treated corneas can also be enhanced by increasing the cumulative energy dose and allowing additional type I photochemical cross-linking to occur. The improvement in enzymatic resistance was evidenced by the Ion-CXL and TC-ion-CXL corneas treated with a total energy dose of 6.75 J/cm^2 persisting for longer in enzyme digest solution than those that received a lower energy dose of 5.4 J/cm^2. The absence of any difference in their dry weights after 11 days of digestion is likely explained by the fact that at this stage of the digestion process, the rate of digestion was similar for both the high and low energy treatment groups and significant differences in average corneal disk diameter were not observed until day 24.

The enzymatic resistance achieved with the TC-ion-CXL 6.75 J/cm^2 protocol was closest to that of the standard epi-off-CXL 5.4 J/cm^2 protocol, suggesting that this technique may be the best trans-epithelial alternative for epi-off-CXL. Its slightly lower efficacy compared to epi-off-CXL, demonstrated by measurements of corneal disk diameter and tissue dry weight, may be due to a reduced riboflavin stromal absorption or due to other factors. These might include absorption of UVA by riboflavin within the epithelium, resulting in shielding of the underlying stroma and a reduced UVA dosage to the stroma, although this is unlikely as a 3 min PBS wash of the ocular surface was performed before UVA exposure. Another possible cause of the reduced efficacy might be the oxygen consumption by the epithelium itself (Harvitt and Bonanno, 1998), which could reduce the amount of oxygen available to the stroma to drive the CXL process (McCall et al., 2010). Such problems may be overcome by additional manipulation of the UVA dosage, in terms of its intensity and duration and/or by increasing oxygen availability and require further investigation. One further explanation may be the limitation of our porcine model. As the porcine cornea has a much thicker corneal epithelium than the human cornea (90 μm and 50 μm respectively), the results of the current study should be regarded as a conservative assessment of the effectiveness of trans-epithelial CXL. Unfortunately, human donor corneas are unsuitable for examining the effects of CXL on enzymatic resistance due to the fact that donors are typically over 60 years old, and the naturally occurring cross-links which increase with age, may mask the effects of the CXL treatment under investigation. However, it would be interesting to repeat our methodology in the rabbit model which has a thinner epithelium (40 μm) and is closer in thickness to that of the human cornea. Such a study would complement our current findings by providing a more liberal estimate of the effectiveness of trans-epithelial cross-linking.

This study, which shows our St Thomas'/Cardiff modified iontophoresis protocol (TC-ion-CXL) to be more effective than other trans-epithelial CXL protocols at increasing the enzymatic resistance of the cornea supports the concept that iontophoresis-assisted CXL may, with modifications in terms of riboflavin concentration, duration of iontophoretic treatment, riboflavin soak-time and UVA energy dose, be an effective technique to prevent the progression of keratoconus and avoid the postoperative pain associated with epithelial debridement. Such a technique is envisaged to be especially useful for eyes that are not eligible for treatment with epi-off-CXL due to minimum corneal thickness values less than 400 μm. Further laboratory studies to optimize this protocol and randomized, prospective clinical studies to compare its efficacy with epi-off CXL are indicated and are currently being undertaken (O'Brart D, personal communication, International Standard Randomized Controlled Trials Number: 04451470).

Financial disclosure

No author has a financial or proprietary interest in any material or method mentioned.

Conflict of interest

The authors have no conflicts of interest to disclose.

Acknowledgements

This work was supported by MRC programme grant MR/K000837/1 and King Saud University funding KSU1269. The funders had no role in study design, data collection and analysis, decision to publish or preparation of the manuscript. The authors indicate no financial disclosures. We wish to thank Veni Vidi (Halifax, UK) for their generous provision of riboflavin for this study. Contributions of authors: design of the study (NA, SH, DO,

KM); conduct of the study (NA, SH, NO); management and analysis of the data (NA), interpretation of the data (NA, DO and SH); and preparation, review, or approval of manuscript (NA, SH, DO, KM).

References

Aldahlawi, N.H., Hayes, S., O'Brart, D.P.S., Akhbanbetova, A., Littlechild, S.L., Meek, K.M., 2016. Enzymatic resistance of corneas crosslinked using riboflavin in conjunction with low energy, high energy, and pulsed UVA irradiation modes. Investig. Ophthalmol. Vis. Sci. 57 (4), 1547–1552.

Aldahlawi, N.H., Hayes, S., O'Brart, D.P.S., Meek, K.M., 2015. Standard versus accelerated riboflavin-ultraviolet corneal collagen crosslinking: resistance against enzymatic digestion. J. Cataract. Refract. Surg. 41 (9), 1989–1996.

Alhamad, T.A., O'Brart, D.P.S., O'Brart, N.A.L., Meek, K.M., 2012. Evaluation of transepithelial stromal riboflavin absorption with enhanced riboflavin solution using spectrophotometry. J. Cataract. Refract. Surg. 38 (5), 884–889.

Andreassen, T.T., Simonsen, A.H., Oxlund, H., 1980. Biomechanical properties of keratoconus and normal corneas. Exp. Eye Res. 31 (4), 435–441.

Bikbova, G., Bikbov, M., 2014. Transepithelial corneal collagen cross-linking by iontophoresis of riboflavin. Acta Ophthalmol. 92 (1), E30–E34.

Boxer Wachler, B.S., Pinelli, R., Ertan, A., Chan, C.C.K., 2010. Safety and efficacy of transepithelial crosslinking (C3-R/CXL). J. Cataract. Refract. Surg. 36 (1), 186–188.

Buzzonetti, L., Petrocelli, G., 2012. Transepithelial corneal cross-linking in pediatric patients: early results. J. Refract. Surg. 28 (11), 763–767.

Buzzonetti, L., Petrocelli, G., Valente, P., Iarossi, G., Ardia, R., Petroni, S., 2015. Iontophoretic transepithelial corneal cross-linking to halt keratoconus in pediatric cases: 15-Month follow-up. Cornea 34 (5), 512–515.

Caporossi, A., Baiocchi, S., Mazzotta, C., Traversi, C., Caporossi, T., 2006. Parasurgical therapy for keratoconus by rib oflavin-ultraviolet type A rays induced cross-linking of corneal collagen - preliminary refractive results in an Italian study. J. Cataract. Refract. Surg. 32 (5), 837–845.

Cassagne, M., Laurent, C., Rodrigues, M., Galinier, A., Spoerl, E., Galiacy, S.D., Soler, V., Fournie, P., Malecaze, F., 2016. Iontophoresis transcorneal delivery technique for transepithelial corneal collagen crosslinking with riboflavin in a rabbit model. Investig. Ophthalmol. Vis. Sci. 57 (2), 594–603.

Chan, C.C.K., Sharma, M., Wachler, B.S.B., 2007. Effect of inferior-segment Intacs with and without C3-R on keratoconus. J. Cataract. Refract. Surg. 33 (1), 75–80.

Cinar, Y., Cingu, A.K., Turkcu, F.M., Yuksel, H., Sahin, A., Yildirim, A., Caca, I., Cinar, T., 2014. Accelerated corneal collagen cross-linking for progressive keratoconus. Cutan. Ocular Toxicol. 33 (2), 168–171.

Cummings, A.B., McQuaid, R., Naughton, S., Brennan, E., Mrochen, M., 2016. Optimizing corneal cross-linking in the treatment of keratoconus: a comparison of outcomes after standard- and high-intensity protocols. Cornea 35 (6), 814–822.

Davidson, A.E., Hayes, S., Hardcastle, A.J., Tuft, S.J., 2014. The pathogenesis of keratoconus." Eye 28 (2), 189–195.

Fang, J.Y., Lin, H.H., Chen, H.I., Tsai, Y.H., 1998. Development and evaluation on transdermal delivery of enoxacin via chemical enhancers and physical iontophoresis. J. Control. Release 54 (3), 293–304.

Filippello, M., Stagni, E., O'Brart, D., 2012. Transepithelial corneal collagen cross-linking: bilateral study. J. Cataract. Refract. Surg. 38 (2), 283–291.

Gkika, M., Labiris, G., Kozobolis, V., 2011. Corneal collagen cross-linking using riboflavin and ultraviolet-A irradiation: a review of clinical and experimental studies. Int. Ophthalmol. 31 (4), 309–319.

Gore, D.M., Margineanu, A., French, P., O'Brart, D., Dunsby, C., Allan, B.D., 2014. Two-photon fluorescence microscopy of corneal riboflavin absorption. Investig. Ophthalmol. Vis. Sci. 55 (4), 2476–2481.

Harvitt, D.M., Bonanno, J.A., 1998. Oxygen consumption of the rabbit cornea. Investig. Ophthalmol. Vis. Sci. 39 (2), 444–448.

Hayes, S., Kamma-Lorger, C.S., Boote, C., Young, R.D., Quantock, A.J., Rost, A., Khatib, Y., Harris, J., Yagi, N., Terrill, N., Meek, K.M., 2013. The effect of riboflavin/UVA collagen cross-linking therapy on the structure and hydrodynamic behaviour of the ungulate and rabbit corneal stroma. Plos One 8 (1), e52860. http://dx.doi.org/10.1371/journal.pone.0052860.

Hayes, S., Morgan, S.R., O'Brart, D.P., O'Brart, N., Meek, K.M., 2015. A study of stromal riboflavin absorption in ex vivo porcine corneas using new and existing delivery protocols for corneal cross-linking. Acta Ophthalmol. 94 (2), E109–E117.

Huang, A.J.W., Tseng, S.C.G., Kenyon, K.R., 1989. Paracellular permeability of corneal and conjunctival epithelia. Investig. Ophthalmol. Vis. Sci. 30 (4), 684–689.

Kanellopoulos, A.J., 2012. Long term results of a prospective randomized bilateral eye comparison trial of higher fluence, shorter duration ultraviolet A radiation, and riboflavin collagen cross linking for progressive keratoconus. Clin. Ophthalmol. 6, 97–101 (Auckland, N.Z.).

Kissner, A., Spoerl, E., Jung, R., Spekl, K., Pillunat, L.E., Raiskup, F., 2010. Pharmacological modification of the epithelial permeability by benzalkonium chloride in UVA/riboflavin corneal collagen cross-linking. Curr. Eye Res. 35 (8), 715–721.

Kocak, I., Aydin, A., Kaya, F., Koc, H., 2014. Comparison of transepithelial corneal collagen crosslinking with epithelium-off crosslinking in progressive keratoconus. J. Fr. D Ophtalmol. 37 (5), 371–376.

Koller, T., Mrochen, M., Seiler, T., 2009. Complication and failure rates after corneal crosslinking. J. Cataract. Refract. Surg. 35 (8), 1358–1362.

Koppen, C., Wouters, K., Mathysen, D., Rozema, J., Tassignon, M.-J., 2012. Refractive and topographic results of benzalkonium chloride–assisted transepithelial crosslinking. J. Cataract. Refract. Surg. 38 (6), 1000–1005.

Kymionis, G.D., Grentzelos, M.A., Kankariya, V.P., Liakopoulos, D.A., Portaliou, D.M., Tsoulnaras, K.I., Karavitaki, A.E., Pallikaris, A.I., 2014a. Safety of high-intensity corneal collagen crosslinking. J. Cataract Refract. Surg. 40 (8), 1337–1340.

Kymionis, G.D., Tsoulnaras, K.I., Grentzelos, M.A., Liakopoulos, D.A., Tsakalis, N.G., Blazaki, S.V., Paraskevopoulos, T.A., Tsilimbaris, M.K., 2014b. Evaluation of corneal stromal demarcation line depth following standard and a modified-accelerated collagen cross-linking protocol. Am. J. Ophthalmol. 158 (4), 671–675.

Leccisotti, A., Islam, T., 2010. Transepithelial corneal collagen cross-linking in keratoconus. J. Refract. Surg. 26 (12), 942–948.

Lombardo, M., Serrao, S., Rosati, M., Ducoli, P., Lombardo, G., 2014. Biomechanical changes in the human cornea after transepithelial corneal crosslinking using iontophoresis. J. Cataract. Refract. Surg. 40 (10), 1706–1715.

Magli, A., Forte, R., Tortori, A., Capasso, L., Marsico, G., Piozzi, E., 2013. Epithelium-off corneal collagen cross-linking versus transepithelial cross-linking for pediatric keratoconus. Cornea 32 (5), 597–601.

Mastropasqua, L., Lanzini, M., Curcio, C., Calienno, R., Mastropasqua, R., Colasante, M., Mastropasqua, A., Nubile, M., 2014. Structural modifications and tissue response after standard epi-off and iontophoretic corneal crosslinking with different irradiation procedures. Investig. Ophthalmol. Vis. Sci. 55 (4), 2526–2533.

McCall, A.S., Kraft, S., Edelhauser, H.F., Kidder, G.W., Lundquist, R.R., Bradshaw, H.E., Dedeic, Z., Dionne, M.J.C., Clement, E.M., Conrad, G.W., 2010. Mechanisms of corneal tissue cross-linking in response to treatment with topical riboflavin and long-wavelength ultraviolet radiation (UVA). Investig. Ophthalmol. Vis. Sci. 51 (1), 129–138.

Nawaz, S., Gupta, S., Gogia, V., Sasikala, N.K., Panda, A., 2015. Trans-epithelial versus conventional corneal collagen crosslinking: a randomized trial in keratoconus. Oman J. Ophthalmol. 8 (1), 9–13.

O'Brart, D.P.S., Chan, E., Samaras, K., Patel, P., Shah, S.P., 2011. A randomised, prospective study to investigate the efficacy of riboflavin/ultraviolet A (370 nm) corneal collagen cross-linkage to halt the progression of keratoconus. Br. J. Ophthalmol. 95 (11), 1519–1524.

Raiskup, F., Pinelli, R., Spoerl, E., 2012. Riboflavin osmolar modification for trans-epithelial corneal cross-linking. Curr. Eye Res. 37 (3), 234–238.

Razmjoo, H., Rahimi, B., Kharraji, M., Koosha, N., Peyman, A., 2014. Corneal haze and visual outcome after collagen crosslinking for keratoconus: a comparison between total epithelium off and partial epithelial removal methods. Adv. Biomed. Res. 3, 221.

Rechichi, M., Daya, S., Scorcia, V., Meduri, A., Scorcia, G., 2013. Epithelial-disruption collagen crosslinking for keratoconus: one-year results. J. Cataract. Refract. Surg. 39 (8), 1171–1178.

Richoz, O., Mavrakanas, N., Pajic, B., Hafezi, F., 2013. Corneal collagen cross-linking for ectasia after LASIK and photorefractive keratectomy long-term results. Ophthalmology 120 (7), 1354–1359.

Rossi, S., Orrico, A., Santamaria, C., Romano, V., De Rosa, L., Simonelli, F., De Rosa, G., 2015. Standard versus trans-epithelial collagen cross-linking in keratoconus patients suitable for standard collagen cross-linking. Clin. Ophthalmol. 9, 503–509.

Scarcelli, G., Kling, S., Quijano, E., Pineda, R., Marcos, S., Yun, S.H., 2013. Brillouin microscopy of collagen crosslinking: noncontact depth-dependent analysis of corneal elastic modulus. Investig. Ophthalmol. Vis. Sci. 54 (2), 1418–1425.

Sherif, A.M., 2014. Accelerated versus conventional corneal collagen cross-linking in the treatment of mild keratoconus: a comparative study. Clin. Ophthalmol. 8, 1435–1440.

Shetty, R., Pahuja, N.K., Nuijts, R.M.M.A., Ajani, A., Jayadev, C., Sharma, C., Nagaraja, H., 2015. Current protocols of corneal collagen cross-linking: visual, refractive, and tomographic outcomes. Am. J. Ophthalmol. 160 (2), 243–249.

Soeters, N., Wisse, R.P.L., Godefrooij, D.A., Imhof, S.M., Tahzib, N.G., 2015. Trans-epithelial versus epithelium-off corneal cross-linking for the treatment of progressive keratoconus: a randomized controlled trial REPLY. Am. J. Ophthalmol. 160 (2), 400–400.

Spoerl, E., Huhle, M., Seiler, T., 1998. Induction of cross-links in corneal tissue. Exp. Eye Res. 66 (1), 97–103.

Spoerl, E., Wollensak, G., Seiler, T., 2004. Increased resistance of crosslinked cornea against enzymatic digestion. Curr. Eye Res. 29 (1), 35–40.

Touboul, D., Gennisson, J.-L., Nguyen, T.-M., Robinet, A., Roberts, C.J., Tanter, M., Grenier, N., 2014. Supersonic shear wave elastography for the in vivo evaluation of transepithelial corneal collagen cross-linking. Investig. Ophthalmol. Vis. Sci. 55 (3), 1976–1984.

Uematsu, M., Kumagami, T., Kusano, M., Yamada, K., Mishima, K., Fujimura, K., Sasaki, H., Kitaoka, T., 2007. Acute corneal epithelial change after instillation of benzalkonium chloride evaluated using a newly developed in vivo corneal transepithelial electric resistance measurement method. Ophthalmic Res. 39 (6), 308–314.

Vinciguerra, P., Mencucci, R., Romano, V., Spoerl, E., Camesasca, F.I., Favuzza, E., Azzolini, C., Mastropasqua, R., Vinciguerra, R., 2014a. Imaging mass spectrometry by matrix-assisted laser desorption/ionization and stress-strain measurements in iontophoresis transepithelial corneal collagen cross-linking. Biomed. Res. Int. 404587.

Vinciguerra, P., Randleman, J.B., Romano, V., Legrottaglie, E.F., Rosetta, P., Camesasca, F.I., Piscopo, R., Azzolini, C., Vinciguerra, R., 2014b. Transepithelial iontophoresis corneal collagen cross-linking for progressive keratoconus: initial clinical outcomes. J. Refract. Surg. 30 (11), 747–754.

Wittig-Silva, C., Chan, E., Islam, F.M.A., Wu, T., Whiting, M., Snibson, G.R., 2014. A randomized, controlled trial of corneal collagen cross-linking in progressive keratoconus three-year results. Ophthalmology 121 (4), 812–821.
Wollensak, G., Iomdina, E., 2009. Biomechanical and histological changes after corneal crosslinking with and without epithelial debridement. J. Cataract. Refract. Surg. 35 (3), 540–546.
Wollensak, G., Spoerl, E., Seiler, T., 2003. Riboflavin/ultraviolet-A-induced collagen crosslinking for the treatment of keratoconus. Am. J. Ophthalmol. 135 (5), 620–627.
Zhou, L., Sawaguchi, S., Twining, S.S., Sugar, J., Feder, R.S., Yue, B.Y.J.T., 1998. Expression of degradative enzymes and protease inhibitors in corneas with keratoconus. Investig. Ophthalmol. Vis. Sci. 39 (7), 1117–1124.

Enzymatic Resistance of Corneas Crosslinked Using Riboflavin in Conjunction With Low Energy, High Energy, and Pulsed UVA Irradiation Modes

Nada H. Aldahlawi,[1,2] Sally Hayes,[1,2] David P. S. O'Brart,[3] Alina Akhbanbetova,[1,2] Stacy L. Littlechild,[1,2] and Keith M. Meek[1,2]

[1]Structural Biophysics Research Group, School of Optometry and Vision Sciences, Cardiff University, Cardiff, United Kingdom
[2]Cardiff Institute for Tissue Engineering and Repair (CITER), Cardiff University, Cardiff, United Kingdom
[3]Keratoconus Research Institute, Department of Ophthalmology, St. Thomas' Hospital, London, United Kingdom

Correspondence: Keith M. Meek, Structural Biophysics Research Group, School of Optometry and Vision Sciences, Cardiff University, Maindy Road, Cardiff CF24 4HQ, UK; MeekKM@cardiff.ac.uk.

Submitted: November 30, 2015
Accepted: January 20, 2016

Citation: Aldahlawi NH, Hayes S, O'Brart DPS, Akhbanbetova A, Littlechild SL, Meek KM. Enzymatic resistance of corneas crosslinked using riboflavin in conjunction with low energy, high energy, and pulsed UVA irradiation modes. *Invest Ophthalmol Vis Sci*. 2016;57:1547–1552. DOI:10.1167/iovs.15-18769

Purpose. To investigate the effect of various riboflavin/ultraviolet light (UVA) crosslinking (CXL) protocols on corneal enzymatic resistance.

Methods. A total of 66 enucleated porcine eyes, with the corneal epithelium removed, were divided into 6 groups. Group 1 remained untreated. Groups 2 to 6 received riboflavin/dextran for 30 minutes. Group 3 underwent standard CXL (SCXL) with 3 mW/cm^2 UVA for 30 minutes (total energy dose 5.4 J/cm^2). Groups 4 and 5 underwent high intensity CXL (HCXL) using 30 mW/cm^2 UVA for 3 minutes (5.4 J/cm^2) and 30 mW/cm^2 for 4 minutes (7.2 J/cm^2), respectively. Group 6 was exposed to 8 minutes of 30 mW/cm^2 UVA in a 10-second on/10-second off pulsed-radiation mode (p-HCXL; 7.2 J/cm^2). A central 8-mm disk from each cornea was submerged in pepsin digest solution at 23°C and measured daily. After 13 days, the dry weight was recorded from 5 samples in each group.

Results. The CXL-treated corneas took longer to digest than nonirradiated corneas ($P < 0.0001$). Differences in digestion time also were observed between CXL groups, such that, HCXL (5.4 J/cm^2) < SCXL (5.4 J/cm^2) < HCXL (7.2 J/cm^2) < p-HCXL (7.2 J/cm^2; $P < 0.0001$). The dry weight of the SCXL (5.4 J/cm^2) group was higher than the HCXL (5.4 and 7.2 J/cm^2; $P < 0.001$) and p-HCXL 7.2 J/cm^2 ($P < 0.05$) groups. No difference was detected between the HCXL and p-HCXL 7.2 J/cm^2 groups.

Conclusions. The intensity and distribution of the crosslinks formed within the cornea vary with different UVA protocols. The precise location and amount of crosslinking needed to prevent disease progression is unknown.

Keywords: keratoconus, crosslinking, accelerated crosslinking, CXL, enzymatic digestion

Keratoconus is a degenerative corneal dystrophy, characterized by progressive corneal thinning and subsequent impairment of corneal biomechanics.[1–3] The resultant conical ectasia causes irregular astigmatism and associated reduction of visual performance, which can be significant.[4] It typically presents in adolescence and is the most common of all corneal dystrophies with a reported incidence of 1 in 1750.[1–3] Its precise pathophysiology is as yet undetermined, but it has been shown to be associated with an upregulation of degradative proteolytic enzymes.[5] Riboflavin and ultraviolet A (UVA) corneal crosslinking (CXL) was first postulated in 1998 as a means of strengthening the corneal stroma, increasing its resistance to enzymatic digestion and stabilizing cases of progressive keratoconus.[6] It has since been the subject of a plethora of research articles investigating and confirming its safety and efficacy.[7–10]

The standard CXL protocol (SCXL), first clinically tested by Wollensak et al.,[8] involves removing the central 9 mm of corneal epithelium, soaking the exposed stromal surface with 0.1% riboflavin for 30 minutes, and irradiating the riboflavin-laden stroma with 370 nm UVA light with an intensity of 3 mW/cm^2 (resulting in a cumulative dose of 5.4 J/cm^2). This protocol requires in excess of 1 hour of treatment time. Given its frequency of occurrence, the potential numbers of patients with progressive keratoconus requiring CXL is large and represents a not inconsiderable burden to health services. In an attempt to reduce the treatment time, a number of modifications to the existing SCXL protocol have been proposed. These changes are based primarily on current understanding of the photochemical kinetics of UVA exposure and the theoretical principles of the Bunsen–Roscoe law of reciprocity,[11] which states that a certain biological effect is directly proportional to the total energy dose irrespective of the administered regimen. However, as has been shown with other photochemical reactions,[12] this law may only be valid within a certain dose range and this must be defined individually for each reaction.

The precise photochemical mechanism involved in riboflavin/UVA CXL currently is uncertain. What has been shown, however, is that oxygen is essential to drive the process and in the absence of oxygen, CXL is impaired.[13] It has been suggested that higher intensity UVA, or so-called "accelerated" CXL protocols, result in more rapid oxygen depletion thereby reducing efficacy.[14,15] It has been shown that by ceasing UV

irradiation, oxygen can be restored to its normal level within 3 to 4 minutes[16] and, on this basis, it has been proposed that by pulsing the UV light throughout the procedure, oxygen levels may be replenished so that the CXL process is no longer impaired.[17,18] In addition to pulsing, it also has been suggested that the efficacy of accelerated protocols may be improved by increasing the exposure time by 30% to 40%.[19,20]

To further investigate these issues and compare the efficacy of accelerated CXL, extended accelerated CXL and pulsed CXL protocols with the "gold standard" SCXL protocol, we analyzed the rate of enzymatic digestion after CXL in an ex vivo porcine model.

Methods

Study Design

A total of 66 fresh porcine eyes, with transparent corneas and an intact corneal epithelium, were obtained from a local European Community licensed abattoir and used within 6 hours of death. Following a complete debridement of the corneal epithelium using a single-edged razor blade, the eyes were divided randomly and equally into the 6 groups described below (in which Groups 1 and 2 served as controls).

1. Untreated (U): no treatment performed.
2. Riboflavin only (R): a 0.1% riboflavin solution containing 20% dextran T-500 (Mediocross D; Peschke Meditrade, Huenenberg, Switzerland) was applied to the anterior corneal surface for 30 minutes using an annular suction ring.
3. Standard low-intensity CXL (SCXL 5.4 J/cm^2): a 0.1% riboflavin solution containing 20% dextran T-500 was applied to the anterior corneal surface for 30 minutes (as above). The cornea then was exposed to 3 mW UVA for 30 minutes (total energy dose of 5.4 J/cm^2) during which time riboflavin was reapplied at 5-minute intervals.
4. High intensity 30 mW/3 min CXL (HCXL 5.4 J/cm^2): a 0.1% riboflavin solution containing 20% dextran T-500 was applied to the anterior corneal surface for 30 minutes. The cornea then was exposed to 30 mW UVA for a period of 3 minutes (total energy dose of 5.4 J/cm^2) during which time riboflavin was reapplied once.
5. High intensity 30 mW/4 min CXL (HCXL 7.2J/cm^2): a 0.1% riboflavin solution containing 20% dextran T-500 was applied to the anterior corneal surface for 30 minutes. The cornea then was exposed to 30 mW UVA for a period of 4 minutes (total energy dose of 7.2 J/cm^2) during which time riboflavin was reapplied once.
6. High intensity 30 mW/8min pulsed CXL (p-HCXL7.2 J/cm^2): a 0.1% riboflavin solution containing 20% dextran T-500 was applied to the anterior corneal surface for 30 minutes. The cornea then was exposed to 30 mW UVA in a pulsed radiation mode of 10 seconds on and 10 seconds off for a period of 8 minutes (total energy dose of 7.2 J/cm^2). During irradiation the riboflavin solution was reapplied twice.

All of the irradiation protocols were performed using the Phoenix CXL System (Peschke Meditrade) with a wavelength of 365 nm, a 50 mm working distance, and a 9 mm aperture. Central corneal thickness was measured via ultrasound pachymetry (DGH Pachmate 55; DGH Technologies, Exton, PA, USA) before treatment (after epithelial debridement), after riboflavin application, and after UVA exposure.

Following treatment, an 8 mm full-tissue-thickness biopsy was trephined from the center of each cornea. The corneal disks were placed in individual sealed tubes containing 5 mL pepsin digest solution (1 g 600 to 1200 U/mg pepsin from porcine gastric mucosa [Sigma-Aldrich, Dorset, UK] in 10 mL 0.1 M HCL at pH 1.2) and incubated in a water bath at 23°C. As our previous studies suggest that CXL causes the formation of crosslinks not only at the collagen fibril surface but also in the protein network surrounding the collagen,[21] pepsin was selected in preference to collagenase as the enzyme of choice for this study.

Using electronic digital calipers, the diameter of the anterior surface of each corneal disk was recorded daily until the tissue could no longer be distinguished from the surrounding pepsin solution (even under microscopic examination). At this point the tissue was considered to have undergone "complete digestion." We recorded the daily diameter of the trephined corneal disks, rather than corneal thickness, as corneal disks placed in pepsin are known to undergo significant stromal swelling (predominantly in the posterior stroma) during the first 24 hours.[22]

To assess further the effect of each treatment on enzymatic resistance, 5 corneal disks from each group were removed from the pepsin digest solution after 13 days and placed in a 60°C oven until a constant dry weight was obtained. The average corneal dry weight then was calculated for each group.

The corneal disk diameter measurements provide valuable information about the structural integrity of the most anterior layers of the cornea, while the dry weight measurements, representing the total mass of undigested tissue, negate the complications associated with within-sample variations in corneal thickness and between sample differences in hydration and provide information about the effective depth of CXL.

Data Analysis

Data are shown as mean measurements (±SD) for corneal thickness, dry weight, and complete digestion time. Measurements of corneal disk diameter are presented as a daily cumulative measurement for each treatment group. Statistical analysis was performed using a one-way ANOVA and Bonferroni multiple comparisons in a depth-wise manner. All statistical analyses were performed with the Statistical Package for the Social Sciences (SPSS Statistics 20; IBM, Armonk, NY, USA). A probability value of $P < 0.05$ was considered significant.

Results

Corneal Thickness

The average stromal thickness at each stage of treatment is shown in Figure 1. Before treatment, the average stromal thickness did not differ significantly between groups. However, a 30-minute application of riboflavin–dextran solution (groups 2–6) resulted in a significant decrease in stromal thickness ($P < 0.0001$). The subsequent irradiation of corneas in groups 3 to 6 produced no further changes in corneal thickness and the final stromal thickness did not differ significantly between any of the CXL groups.

Time Taken for Complete Digestion

Stromal swelling, in a posterior–anterior direction was observed in all corneal disks within 1 day of submersion in pepsin digest solution (Fig. 2). After 2 days of digestion, a loss of structural integrity was seen in the untreated corneas but the crosslinked corneas remained intact (Fig. 2). By day 7 of the digestion process, the anterior portion of each treated and untreated corneal button had separated from the posterior portion and by day 10, the posterior portion had been

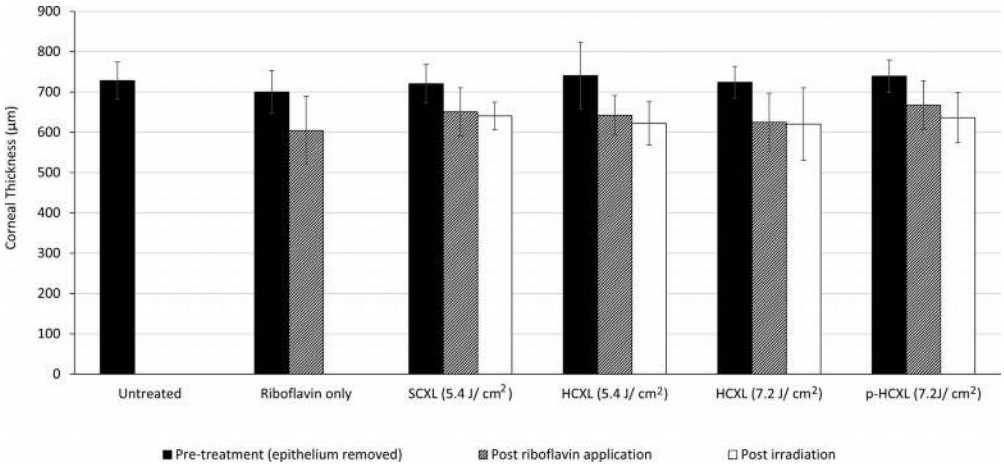

Figure 1. Average corneal thickness measured before, during, and after treatment.

completely digested in all cases. The anterior corneal disk persisted considerably longer (particularly in the CXL-treated corneas) and maintained its form sufficiently to allow reliable measurements of corneal disk diameter to be recorded daily.

The time required for complete digestion of the crosslinked corneas (groups 3–6) was significantly longer than that required for the nonirradiated specimens (groups 1 and 2; $P < 0.0001$; Fig. 3). After 13 days of digestion, all nonirradiated corneas had undergone complete digestion and the average diameter of all the crosslinked corneal disks had decreased in diameter from their original value.

Corneas crosslinked with higher energy dose treatments (7.2 J/cm^2) using continuous (group 5) or pulsed (group 6) light took significantly longer to digest than corneas crosslinked using lower (5.4J/cm^2) energy dose treatments (groups 3 and 4; $P < 0.0001$). A direct comparison between treatments using the same energy dose revealed that corneas crosslinked using the SCXL (5.4 J/cm^2) procedure took longer to digest than corneas crosslinked using the accelerated HCXL (5.4 J/cm^2) procedure ($P < 0.0001$), and corneas crosslinked using the pulsed irradiation p-HCXL (7.2 J/cm^2) procedure took significantly longer to digest than those treated with the continuous irradiation HCXL (7.2J/cm^2) procedure ($P < 0.0001$).

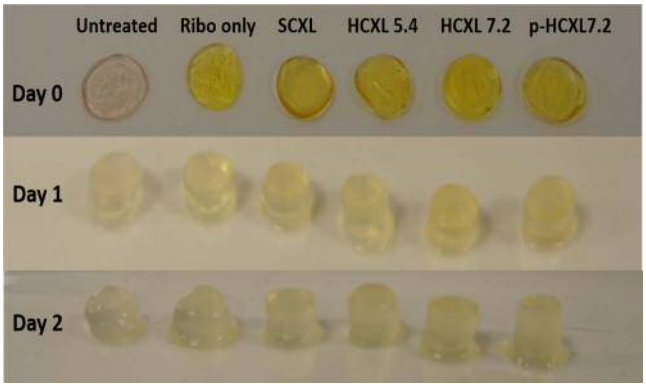

Figure 2. Photographs of a representative corneal disk from each treatment group before immersion in pepsin digest solution (day 0) and after 1 and 2 days of digestion.

Undigested Tissue Mass

After 13 days in pepsin digest solution, only the CXL-treated corneas remained (Fig. 4). At this time point, the average stromal dry weight of the SCXL (5.4 J/cm^2)–treated corneas was significantly higher than that of the HCXL 5.4 J/cm^2– ($P < 0.0001$), HCXL 7.2 J/cm^2– ($P < 0.001$), and p-HCXL 7.2J/cm^2–treated corneas ($P < 0.05$). The stromal dry weight did not differ significantly between the two higher energy treatment groups which used continuous (HCXL 7.2 J/cm^2) and pulsed (p-HCXL 7.2 J/cm^2) irradiation, but the corneas treated with p-HCXL 7.2 J/cm^2 had a higher stromal dry weight than the corneas treated with HCXL 5.4 J/cm^2 ($P < 0.0001$).

Discussion

Crosslinking has been shown to be a safe and effective treatment for keratoconus[7–10] and other corneal ectatic disorders.[23,24] The efficacy of CXL can be attributed, at least in part, to its ability to increase the enzymatic resistance of corneal tissue, as enzymatic digestion is known to be involved in the pathogenesis of keratoconus.[25]

An increase in enzymatic resistance following CXL with irradiances of 2 and 3 mW/cm^2 UVA was first evidenced by Spoerl et al.[22] and later by others.[21] It since has been shown that the use of CXL with irradiances of 9 and 18 mW/cm^2 also results in enhanced enzymatic resistance.[26] However measurements of undigested tissue mass midway through the digestion process revealed significant differences between treatment groups that indicated that the amount of CXL may be less when higher intensity "accelerated" protocols, with the same cumulative dose as SCXL, are used.[26] While some studies show little differences between SCXL and accelerated CXL, a possible reduction in efficacy with high-intensity UVA protocols has been documented recently by some clinical investigators. Ng et al.[27] compared 9 mW/cm^2 for 10 minutes to SCXL and reported a statistically greater reduction in maximum and mean keratometry and deeper demarcation lines in SCXL-treated eyes.[27] Similar results were reported in a retrospective study by Brittingham et al.[14]

Oxygen is essential to drive the riboflavin/UVA CXL process and in its absence crosslink formation is impaired.[13] It has been postulated that reduced efficacy with accelerated CXL protocols is due to more rapid oxygen depletion compared to the more prolonged but less intense UVA exposure in SCXL.[14,15] As oxygen can be restored to its normal tissue levels

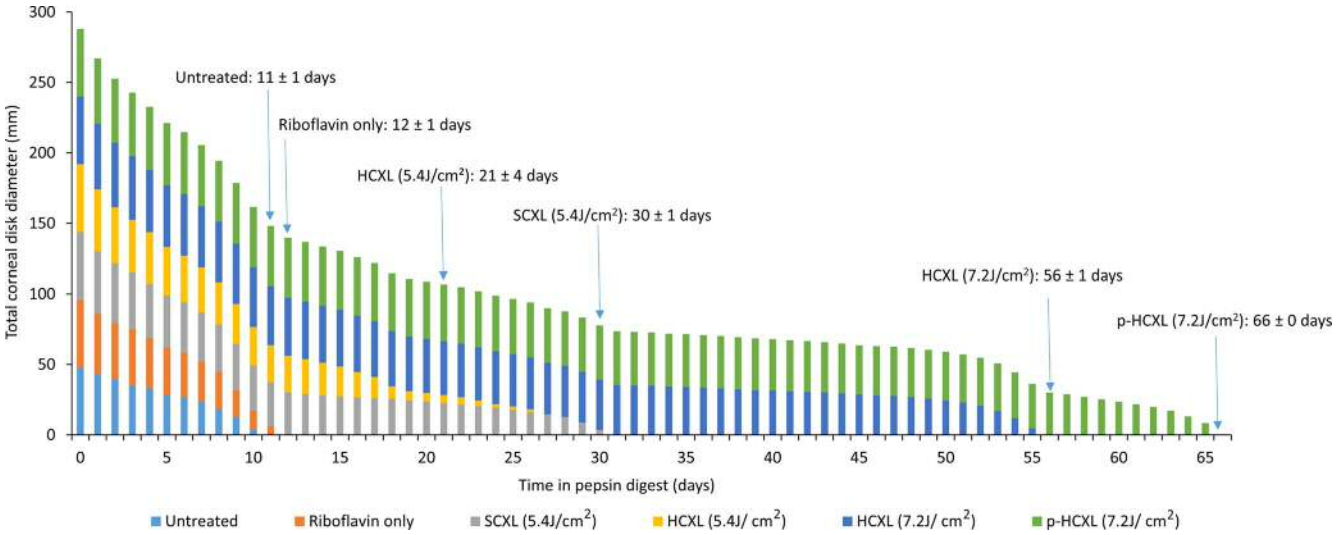

Figure 3. The summed diameter of all corneal disks ($n = 6$) within each crosslinked and noncrosslinked treatment group is shown as a function of time in pepsin digest solution. In addition, the average time (±SD) required for complete digestion of each treatment group has been added to the time-line.

within 3 to 4 minutes of cessation of UVA radiation,[16] it has been postulated that by pulsing the UV light, oxygen levels may be replenished so that the CXL process is no longer impaired.[17,18] In addition to pulsing, some investigators have demonstrated that the efficacy of accelerated CXL protocols may be improved by increasing the UVA exposure time, and, hence, the overall cumulative dosage, by 30% to 40%.[19,20] In this present study, we tested a number of these newer commercially available extended and pulsed accelerated protocols by investigating their resistance to enzymatic (pepsin) digestion.

All eyes treated in our study received an application of an isoosmolar riboflavin solution (containing 20% dextran) to the deepithelialized corneal surface. Consistent with previous studies,[21,28] this resulted in a significant decrease in corneal thickness. The corneal thinning can be attributed primarily to the deturgescent effect of the dextran but also, possibly, to the presence of riboflavin,[26] which has the effect of increasing the ionic strength of the applied solution and presumably further lowering the hydration of the cornea.[29]

Due to treatment-induced variations in corneal thickness and the swelling of the trephined corneal disks (in the posterior-anterior direction) during the first 24 hours of immersion in pepsin digest solution,[26] corneal thickness measurements were considered to be an unreliable measure of the rate of enzymatic digestion. Instead, in this current study, daily measurement of the diameter of the anterior corneal surface and the dry weight of the undigested tissue after 13 days of digestion was performed. These measurements provided a more accurate assessment of the structural integrity of the anterior corneal stroma and the effective depth of CXL following each treatment variation.

The discovery that corneas treated with HCXL (5.4 J/cm^2) had a lower residual mass after 13 days of digestion, and took less time to undergo complete digestion than SCXL-treated corneas, suggests a reduced CXL effect and a failure of the Bunsen–Roscoe law of reciprocity at higher UVA intensities. This supports the findings of biomechanical studies which have reported a reduced corneal stiffening effect with increasing UVA intensity up to 18mW,[30] and a sudden decrease in efficacy with very high intensities greater than 45 mW/cm^2.[31] The failure of the Bunsen-Roscoe law of reciprocity in cases of very high intensity and short illumination time is not yet fully understood, but is thought to be caused, as discussed above, by insufficient oxygen availability inhibiting the CXL process.[13] This hypothesis is supported by our findings of increased enzymatic resistance in p-HCXL treated eyes, where oxygen availability theoretically should be greater than in the nonpulsed HCXL treatments.

The precise photochemical mechanisms involved in riboflavin/UVA CXL are unknown. It has been postulated that the process commences under aerobic conditions with a brief type II photochemical reaction, in which sensitized photooxidation of stromal proteins occurs, mainly by their reaction with photochemically generated reactive oxygen species.[16] As oxygen becomes depleted, after the initial 15 seconds of exposure to UVA, a type I photosensitizing mechanism then may predominate, in which radical ions are produced that can induce covalent CXL of stromal macromolecules.[16] In SCXL, where UVA exposure occurs over 30 minutes, the oxygen

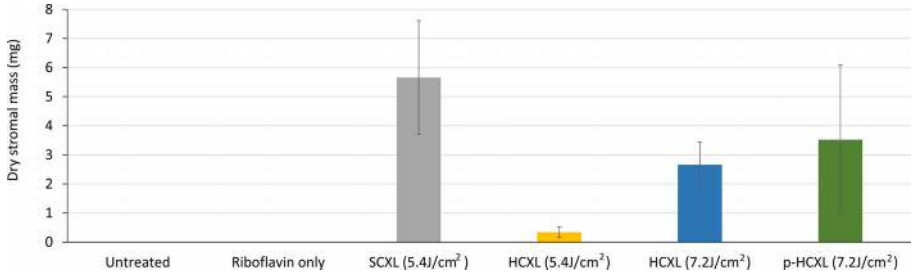

Figure 4. Corneal disk dry weight after 13 days of digestion.

concentration in the cornea may slowly increase, during the later stages of the treatment, to a level at which a type-II mechanism may once again begin.[16]

The enhanced enzymatic resistance we observed when the exposure time of the cornea to 30 mW UVA was increased from 3 to 4 minutes may be attributed to the increase in the total energy dose from 5.4 to 7.2 J/cm^2, which allowed additional type I photochemical CXL to occur. It is unlikely that the increased CXL effect is due to the extended treatment providing additional time for the oxygen levels to be replenished to a level at which the type II CXL reaction could be restarted as, even when SCXL is performed, the oxygen concentration is thought only to reach sufficient levels in the latter half of the 30-minute treatment.[16]

Although corneas treated with HCXL and p-HCXL and a total energy dose of 7.2 J/cm^2 persisted longer in enzyme digest solution than SCXL (5.4J/cm^2)–treated corneas, the dry weight of the SCXL-treated corneas was higher when measured midway through the digestion process. This suggested that differences in the distribution of CXL may exist within the tissue. It can be postulated that CXL using a higher UVA intensity and a greater total energy dose results in superior CXL efficacy within the most anterior stromal layers and/or the mid-corneal region, resulting in longer overall digestion times. However, the depth of CXL may be shallower or there may be a more rapid decrease in the intensity of CXL as a function of depth, compared to SCXL, resulting in a reduced overall mass of crosslinked tissue. It is of interest that Brillouin microscopy studies of SCXL-treated corneas have shown that the intensity of CXL is depth-dependent, with the anterior stroma contributing the most to the increase in mechanical stiffness, and examination of the effect of varying UVA exposure time (0–30 minutes) has shown a dose-dependent tissue stiffening in the anterior third of the cornea.[32]

The clinical relevance of these findings is uncertain, as the precise amount and location of crosslinked tissue required to prevent keratoconic progression has yet to be determined. Clinical studies comparing CXL with accelerated CXL protocols are limited and somewhat conflicting. Tomita et al.,[33] in a study comparing SCXL with 30 mW/cm^2 for 3 minutes, found no differences in visual and topographic indices and similar demarcation line depths at 6 months, while Shetty et al.,[34] in a randomized clinical study in 138 eyes with 12-month follow-up, found poorer refractive and tomographic outcomes with 30 mW/cm^2 for 3 minutes. A small clinical trial involving 20 patients treated with either pulsed or continuous light HCXL showed keratoconus stability in both groups at 1 year follow-up, although the pulsed light treatment produced better functional outcomes and a deeper stromal penetration.[17] Similarly, a retrospective assessment of 60 patients treated with HCXL found the demarcation line to be significantly deeper in patients treated with pulsed rather than continuous light.[35] Clearly further, comparative clinical studies are required especially comparing the outcomes of p-HCXL with standard CXL, both of which appeared on this basis of this study to offer the best outcomes in terms of resistance to enzyme digestion.

Acknowledgments

The authors thank Veni Vidi for their provision of riboflavin for this study and loan of the Phoenix CXL System, and Philip Almond for assistance in the set-up of the Phoenix CXL System.

Supported by MRC Programme Grant MR/K000837/1 and King Saud University funding R1269. The authors alone are responsible for the content and writing of this paper.

Disclosure: **N.H. Aldahlawi**, None; **S. Hayes**, None; **D.P.S. O'Brart**, None; **A. Akhbanbetova**, None; **S.L. Littlechild**, None; **K.M. Meek**, None

References

1. Kennedy RH, Bourne WM, Dyer JA. A 48-year clinical and epidemiologic study of keratoconus. *Am J Ophthalmol*. 1986; 101:267–273.
2. Krachmer JH, Feder RS, Belin MW. Keratoconus and related non-inflammatory corneal thinning disorders. *Surv Ophthalmol*. 1984;28:293–322.
3. Rabinowitz YS: Keratoconus. *Surv Ophthalmol*. 1998;42:297–319.
4. Kymes SM, Walline JJ, Zadnik K, Gordon MO. Group CLEOKS: quality of life in keratoconus. *Am J Ophthalmol*. 2004;138: 527–35.
5. Zhou LL, Sawaguchi S, Twining SS, Sugar J, Feder RS, Yue BY. Expression of degradative enzymes and protease inhibitors in corneas with keratoconus. *Invest Ophthalmol Vis Sci*. 1998; 39:1117–1124.
6. Spoerl E, Huhle M, Seiler T. Induction of cross-links in corneal tissue. *Exp Eye Res*. 1998;66:97–103.
7. Meek KM, Hayes S. Corneal cross-linking - a review. *Ophthalmic Physiol Opt*. 2013;33:78–93.
8. Wollensak G, Spoerl E, Seiler T. Riboflavin/ultraviolet-A-induced collagen crosslinking for the treatment of keratococnus. *Am J Ophthalmol*. 2003;135:620–627.
9. O'Brart D. Corneal collagen cross linking: a review. *J Optom*. 2014;7:113–124.
10. O'Brart D, Patel P, Lascaratos G, Wagh V, Tam C, Lee J. Seven year follow-up of riboflavin/ultraviolet A corneal cross-linking to halt the progression of keratoconus and corneal ectasia. *Am J Ophthalmol*. 2015;160:1154–1163.
11. Bunsen R, Roscoe H. Photochemical researches - Part V. On the measurement of the chemical action of direct and diffuse sunlight. *Proc R Soc Lond*. 1862;12:306–312.
12. Potapenko A, Agamalieva M, Nagiev A, Lysenko E, Bezdetnaya L, Sukhorukov V. Photochemolysis sensitzed by psoralen: reciprocity law is not fulfilled. *Photochem Photobiol*. 1991;54: 375–379.
13. McCall A, Kraft S, Edelhauser H, et al. Mechanisms of corneal tissue cross-linking in response to treatment with topical riboflavin and long-wavelength ultraviolet radiation (UVA). *Invest Ophthalmol Vis Sci*. 2010;51:129–138.
14. Brittingham S, Tappeiner C, Frueh B. Corneal cross-linking in keratoconus using the standard and rapid treatment protocol: differences in demarcation line and 12-month outcomes. *Invest Ophthalmol Vis Sci*. 2014;55:8371–8376.
15. Touboul D, Efron N, Smadja D, Praud D, Malet F, Colin J. Corneal confocal microscopy following conventional, trans-epithelial, and accelerated corneal collagen cross-linking procedures for keratoconus. *J Refract Surg*. 2012;28:769–776.
16. Kamaev P, Friedman M, Sherr E, Muller D. Photochemical kinetics of corneal Cross-Linking with riboflavin. *Cornea*. 2012;53:2360–2367.
17. Mazzotta C, Traversi C, Paradiso A, Latronico M, Rechichi M. Pulsed light accelerated crosslinking versus continuous light accelerated crosslinking: one-year results. *J Ophthalmol*. 2014;2014:604731.
18. Krueger R, Herekar S, Spoerl E. First proposed efficacy study of high versus standard irradiance and fractionated riboflavin/ultraviolet a cross-linking with equivalent energy exposure. *Eye Contact Lens*. 2014;40:353–357.
19. Kymionis G, Tsoulnaras K, Grentzelos M, et al. Evaluation of corneal stromal demarcation line depth following standard

and a modified-accelerated collagen cross-linking protocol. *Am J Ophthalmol*. 2014;158:671–675.

20. Sherif A. Accelerated versus conventional corneal collagen cross-linking in the treatment of mild keratoconus: a comparative study. *Clin Ophthalmol*. 2014;2:1435–1440.
21. Hayes S, Kamma-Lorger C, Boote C, et al. The effect of riboflavin/UVA collagen cross-linking therapy on the structure and hydrodynamic behaviour of the ungulate and rabbit corneal stroma. *PLoS One*. 2013;8:e52860.
22. Spoerl E, Wollensak G, Seiler T. Increased resistance of crosslinked cornea against enzymatic digestion. *Curr Eye Res*. 2004;29:35–40.
23. Hafezi F, Kanellopoulos J, Wiltfang R, Seiler T. Corneal collagen crosslinking with riboflavin and ultraviolet A to treat induced keratectasia after laser in situ keratomileusis. *J Cataract Refract Surg*. 2007;33:2035–2040.
24. Spadea L. Corneal collagen cross-linking with riboflavin and UVA irradiation in pellucid marginal degeneration. *J Refract Surg*. 2010;26:375–377.
25. Davidson A, Hayes S, Hardcastle A, Tuft S. The pathogenesis of keratoconus. *Eye*. 2014;28:189–195.
26. Aldahlawi N, Hayes S, O'Brart D, Meek K. Standard versus accelerated riboflavin/ultraviolet corneal cross-linking: resistance against enzymatic digestion. *J Cataract Refract Surg*. 2015;41:1989–1996.
27. Ng A, Chan T, Cheng A. Conventional versus accelerated corneal collagen cross-linking in the treatment of keratoconus. *Clin Experiment Ophthalmol*. 2016;44:8–14.
28. Hassan Z, Modis L, Szalai E Jr, Berta A, Nemeth G. Intraoperative and postoperative corneal thickness change after collagen crosslinking therapy. *Eur J Ophthalmol*. 2014; 24:179–185.
29. Huang Y, Meek K. Swelling studies on the cornea and sclera: the effects of pH and ionic strength. *Biophys J*. 1999;77:1655–1665.
30. Hammer A, Richoz O, Arba Mosquera S, Tabibian D, Hoogewould F, Hafezi F. Corneal biomechanical properties at different corneal cross-Linking (CXL) irradiances. *Invest Ophthalmol Vis Sci*. 2014;55:2881–2884.
31. Wernli J, Schumacher S, Spoerl E, Mrochen M. The efficacy of corneal cross-linking shows a sudden decrease with very high intensity UV light and short treatment time. *Invest Ophthalmol Vis Sci*. 2013;54:1176–1180.
32. Scarcelli G, Kling S, Quijano E, Pineda R, Marcos S, Yun S. Brillouin microscopy of collagen crosslinking: noncontact depth-dependent analysis of corneal elastic modulus. *Invest Ophthalmol Vis Sci*. 2013;54:1418–1425.
33. Tomita M, Mita M, Huseynova T. Accelerated versus conventional corneal collagen crosslinking. *J Cataract Refract Surg*. 2014;40:1013–1020.
34. Shetty R, Pahuja N, Nuijts R, et al. Current protocols of corneal collagen cross-linking: visual, refractive, and tomographic outcomes. *Am J Ophthalmol*. 2015;160:243–249.
35. Moramarco A, Iovieno A, Sartori A, Fontana L. Corneal stromal demarcation line after accelerated crosslinking using continuous and pulsed light. *J Cataract Refract Surg*. 2015;41:2546–2551.

Investigative Ophthalmology & Visual Science

An Investigation of the Effects of Riboflavin Concentration on the Efficacy of Corneal Cross-Linking Using an Enzymatic Resistance Model in Porcine Corneas

Naomi A. L. O'Brart,[1] David P. S. O'Brart,[2] Nada H. Aldahlawi,[3] Sally Hayes,[3] and Keith M. Meek[3]

[1]Moorfields Eye Hospital, City Road, London, United Kingdom
[2]Keratoconus Research Institute, Department of Ophthalmology, St. Thomas' Hospital, London, United Kingdom
[3]Structural Biophysics Research Group, School of Optometry and Vision Sciences, Cardiff University, Maindy Road, Cardiff

Correspondence: David P. S. O'Brart, Department of Ophthalmology, Guy's and St. Thomas' NHS Foundation Trust, Lambeth Palace Road, London SE1 7EH, England; davidobrart@aol.com.

NALO'B and DPSO'B are joint first authors.

Submitted: September 19, 2017
Accepted: January 25, 2018

Citation: O'Brart NAL, O'Brart DPS, Aldahlawi NH, Hayes S, Meek KM. An investigation of the effects of riboflavin concentration on the efficacy of corneal cross-linking using an enzymatic resistance model in porcine corneas. *Invest Ophthalmol Vis Sci*. 2018;59:1058–1065. https://doi.org/10.1167/iovs.17-22994

Purpose. To investigate riboflavin concentration on enzymatic resistance following corneal cross-linking (CXL).

Methods. Ninety-six porcine eyes were divided into five groups in two treatment runs. Group 1 remained untreated. Group 2 received riboflavin 0.05%, group 3 riboflavin 0.1%, group 4 riboflavin 0.2%, and group 5 riboflavin 0.3%. Treated eyes underwent CXL with ultraviolet A at 9 mW/cm^2 for 10 minutes. Eight-millimeter discs from each cornea were submerged in pepsin digest solution. In the first run, disc diameters were measured daily. After 10 days, dry weights were recorded from five samples in each group. In the second run, dry weights were recorded in five samples in each group at 10 and 20 days.

Results. CXL-treated corneas took longer to digest than untreated ($P < 0.001$). Although eyes treated with higher riboflavin concentrations generally took longer to digest, there were no significant differences between groups ($P = 0.3$). Dry weights at 10 days demonstrated, with each increase in concentration, an increase in weight of residual undigested tissue ($P < 0.001$). In the second run, with each increase in riboflavin concentration there was an increase in weight of residual tissue ($P < 0.001$) at 10 days. At 20 days, the dry weight was lower with 0.05% riboflavin compared to 0.3% ($P < 0.001$) and 0.2% and 0.1% solutions ($P < 0.05$), with no other difference between groups.

Conclusions. There is a consistent dose-response curve with higher concentrations of riboflavin achieving greater CXL efficacy, suggesting that manipulation of riboflavin dosage as well as the UVA protocol can be used to optimize CXL.

Keywords: keratoconus, corneal cross-linking, riboflavin, enzymatic digestion

The current management of corneal ectatic diseases such as keratoconus depends on the severity and extent of the degree of irregular astigmatism.[1] Mild cases can be corrected with spectacles and soft toric contact lenses.[2] However, such modalities are limited in their effectiveness as the cornea becomes more irregular. In advanced disease, special soft, rigid gas-permeable, and scleral contact lenses become a more suitable solution to restore vision.[3] Despite the use of such special contact lenses, studies indicate that over 25% of patients with keratoconus can progress to such an extent that they require corneal transplantation,[4] with this disease remaining the most common indication for penetrating keratoplasty in Europe, Australia, South America, Africa, and the Middle East.[5]

The introduction of cross-linking (CXL) has heralded a new era in the treatment of corneal ectatic disorders. CXL utilizing riboflavin/ultraviolet A (UVA) is now a widely established intervention that has been shown to halt the progression of the disease process in keratoconus, post-LASIK ectasia, and pellucid marginal degeneration.[6,7] The rationale of CXL is to enhance the biomechanical rigidity of the cornea[6,7] and its resistance to enzymatic digestion[8] by creating cross-links between both collagen and proteoglycan molecules within the corneal stroma.[9–11] Not only does CXL appear to stabilize corneal ectasia at a stage when contact lenses can still be utilized, it also has been shown in many treated individuals to reduce topographic steepness and corneal high-order aberrations, resulting in improved vision.[12] Indeed, a recent study in the Netherlands demonstrated a significant reduction in the number of corneal transplants for keratoconus following the nationwide introduction of CXL.[13]

The standard CXL (SCXL) protocol, first described clinically by Wollensak et al.[7] in 2003, involves debridement of the central 9 mm of corneal epithelium, followed by soaking the exposed stromal surface with 0.1% riboflavin for 30 minutes and irradiation with 370-nm UVA light with an intensity of 3.0 mW/cm^2 for 30 minutes (a total dose of 5.4 J/cm^2). This protocol requires more than 1 hour of treatment time. To shorten this procedure time, given the large potential numbers of patients with progressive keratoconus requiring CXL and its resultant burden to health service delivery, and to improve patient and surgeon convenience alike, accelerated CXL (ACXL) protocols have been introduced.[14] These ACXL techniques are based on the Bunsen-Roscoe law of photochemical reciprocity and are modeled on the understanding that the same photochemical effect can be achieved with a reduced irradiation interval, provided that the total energy level is kept

Table 1. Treatment Groups for the Two Separate Experimental Runs, Detailing the Differing Riboflavin Concentrations Utilized

Groups	Riboflavin Soak Time	CXL Time	No. of Eyes	
			Run 1	Run 2
1. Untreated corneas	30 minutes	9 mw/cm^2 for 10 min	6	6
2. Riboflavin 0.05%	30 minutes	9 mw/cm^2 for 10 min	11	10
3. Riboflavin 0.1%	30 minutes	9 mw/cm^2 for 10 min	11	10
4. Riboflavin 0.2%	30 minutes	9 mw/cm^2 for 10 min	11	10
5. Riboflavin 0.3%	30 minutes	9 mw/cm^2 for 10 min	11	10

constant by a corresponding increase in irradiation intensity.[15] However, as has been demonstrated with other photochemical reactions, this law may be valid only within a certain dose range and varies with different types of photochemical processes.[16] Certainly, while efficacy has been demonstrated, it appears both in the laboratory[17] and clinically[18,19] that ACXL may be less effective than SCXL, although the minimum effective amount of CXL needed for stabilization of ectasia has not yet been established.[17,20]

The precise reasons for the reduced efficacy of ACXL protocols are unclear, and the exact mode of action of CXL at a molecular level is undetermined.[21] It is postulated that riboflavin acts as a photosensitizer to produce both oxygen singlets and riboflavin triplets,[22] which then drive the CXL process within the corneal stroma.[23] What is understood is that oxygen is essential to drive the process, and in the absence of oxygen, CXL is impaired.[24] It has been hypothesized that the reduced efficacy associated with ACXL protocols might be the result of more rapid oxygen depletion.[25,26] Kameav et al.[27] showed that, oxygen consumption occurs within seconds during UVA irradiation and that following cessation of irradiation, oxygen levels can take several minutes to be restored. As such it has been hypothesized that by pulsing the UVA light during irradiation, oxygen levels within the stroma might be replenished/maintained so that the CXL process is not compromised.[28,29] Other investigators have advocated that in addition to pulsing optimization of ACXL protocols can be achieved by extending the UVA dosage by 30% to 40%.[30,31] Indeed, in a laboratory study utilizing the same resistance to enzymatic digestion methodology employed in this present study, our group demonstrated increased efficacy with both extended and pulsed UVA dosages with ACXL protocols, although the results suggested that the distribution of cross-links may be different compared to SCXL.[23] As described above, to date virtually all research directed at optimizing CXL protocols has been targeted at manipulating the UVA irradiation dosage of the treatment. Indeed, except for some transepithelial CXL protocols,[32] published CXL research, including those with varying riboflavin formulations, has almost universally maintained a riboflavin concentration of 0.1%. Almost 15 years after publication of the first clinical paper,[7] the optimal stromal riboflavin dosage for CXL is yet to be determined.[22] This present study aims to investigate this issue by determining the efficacy of CXL using an enzymatic (pepsin) resistance model in ex vivo porcine corneas with varying concentrations of riboflavin (0.05%, 0.1%, 0.2%, and 0.3%).

Methods

A total of 96 fresh porcine eyes were utilized in this study. All had transparent corneas and an intact corneal epithelium on inspection. They were obtained and transported on ice from a local European Community licensed abattoir and used within 12 hours of death. The experiment was conducted using two separate treatment runs to ensure the consistency of the results. In the first run, 50 eyes were utilized, and in the second, conducted 8 weeks later, 46 eyes were used.

Our pepsin digestion methodology has been published previously.[17,23] We chose this method as it facilitates relatively slow digestion rates. This has allowed us in our past studies to not only detect significant differences in the digestion rates in terms of disc diameter measurements and time to complete digestion but also to measure dry weights at 10 days, which has highlighted significant differences between treatment protocols that are not evident by just measuring disc diameters and time to digestion alone.[17,23] In addition, using this same protocol we have repeatedly shown that there are no differences in digestion times in nonirradiated corneas that have not received riboflavin drops and those soaked in riboflavin for 30 minutes.[17,23] This allowed us in this study to reduce the number of control groups and just use de-epithelialized, nontreated, nonirradiated corneas as a sole control group. In brief, following complete debridement of the corneal epithelium using a single-edged razor blade, the eyes were divided randomly into the five groups described in Table 1, in which group 1 (no riboflavin administered and no UVA exposure) served as an untreated control and groups 2, 3, 4, and 5 received varying concentrations of riboflavin solution (0.05%, 0.1%, 0.2%, 0.3%, respectively) for a period of 30 minutes. All riboflavin solutions contained 20% dextran and were identical in formulation except for the riboflavin concentration. The riboflavin was applied using a 10-mm suction ring/container (J2294; E. Janach srl, Como, Italy) that was completely filled to its brim with the relevant riboflavin solution concentration after being placed and suctioned over the central cornea. Following the 30-minute riboflavin diffusion period, all eyes in groups 2, 3, 4, and 5 underwent irradiation using a CCL-VARIO corneal cross-linking UVA lamp (Peschke Meditrade GmbH, Huenenberg, Switzerland) with a wavelength of 365 nm and a 9.0-mm aperture, with an intensity of 9 mW/cm^2 for 10 minutes (total energy dose 5.4 J/cm^2). An accelerated treatment protocol was chosen, as we needed to treat 44 eyes in each experimental run and wished to use only one UVA irradiation device so that fluence levels and UV beam profile were consistent between treatments. If we had used the standard protocol of 3 mW/cm^2 for 30 minutes, it would have taken 22 hours to complete the treatments in radiation time alone. This would mean that the eyes being treated last would be well over 24 hours old since time from enucleation. Even though we treated one eye from each group sequentially to minimize any effects of some eyes being treated later than others, we did not want to include any eyes in which treatment occurred after 24 hours. This was undertaken to diminish any effects of natural decomposition, endothelial and epithelial cell death with subsequent changes in corneal hydration, and possible fungal/bacterial contamination. By using an accelerated treatment of 9 mW/cm^2 for 10 minutes, we could reduce the total irradiation time to just over 7 hours and treat all eyes with 12 hours.

Central corneal thickness measurements were taken manually using a handheld ultrasonic pachymeter (Pachmate 55; DGH Technology, Inc., Exton, PA, USA) after epithelial removal, after riboflavin administration, and after UVA irradiation in the treatment groups 2, 3, 4, and 5 in the first experimental run (44 eyes).

On completion of the treatments, an 8-mm full-tissue-thickness biopsy was trephined from the center of each cornea. The corneal discs were placed in individual sealed tubes containing 5 mL pepsin digest solution, 1 g $\geq$ 500 U/mg pepsin from porcine gastric mucosa (Sigma-Aldrich Corp., Dorset, UK) in 10 mL 0.1 M hydrochloric acid at pH 1.2 and incubated them in a water bath at 23°C. As previous studies have indicated that CXL results in cross-links not only at the collagen fibril surface but also in the proteoglycan network surrounding the collagen,[11] we selected pepsin for enzymatic digestion as it is a nonspecific endopeptidase that breaks down both collagen and proteoglycan core proteins.

To reduce the risk of fungal/bacterial contamination, sterility was maintained by undertaking the preparation of the sample specimens with sterile instruments, which were cleaned with an ethanol alcohol spray (Spiriclens DEB; Ecolab Ltd., Leeds, UK) between specimen preparation. The sealed tubes into which the corneal discs were placed were clean and sterile prior to usage. To avoid contamination, from the water bath, 30 mL chlorine-based disinfecting solution (Milton sterilizing fluid; Milton Pharmaceutical Company, Bournemouth, UK) was added to the bath water every 3 days and the water replaced every 12 days. All instruments used when handling samples for measurement were cleaned before and between sample measurement and left to dry using ethanol alcohol spray. At day 26, in the first experimental run the pepsin digest solution in each sealed tube was replaced, both to enhance further digestion and to attempt to maintain sterility.

First Experimental Run

In the first experimental run (involving 50 eyes), electronic digital calipers were used to perform daily measurements of the longest diameter of the anterior surface of each corneal disk. This was facilitated by microscopic examination at 10× magnification after the disk had been poured into a sterile petri dish and separated from the pepsin digest solution using a sterilized pipette. This magnified examination allowed the longest diameter of the disc to be identified and precisely measured with the electronic calipers. Measurements were performed until the tissue could no longer be distinguished from the surrounding pepsin solution, at which time point the tissue was considered to have undergone complete digestion.

Measurements of anterior corneal disc diameter, rather than stromal thickness, were used to assess the rate of enzymatic digestion as the corneal discs underwent significant posterior stromal swelling (in the vertical direction) during immersion in pepsin digest solution, and the more-resistant anterior portion of the cornea then separated from the posterior stroma after 4 to 6 days.[17,23]

To further evaluate the effect of different riboflavin concentrations on corneal enzymatic resistance, five randomly selected corneal discs from each CXL-treated group (groups 2, 3, 4, and 5) were removed from the pepsin digest solution after 10 days, placed in a 60°C oven, and weighed daily until a constant dry weight was obtained. The average dry weight was then calculated for each group. There were no differences between the groups in the mean times each of the groups were in the oven (median 7 days). This methodology was undertaken to ensure the samples were completely dehydrated and the true dry tissue weight verified.

The remaining six discs in each of the CXL treatment groups 2, 3, 4, and 5 remained in pepsin digest solution and were measured daily, as described above, until digestion was complete. At day 26 it appeared that the discs had stopped digesting so the digest solution in each sealed tube was replaced with freshly prepared pepsin digest solution (with the same formulation as described previously), and the temperature of the water bath was increased to 26°C to accelerate the digestion process.

Second Experimental Run

To ensure the consistency of the results, a second experimental run of 50 eyes was conducted (Table 1). While previous enzymatic digestion studies from our group[17,23] have indicated that the corneal disc diameter measurements appear to provide information about the structural integrity of the most anterior layers of the cornea, they can be subject to variation. This occurs especially in the later stages of digestion when the tissue tends to lose its circular shape and become irregular in outline, making the longest diameter of the tissue difficult to determine. As the dry weight measurements represent the total mass of undigested tissue and negate any of the problems associated with tissue shape and between-sample differences in hydration, in the second experimental run we replaced reliance on this more-reproducible methodology. In this run, after being immersed in pepsin solution, the discs remained in their sealed containers and were incubated at 23°C until day 10, when five corneal discs from each CXL treatment group (groups 2, 3, 4, and 5) were removed from the digest solution and placed in the 60°C oven until a constant dry weight was obtained and the average corneal dry weight calculated for each group. This process was repeated at 20 days, when the remaining five corneal discs from each group were removed from the pepsin digest, placed in the 60°C oven, and their constant dry weights recorded. The digest solution was not renewed during this second run, and the water bath temperature was maintained at 23°C.

Statistical Analysis

Data are shown as average measurements (± SD) for corneal thickness, dry weight, and complete digestion time. Measurements of corneal disk diameter are presented as a daily cumulative measurement for each treatment group. Statistical analysis was performed using a 1-way ANOVA and Bonferroni multiple comparisons in a depth-wise manner. All statistical analyses were performed with the Statistical Package for the Social Sciences (SPSS Statistics 20; IBM, Armonk, NY, USA). A probability value of $P < 0.05$ was considered significant.

Results

Corneal Thickness

The average stromal thicknesses pretreatment (after epithelial debridement), after riboflavin administration and after UVA irradiation in the first experimental run are shown in Figure 1. There was a significant decrease in thickness following CXL (from pretreatment to after CXL) in all groups ($P < 0.001$), but there were no differences in thicknesses between the groups at any stage.

Time Taken for Complete Digestion

As previously reported,[17,23] in all corneal discs significant stromal swelling, in a posterior–anterior direction, was documented within 24 hours of submersion in the pepsin

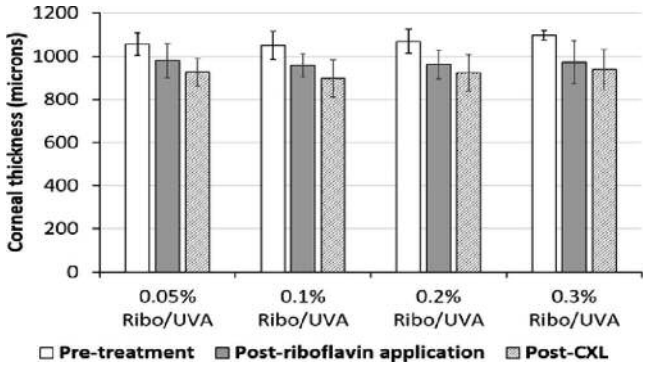

Figure 1. Corneal thickness measurements for each group in the first experimental run are shown before treatment (after epithelial debridement), following riboflavin administration for 30 minutes, and after CXL ($n = 11$ per group). Data are shown as the mean value ± SD.

digest solution. By 4 to 6 days, the anterior portion of each corneal disc had separated from the posterior portion, and by days 8 to 10 the posterior portion of each disc had undergone complete digestion. The anterior portion of the corneal discs persisted to allow daily measurements of diameter (Fig. 2; Table 2).

The time required for complete digestion of the CXL-treated corneal discs (groups 2, 3, 4, and 5) was significantly longer than that required for the untreated specimens in group 1 ($P < 0.001$) (Fig. 2; Table 2). After 10 days, all untreated corneas (group 1) had undergone complete digestion in both experimental runs. Based on cumulative measurements of corneal disc diameter for each treatment group, the irradiated corneas treated with a higher concentration of riboflavin appeared to take longer to undergo complete digestion than those treated with lower concentrations of riboflavin. However, this was largely due to the persistence of a minority of samples within the higher riboflavin concentration groups (Fig. 2), and the average time taken for complete digestion to occur did not differ significantly between the CXL-treated groups ($P = 0.3$) (Table 2).

Dry Weight Measurements

After 10 days in the pepsin digest solution, only the CXL-treated corneas remained, with all the untreated discs being completely digested in both experimental runs (Fig. 2; Table 2).

Table 2. Time in Days Taken for Complete Digest to Occur in All Groups

Group	Time Taken for Complete Digestion to Occur		
	Minimum, d	Maximum, d	Average, d (±SD)
Untreated	6	10	8 (±2)
0.05% Ribo/UVA	36	40	39 (±2)
0.1% Ribo/UVA	36	42	39 (±2)
0.2% Ribo/UVA	39	45	41 (±2)
0.3% Ribo/UVA	38	46	41 (±3)

Ribo/UVA, Riboflavin/UVA.

First Experimental Run

In the first experimental run, there was a statistically significant difference in dry weight measurements between all treated groups (2, 3, 4, and 5) at 10 days ($P < 0.001$). For each group with an increased riboflavin concentration, there was a significant increase in the dry weight of residual undigested corneal tissue, denoting an increased resistance of the tissue to pepsin digestion ($P < 0.001$) (Fig. 3A; Table 3).

Second Experimental Run

Similarly, in the second experimental run, there was a statistically significant difference in dry weight measurements between all treated groups (groups 2, 3, 4, and 5) at 10 days ($P < 0.001$). For each group with an increased riboflavin concentration, there was a significant increase in the dry weight of residual undigested corneal tissue, denoting an increased resistance of the tissue to pepsin digestion ($P < 0.001$) (Fig. 3B; Table 3), with comparable average dry weights for each of the treatment groups in the two experimental runs (Table 3).

In the second experimental run at 20 days, measurement of the average stromal dry weight was significantly lower in the 0.05% riboflavin treatment group (group 2) than in the 0.3% ($P < 0.001$) and the 0.2% and 0.1% treatment groups ($P < 0.05$) (groups 3, 4, and 5). There was no significant difference between 0.1%, 0.2%, and 0.3% riboflavin/UVA treated groups (groups 3, 4, and 5) at 20 days of digestion (Fig. 4; Table 4).

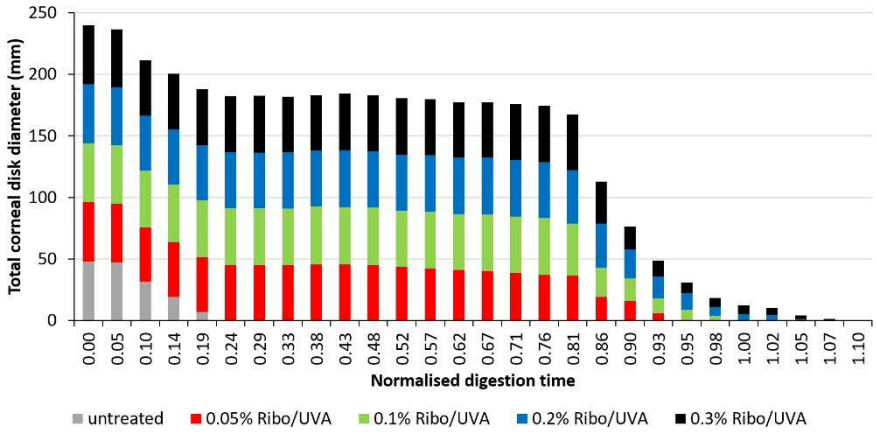

Figure 2. The summed longest diameter of the corneal discs in each group in the first experimental run is shown as a function of time, which has been normalized against the maximum time taken for corneas cross-linked using the standard 0.1% riboflavin formulation (42 days) to undergo complete digestion. The discs appeared to stop digesting at approximately day 26 (normalized time of 0.62) so temperature was increased to 26°C and the digest solution renewed.

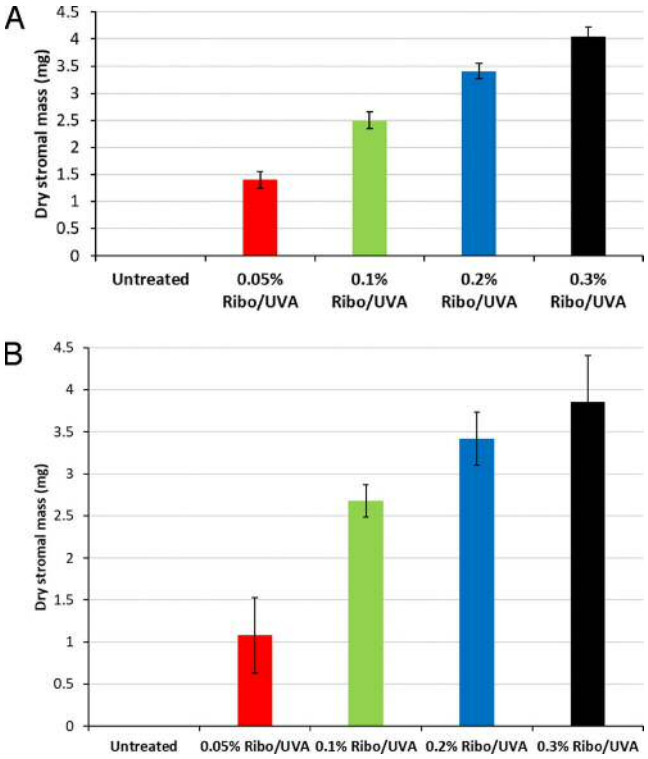

FIGURE 3. (**A**) Average stromal dry weight of the untreated and treated groups ($n = 5$ samples per group) at day 10 in the first experimental run. *Error Bars*: ±1 SD. There was a statistically significant difference in dry weights between all groups ($P < 0.001$) at 10 days. (**B**) Average stromal dry weight of the untreated and CXL-treated groups ($n = 5$ samples per group) at day 10 in the second experimental run. *Error Bars*: ±1 SD. There was a statistically significant difference in dry weights between all groups ($P < 0.001$) at 10 days.

DISCUSSION

SCXL has been shown to be efficient in arresting the progression of corneal ectatic disease in most treated eyes with up to 10 years follow-up.[33,34] Although numerous modifications of the epithelium-off CXL technique have been postulated, these have almost universally focused on variation in the UVA protocol and additives to the standard riboflavin 0.1% solution.[21] Indeed, except for some epithelium-on CXL formulations that utilize 0.25% riboflavin concentrations,[32] virtually all currently used epithelium-off protocols use a riboflavin concentration of 0.1%.[21,22] Despite the passage of almost two decades since the first human clinical CXL treatments,[7] the optimum riboflavin dosage for CXL is undetermined,[22] but to fully evaluate the efficacy and safety of any drug, it is vital to determine its dose-response curve.[35]

There are multiple problems with determining this dose-response curve, the not least of which is the difficulty in measuring the biomechanical changes induced by CXL. As yet there are no reliable ways to measure these changes in vivo,[36] a problem that compounded by the fact that any measurable clinical changes take months to become evident and years to stabilize.[33,34] Even in vitro, the measurement of biomechanical changes after CXL are beset with difficulty. Standard biomechanical measurement methodologies, such as stress-strain extensiometry, have inherent deficiencies when applied to the assessment of biological tissues such as the cornea.[37] Such biological tissues do not behave like metals and polymers with homogeneous chemical/molecular bonds but rather have nonhomogeneous chemical bonds and molecular interactions that result in viscoelastic material properties. In addition, strip specimens from corneas are originally part of a spherical surface, so the length of the strip along its longitudinal centerline is longer than its sides and there is variation in thickness between the corneal center and its periphery.[37] All these factors can lead to poor measurement reliability, which has led investigators to explore other potential methodologies such as inflation techniques,[38] scanning acoustic microscopy,[39] and Brillouin microscopy,[40] none of which have yet to become a reliable gold standard measurement technique to determine biomechanical changes after CXL.

An increase in activity of proteinase enzymes and reduction of proteinase inhibitors have been identified in keratoconic corneas[41] and are liable to be important factors in the pathophysiology of the condition and disease progression. The main aim of corneal cross-linking is to halt the progression of corneal ectasia. While cross-linking the macromolecules within the corneal stroma undoubtedly augments its mechanical strength, it also increases its resistance to enzymatic

TABLE 3. Average Stromal Dry Weight of Control Group 1 and Treated Groups 2, 3, 4, and 5 ($n = 5$) at Day 10 in First and Second Experimental Runs

	Mean Dry Weight After 10 Days of Digestion, mg ±1 SD	
Group	Run 1	Run 2
Untreated	0	0
0.05% Ribo/UVA	1.4 ± 0.16	1.08 ± 0.45
0.1% Ribo/UVA	2.5 ± 0.16	2.68 ± 0.19
0.2% Ribo/UVA	3.4 ± 0.14	3.42 ± 0.32
0.3% Ribo/UVA	4.04 ± 0.18	3.86 ± 0.54

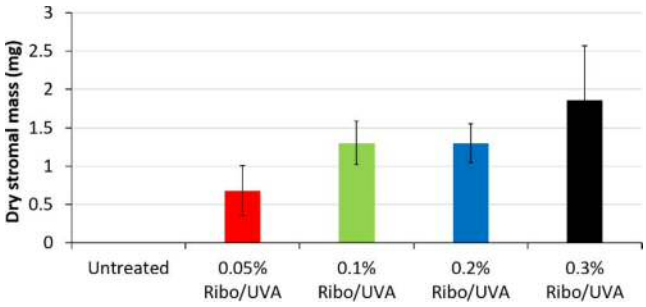

FIGURE 4. Average stromal dry weight (milligrams) of control group 1 and treated groups 2, 3, 4, and 5 ($n = 5$) at day 20 in a second experimental run. *Error Bars*: ±1 SD. The average stromal dry weight was significantly lower in the 0.05% riboflavin treatment group (group 2) than in the 0.3% ($P < 0.001$) and the 0.2% and 0.1% treatment groups ($P < 0.05$) (groups 3, 4, and 5).

TABLE 4. Average Stromal Dry Weight of the Untreated and CXL-Treated Groups ($n = 5$ samples per group) at Day 20 in the Second Experimental Run

Group	Mean Dry Weight at 20 Days in Second Experimental Run, mg ±1 SD
Untreated	0
0.05% Ribo/UVA	0.68 ± 0.33
0.1% Ribo/UVA	1.3 ± 0.28
0.2% Ribo/UVA	1.3 ± 0.25
0.3% Ribo/UVA	1.86 ± 0.71

digestion. Spoerl et al.[42] were the first to demonstrate this increased resistance of the corneal stroma to enzymatic digestion after CXL. The ability of CXL to increase corneal stromal resistance to enzymatic digestion can therefore be expected to be a significant factor with regard to efficacy of the procedure in halting disease progression. To what extend and precisely how resistance to enzymatic digestion and increase in biomechanical strength after CXL are responsible for and contribute to its efficacy is yet undetermined, but both can undoubtedly be used as a measure of CXL efficacy. It is for such reasons, as well as poor measurement reliability of current methods of corneal biomechanical assessment (which we discussed above), that in this study we employed an enzymatic digestion methodology. We have previously demonstrated the efficacy of this methodology in determining differences in both ACXL and epithelium-on CXL protocols compared to SCXL.[17,23]

We employed two experimental runs in this study to ensure consistency and verify our dry weight measurements, as well as to simplify and improve our methodology. While daily measurements of the disc diameters until digestion do provide information about the structural integrity of the anterior layers of the cornea to which CXL is directed,[17,23] their measurement, as well as being time-consuming, is subject to variation. This is especially true in the later stages of digestion, when the repeatability and hence reliability of the measurements are reduced due to the smaller dimensions of the tissue and its increasingly irregular outline. In addition, with time the pepsin solution in which the discs are immersed loses its digestive activity. Indeed, in the first experimental run we perceived that the discs had stopped digesting at about day 26; therefore, in order to complete the experiment, we had to renew the pepsin solution. As dry weight measurements, which represent the total mass of undigested tissue, were found to be highly reproducible because they negate any problems associated with within-sample variations in corneal thickness, shape, and between-sample differences in hydration, in the second experimental run we relied solely on this methodology and collected dry weight measurements at day 10 and day 20 of digestion.

All CXL-treated eyes in our study received an application of an iso-osmolar riboflavin solution containing 20% dextran. Consistent with previous studies,[17,23,43] this resulted in a significant decrease in corneal thickness (Fig. 1), probably attributable to the deturgescent effect of the 20% dextran and dehydration of the de-epithelialized cornea during cross-linking. As might be expected, the concentration of riboflavin over the ranges we used had no effect on corneal thickness.

In previous studies using an identical methodology, we have shown that there are no differences at all between digestion times in nonirradiated corneal controls that have not received riboflavin drops and those soaked in riboflavin for 30 minutes.[16,23] This allowed us, in this present study, to reduce the number of control groups and use only completely de-epithelialized, nontreated, nonirradiated corneas as a sole control group. As we have documented previously,[17,23] the time required for complete digestion of the treated CXL corneal discs was significantly longer than the untreated controls, demonstrating the reproducibility of this technique in detecting changes between CXL-treated and untreated corneas. However, despite an evident trend for the higher-concentration riboflavin-treated corneas to take longer to digest completely, the differences between groups were not significant. In contrast, the dry weight measurements after 10 days of digestion (Figs. 3A, 3B; Table 3) and to a lesser extent at 20 days (Fig. 4; Table 4), demonstrated significant differences between the treatment groups, indicating that an increase in riboflavin concentration from 0.05% to 3% results in a progressive improvement in the resistance of cross-linked corneas to enzymatic digestion. This suggests that measurement of the time until digestion is complete is not sensitive enough to detect subtle (but probably clinically important) differences in CXL efficacy with differing protocols. Certainly, in a previous study using this methodology to investigate SCXL versus ACXL protocols,[18] time to complete digestion showed no differences, whereas dry weight measurements indicated significant differences, with better results in SCXL.[17] Clinical investigations confirmed and supported such laboratory findings of a reduced efficacy with ACXL.[18,19]

The similarity between runs 1 and 2 in terms of the average dry weight measurements for each group after 10 days of digestion confirmed our belief that the dry weight technique is a less time-consuming and a more accurate and reproducible technique for investigating CXL efficacy than are daily measurements of corneal diameter (Fig. 3A, 3B; Table 3).

Over the ranges we tested, such outcomes support a dose-response curve of riboflavin in CXL, with higher concentrations, up to 0.3%, achieving greater efficacy. How these results will transfer into clinical efficacy is undetermined until clinical trials with higher concentrations are undertaken, but they may have important implications. In this study, all treatments were conducted using an ACXL technique of 9 mW/cm^2 for 10 minutes (total energy dose 5.4 J/cm^2), yet manipulation of riboflavin dosage and hence stromal concentration resulted in improved efficacy. This occurred without oxygen supplementation or pulsing, which some authors, both in laboratory[23] and clinical studies,[28,29] have hypothesized may augment the CXL process, especially with ACXL protocols. A riboflavin dose-response curve might suggest that while oxygen and type II photochemical (aerobic) reactions are undoubtedly important in the CXL process,[24] type I photochemical (anaerobic) pathways, with direct interaction between excited riboflavin triplets and stromal proteins resulting in cross-linking, play a significant role and may be augmented by increasing riboflavin concentrations during CXL. As such, the efficacy of ACXL might be improved not only by increasing the UVA dosage and perhaps the addition of supplemental oxygen and/or pulsing but also by simply increasing stromal riboflavin concentration. With manipulation of such parameters, it might be possible with ACXL to reduce the overall treatment time while maintaining the same clinical efficacy as SCXL.

Such results may also have important implications for epithelium-on CXL, where reports of reduced efficacy compared to SCXL[44] are likely to be related to limited riboflavin absorption through the intact corneal epithelium and low stromal riboflavin concentrations. A dose-response curve of riboflavin with higher concentrations, at least up to 0.3%, achieving greater efficacy would support such a hypothesis. It is of note that by using two-photon fluorescence, we have previously shown that stromal riboflavin concentrations with currently commercially available protocols are only 10% to 30% of that achieved with SCXL[45] and that in laboratory studies, manipulation of such epithelium-on protocols can result in higher achieved stromal riboflavin concentrations[46] and resultant increased CXL efficacy.[47]

Finally, in the CXL process riboflavin has two basic functions. As well as acting as a photosensitizer to produce both oxygen singlets and riboflavin triplets to drive the CXL process,[22] it also absorbs the UVA photons within the anterior corneal stromal to reduce UVA toxicity and potential damage to internal ocular structures such as the endothelium.[48] The use of higher-strength riboflavin solutions resulting in increased stromal riboflavin concentrations and therefore increased UVA absorption within the anterior stroma, should theoretically reduce the amount of UVA radiation reaching deeper layers of

Investigative Ophthalmology & Visual Science

the cornea, reducing the risk of endothelial toxicity as well as allowing for the possible treatment of thinner corneas.[49] It is interesting that while it might be supposed that increased absorption of UVA photons within the anterior stroma by higher riboflavin concentrations might result in an increased but more superficial cross-linking effect, our dry weight results of a significant increase in the mass of residual undigested corneal tissue with increasing riboflavin concentration, while there were no differences in disc diameter measurements, suggest that this is probably not the case. We can postulate from such results that more volume of tissue is being cross-linked, including that in deeper stromal layers with higher riboflavin concentrations, and that we are not merely getting a more intense, but superficial effect, that one might expect not to affect the dry weight measurements but to result in differences in disc diameter measurements during the digestion process.

Conclusions

Our results demonstrate a dose-response curve with increasing riboflavin solution concentrations up to 0.3% achieving greater CXL efficacy. This suggests that by simply increasing the riboflavin concentration, at least within the limits we tested, it may be possible to increase the efficacy of ACXL to match that of SCXL. The use of higher concentrations of riboflavin solution may also improve the outcomes of epithelium-on CXL as well and allow the safe treatment of thin corneas. Whether or not higher concentrations of riboflavin in CXL may result in any adverse complications (such as increased haze) is as yet undetermined, but this study appears to support the commencement of clinical trials of CXL with moderately increased higher riboflavin concentration solutions.

Acknowledgments

Disclosure: **N.A.L. O'Brart**, None; **D.P.S. O'Brart**, Sooft Italia SPA (C), Alcon, Inc. (C, F); **N.H. Aldahlawi**, None; **S. Hayes**, None; **K.M. Meek**, None

References

1. Ortiz-Toquero S, Rodriguez G, de Juan V, Martin R. Rigid gas permeable contact lens fitting using new software in keratoconic eyes. *Optom Vis Sci*. 2016;93:286–292.
2. Rathi VM, Mandathara PS, Dumpati S. Contact lens in keratoconus. *Indian J Ophthalmol*. 2013;61:410–415.
3. Wu Y, Tan Q, Zhang W, et al. Rigid gas permeable contact lens related life quality in keratoconic patients with different grades of severity. *Clin Exp Ophthalmol*. 2015;98:150–154.
4. Javadi MA, Motlagh BF, Jafarinasab MR, et al. Outcomes of penetrating keratoplasty in keratoconus. *Cornea*. 2005;24:941–946.
5. Matthaei M, Sandhaeger H, Hermel M, et al. Changing indications in penetrating keratoplasty: a systematic review of 34 years of global reporting. *Transplantation*. 2017;101:1387–1399.
6. Gore DM, Short AJ, Allan BD. New clinical pathways for keratoconus. *Eye*. 2013;27:329–339.
7. Wollensak G, Spoerl E, Seiler T. Riboflavin/ultraviolet-A–induced collagen crosslinking for the treatment of keratoconus. *Am J Ophthalmol*. 200331;135:620–627.
8. Beshtawi IM, O'Donnell C, Radhakrishnan H. Biomechanical properties of corneal tissue after ultraviolet-A–riboflavin crosslinking. *J Cataract Refract Surg*. 2013;39:451–462.
9. Gatinel D. Effectiveness of corneal collagen crosslinking in vivo for corneal stiffening. *J Cataract Refract Surg*. 2014;40:1943–1944.
10. Kobashi H, Rong SS. Corneal collagen cross-linking for keratoconus: systematic review. *Biomed Res Int*. 2017;2017:8145651.
11. Hayes S, Kamma-Lorger C, Boote C, et al. The effect of riboflavin/UVA collagen cross-linking therapy on the structure and hydrodynamic behaviour of the ungulate and rabbit corneal stroma. *PLoS One*. 2013;8:e52860.
12. Vinciguerra P, Albé E, Frueh BE, Trazza S, Epstein D. Two-year corneal cross-linking results in patients younger than 18 years with documented progressive keratoconus. *Am J Ophthalmol*. 2012;154:520–526.
13. Godefrooij DA, Gans R, Imhof SM, Wisse RP. Nationwide reduction in the number of corneal transplantations for keratoconus following the implementation of cross-linking. *Acta Ophthalmol*. 2016;94:675–678.
14. Mastropasqua L. Collagen cross-linking: when and how? A review of the state of the art of the technique and new perspectives. *Eye Vis*. 2015;2:19.
15. Bunsen R, Roscoe H. Photochemical researches. Part V. On the measurement of the chemical action of direct and diffuse sunlight. *Proc R Soc Lond*. 1862;12:306–312.
16. Potapenko A, Agamalieva M, Nagiev A, Lysenko E, Bezdetnaya L, Sukhorukov V. Photochemolysis sensitized by psoralen: reciprocity law is not fulfilled. *Photochem Photobiol*. 1991;54:375–379.
17. Nada H, Aldahlawi AH, Hayes S, O'Brart DPS, Meek KM. Standard versus accelerated riboflavin/ultraviolet corneal cross-linking: resistance against enzymatic digestion. *J Cataract Refract Surg*. 2015;41:1989–1996.
18. Ng AL, Chan TC, Cheng AC. Conventional versus accelerated corneal collagen cross-linking in the treatment of keratoconus. *Clin Exp Ophthalmol*. 2016;44:8–14.
19. Chow VW, Chan TC, Yu M, Wong VW, Jhanji V. One-year outcomes of conventional and accelerated collagen cross-linking in progressive keratoconus. *Sci Rep*. 2015;25:14425.
20. Kymionis GD, Grentzelos MA, Kankariya VP, et al. Safety of high-intensity corneal collagen crosslinking. *J Cataract Refract Surg*. 2014;40:1337–1340.
21. O'Brart DPS. Corneal collagen cross-linking for corneal ectasias: a review. *Eur J Ophthalmol*. 2017;27:253–269.
22. O'Brart DP. Riboflavin for corneal cross-linking. *Drugs Today (Barc)*. 2016;52:331–346.
23. Aldahlawi NH, Hayes S, O'Brart DP, Akhbanbetova A, Littlechild SL, Meek KM. Enzymatic resistance of corneas cross-linked using riboflavin in conjunction with low energy, high energy, and pulsed UVA irradiation modes. *Invest Ophthalmol Vis Sci*. 2016;57:1547–1552.
24. McCall A, Kraft S, Edelhauser H, et al. Mechanisms of corneal tissue cross-linking in response to treatment with topical riboflavin and long-wavelength ultraviolet radiation (UVA). *Invest Ophthalmol Vis Sci*. 2010;51:129–138.
25. Brittingham S, Tappeiner C, Frueh B. Corneal cross-linking in keratoconus using the standard and rapid treatment protocol: differences in demarcation line and 12-month outcomes. *Invest Ophthalmol Vis Sci*. 2014;55:8371–8376.
26. Touboul D, Efron N, Smadja D, Praud D, Malet F, Colin J. Corneal confocal microscopy following conventional, transepithelial, and accelerated corneal collagen cross-linking procedures for keratoconus. *J Refract Surg*. 2012;28:769–776.
27. Kamaev P, Friedman M, Sherr E, Müller D. Photochemical kinetics of corneal cross-linking with riboflavin. *Cornea*. 2012;53:2360–2367.

Investigative Ophthalmology & Visual Science

28. Mazzotta C, Traversi C, Paradiso A, Latronico M, Rechichi M. Pulsed light accelerated crosslinking versus continuous light accelerated crosslinking: one-year results. *J Ophthalmol*. 2014;2014:604731.
29. Krueger R, Herekar S, Spoerl E. First proposed efficacy study of high versus standard irradiance and fractionated riboflavin/ultraviolet a cross-linking with equivalent energy exposure. *Eye Contact Lens*. 2014;40:353–357.
30. Kymionis G, Tsoulnaras K, Grentzelos M, et al. Evaluation of corneal stromal demarcation line depth following standard and a modified-accelerated collagen cross-linking protocol. *Am J Ophthalmol*. 2014;158:671–675.
31. Sherif A. Accelerated versus conventional corneal collagen cross-linking in the treatment of mild keratoconus: a comparative study. *Clin Ophthalmol*. 2014;2:1435–1440.
32. Gore DM, O'Brart D, Dunsby C, French P, Allan BD. A comparison of different corneal iontophoresis protocols for promoting transepithelial riboflavin penetration. *Invest Ophthalmol Vis Sci*. 2015;56:7908–7914.
33. Raiskup F, Theuring A, Pillunat LE, Spoerl E. Corneal collagen crosslinking with riboflavin and ultraviolet-A light in progressive keratoconus: ten-year results. *J Cataract Refract Surg*. 2015;41:41–46.
34. O'Brart DP, Patel P, Lascaratos G. Corneal cross-linking to halt the progression of keratoconus and corneal ectasia: seven-year follow-up. *Am J Ophtlamol*. 2015;160:1154–1163.
35. Prickaerts J, Van Goethem NP, Gulisano W, Argyrousi EK, Palmeri A, Puzzo D. Physiological and pathological processes of synaptic plasticity and memory in drug discovery: do not forget the dose-response curve. *Eur J Pharmacol*. 2017;817:59–70.
36. Steinberg J, Frings A, Mousli A, et al. New Scheimpflug dynamic in vivo curve analyses to characterize biomechanical changes of the cornea after cross-linking for progressive keratoconus. *J Refract Surg*. 2016;32:34–39.
37. Elsheikh A, Anderson K. Comparative study of corneal strip extensometry and inflation tests. *J R Soc Interface*. 2005;2:177–185.
38. Kling S, Remon L, Pérez-Escudero A, Merayo-Lloves J, Marcos S. Corneal biomechanical changes after collagen cross-linking from porcine eye inflation experiments. *Invest Ophthalmol Vis Sci*. 2010;51:3961–3968.
39. Beshtawi IM, Akhtar R, Hillarby MC, et al. Biomechanical properties of human corneas following low- and high-intensity collagen cross-linking determined with scanning acoustic microscopy. *Invest Ophthalmol Vis Sci*. 2013;54:5273–5280.
40. Scarcelli G, Kling S, Quijano E, Pineda R, Marcos S, Yun SH. Brillouin microscopy of collagen crosslinking: noncontact depth-dependent analysis of corneal elastic modulus. *Invest Ophthalmol Vis Sci*. 2013;54:1418–1425.
41. Zhou L, Sawaguchi S, Twining SS, Sugar J, Feder RS, Yue BYJT. Expression of degradative enzymes and protease inhibitors in corneas with keratoconus. *Invest Ophthalmol Vis Sci*. 1998;39:1117–1124.
42. Spoerl E, Wollensak G, Seiler T. Increased resistance of crosslinked cornea against enzymatic digestion. *Curr Eye Res*. 2004;29:35–40.
43. Hassan Z, Modis L Jr, Szalai E, Berta A, Nemeth G. Intraoperative and postoperative corneal thickness change after collagen crosslinking therapy. *Eur J Ophthalmol*. 2014;24:179–185.
44. Bikbova G, Bikbov M. Standard corneal collagen crosslinking versus transepithelial iontophoresis-assisted corneal cross-linking, 24 months follow-up: randomized control trial. *Acta Ophthalmol*. 2016;94:e600–e606.
45. Gore DM, O'Brart D, Dunsby C, French P, Allan BD. Transepithelial riboflavin absorption in an ex-vivo rabbit corneal model. *Invest Ophthamol Vis Sci*. 2015;56:5006–5011.
46. Gore DM, O'Brart D, Dunsby C, French P, Allan BD. A comparison of different corneal iontophoresis protocols for promoting transepithelial riboflavin penetration. *Invest Ophthalmol Vis Sci*. 2015;56:7908–7914.
47. Aldahlawi NH, Hayes S, O'Brart DPS, O'Brart NA, Meek KM. An investigation into corneal enzymatic resistance following epithelium-off and epithelium-on corneal cross-linking protocols. *Exp Eye Res*. 2016;153:141–151.
48. Spoerl E, Mrochen M, Sliney D, Trokel S, Seiler T. Safety of UVA-riboflavin cross-linking of the cornea. *Cornea*. 2007;26:385–389.
49. Jui-Teng L. Efficacy and z* formula for minimum corneal thickness in ultraviolet light cross-linking. *Cornea*. 2017;36:30–31.

Investigative Ophthalmology & Visual Science

Appendix C: Raw data of SAXS fibrillar parameter

Group	Ex/In Vivo	Sample	Interfibrillar Peak (nm)	D Period (nm)	Fibril Diameter (nm)	BC Interfibrillar Peak (nm)
Control	In vivo	C1	56.2	65.9	41.083	55.1
		C2	56.2	65.9	43	54
		C3	57.3	65.9	43.035	55.1
		C4	57.3	65.9	40.8	56.2
		C5	55.1	65.9	43.035	54
		C6	56.2	65.9	41.083	55.1
		Average	56.38	65.90	42.01	54.92
		SD	0.83	0.00	1.12	0.83
	Ex vivo	E1C	63.9	65.9	39.09	59.8
		E2C	66.9	65.9	39.952	65.3
		E3C	62.4	65.9	38.74	59.8
		E4C	59.8	65.9	39.09	58.5
		E5C	59.8	65.9	40.471	58.5
		E6C	65.3	65.9	38.811	63.9
		E7C	59.8	65.9	38.811	58.5
		E8C	63.9	65.9	38.811	59.8
		E9C	59.8	65.9	39.952	58.5
		E10C	59.6	65.9	38.74	58.5
		E11C	59.8	65.9	39.877	57.3
		E12C	59.8	65.9	39.66	58.5
		Average	61.73	65.90	39.33	59.74
		SD	2.63	0.00	0.61	2.40
Treated	In vivo	T1	56.2	65.9	42.449	53
		T2	56.2	65.9	43.818	53
		T3	56.2	65.9	40.548	53
		T5	54	65.9	42.12	52
		T6	54	65.9	39.952	52
		Average	55.32	65.9	41.78	52.6
		SD	1.20	0.00	1.51	0.55
	Ex vivo	E1T	65.3	65.9	39.261	63.9
		E2T	63.9	65.9	39.836	58.5
		E3T	58.5	65.9	39.373	55.1
		E4T	59.8	65.9	39.546	57.3
		E5T	59.8	65.9	39.373	58.5
		E6T	58.5	65.9	38.264	57.3
		E7T	62.4	65.9	39.546	58.5
		E8T	65.3	65.9	39.546	59.8
		E9T	65.3	65.9	38.701	63.9
		E10T	63.9	65.9	39.373	58.5
		E11T	59.8	65.9	40.548	58.5
		E12T	65.3	65.9	38.979	59.8
		Average	62.32	65.90	39.36	59.13
		SD	2.84	0.00	0.57	2.55

Appendix D: preliminary studies prior to corneal enzymatic resistance studies

Prior to launching the main enzymatic resistance studies, the following two preliminary tests were performed to optimise the pepsin digest method used for assessing corneal resistance to enzymatic digestion.

(i) Optimization of water bath temperature for enzyme digest studies

Water baths were set at three different temperatures (23 ºC, 25 ºC and 28 ºC) in order to select the optimum water bath temperature for untreated and cross-linked 4-5 porcine corneal disks of 8 mm diameter with epithelial debridement (**Table D.1.**) to digest in a pepsin solution comprising 1 g of 600-1200 U/mg pepsin from porcine gastric mucosa (Sigma-Aldrich, Dorset, UK) in 10 ml 0.1M HCl at pH 1.2. As shown in **Table D.1.**, the corneal disks placed in a 23 ºC water bath temperature digested at a rate slow enough to allow differences between treatment groups to be detected but fast enough to ensure that the pepsin remained active throughout as it is continue digesting the disk.

Table D.1. Three different temperatures set up (23 ºC, 25 ºC and 28ºC) in order to select the optimum water bath temperature for porcine corneal disks.

Temperature	Group	n	Time taken for complete digestion (days)	Significantly difference from control groups
28ºC	Untreated	5	3.6 ± 0.5	
	ACXL 9mW	4	4 ± 0	
25ºC	Untreated	4	6.25 ± 0.5	
	SCXL 3mW	4	9 ± 1.6	*($p < 0.018$)
	ACXL 9mW	4	9.75 ± 0.5	*($p < 0.006$)
23ºC	Untreated	4	9.5 ± 0.6	
	SCXL 3mW	4	20.5 ± 3.7	*($p < 0.004$)
	ACXL 9mW	4	19.75 ± 3.7	*($p < 0.006$)

(ii) Assessment of the effects of hydrochloric acid on corneal tissue digestion

As hydrochloric acid is a component of the pepsin digest solution described above, it was necessary to ascertain the effects of the hydrochloric acid on the corneal tissue prior to beginning the pepsin digestion studies. Briefly, six 8 mm corneal disks (with epithelium removed) were immersed into 6 ml of 1 M HCl at pH 1.2. The diameter of the corneal disks was monitored at regular intervals for a period of four months. Our preliminary *ex vivo* data showed that HCl at the concentration used in the pepsin digest solution does not result in any changes in the diameter of the porcine eyes even after 126 days (**Figure D.1.**). Therefore, it

can be sure that during the pepsin digest studies any changes in corneal tissue diameter are due to enzymatic digestion.

Figure D.1. Measurement of corneal disk diameter using digital calipers. The diameter of the porcine corneal disks remained unchanged after 126 days in HCl.

Appendix E: A preliminary study of corneal biomechanical properties

(i) Optimising corneal hydration control during strip extensometry

Previous studies confirmed that both hydration and collagen cross-linking treatment influence biomechanical properties of the cornea (Hatami-Marbini and Rahimi, 2015a, Hatami-Marbini and Rahimi, 2015b, Kling and Marcos, 2013). Thus, an accurate assessment of the stiffening effect of different CXL procedures by means of uniaxial tensile testing is only possible if the hydration of the samples is completely controlled. In this preliminary study the optimal method for maintaining the hydration of corneal strips during biomechanical testing. Ten corneal strips were positioned in a custom made sample holder that was compatible with a Lloyd extensometer and comprised metal clamps for securing the tissue strip and a detachable Perspex enclosure designed to minimise sample evaporation during biomechanical testing. The corneal strips were exposed to a variety of environmental conditions: (1) a cotton pad soaked with distilled water positioned within the sample enclosure beneath the tissue strip, (2) blue roll soaked with distilled water positioned within the sample enclosure beneath the tissue strip, (3) 1.5 ml of distilled water within the sample enclosure beneath the tissue strip, (4) 4 ml of distilled water within the sample enclosure beneath the tissue strip, (5) one drop of distilled water applied to the corneal strip without use of the sample enclosure and (6) no hydration control method or sample enclosure used (**Figure E.1**). Wet weight measurements for each strip were performed before securing the specimen into the sample holder and again after 35 minutes (the usual time required to perform a biomechanical testing measurement). All strips were then placed in a 60°C oven for three days, after which their dry weight was recorded. The percent of water content was calculated according to Equation 1.

% water content = ((wet weight – dry weight) / wet weight) * 100 (1)

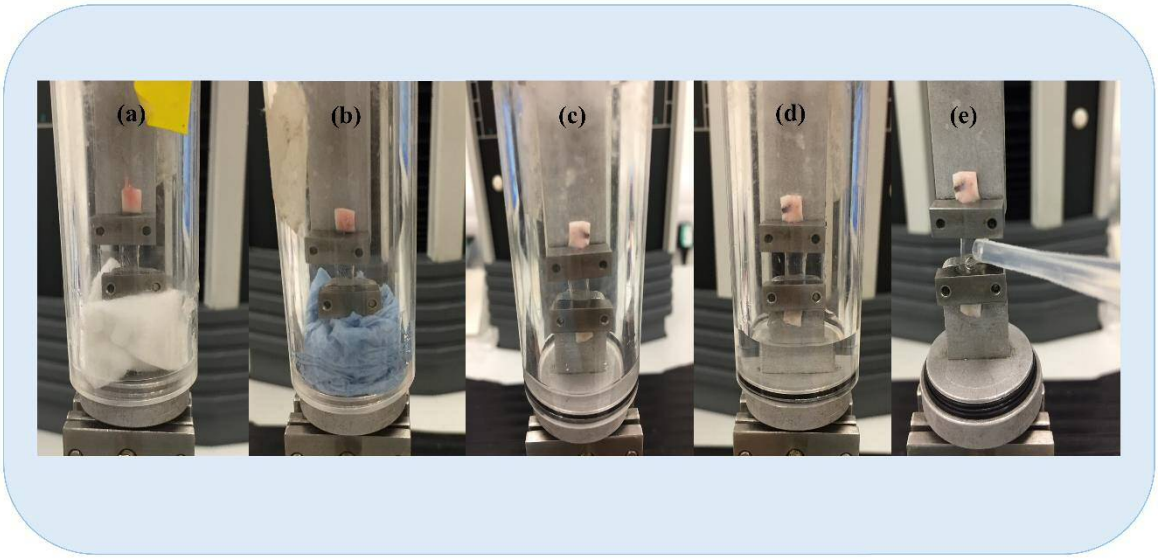

Figure E.1. Preliminary study five various conditions of hydration control. These conditions were (a) cotton pad soaked in distilled water, (b) blue paper soaked in distilled water, (c) 1.5

ml distilled water, (d) 4 ml distilled water and (e) the application of one drop of distilled water to the corneal strip without use of the sample enclosure.

Table E.1 Humidity chamber conditions showing that the cotton pad soaked in distilled water reduced the percent of water content by about 0.4% (indicated in bold).

Control		% decreased of water content	Hydration conditions	Hydration		% decreased of water content
% water content				% water content		
start	after 35 min			start	after 35 min	
81.1	75.1	6.0	cotton pad soaked in distilled water	**80.1**	**79.7**	**0.4**
81.3	76.3	5.1	blue paper soaked in distilled water	81.5	79.7	1.8
81.3	69.8	11.5	1.5 ml distilled water	81.5	79.6	1.8
81.7	76.1	5.6	4 ml distilled water	80.4	77.9	2.5
80.7	74.6	6.1	apply one drop of distilled water	81.1	80.1	1.1

The results of this preliminary study indicated that the hydration of porcine corneal strips could be best maintained during biomechanical testing by placing a cotton pad soaked in distilled water directly beneath the sample within the sample enclosure (**Table E.1**).

Appendix F: The stress-strain data for accelerated cross-linking protocols

The stress-strain data are presented here to support information in **Chapter 3**.

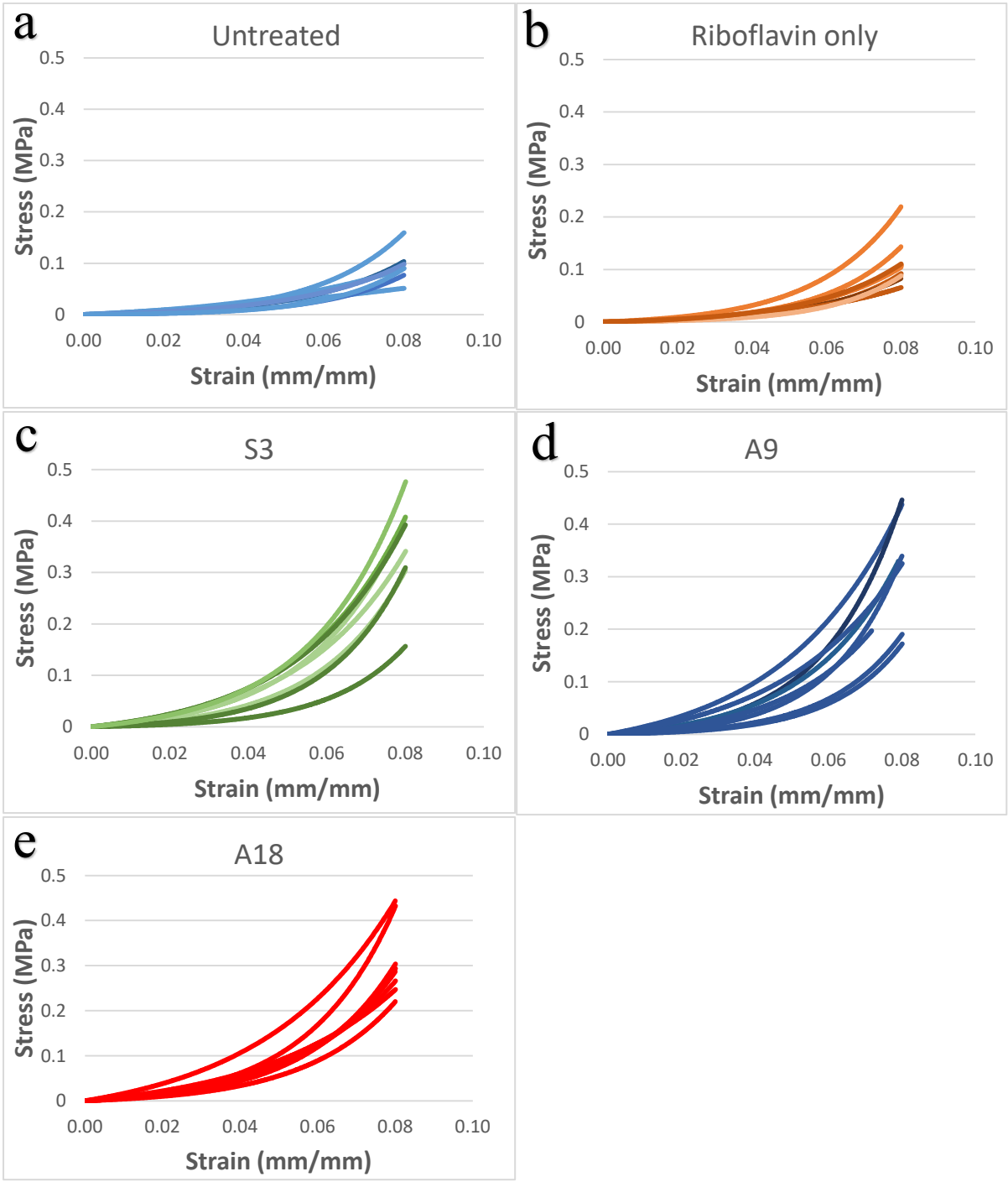

Figure F.1. The stress-strain data was plotted for each sample within a single treatment group: (a) untreated; (b) riboflavin-only; (c) standard cross-linking with 3 mW UVA (S3); accelerated cross-linking using (d) 9 mW (A9) and (e) 18 mW (A18) UVA.

Appendix G: The stress-strain data for modified cross-linking protocols

The stress-strain data are presented here to support information in **Chapter 6**.

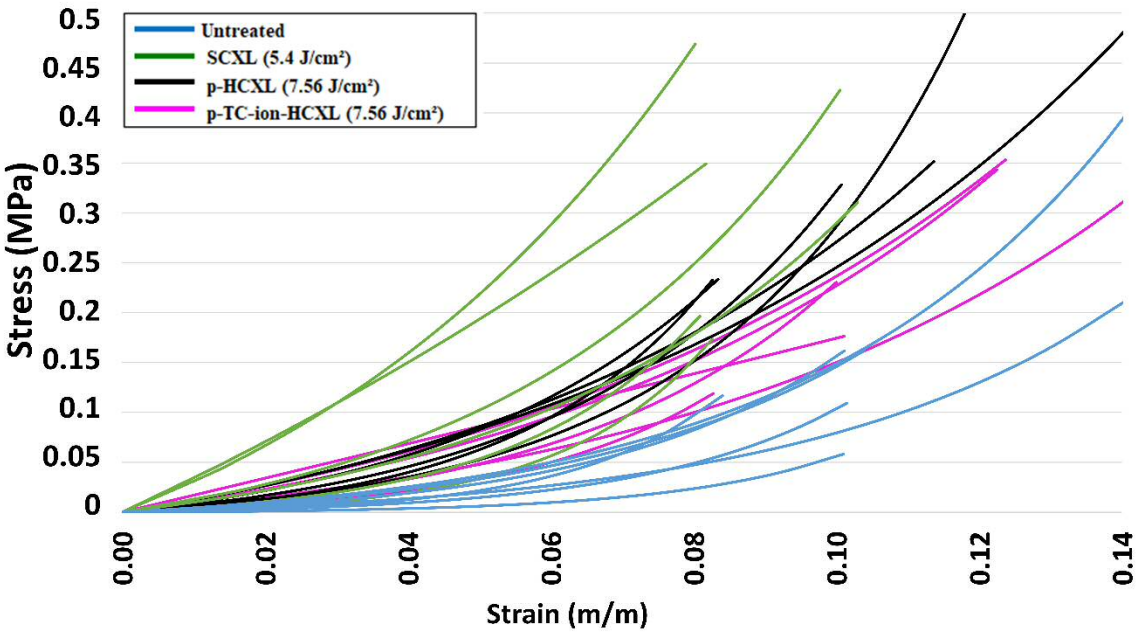

Figure G.1. The stress-strain data was plotted for each sample within a single treatment group: untreated (blue lines); SCXL (5.4 J/cm²) (standard cross-linking) (Green lines); p-HCXL (7.56 J/cm²) (pulsed, high intensity and high energy UVA cross-linking) (Black lines) and p-TC-ion-HCXL (7.56 J/cm²) (pulsed, high intensity and high energy UVA cross-linking with iontophoretic riboflavin delivery) (Pink lines).

Appendix H: Supplementary Electron Microscopy Images

Extra electron micrographs are presented here to support information in **Chapter 7**.
Only representative images appeared in **Chapter 7**.

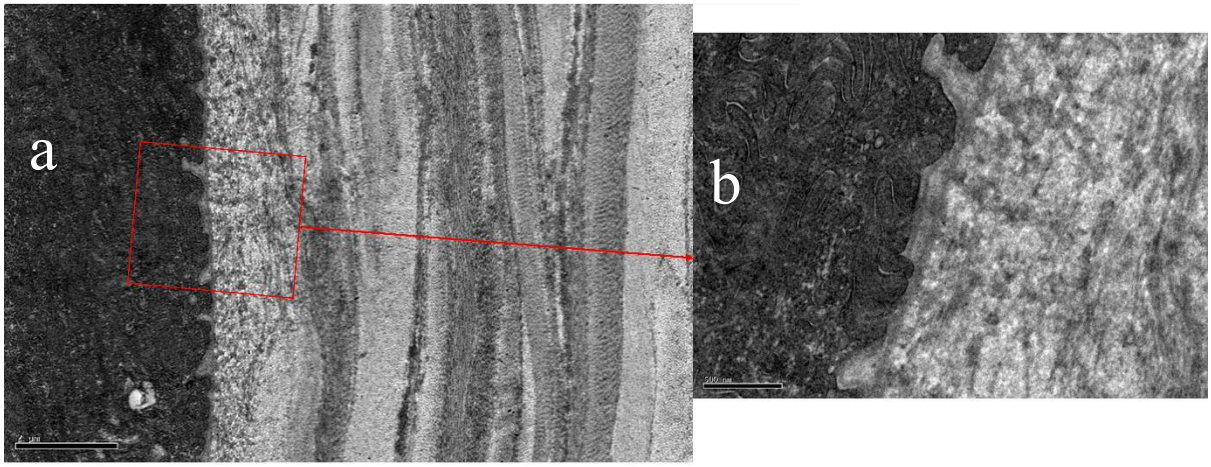

Figure H.1 Electron microscopy images of the corneal epithelium of WST-D treatment showing a double basal lamina, fewer and more irregular basal epithelial cell hemidesmosomes than normal The scale bar for (a) is 2 µm (×2000), and the scale bar for (b) is 500 nm with higher magnification(×10K).

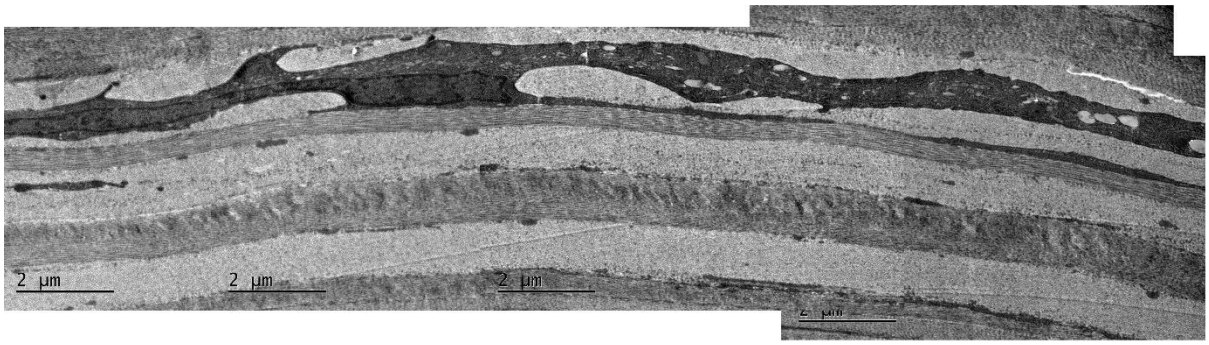

Figure H.2a Montage electron microscopy images of anterior corneal stroma of the WST-D/NIR treatment, showing an active keratocytes of an increased size, with a number of organelles and an altered morphology. Scale bar is 2 µm.

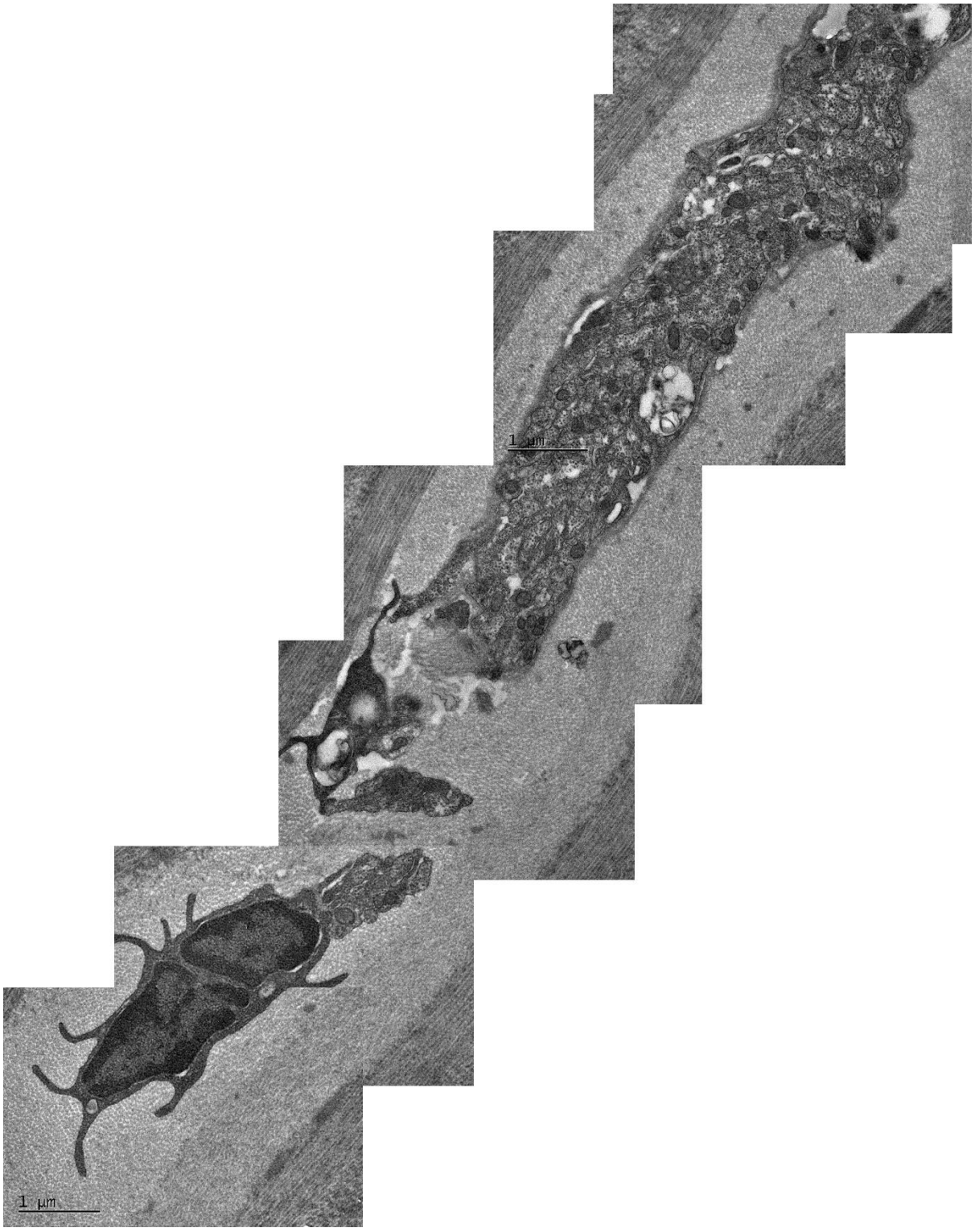

Figure H.2b Montage electron microscopy images of anterior corneal stroma of the WST-D/NIR treatment, showing an active keratocytes of an increased size, with a larger number of organelles and an altered morphology. Scale bar is 1 µm.

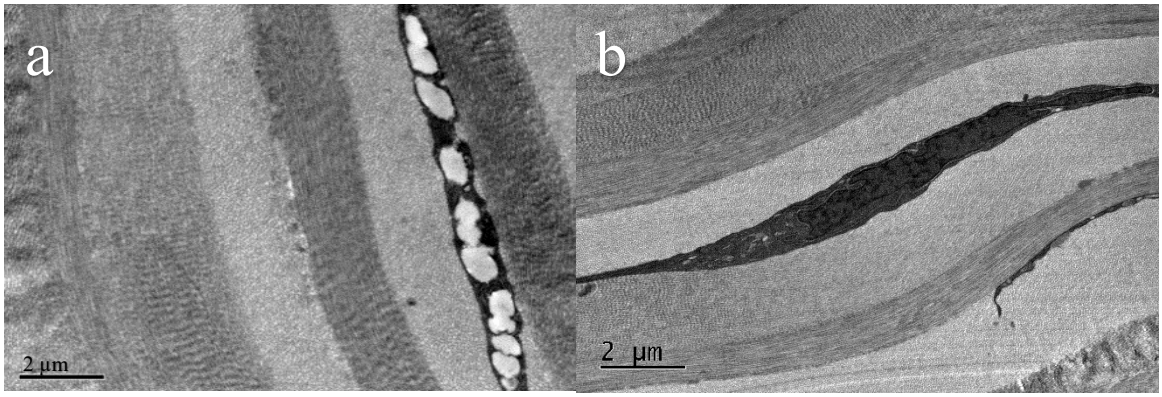

Figure H.3 In the same cornea, (a) intra-cytoplasmic deposits of lipid material with vacuoles could be seen in the anterior stroma of WST-D/NIR corneas with few flat keratocytes (b). Scale bar is 2 µm.

In the anterior stroma of WST-D/NIR corneas, activated keratocytes of an increased size, with a larger number of organelles and an altered morphology were observed (Figure 7.12 c, appendix, **Figure H.2a and Figure H.2b**). Moreover, intra-cytoplasmic deposits of lipid material with vacuoles could be seen in the anterior stroma of WST-D/NIR corneas with few flat keratocytes (appendix, **Figure H.3**). The posterior WST-D/NIR stroma had flat quiescent keratocytes (Figure 7.12 d). However, in the anterior stroma of riboflavin/UVA corneas, keratocytes were flattened (Figure 7.12 j). Meanwhile, the posterior stroma of riboflavin/UVA corneas showed some active keratocytes (Figure 7.12 h) with some flat keratocytes (appendix, **Figure H.4**).

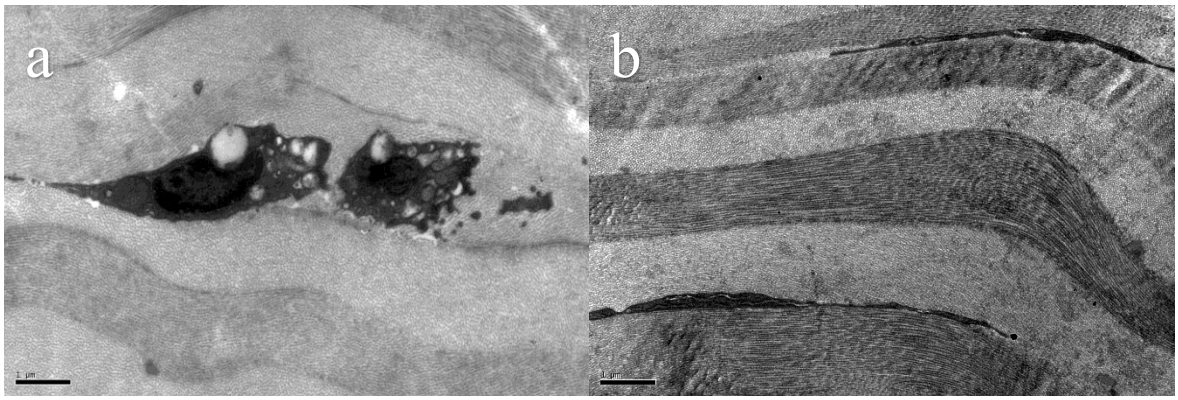

Figure H.4 The posterior stroma of riboflavin/UVA corneas showed (b) some active keratocytes (b) with some flat keratocytes. Scale bar is 1 µm.

Appendix I: Graphical Abstract

To examine the potential of a range of CXL therapies

Compare the effectiveness of epi-on & epi-off

By examining the impact of changes

The intensity and distribution of the crosslinks formed within the cornea vary with different UVA protocols.

Chapter 3

UVA intensity

- 9 mW/cm^2 for 10 min
- 18 mW/cm^2 for 5 min

→ High intensity protocols result in more CXL in the anterior-most stroma but the depth of CXL may be shallower.

Chapter 4

Riboflavin solution — Increase concentrations

UVA dosage — Increase by 25% from 5.4 to 6.75 J/cm^2

→ epi-on CXL < epi-off CXL in terms of enzymatic resistance, the outcome of epi-on CXL may be significantly improved by:

1. the use of higher concentrations of riboflavin solution.
2. Increase riboflavin soakage time.
3. a longer duration of iontophoresis.
4. an increase in UVA radiance.

Chapter 5

UVA delivery mode (pulsed vs continuous) — 30 mW for 4 min (p-HCXL 7.2)

→ Pulsing UVA during high intensity/high energy procedures can increase the enzymatic resistance of the cornea by increasing oxygen availability.

Develop epi-on method that is equally effective to SCXL

Chapter 6

Combine all of the above — 9 mW for 14 min (p-TC-ion-HCXL 7.56)

→ The optimised St Thomas'/Cardiff TE CXL protocol may be a promising, less painful, but equally effective alternative to SCXL.

Chapter 7

Assess the effect of another novel corneal stiffening treatment involve WST-D

The organisation of collagen within the corneal stroma as primary step to assessing its clinical potential.

- Slower healing processing of epithelium and anterior stromal in WST-D/NIR treatment compared to standard riboflavin/UVA treatment.
- No alterations in collagen structural parameters following treatment supports the idea that WST-D/NIR treatment is a suitable method for safely strengthening diseased or surgically weakened corneas.